# Investigation of the Role of Nephrin Phosphorylation and Associated Signaling Pathways in Kidney Podocytes

**by**

**Laura Alexandra New**

**A Thesis**
**presented to**
**The University of Guelph**

**In partial fulfilment of requirements**
**for the degree of**
**Doctor of Philosophy**
**in**
**Molecular and Cellular Biology**

**Guelph, Ontario, Canada**

# ABSTRACT

## INVESTIGATION OF THE ROLE OF NEPHRIN PHOSPHORYLATION AND ASSOCIATED SIGNALING PATHWAYS IN KIDNEY PODOCYTES

**Laura Alexandra New** **Advisor:**
**University of Guelph, 2014** **Dr. Nina Jones**

The integrity of the glomerulus plays a key role in prevention of kidney damage. The specialized function of the glomerular filter has led to the evolution of a unique cell type—the podocyte—whose shape and function depends on its network of actin-based 'foot processes'. Damage to the filter—the slit diaphragm junction—formed between foot processes leads to proteinuria and can result in kidney failure. The slit diaphragm supports podocyte architecture through the IgG protein nephrin, whose cytoplasmic tail contains several conserved tyrosine residues within YDxV motifs which are phosphorylated by Fyn kinase. The significance of these tyrosines has remained elusive, but they have recently been shown to recruit the essential podocyte protein Nck. We hypothesize that phosphorylated nephrin signaling via Nck is important in the podocyte and that removal of the YDxV motifs from nephrin *in vivo* will result in a loss of Nck signaling and the collapse of the podocyte actin cytoskeleton.

To study nephrin phosphorylation on specific tyrosines, we generated phospho-nephrin antibodies against individual YDxV motifs. These antibodies allowed us to validate that these sites are indeed phosphorylated *in vivo* and to demonstrate that phosphorylation on these tyrosines is altered in a podocyte injury model. This work was complemented by further study of the regulation of nephrin phosphorylation, which outlined a mechanism whereby nephrin phosphorylation is positively regulated by Nck. Recruitment of Nck to phosphorylated nephrin via its SH2 domain enables its SH3 domains to bind and activate Fyn kinase, thus increasing nephrin tyrosine phosphorylation and promoting continued engagement of nephrin signaling pathways.

Finally, we investigated the importance of nephrin tyrosine phosphorylation *in vivo* through the nephrin$^{Y3F}$ mouse model, which contains mutations preventing nephrin phosphorylation on the YDxV tyrosine motifs. The inability to phosphorylate these tyrosines *in vivo* does not prevent slit diaphragm formation, but results in podocyte foot process effacement and proteinuria with age. These results highlight the importance of phospho-nephrin signaling pathways in the podocyte, and—as altered nephrin phosphorylation is observed in human kidney disease—may contribute to a better understanding of how these pathways can be therapeutically manipulated to restore damaged podocytes.

# DEDICATION

This thesis is dedicated to the memory of two scientists,

my maternal grandmother, Lillian Gladys Alonso Wozniak (1914 – 2012)

and

Dr. Jones' post-doctoral advisor, Dr. Anthony James Pawson (1952 – 2013)

whose inspiration and support, directly and indirectly, made this thesis possible.

# ACKNOWLEDGMENTS

The completion of a graduate degree is a process which is not carried out in isolation, and there are many people to whom I owe a thank you for their assistance during my project.

I'd like to begin by thanking my advisor, Nina, for taking a chance on me back at the beginning when she was starting up her lab. The time I have spent in her lab has been a very valuable education, one which I will take with me for the future. It's taken me a while to make it here, along the way she has been the very best kind of supervisor that anyone could hope for. She has been supportive of my project, and challenged me to take things to the next level. She has generously given me the means to pursue extraordinary opportunities to share my work on the global stage. She has provided me with opportunities to practice all aspects of being a researcher, from assisting with grant applications, to drafting animal utilization protocols, and writing manuscripts.

My next thanks goes to all of the mice whose contributions to science made my project possible and to all of the people at the Central Animal Facility who helped look after them. Our research animal technician, Martha (Manning) Smith, was a blessing. She was always willing to help find me additional equipment to make things work better and she collected urine from all of my mice without complaint. I'd also like to thank Jackie Roombeck for helping me with perfusions and teaching me how to collect blood. On the administrative side, Mary Zouthout and Helen Donaldson patiently answered my questions and explained the meanings of countless requirements and Mary Fowler made sure everything ran smoothly.

I was fortunate to have many excellent collaborators. At Guelph, I owe a big thank you to Matt Platt and Jeremy Simpson for collecting cardiac function data and tissues from all of the mice. Sandy Smith and showed me how to do electron microscopy myself from start to finish, and she and Dianne Moyles helped me to image samples on the TEM scope. John Armstrong helped me to perform an important experiment. In Toronto, Rizaldy Scott provided experimental protocols and assisted with imaging all of my SEM samples and he even came to Guelph to give

me a hand. In Boston, Peter Mundel let me be part of his lab for a summer and taught me how to grow podocytes and Joel Henderson analyzed my slides with the eyes of a pathologist. Lastly, I'd like to thank Sean Taylor, who went above and beyond the standard level of customer service to help me with the analysis of my qPCR data.

I must also thank all of my labmates over the years for being a great bunch to work with and the members of the Van Raay, Mosser and Bendall labs for giving me additional resources to ask for help about unfamiliar techniques. In the Jones lab, Ava stepped up when I was in a pinch and helped me to finish up my first paper. Colin took care of my mice for me when I was away. Claire was always willing to talk about podocytes. Melanie was a great bench mate and asked good questions during lab meeting.

Lastly, I'd like to thank those family and friends who have supported me personally on the path to finishing my thesis. Margaret Hundleby put her keen eye to the text and it has been significantly improved by her efforts. Cheryl Cragg got me to join an intermural hockey team which helped me to be more confident. Joan and Richard Barham's dinners were a lovely chance to visit with friends. The members of the Unitarian Congregation of Guelph and St. Matthias helped me to feel connected with the larger community. Suzanne and Lynda were always willing to listen.

I am grateful for all of the support I have received during my project, especially from NSERC (Alexander Graham Bell Canada Graduate Scholarships, as well as a Canada Graduate Scholarship Michael Smith Foreign Study Supplement which enabled me to travel to Boston), and for a CIHR Institute of Nutrition, Metabolism and Diabetes Community Support Travel Award which allowed me to present my work to the American Society of Nephrology.

As for my family, my parents have believed in me from the beginning, and their support was essential. My grandmother Lillian was proud that I was following in her footsteps. Both David and Liam, and their respective families, helped me to make Guelph my home. Tim believed in me when I needed it most and help me to create a place to get started writing. And my partner, Hal, kept me motivated and convinced me that I could make it to the finish line.

# TABLE OF CONTENTS

# LIST OF TABLES

# LIST OF FIGURES

# LIST OF ABBREVIATIONS

| | |
|---|---|
| ACE | angiotensin-converting enzyme |
| ACR | albumin/creatinine ratio |
| ADAP | adhesion and degranulation promoting adaptor protein |
| ANOVA | analysis of variance |
| AP-1 | activator protein 1 |
| aPKC | atypical protein kinase C |
| Arp2/3 | actin-related protein 2/3 |
| BCA | bicinchoninic acid |
| CAS | chemical abstracts service |
| CD2AP | CD2 associated protein |
| CDC42 | cell division control protein 42 |
| cDNA | complementary DNA |
| c-mip | c-Maf inducing protein |
| CNF | congenital nephrotic syndrome of the Finnish type |
| Csk | c-src tyrosine kinase |
| DNA | deoxyribonucleic acid |
| Dock | dreadlocks |
| Dox | doxycycline |
| EDTA | ethylenediaminetetraacetate |
| EGFR | epidermal growth factor receptor |
| EGTA | [Ethylenebis(oxyethylenenitrilo)]tetraacetic acid |
| ELISA | enzyme-linked immunosorbent assay |
| FBS | fetal bovine serum |
| FSGS | focal segmental glomerulosclerosis |
| GAPDH | glyceraldehyde-3-phosphate dehydrogenase |
| GBM | glomerular basement membrane |
| GFP | green fluorescent protein |

| | |
|---|---|
| GLEPP1 | glomerular epithelial protein 1 (see also PTPRO) |
| Grb2 | growth-factor receptor binder 2 |
| HEPES | 4-(2-Hydroxyethyl)-1-piperazineethanesulfonic acid |
| HSN | hermaphrodite-specific neuron (C. elegans) |
| i.p. | intraperitoneal(ly) |
| Ig | immunoglobulin |
| IP | immunoprecipitate |
| IPCs | interommatidial precursor cells (Dros) |
| IQGAP1 | IQ motif containing GTPase activating protein 1 |
| IrreC | irregular-chiasm C |
| Kirre | kin-of-IrreC |
| Kirrel | kin-of-IrreC-like |
| LPS | Lipopolysaccharide |
| MAGI | membrane-associated guanylate kinase inverted |
| MAP | mean arterial pressure |
| MCD | minimal change disease |
| MDCK | Madin Darby canine kidney |
| MN | membranous nephropathy |
| mRNA | messenger RNA |
| Nck | non catalytic kinase |
| neph | nephrin-like |
| NOS | not otherwise specified |
| N-WASp | neuronal Wiskott-Aldrich syndrome protein |
| OMIM | Online mendelian inheritance in man |
| p | phospho |
| PAAS | Periodic acid-ammoniacal silver |
| PAGE | polyacrylamide gel electrophoresis |
| Pak | p21 activated kinase |
| PAN | puromycin aminonucloside |
| PAS | Periodic acid–Schiff |
| PBS | phosphate-buffered saline |

| | |
|---|---|
| PCR | polymerase chain reaction |
| PDGFR | platelet derived growth factor β receptor |
| PHN | passive Heymann nephritis |
| PI3K | phosphatidylinositol 3-kinase |
| PLA2R | phospholipase A2 receptor |
| PLC | phospholipase C |
| PMSF | phenylmethylsulfonyl fluoride |
| PP2 | 4-amino-5-(4-chlorophenyl)-7-(t-butyl)pyrazolo[3,4-d]pyrimidine |
| PPi | inorganic pyrophosphate |
| PTP | protein tyrosine phosphatase |
| PTPRO | protein tyrosine phosphatase, receptor type, O (see also GLEPP1) |
| PVDF | poly(vinylidene difuloride) |
| RAbMAbs | rabbit monoclonal antibodies |
| Rac1 | Ras-related C3 botulinum substrate 1 |
| RhoA | Ras homolog family member A |
| RIN | RNA integrity number |
| RIPA | radio immuno-precipitation assay |
| RNA | ribonucleic acid |
| rpm | revolutions per minute |
| rtTA | reverse tetracycline trans-activator |
| S.E.M. | standard error of mean |
| SDS | sodium dodecyl sulfate |
| SEM | scanning electron microscopy |
| SFK | Src family kinase |
| SH2 | Src homology domain 2 |
| SH3 | Src homology domain 3 |
| SHP-2 | SH2 domain-containing protein tyrosine phosphatase-2 |
| siRNA | short interfering RNA |
| SIRPα | signal-regulatory protein alpha |
| SLP-76 | SH2 domain containing leukocyte protein of 76kDa |
| SNS | sticks-and-stones |

| | |
|---|---|
| Sos | son of sevenless |
| TBST | Tris-buffered saline with tween |
| TEM | transmission electron microscopy |
| Tris | tris(hydroxymethyl)aminomethane |
| VAMP2 | vesicle-associated membrane protein 2 |
| VEGFR-2 | vascular endothelial growth factor receptor 2 |

# CHAPTER 1:

# INTRODUCTION

## 1.1 RELEVANCE OF KIDNEY DISEASE

Kidney failure is one of the top ten causes of death among Canadians; it significantly increases risk of death when combined with cardiovascular complications. The 12% of Canadians (3 million) who live with some stage of chronic kidney disease includes 30% of people over the age of 65 (Arora *et al.*, 2013). The challenge of kidney failure is not limited to Canada; the global incidence of end-stage kidney disease has been steadily increasing, with at least 1 million people worldwide undergoing dialysis (Dirks, 2005).

The primary function of the kidney is to remove waste products from the blood efficiently. The kidney also controls fluid balance, pH and blood pressure as well as performing some endocrine functions. Each kidney is comprised of many copies of its functional unit, the nephron, numbering about one million in a single human kidney. Blood flows into the kidney via the renal artery, which branches until it reaches the capillary beds of individual nephrons. It enters the nephron through the glomerulus, where filtration occurs. Filtration is a tightly controlled process; failure of the filtration system damages the kidney, leading to kidney disease and eventually to kidney failure.

Once kidney failure occurs, there is no way to reverse the process. Currently, the only viable treatment options for patients suffering from kidney failure are dialysis and kidney transplantation. Therefore, it is important to fully understand the molecular changes underlying the various routes which can lead to the development of kidney disease. If we can increase our understanding of how signaling pathways involved in normal kidney function are perturbed during the development of kidney disease, then we may be able to use this knowledge to discover new ways to prevent the progression of kidney damage into kidney disease.

## 1.2 THE GLOMERULUS

### 1.2.1 *THE GLOMERULUS AS A HOMEOSTASIS MAINTENANCE MECHANISM*

The glomerulus resembles a twisted ball of capillaries in a circular shape (Figure 1.1A-C). Blood enters the glomerulus through the afferent arteriole and exits the glomerulus through the efferent arteriole. Within the glomerulus, the capillary branches and forms a number of loops. These loops are held in place by mesangial cells. Glomerular capillaries are lined with endothelial cells, which are highly fenestrated. The outer surface of glomerular capillaries is covered by epithelial cells called podocytes. Podocytes and endothelial cells are both attached to the glomerular basement membrane (GBM) which spans between them. The GBM forms a continuous surface and is directly connected to the mesangium in some areas. The GBM also connects to the outer surface of the glomerulus called Bowman's capsule, which is lined by parietal epithelial cells. The filtrate exits the glomerulus and continues through the nephron, traveling through the collecting ducts and the loop of Henle where salts and water are re-absorbed. The filtrate continues to be concentrated as it exits the kidney into the ureter, ultimately being released as urine.

The glomerulus acts as a filter by retaining large proteins in the blood while allowing waste products to exit the blood stream, and this process is essential for the maintenance of homeostasis (Haraldsson *et al.*, 2008). If the filter is damaged, this allows proteins to pass through the rest of the nephron and into the urine. The passage of protein through the tubules of the nephron causes damage which can result in increased blood pressure, and develop into kidney disease. The detection of high levels of protein, typically albumin, in the urine represents one of the clinical hallmarks of kidney damage, proteinuria. The maintenance of proper filtration within the glomerulus is an integral aspect of the prevention of kidney damage.

### 1.2.2 *THE GLOMERULUS AS A FILTRATION BARRIER*

The glomerular filtration barrier is composed of three components—the podocyte, the GBM and the endothelium (Figure 1.2A and B)—supported by the mesangium, all of which are required for filtration (Patrakka and Tryggvason, 2010). This thesis focuses on podocyte structure and function; there are excellent review articles detailing the contributions of the GBM (Miner, 2012; Suh and Miner, 2013), endothelium (Haraldsson and Nystrom, 2012; Obeidat *et al.*, 2012) and mesangium (Lemley *et al.*, 1992; Schlondorff and Banas, 2009) to the glomerular filtration barrier. The outer surface of glomerular capillary is covered by an elaborate network of podocyte cells which adopt a complex architecture (Figure 1.3A). Like other arborized cells such as neurons (Kobayashi *et al.*, 2004), the podocyte cell body extends a number of primary and secondary processes comprised of microtubules and the intermediate filaments vimentin and desmin (Pavenstadt *et al.*, 2003). Branching off from these processes are numerous smaller actin rich foot processes, which interdigitate with foot processes from adjacent podocytes.

## 1.3 **THE PODOCYTE**

### 1.3.1 *SPECIALIZED ARCHITECTURE OF THE PODOCYTE*

The specialized architecture of the podocyte is adapted to the biophysical challenges of filtration. The human body filters blood through size selective pores with a cutoff of approximately 70 kDa at a rate of roughly 120 mL/min through its two kidneys (Haraldsson *et al.*, 2008). Based on estimates derived from electron micrographs, there are roughly 19 km of glomerular capillaries with a total surface area of 6000 $cm^2$, though only a portion of that surface area is available to be used as a filter (Rodewald and Karnovsky, 1974; Bohle *et al.*, 1998). From an engineering perspective, there are two requirements to be able to achieve such a high filtration rate. The first is to increase the available surface area. The estimated available filtration area of glomerular capillaries is 5-8% of the total surface area as compared to 0.01% in muscle (Rodewald and Karnovsky, 1974; Bohle *et al.*, 1998). The increase in surface area is accomplished by the branched network of podocyte foot processes. The filter is formed by a

specialized intercellular junction between podocyte foot processes known as the slit diaphragm. As a result, the amount of surface area available for filtration will be directly proportional to the total length of foot processes and thus to the length of the slit diaphragm (Figure 1.3B).

The second requirement for achieving a rapid filtration rate under these specific conditions, mechanical strength, is based on purely hydrodynamic considerations. The filtration rate generates significant hydrostatic pressure, reaching a pressure differential across a glomerular capillary that has been estimated to measure 40 mmHg (Endlich and Endlich, 2012). This creates a significant outward force on the glomerular capillaries which is counteracted via forces generated by the actin cytoskeleton of podocyte foot processes.

Not surprisingly, these forces require that podocytes be strongly attached to the GBM, as illustrated in Figure 1.4. The most critical components of the GBM are laminin and type IV collagen, and specific isoforms of both are found in the glomerular GBM (Abrahamson, 2012). The GBM of the mature glomerulus is composed of laminin-521 and type IV collagen (α3α4α5). The podocyte is linked to the GBM through a number of proteins (Hu and Jiao, 2013). Laminin receptors in the podocyte include α3β1 integrin and dystroglycan. Type IV collagen receptors include α1β1 and α2β1 integrin and discoidin domain receptor 1 (DDR1).

### 1.3.2 *MOLECULAR MAKEUP OF THE PODOCYTE SLIT DIAPHRAGM*

A series of elegant microscopy experiments in the 1970s established the presence of the slit diaphragm as an electron-dense structure spanning podocyte foot processes (Rodewald and Karnovsky, 1974). It took another 25 years for scientists to be able to identify the molecular components of the slit diaphragm. The slit diaphragm (Figure 1.4) is a unique type of intercellular junction which forms a critical component of the podocyte's contribution to the glomerular filtration barrier (Grahammer *et al.*, 2013); though unique in its composition, the slit diaphragm contains elements of classical adherens (Reiser *et al.*, 2000a) and tight (Fukasawa *et al.*, 2009) junctions, and, like both types of junctions, it is anchored to the actin cytoskeleton.

The junction is formed primarily by members of the immunoglobulin (Ig)-like transmembrane protein nephrin family, including nephrin and the nephrin-like (neph) family

(neph1-3) (George and Holzman, 2012), though the cadherins P-cadherin and Fat also contribute to the slit diaphragm. On the intracellular side of the slit diaphragm, nephrin forms a complex with a number of proteins. These include the stomatin-like protein podocin (Schwarz *et al.*, 2001), the tyrosine kinase Fyn (Verma *et al.*, 2003) and the adaptor CD2AP (Shih *et al.*, 2001). While disruption of most of the above proteins leads to kidney disease, arguably the most critical to the functioning of the slit diaphragm is the nephrin family.

## 1.4 NEPHRIN

### 1.4.1 *DISCOVERY OF NEPHRIN AS A PODOCYTE PROTEIN*

In the 1990s, genetic work with the families of patients with an inherited form of kidney disease, congenital nephrotic syndrome of the Finnish type (CNF) (OMIM #602716), led to identification of *NPHS1* as the gene mutated in the syndrome (Kestila *et al.*, 1998). The protein involved, which was named nephrin, was cloned and subsequently localized to the podocyte slit diaphragm (Kestila *et al.*, 1998; Holthofer *et al.*, 1999; Holzman *et al.*, 1999; Ruotsalainen *et al.*, 1999). Genetic analysis identified two nephrin mutations which account for 90% of cases of the Finnish syndrome (Kestila *et al.*, 1998). The most common mutation, $Fin_{major}$, is a frameshift that results in the production of a truncated (90 amino acids out of 1241), non-functional protein. As well, the kidneys of patients with the mutation were found to lack slit diaphragms, providing a major breakthrough in glomerular research.

### 1.4.2 *NEPHRIN EXPRESSION*

The nephrin gene encodes an 180 kDa adhesion protein of the immunoglobulin superfamily that has an extracellular domain composed of eight IgG-like domains and a single fibronectin type-3 motif, followed by a transmembrane domain and a short cytoplasmic domain (Figure 1.5A). Initially, the phenotype of patients with congenital nephrotic syndrome suggested that the absence of nephrin affected only kidney function. Subsequently, some reports using mouse models detected nephrin transcripts in the kidney, brain and pancreas (Moeller *et al.*, 2000;

Putaala *et al.*, 2001) as well as the testes (Liu *et al.*, 2001). Other efforts have confirmed nephrin expression in the brain (Beltcheva *et al.*, 2003; Morikawa *et al.*, 2007; Nishida *et al.*, 2010; Li *et al.*, 2011) and pancreas (Palmen *et al.*, 2001; Beltcheva *et al.*, 2003; Zanone *et al.*, 2005). One group observed, however, that nephrin expression was restricted to the kidney in both human and porcine species (Kuusniemi *et al.*, 2004). More recently, roles for nephrin have been proposed in skeletal muscle (Komori *et al.*, 2008; Sohn *et al.*, 2009) and heart (Wagner *et al.*, 2011) and there has been a single report of nephrin expression in the human lymphatic system (Astrom *et al.*, 2006) and another of nephrin expression in the rat placenta (Beall *et al.*, 2005). In the process, researchers have identified some of the promoter regions responsible for directing tissue specific-expression patterns (Moeller *et al.*, 2000; Moeller *et al.*, 2002; Beltcheva *et al.*, 2003; Guo *et al.*, 2004; Wagner *et al.*, 2004; Nishida *et al.*, 2010; Beltcheva *et al.*, 2010) and some of the transcription factors responsible for controlling nephrin expression (Matsui *et al.*, 2007; Takano *et al.*, 2007; Okamura *et al.*, 2009; Ristola *et al.*, 2009; Saito *et al.*, 2010; Nishida *et al.*, 2010; Deb *et al.*, 2011; Ristola *et al.*, 2012; Ristola *et al.*, 2013).

### 1.4.3 *THE NEPH FAMILY OF PROTEINS*

The characterization of nephrin led to the discovery of a family of nephrin-like (neph) proteins. Humans and mice have three family members—neph1/Kirrel, neph2/Kirrel3, and neph3/Kirrel2/filtrin—which contain 5 IgG-like domains in the extracellular portion, followed by a transmembrane domain and cytoplasmic tail (Figure 1.5B). Expression of the three neph proteins is not restricted to the glomerulus and each has a distinct expression pattern (Volker *et al.*, 2012). The loss of neph1 in mice leads to the development of proteinuria (Donoviel *et al.*, 2001), whereas the absence of neph2 does not appear to impact kidney function (Prince *et al.*, 2013). The importance of neph3 in mice is unknown, though it is expressed in podocytes (Ristola *et al.*, 2009).

### 1.4.4 *NEPH-NEPHRIN INTERACTIONS FORM AN EVOLUTIONARILY CONSERVED ADHESION MODULE*

The signaling module composed of neph and nephrin proteins is evolutionarily conserved (Fischbach *et al.*, 2009). In other species, neph-nephrin interactions mediate connections between two different cell types leading to intercellular adhesion. For example, in *C. elegans*, syg-1 (neph-like) is expressed on HSN axons and mediates interaction with syg-2 (nephrin-like) expressed on guidepost cells (Shen *et al.*, 2004; Chao and Shen, 2008; Wanner *et al.*, 2011). In *Drosophila*, there are two nephrin-like proteins, Hibris and Sticks-and-stones (Sns), and two neph-like proteins, irregular-chiasm (IrreC)/Roughest and Dumbfounded/Kin-of-IrreC (Kirre) (Fischbach *et al.*, 2009). The neph-nephrin module is used in multiple organs during development. Eye organization is coordinated by interactions between Hibris (nephrin-like) expressing pigment cells and Roughest (neph-like) expressing IPC cells (Bao and Cagan, 2005; Bao *et al.*, 2010). Neph and nephrin-like proteins play a role in myoblast fusion as well, through their expression exclusively in founder cells and fusion competent myoblasts respectively (Shelton *et al.*, 2009; Abmayr and Pavlath, 2012; Kaipa *et al.*, 2013). They also function in selective adhesion processes which pattern wing margin hairs (Takemura and Adachi-Yamada, 2011) and the visual retinotopic map (Sugie *et al.*, 2010). In the *Drosophila* nephrocyte, which shares some structural similarities with the mammalian glomerulus, expression of both Sns (nephrin-like) and Kirre (neph-like) are required for adhesion and fusion of garland cells during development and in the adult nephrocyte (Weavers *et al.*, 2009; Zhuang *et al.*, 2009; Zhang *et al.*, 2013).

Across species, all three mammalian neph proteins were able to rescue *C. elegans* syg-1 mutants (Neumann-Haefelin *et al.*, 2010), whereas only neph1 was able to compensate for *Drosophila* Kirre (Helmstadter *et al.*, 2012). In *Drosophila* myoblast fusion, both the PDZ motif and serines in the cytoplasmic tail of Sns were dispensable, but the tyrosines and PxxP motifs were required (Kocherlakota *et al.*, 2008). Although both Sns and its paralog Hibris contain tyrosine phosphorylation sites in their cytoplasmic tails, there appears to be little conservation between the cytoplasmic tail of Sns and that of nephrin (Kocherlakota *et al.*, 2008).

### 1.4.5 *NEPH-NEPHRIN INTERACTIONS IN THE PODOCTYE*

In the evolutionarily conserved neph-nephrin adhesion module, interactions occur between two distinct cell types, with one expressing nephrin and the other expressing neph to control spatial positioning. In the glomerulus however, interactions occur between two cells of the same type, the podocyte, which expresses both nephrin and neph proteins. The dynamics of the possible modes of neph-nephrin signaling in the podocyte are poorly characterized. One possibility is that *cis* and *trans* modes of interaction result in different types of signaling, as occurs for other *trans*-membrane receptors such as Notch and Eph (Sprinzak *et al.,* 2010; Pitulescu and Adams, 2010).

In non-mammalian species, heterodimeric *trans* neph-nephrin interactions mediate cell-cell adhesion and signaling. In contrast, homodimeric *trans* neph-neph and nephrin-nephrin interactions do not appear to induce adhesion. In an *in vitro* context, most studies have examined the effects of *trans* interactions between adhesive proteins on cell-cell adhesion. In cell aggregation assays using non-adhesive cell lines (Jurkat and L-cells), *trans* nephrin-nephrin interactions do not lead to adhesion (Nishida *et al.*, 2010; Heikkila *et al.*, 2011), however, nephrin expression induced formation of aggregates in an adhesive cell line (HEK 293T) growing as a monolayer (Khoshnoodi *et al.*, 2003). In contrast, adhesive *trans* neph1-neph1 (Heikkila *et al.*, 2011) and neph3-neph3 interactions have been reported (Nishida *et al.*, 2010; Heikkila *et al.*, 2011), and one group also observed *trans* nephrin-neph3 adhesion (Heikkila *et al.*, 2011).

Interactions between nephrin and nephs have also been examined; however, these experiments have usually relied on the expression of both proteins simultaneously in cultured cells, making it difficult to be certain that the interactions reported are only the result of *cis* interactions within the same cell and not also from *trans* interactions between adjacent cells. Using this type of experimental approach, there is significant evidence for nephrin-nephrin interactions (Barletta *et al.*, 2003; Gerke *et al.*, 2003; Khoshnoodi *et al.*, 2003; Nishida *et al.*, 2010), as well as reports of nephrin-neph1 (Barletta *et al.*, 2003; Gerke *et al.*, 2003; Liu *et al.*, 2003), nephrin-neph2 (Gerke *et al.*, 2005) and nephrin-neph3 (Nishida *et al.*, 2010; Heikkila *et*

*al.*, 2011) interactions. There may or may not be neph1-neph1 (Barletta *et al.*, 2003; Gerke *et al.*, 2003) and neph2-neph2 (Gerke *et al.*, 2005) interactions, though neph1-neph2 interactions were not observed (Gerke *et al.*, 2005). Additionally, two groups have reported cytoplasmic nephrin-neph1 interactions (Barletta *et al.*, 2003; Heikkila *et al.*, 2011), though another did not (Liu *et al.*, 2003), and there has been one report of cytoplasmic neph1-neph3 and neph3-neph3 interactions (Heikkila *et al.*, 2011).

### 1.4.6 *ENGAGEMENT OF NEPHRIN RESULTS IN NEPHRIN TYROSINE PHOSPHORYLATION*

Evidence suggests that the presence of nephrin in lipid rafts is important to maintain proper nephrin signaling (Simons *et al.*, 2001). Both nephrin and podocin form higher order structures when localized in rafts (Schwarz *et al.*, 2001); nephrin likely contributes to the architecture of the slit diaphragm, while podocin may play an additional role as a possible sensor of dynamic changes to the podocyte (Huber *et al.*, 2007; Schermer and Benzing, 2009). In addition, podocin has been shown to play a key role in the recruitment of nephrin into the lipid rafts (Schwarz *et al.*, 2001; Huber *et al.*, 2003a). Other slit diaphragm-associated proteins are also found in detergent resistant fractions in podocytes including CD2AP (Schwarz *et al.*, 2001) and Fyn (Verma *et al.*, 2003), suggesting that this environment contains all of the components necessary to promote nephrin signaling. It was subsequently established that nephrin can be tyrosine phosphorylated by Src family kinases such as Fyn and that raft-associated nephrin is tyrosine phosphorylated *in vivo* (Lahdenpera *et al.*, 2003; Verma *et al.*, 2003).

Raft association and induction of nephrin tyrosine phosphorylation and signaling appear to be intimately linked. Endocytosis is an important regulator of signaling (Le Roy and Wrana, 2005), and endocytosis of nephrin can occur through both clathrin and raft-mediated mechanisms (Qin *et al.*, 2009). Nephrin phosphorylation may affect the mode of nephrin endocytosis. Phosphorylated nephrin was more efficiently internalized by raft-mediated endocytosis than a nephrin mutant lacking key phosphorylation sites (Qin *et al.*, 2009). A point mutation (V822M) was recently identified in the extracellular domain of nephrin in a patient prone to relapsing nephropathy (Shono *et al.*, 2009). The mutant nephrin decreased stability of the nephrin complex in lipid rafts, leading to inadequate engagement of nephrin signaling as evidenced by reduced

nephrin phosphorylation relative to wildtype nephrin (Shono *et al.*, 2009). Disease causing mutations in podocin can also result in the absence of nephrin from lipid rafts due to failure of mutant podocin to associate with lipid rafts despite being present on the plasma membrane (Huber *et al.*, 2003a).

### 1.4.7 *SIGNALING PARTNERS OF THE CYTOPLASMIC TAIL OF NEPHRIN*

The 155 amino acid cytoplasmic tail of nephrin contains a number of conserved tyrosine residues which can be phosphorylated (key tyrosine residues are illustrated in Figure 1.5A and Figure 1.6). In addition to the $Fin_{major}$ mutation, a second, less frequent, mutation, $Fin_{minor}$, displays an identical clinical manifestation. The $Fin_{minor}$ mutation results in the insertion of a stop codon at position 1109, leading to the truncation of 132 amino acids from the C-terminal end of the cytoplasmic tail of nephrin. As both $Fin_{major}$ and $Fin_{minor}$ mutations produce a similar phenotype, this suggests that the 132 amino acid segment lost due to the $Fin_{minor}$ mutation from the cytoplasmic tail of nephrin, which contains all the tyrosine residues, is essential for nephrin function.

The presence of phosphorylatable tyrosine residues in the cytoplasmic tail of nephrin means that nephrin binding partners (Figure 1.6) can be broadly classified into those whose interaction with nephrin is phosphorylation-dependent and those whose interaction is phosphorylation-independent. Of the six most highly conserved tyrosine residues among human, mouse and rat nephrin, the majority can be phosphorylated by the tyrosine kinase Fyn *in vitro*, though each residue may not be phosphorylated to the same extent (Jones *et al.*, 2006; Harita *et al.*, 2009). Tyrosine phosphorylated nephrin has multiple binding partners. Fyn binds to phosphorylated nephrin (Verma *et al.*, 2003; Liu *et al.*, 2005), presumably to some of the various tyrosine residues which it can phosphorylate. Several interactions have been described which require phosphorylation of specific tyrosine residues. The p85 subunit of phosphoinositide 3-kinase (PI3K) can bind to two different phosphorylated residues, Y1114 and Y1138 (Huber *et al.*, 2003b; Zhu *et al.*, 2008; Garg *et al.*, 2010). PLC-γ binds only to phosphorylated Y1193 (Harita *et al.*, 2009), while Nck can bind to three different phosphorylated residues, Y1176, Y1193 and Y1217 (Li *et al.*, 2006; Verma *et al.*, 2006; Jones *et al.*, 2006; Blasutig *et al.*, 2008).

Other nephrin interacting partners do not require nephrin phosphorylation to bind nephrin. These include CD2AP (Shih *et al.*, 2001; Schwarz *et al.*, 2001), podocin (Li *et al.*, 2004), β-arrestin (Quack *et al.*, 2006) and Par3 (Hartleben *et al.*, 2008). However, nephrin phosphorylation does affect nephrin interactions with podocin and β-arrestin. The nephrin-podocin interaction is enhanced by nephrin phosphorylation on Y1193 (Li *et al.*, 2004; Quack *et al.*, 2006). The nephrin-β-arrestin interaction is enhanced by nephrin serine/threonine phosphorylation within binding site residues 1120-1125 (Quack *et al.*, 2011); however, the interaction is inhibited when nephrin is phosphorylated on Y1193 (Quack *et al.*, 2006).

In addition to these well characterized interactions, nephrin interactions have been reported with 14-3-3θ (Hussain *et al.*, 2009), anion exchanger 1 (Wu *et al.*, 2010), aPKCζ (Hussain *et al.*, 2009) and aPKCλ/ι (Huber *et al.*, 2009), BKCa channel $Slo1_{VEDEC}$ (Kim *et al.*, 2008), IQGAP1 (Liu *et al.*, 2005; Lehtonen *et al.*, 2005; Rigothier *et al.*, 2012), MAGI-1 (Hirabayashi *et al.*, 2005) and MAGI-2 (Lehtonen *et al.*, 2005), Par3 (Hartleben *et al.*, 2008; Hirose *et al.*, 2009), $PlexinA_1$ (Reidy *et al.*, 2013), septin-7 (Wasik *et al.*, 2012), SIRPα (Kajiho *et al.*, 2012), Trpc6 (Reiser *et al.*, 2005; Kanda *et al.*, 2011), VAMP2 (Coward *et al.*, 2007), and VEGFR2 (Veron *et al.*, 2010; Bertuccio *et al.*, 2011).

### 1.4.8 *PHOSPHO-NEPHRIN SIGNALING LINKS THE SLIT DIAPHRAGM TO THE ACTIN CYTOSKELETON*

Data from a number of *in vitro* studies has been essential to define the role of phospho-nephrin signaling pathways. Engagement of the extracellular domain of nephrin *in vitro* by application of anti-nephrin antibodies results in nephrin clustering and phosphorylation of the cytoplasmic tail of nephrin (Simons *et al.*, 2001; Lahdenpera *et al.*, 2003). Replication of this process has been achieved using a chimeric system which combines the extracellular domain of CD16 with the cytoplasmic tail of nephrin. The chimeric CD16-nephrin is clustered by treatment with anti-CD16 antibodies, which results in similar activation of signaling via the cytoplasmic tail of nephrin (Verma *et al.*, 2006; Jones *et al.*, 2006). In this way, researchers have mapped out how nephrin engagement leads to the activation of phospho-nephrin-dependent signaling.

The cytoplasmic tail of nephrin contains multiple tyrosine residues, but not all of them have been shown to have a direct role in nephrin signaling. Nephrin signaling pathways can be loosely defined based on their dependence on each of two different sets of tyrosine residues that coordinate signaling pathways either independently or in concert (as shown in Figure 1.6). The group A set of tyrosines is composed of Y1114 and Y1138/9. The group B tyrosines are Y1176, Y1193 and Y1217. Intially, nephrin phosphorylation of group A tyrosines leads to recruitment of p85/PI3K (Huber *et al.*, 2003b; Zhu *et al.*, 2008; Garg *et al.*, 2010), and phosphorylation of the group B tyrosines leads to the recruitment of Nck (Li *et al.*, 2006; Verma *et al.*, 2006; Jones *et al.*, 2006; Blasutig *et al.*, 2008; Zhu *et al.*, 2010; Venkatareddy *et al.*, 2011) and PLCy (Harita *et al.*, 2009). These direct phospho-nephrin binding partners serve as the basis for the assembly of a phospho-nephrin signaling platform through the recruitment and activation of additional proteins. Group A signaling through p85/PI3K leads to activation of Akt (Zhu *et al.*, 2008) and Rac1 (Zhu *et al.*, 2008) and the recruitment of cofilin (Zhu *et al.*, 2008; Garg *et al.*, 2010). Group B signaling through Nck brings both Pak (Zhu *et al.*, 2010; Venkatareddy *et al.*, 2011) and N-Wasp (Blasutig *et al.*, 2008) to the complex. Nck mediated recruitment of Pak then leads to the recruitment and phosphorylation of Filamin (Venkatareddy *et al.*, 2011), which can then bind Ship2 (Venkatareddy *et al.*, 2011). Together, signaling mediated by the activation of both group A and group B tyrosines indirectly leads to the recruitment (via group A signaling) and the phosphorylation (via group B signaling) of Cas (George *et al.*, 2012), which recruits Crk1/2 (George *et al.*, 2012). Group A recruitment of p85/PI3K combined with the group B mediated recruitment of Ship2 outlined above leads to the generation of PI(3,4)P2 which recruits lamellipodin (Venkatareddy *et al.*, 2011).

Engagement of nephrin results in the activation of signaling pathways governing two different actin-based processes, a general reorganization of the cytoskeleton that can produce lamellipodia like structures and the growth of actin tails or ‘comets’ at the base of individual nephrin punctae. Phospho-nephrin-dependent lamellipodium formation requires a number of signaling events. It is p85/PI3K-dependent (Zhu *et al.*, 2008; George *et al.*, 2012), and requires Akt phosphorylation (Zhu *et al.*, 2008) and Rac activation (Zhu *et al.*, 2008), Cas-mediated recruitment of Crk (George *et al.*, 2012), and the presence of lamellipodin (mediated via Pak-

Filamin-Ship2 generated PI(3,4)P2) (Venkatareddy *et al.*, 2011). Nck recruitment is not essential for lamellipodium formation (George *et al.*, 2012), though phosphorylation of the Group B tyrosines is required (George *et al.*, 2012). In a separate study, recruitment of Pak/Filamin/Ship2 was shown to be necessary for lamellipodium formation, and the initial step, the recruitment of Pak, was Nck-dependent (Venkatareddy *et al.*, 2011). The reported differences regarding the requirement of Nck in lamellipodium formation requires further investigation.

The production of actin tails at nephrin punctae is dependent on phosphorylation of the group B tyrosines. If all three tyrosines are mutated, no actin tails are formed (Jones *et al.*, 2006), but the phosphorylation of a single one of the three tyrosines is sufficient to generate actin tails (Blasutig *et al.*, 2008). It is also dependent on the recruitment of Nck (Verma *et al.*, 2006; Jones *et al.*, 2006), but recruitment of Crk is not required (George *et al.*, 2012). The dynamics of actin tail formation is affected by mutation of the group A tyrosines, which generates elongated actin structures (Garg *et al.*, 2010). This effect is likely related to the absence of p85-mediated cofilin activation when the group A tyrosines are mutated, since the knockdown of cofilin has a similar effect (Garg *et al.*, 2010). In cells with a knockdown of Ship2 or Filamin, nephrin engagement results in large actin aggregates within the cell instead of many small punctae (Venkatareddy *et al.*, 2011). Overall, the phospho-nephrin signaling platform is an important regulator of actin dynamics in the podocyte—a process that plays a key role in the development of disease as podocyte foot process effacement is highly dependent on rearrangement of the podocyte actin cytoskeleton.

### 1.4.9 *REGULATION OF NEPHRIN PHOSPHORYLATION BY KINASES AND PHOSPHATASES*

Nephrin is phosphorylated by members of the Src kinase family. In particular, Fyn can phosphorylate nephrin on multiple tyrosine residues (Liu *et al.*, 2005; Jones *et al.*, 2006; Verma *et al.*, 2006; Harita *et al.*, 2009). Although nephrin has been reported to be phosphorylated *in vitro* by other Src family kinases, including Src (Li *et al.*, 2004), Yes (Verma *et al.*, 2003), and Lyn (Lahdenpera *et al.*, 2003), phosphorylation by Fyn appears to be the most important (Verma *et al.*, 2003; Lahdenpera *et al.*, 2003; Li *et al.*, 2004; Liu *et al.*, 2005). Nephrin phosphorylation

by Fyn is also relevant *in vivo* as nephrin phosphorylation is decreased in the glomeruli of Fyn knockout mice (Verma *et al.*, 2003).

Removal of phosphate groups is catalyzed by phosphatases. Podocytes express multiple tyrosine phosphatases, including GLEEP1/PTPRO (Wharram *et al.*, 2000; Wang *et al.*, 2000a), SHP-2, PTP-PEST and PTP-1β (Reiser *et al.*, 2000b; Aoudjit *et al.*, 2011). These phosphatases may act directly on nephrin, but may also be involved indirectly through regulation of Fyn activity. Aoudjit *et al*. reported on two of these phosphatases (PTP-1β and PTP-PEST) (Aoudjit *et al.*, 2011). Using rat nephrin, they found that PTP-1β could directly dephosphorylate Y1204 and Y1228, but not Y1152—equivalent to human sites 1193, 1217 and 1138, respectively. It is interesting to note that while PTP-1β could dephosphorylate both Y1204 and Y1228, which contain YDxV motifs, Y1152 (YYSML) was not a target. Also, PTP-1β appeared to have a slightly higher affinity for Y1204 over Y1228. These differences could be a function of the variations among the motifs (YxxM compared to YDxV and YDEV verses YDQV), or they could be a reflection of natural differences among the steady state phosphorylation levels of the individual tyrosine residues. Additionally, the active site of Fyn (Y418) was found to be a substrate for PTP-PEST, therefore indirectly reducing nephrin phosphorylation.

## 1.5 THE NCK FAMILY OF ADAPTER PROTEINS

### 1.5.1 *STRUCTURAL ORGANIZATION OF NCK*

The Nck family is a class of cytoplasmic adaptor proteins; there are two family members, Nck1 (Nckα) and Nck2 (Nckβ/Grb4) which share 70% identity. Nck1 was first identified as an oncogenic factor (Li *et al.*, 1992; Meisenhelder and Hunter, 1992), while Nck2 was discovered during a screen for growth factor receptor binding proteins (Tu *et al.*, 1998; Braverman and Quilliam, 1999). Nck homologs have been identified in many of the mammalian species which have been sequenced, and a single Nck-like protein is present in *Drosophila melanogaster* (dock) (Li *et al.*, 2001) and *C. elegans* (Nck-1A/Nck-1B) (Mohamed and Chin-Sang, 2011). Nck proteins are comprised of four protein-protein interaction domains: three tandem Src Homology 3 (SH3) domains followed by a single C-terminal Src Homology 2 (SH2) domain (Figure 1.7).

### 1.5.2 *NCK PROTEINS ARE IMPORTANT FOR SIGNAL TRANSDUCTION*

Both Nck1 and Nck2 are ubiquitously expressed in nearly all mammalian tissues and appear to carry out redundant functions in the majority of cell types. The Nck family has been implicated in a variety of diverse functions primarily in connection with the actin cytoskeleton (Buday *et al.*, 2002; Lettau *et al.*, 2009; Chaki and Rivera, 2013), including cell migration and axon guidance (Fawcett *et al.*, 2007; Guan *et al.*, 2007), the modulation of protein translation (Kebache *et al.*, 2002), and acting as a component of the DNA damage response (Kremer *et al.*, 2007). These functions are mediated through the many binding partners which associate with its SH3 and SH2 domains. In most cases, phosphorylation of receptors leads to Nck recruitment through its SH2 domain, which in turn leads to recruitment of actin regulators through the SH3 domains of Nck.

### 1.5.3 *NCK SH2 DOMAIN BINDING PARTNERS*

The SH2 domain binds to phosphorylated tyrosine motifs, and there have been over 100 different SH2 domain-containing proteins identified in the human proteome (Huang et al., 2007). Given the wide variety of SH2 domain-containing proteins, crystal structures of SH2 domains have revealed that point mutation of a key arginine residue in the binding pocket to lysine abolishes its ability to bind phosphotyrosine motifs (Mayer *et al.*, 1992). There have been several studies that have sought to identify the target sequences of individual SH2 domains to characterize their differences in specificity (Frese *et al.*, 2006; Wavreille *et al.*, 2007). These works have identified the consensus sequence of pYDxV as being recognized by the binding site of the SH2 domains of Nck1 and Nck2.

Nck SH2 domains can bind to phosphotyrosine motifs on at least ten different proteins (Lettau *et al.*, 2009). Examples of binding partners include activated growth factor receptors such as platelet derived growth factor β receptor (PDGFR) and vascular endothelial growth factor receptor 2 (VEGFR-2) which have been shown to recruit Nck to the plasma membrane

(Lamalice *et al.*, 2006; Rivera *et al.*, 2006). It also may bind to Ephrin receptors in the brain, where it is involved in proper migration of neuronal cells (Fawcett *et al.*, 2007). It also binds to a phosphotyrosine motif on the Tir protein which is inserted into cells by the vaccinia virus, where it serves to recruit actin polymerizing proteins (Gruenheid *et al.*, 2001).

### 1.5.4 *NCK SH3 DOMAIN BINDING PARTNERS*

SH3 domains mediate binding to PxxP (where x is any amino acid) motifs on target proteins. A well-known example of this type of interaction includes the binding of the SH3 domain of Grb2 to a proline-rich region of the Ras activating protein Son of sevenless (Sos) (Downward, 1994). Understanding of the binding groove of the SH3 domain has identified a conserved tryptophan residue which, when mutated to lysine, abolishes PxxP binding ability (Yu *et al.*, 1992).

Nck1 and Nck2 have been shown to bind some 30 different proline-rich proteins (Lettau *et al.*, 2009). These include many involved in regulation of the actin cytoskeleton, such as p21 activated kinase (Pak) and neural Wiskott-Aldrich Syndrome protein (N-WASp) (Buday *et al.*, 2002). Nck recruits Pak for activation by the GTPase Rac to plasma membrane sites of signaling from VEGFR-2 (Lamalice *et al.*, 2006) and PDGFR (Chen *et al.*, 2000; Rivera *et al.*, 2006). Nck is recruited through its SH2 domain to phosphorylated SLP-76 in activated T cells (Zeng *et al.*, 2003), allowing the SH3 domains of Nck to bring N-WASp to the complex where it can be activated by the Rho family GTPase CDC42. Activated N-WASp initiates the formation of new branched actin filaments through the Arp2/3 complex (Pollard and Borisy, 2003).

As Nck proteins contain three SH3 domains, scientists have attempted to determine if all three copies of the domain are required for substrate binding (Liu *et al.*, 2006). There has been a clearly observed cooperative effect in binding, with the interaction strongest in the presence of all three SH3 domains, though some substrates may show a preference for either the middle SH3 domain (N-WASp and Pak), or the first or third SH3 domains (Li *et al.*, 2001).

In addition to canonical PxxP motifs, recent analysis using peptide arrays has suggested that SH3 domains can possibly bind to non-canonical sequences including RxxP and RxxK based motifs (Jia *et al.*, 2005; Hake *et al.*, 2008). Also, while SH3 domain interactions tend to require higher levels of energy to disassociate, it appears that weaker interactions such as the one recently identified between the second SH3 domain of Nck with epidermal growth factor receptor (EGFR) can still be functionally relevant (Hake *et al.*, 2008).

### 1.5.5 *Redundancy between Nck1 and Nck2*

Mice with a single knockout of either Nck1 or Nck2 are viable (Bladt *et al.*, 2003). However, compound homozygous Nck1/2 null mice die at embryonic day 9.5 due to defects in cell migration (Bladt *et al.*, 2003).

### 1.5.6 *Non-compensatory roles of Nck1 and Nck2*

Though there is high homology between the two family members, there appears to be some binding specificity between the SH3 domains of Nck1 and Nck2. For instance, only Nck2 has been observed to bind to the integrin linked protein PINCH (Tu *et al.*, 1998), and was recently implicated in neuronal differentiation through binding to the actin binding protein paxillin (Guan *et al.*, 2007).

### 1.5.7 *Loss of Nck in the podocyte results in foot process effacement*

The podocyte foot process structure requires a specialized actin network to maintain its shape. As the Nck family can recruit N-WASp (Benesch *et al.*, 2002), which activates the Arp2/3 actin nucleating family, and the cytoplasmic tail of nephrin contains conserved Nck binding sites, Nck was hypothesized to link nephrin at the slit diaphragm to the internal actin cytoskeleton of podocyte foot processes (Lahdenpera *et al.*, 2003). In support of this hypothesis, podocyte specific Nck knockout mice presented with proteinuria at birth, and they had an abnormal podocyte morphology and slit diaphragm structures were absent (Jones *et al.*, 2006),

similar to the phenotype of nephrin knockout mice (Putaala *et al.*, 2001). In addition, a separate study detected an interaction between nephrin and Nck in wildtype mouse glomeruli (Verma *et al.*, 2006); this interaction was disrupted in Fyn knockout mice (Verma *et al.*, 2006), which have reduced levels of nephrin phosphorylation and altered podocyte foot process architecture (Verma *et al.*, 2003).

These results strongly implicate nephrin-Nck interactions as an important regulator of Nck-mediated actin dynamics in the podocyte. Nonetheless, as Nck has the potential to interact with additional binding partners in the podocyte, further evidence is required to demonstrate that the phenotype of podocyte-specific Nck knockout mice is a direct consequence of the disruption of nephrin-Nck signaling. Indeed, as suggested by Benzing, we "lack direct proof that Nck proteins exclusively act through the nephrin/slit diaphragm axis *in vivo*. In fact, this has to be addressed in future studies, for instance using knock-in mouse models of nephrin with mutated tyrosine residues." (Benzing, 2009, p. 1426).

## 1.6 PODOCYTE-BASED HUMAN KIDNEY DISEASES AND ASSOCIATED ANIMAL MODELS

There are many different forms of kidney disease in humans. This section describes three common types of glomerular-based kidney disease which are caused by podocyte damage: membranous nephropathy, focal segmental glomerulosclerosis and minimal change disease. It also describes models of podocyte injury using mice and rats which have been studied by investigators in attempts to model those diseases. More recently, genetic approaches have implicated a number of genes in the pathology of kidney disease (Weins and Pollak, 2008); given the diverse nature of those studies, significant coverage of genetic models is beyond the scope of this thesis.

### 1.6.1 *MEMBRANOUS NEPHROPATHY (MN)*

Historically, membranous nephropathy has been characterized as an auto-immune mediated glomerular disease occurring in the absence of other known conditions affecting the immune

system such as lupus erythematosus or drug treatments. In primary membranous nephropathy, circulating auto antibodies (usually of the IgG4 type) bind to a target antigen expressed by podocytes, leading to the deposition of immune complexes in the sub-epithelial region of the GBM (Glassock, 2012). Immune complex accumulation provokes complement activation and podocyte injury. Secondary membranous nephropathy can arise as a consequence of increased circulating immune complexes in response to many different diseases which affect the immune system, and these complexes can be deposited or trapped in the GBM as in primary membranous nephropathy (Glassock, 2012).

Excitingly, recent genetically based studies in humans have finally identified the underlying antigen expressed by human podocytes which appears responsible for most cases of primary membranous nephropathy (Glassock, 2012). The M-type phospholipase A2 receptor (PLA2R), a membrane protein expressed by podocytes, appears to be responsible for over 80% of cases of primary membranous nephropathy (Beck *et al.*, 2009). In addition to PLA2R variants, the disease response is also dependent on polymorphisms at the *HLA-DQA1* locus, which affects antigen-presenting cells (Stanescu *et al.*, 2011). The exact circumstances provoking immune responses and the development of membranous nephropathy are the subject of ongoing investigation (Coenen *et al.*, 2013).

The most common animal model of membranous nephropathy is the passive Heymann nephritis model (PHN) in the rat. The passive Heymann nephritis model was pioneered by Heymann and colleagues as a method to induce membranous nephropathy similar to the human disease by immunizing rats with injections of crude kidney extracts in Freund's adjuvant (Heymann *et al.*, 1959). Characterization of passive Heymann nephritis has revealed that auto-antibodies against intrinsic podocyte antigens (generated after injection) circulate in the blood and bind to target antigens on podocytes (Couser *et al.*, 1978). Immune complex accumulation occurs within the subepithelial region of the GBM below podocyte foot processes (Kerjaschki *et al.*, 1989); this is followed by complement activation and podocyte injury (Couser *et al.*, 1992). The target antigen responsible for passive Heymann nephritis in rats is the glycoprotein Megalin 330 (Farquhar *et al.*, 1995), while in humans it is primarily the phospholipase A2 receptor

(PLA2R) (Beck *et al.*, 2009). Despite the difference in antigens, symptoms of the disease in both species are similar (Glassock, 2012).

### 1.6.2 *FOCAL SEGMENTAL GLOMERULOSCLEROSIS (FSGS)*

FSGS represents a form of glomerular damage that can result from a number of diverse causes. FSGS affects some, but not all, glomeruli. In addition, FSGS lesions are seen in only a portion of each individual glomerulus, with the remainder of the glomerulus unaffected. Lesions can be classified into five different types based on the area of the glomerulus where damage occurs: collapsing, tip lesion, perihilar, cellular, and not otherwise specified (NOS) (D'Agati *et al.*, 2004). In all cases, lesions result in scarring due to fibrosis from excessive production of collagen and other extracellular matrix components, destroying capillary loops. Mutations, including some that are autosomal dominant, in a very diverse set of podocyte proteins and pathways, including integrin signaling, have been linked to the development of FSGS, underscoring the many routes which can lead to this type of glomerular damage (Cho and Kopp, 2008; D'Agati, 2012).

The most common animal model of FSGS is the Adriamycin model, which was historically performed in rats, athough it can also be successfully performed in mice (Pippin *et al.*, 2009). In addition, there are a number of genetic models of FSGS; in-depth coverage of the genetics of FSGS can be found elsewhere (Cho and Kopp, 2008). The Adriamycin (also called Doxorubicin) rat model produces FSGS like lesions; animals develop proteinuria after ~10 days with foot process effacement and eventual development of glomerulosclerosis (Bertani *et al.*, 1982; Pippin *et al.*, 2009). The adriamycin model has also been characterized in mice, however, it is highly strain dependent—BALB/c mice develop the disease, whereas C57Bl/6 mice are resitant (Wang *et al.*, 2000b; Zheng *et al.*, 2005). Adriamycin induces DNA damage; the genetic locus that confers susceptibility to the BALB/c mouse strain (Zheng *et al.*, 2005; Zheng *et al.*, 2006) has recently been identified as a mutation in *Prkdc*, which is involved in repair of DNA strand breaks (Papeta *et al.*, 2010).

### 1.6.3 *MINIMAL CHANGE DISEASE (MCD)*

Minimal change disease is a common cause of renal disease in children (Dember and Salant, 2008; McGrogan *et al.*, 2011). When examined by light microscopy, biopsies from patients show a distinct lack of glomerular lesions, however, transmission electron microscopy reveals extensive podocyte foot process effacement. The disease can be broadly classified into two subtypes: steroid-sensitive disease and steroid-resistant disease. Patients with steroid-sensitive disease respond to treatment with glucocorticoid drugs. In contrast, many cases of steroid-resistant disease are inherited and are commonly caused by mutations in *NPHS2,* the gene for podocin (Johnstone and Holzman, 2006).

Commonly accepted animal models of minimal change disease include the puromycin aminonucloside (PAN) model in rats and the lipopolysacchride (LPS) model in mice (Pippin *et al.*, 2009; Chugh *et al.*, 2012), with some support for the sheep anti-rat nephrotoxic serum model in mice (Pippin *et al.*, 2009; Chugh *et al.*, 2012). The PAN model has many of the characteristics of human minimal change disease. Treatment of rats with puromycin aminonucloside (PAN) impairs ribosomal functions which lead to a spontaneously resolving disease course lasting roughly 4 weeks. Proteinuria becomes evident starting around 3-5 days post injection, peaking at 12-14 days and returning to baseline by 28 days. While PAN has been used almost exclusively in rats, efforts to establish this model in mice in recent years have met with varying degrees of success (Pippin *et al.*, 2009).

### 1.6.4 *ANIMAL MODELS OF RAPID FOOT PROCESS EFFACEMENT*

The most common model of rapid (under 60 minutes) foot process effacement is the protamine sulfate model, though the 27A antibody injection model has also been used (Simons *et al.*, 2001). The outside surface of the podocyte is highly negatively charged (Pavenstadt *et al.*, 2003); while attempting to manipulate these charges, researchers observed that perfusion of positively charged molecules such as protamine sulfate into rat kidneys led to the rapid onset (under 30 minutes) of significant alterations to podocyte foot process architecture (Seiler *et al.*, 1975). Interestingly, the effaced foot processes were restored to their normal shape with a

subsequent perfusion of heparin sulfate which neutralizes the protamine sulfate. The protamine sulfate model has been used to attempt to understand the signaling pathways which are triggered during foot process effacement. Although it was once considered to partially model minimal change disease, this belief is no longer held (Pippin *et al.*, 2009; Chugh *et al.*, 2012).

## 1.7 NEPHRIN PHOSPHORYLATION IN PODOCYTE-BASED KIDNEY DISEASES

### 1.7.1 *NEPHRIN PHOSPHORYLATION IN THE HEALTHY KIDNEY*

Total phosphorylation of nephrin has been examined in an *in vivo* context using anti-phospho-tyrosine antibodies. These studies have established the presence of nephrin tyrosine in the normal adult mouse (Verma *et al.*, 2003) and rat (Jones *et al.*, 2006; Li *et al.*, 2006; Zhu *et al.*, 2008; Zhu *et al.*, 2010; Zhang *et al.*, 2010b) glomerulus. In addition, multiple groups have developed phospho-specific nephrin antibodies recognizing the individual tyrosine residues Y1176/Y1193 (Verma *et al.*, 2006), Y1193 (Uchida *et al.*, 2008; Jones *et al.*, 2009; Harita *et al.*, 2009) and Y1217 (Uchida *et al.*, 2008; Jones *et al.*, 2009). With these reagents, nephrin phosphorylation can be detected in the normal glomerulus on Y1176/Y1193 (Verma *et al.*, 2006; Zhang *et al.*, 2010a), Y1193 (Uchida *et al.*, 2008; Jones *et al.*, 2009) and Y1217 (Uchida *et al.*, 2008; Jones *et al.*, 2009; Ohashi *et al.*, 2010). Both Y1193 and Y1217 are conserved between human, mouse and rat nephrin and phosphorylation of Y1217 (or the equivalent) has been observed in all three species (Uchida *et al.*, 2008; Jones *et al.*, 2009). Phosphorylation of Y1193 has been reported in both mice (Jones *et al.*, 2009; Zhang *et al.*, 2010a) and in rats—by antibody (Uchida *et al.*, 2008; Jones *et al.*, 2009) and also by mass spectrometry (Zhu *et al.*, 2010). However, two separate groups who generated antibodies to both Y1193 and Y1217 found that their Y1193 antibodies were less sensitive than their Y1217 antibodies (Uchida *et al.*, 2008; Jones *et al.*, 2009). This suggests that there could be a difference in basal phosphorylation levels on individual tyrosines, however it is not possible to draw any conclusions as it is likely that any differences also reflect the differences in sensitivity between the two antibodies making it impossible to accurately gauge the degree of phosphorylation between the two sites using antibodies alone.

### 1.7.2 *NEPHRIN PHOSPHORYLATION IN MN AND ASSOCIATED MODELS*

Total nephrin phosphorylation was shown to be increased in PHN rats on day 14 (Li *et al.*, 2004). In contrast, an investigation into nephrin phosphorylation in the biopsies of MN patients using a phospho-Y1217 antibody found that there was no change in nephrin phosphorylation status in the early stages of the diseases, though it decreased in later stages (Ohashi *et al.*, 2010). This difference may indicate a discrepancy between human MN and the PHN model. Recently, increased expression of the protein c-mip—a factor expressed in the glomeruli of MCD patients that was subsequently shown to negatively regulate nephrin phosphorylation (Zhang *et al.*, 2010a) —was also detected in patients with MN and shown to be upregulated in PHN rats after the onset of proteinuria (Sendeyo *et al.*, 2013).

### 1.7.3 *NEPHRIN PHOSPHORYLATION IN FSGS AND ASSOCIATED MODELS*

No studies have directly examined nephrin phosphorylation in patients with FSGS. In the rat ADR model, a study found that nephrin phosphorylation was decreased at the onset of proteinuria (Fan *et al.*, 2009). They also observed that treatment of the rats with either ACE inhibitors or glucocorticoids reduced proteinuria and increased nephrin phosphorylation (Fan *et al.*, 2009).

### 1.7.4 *NEPHRIN PHOSPHORYLATION IN MCD AND ASSOCIATED MODELS*

There is some evidence suggesting that nephrin phosphorylation is reduced in minimal change disease. This phenomenon was initially reported by Uchida et al. who generated a phospho-Y1217 antibody, which they used on glomeruli from control patients and patients with minimal change disease (Uchida *et al.*, 2008). They found that phospho-nephrin was present in the glomeruli of control patients, and that the levels were strongly decreased in patients with minimal change disease (Uchida *et al.*, 2008).

In agreement with clinical data, several reports over the past few years have also demonstrated a decrease in nephrin phosphorylation in the rat PAN model of MCD. In the PAN model, proteinuria peaks at roughly day 7 and returns to baseline by day 28 (Pippin *et al.*, 2009). Decreased total tyrosine phosphorylation of nephrin has been reported at day 7 when significant proteinuria was also observed (Zhu *et al.*, 2008). Decreased phosphorylation on Y1193 and Y1217 on day 7 and day 14 has been shown using phospho-specific antibodies (Uchida *et al.*, 2008). A third study also reported decreased nephrin phosphorylation on Y1217 on day 4, day 7 and day 14 (Jones *et al.*, 2009).

Nephrin phosphorylation is also decreased in the LPS model. Using a phospho-Y1176/Y1193 nephrin antibody, decreased nephrin phosphorylation was reported 24 hours after LPS injection which is the timepoint when maximal proteinuria is observed, and also coincides with increased expression of c-mip, a protein which negatively regulates Fyn activity (Zhang *et al.*, 2010a). The authors were able to show that the decrease in nephrin phosphorylation was mediated by the increase in c-mip expression, as treatment of their animals with siRNA against c-mip prior to LPS treatment both reduced proteinuria and restored nephrin phosphorylation (Zhang *et al.*, 2010a).

### 1.7.5 *NEPHRIN PHOSPHORYLATION IN MODELS OF RAPID FOOT PROCESS EFFACEMENT*

Increased nephrin phosphorylation has been reported in the 27A antibody model, and it was accompanied by apical translocation of nephrin (Simons *et al.*, 2001). Using the protamine sulfate model and their phospho-Y1176/Y1193 nephrin antibody, Verma *et al*. reported minimal nephrin phosphorylation in control mice, but found that there was increased nephrin phosphorylation following protamine sulfate treatment to induce foot process effacement that returned to baseline when protamine sulfate treatment was followed by heparin sulfate treatment which enables the reestablishment of foot process architecture. A different group independently generated a phospho-specific antibody against Y1193 and found that protamine sulfate treatment significantly increased nephrin phosphorylation on Y1193 in rats (Harita *et al.*, 2009). The increase in nephrin phosphorylation in the protamine sulfate model differs from what is observed

in human diseases such as minimal change disease; however, the reasons behind this difference are unknown.

### 1.7.6 *REGULATION OF NEPHRIN PHOSPHORYLATION AND DISEASE*

There have been a number of recent reports which have linked changes in nephrin phosphorylation to the development of disease, in both human disease as well as animal models that develop some form of nephrotic syndrome. These observations can be broadly classified into two categories, correlations between decreased levels of nephrin phosphorylation and disease, such as the onset proteinuria discussed in the previous section (Zhu *et al.*, 2008; Uchida *et al.*, 2008; Fan *et al.*, 2009; Jones *et al.*, 2009; Ohashi *et al.*, 2010) and changes in other podocyte proteins which somehow directly or indirectly modulate nephrin phosphorylation, discussed in this section (Verma *et al.*, 2003; Shimizu *et al.*, 2009; Zhang *et al.*, 2010a).

The carbohydrate binding lectin galectin-1 interacts with the extracellular domain of nephrin (likely via binding of galectin-1 to galactose sugars incorporated in nephrin at N-glycosylation sites) and this interaction results in increased nephrin phosphorylation *in vitro* (Shimizu *et al.*, 2009). Expression of galectin-1 is decreased in patients with MCD and also in the PAN model, which, when combined with the in vitro binding data, suggests that the decreased galectin-1 expression in MCD should result in decreased nephrin phosphorylation as well, though the effect of decreased galectin-1 on nephrin phosphorylation in vivo was not examined (Shimizu *et al.*, 2009).

In support of Fyn being the primary kinase that phosphorylates nephrin, Fyn knockout mice have reduced nephrin phosphorylation, and they also develop proteinuria and foot process effacement (Verma *et al.*, 2003). Interestingly, mice lacking the related SFK Yes have increased nephrin phosphorylation, but they do not show a podocyte phenotype (Verma *et al.*, 2003). However, double Fyn/Yes knockout mice have reduced nephrin phosphorylation and a slightly stronger phenotype than Fyn knockout mice (Verma *et al.*, 2003). Expression of the phosphatase PTP1β, which can dephosphorylate nephrin, is upregulated in PAN treated rats on day 7 and day 14 (Aoudjit *et al.*, 2011). Expression of the phosphatase PTP-PEST, which de-phosphorylates

Fyn on the regulatory tyrosine in its kinase domain (Y416) thus decreasing Fyn activity, is also upregulated on day 14 of the PAN model (Aoudjit *et al.*, 2011).

Increased expression in disease of two additional proteins that negatively regulate Fyn activity has also been described. The protein c-mip, originally identified in a screen for proteins upregulated in T cells of patients with MCD (Grimbert *et al.*, 2003) was also found to be upregulated in the podocytes of patients with MCD (Audard *et al.*, 2010). To characterize the biological function of c-mip, a transgenic mouse was generated which over-expresses c-mip in podocytes to model what is observed in human MCD (Zhang *et al.*, 2010a). In c-mip transgenic mice, c-mip interacted with Fyn, and this was correlated with decreased Fyn activity and nephrin phosphorylation in vivo, suggesting that this mechanism could also be occurring during human MCD.

Expression of the claudin family protein TM4SF10 occurs in a temporally restricted developmental window in podocytes (Bruggeman *et al.*, 2007). TM4SF10 interacts with ADAP (also known as Fyb) and the expression of TM4SF10 blocks Fyn mediated process formation in MDCK cells (Azhibekov *et al.*, 2011). This is likely because TM4SF10-ADAP interaction results in decreased Fyn kinase activity; the interaction also decreases levels of phosphorylated nephrin *in vitro* (Azhibekov *et al.*, 2011). In addition, TM4SF10 expression is upregulated on day 10 of the PAN model, suggesting that TM4SF10 expression could form a link connecting changes in nephrin phosphorylation with altered actin dynamics in the podocyte during disease (Azhibekov *et al.*, 2011).

### 1.7.7 *ALTERED NEPHRIN SIGNALING IN KIDNEY DISEASE*

As described in the previous section, notable changes in nephrin phosphorylation are associated with certain kinds of podocyte-based diseases. Importantly, these changes likely have functional consequences within the podocyte as recent evidence has shown that many of the phospho-nephrin based signaling pathways characterized *in vitro* are altered in those podocyte-based diseases *in vivo.* In the PAN model, both phospho-nephrin interactions mediated by group A tyrosines to p85/PI3K (Zhu *et al.*, 2008) and group B tyrosines to Nck (Li *et al.*, 2006) are

reduced; this has a demonstrated effect on downstream signaling, as phosphorylation of Akt (Zhu *et al.*, 2008) and Pak (Zhu *et al.*, 2010) are also decreased. Similarly, LPS treatment also results in decreased Akt signaling (Zhang *et al.*, 2010a). In human minimal change disease, there is decreased Akt activation (Zhang *et al.*, 2010a) and cofilin activity (Ashworth *et al.*, 2010). C-mip expression is upregulated in minimal change disease, and c-mip transgenic mice, which have podocyte-specific over expression of c-mip to mimic minimal change disease, also have decreased Akt activation (Zhang *et al.*, 2010a).

Fyn knockout mice have reduced nephrin phosphorylation (Verma *et al.*, 2003) and this disrupts nephrin-Nck interactions (Verma *et al.*, 2006). Reduced Fyn activity is found in c-mip transgenic mice, which have a notable decrease in nephrin-Nck interactions as a result (Zhang *et al.*, 2010a). Garg *et al*. reported upregulated nephrin-Nck interactions following PAN treatment compared to control animals (Garg *et al.*, 2007). However, this disagrees with the work of others showing that PAN decreases nephrin phosphorylation and disrupts nephrin-Nck interactions (Li *et al.*, 2006; Uchida *et al.*, 2008; Jones *et al.*, 2009).

### 1.7.8 *EMERGING ROLE OF NEPHRIN PHOSPHORYLATION IN KIDNEY DISEASE*

The function of nephrin tyrosine phosphorylation has been the subject of active debate in the literature (Patrakka and Tryggvason, 2007) and there have been conflicting reports about the importance of nephrin phosphorylation in the mature podocyte, as well as whether nephrin phosphorylation plays a positive or negative role in the processes of podocyte effacement and recovery. A number of studies have examined the dynamics of nephrin phosphorylation in a variety of conditions involving both human kidney diseases and related animal disease models. As a whole, these studies have established that kidney disease leads to alterations in nephrin phosphorylation, however it has not been possible to determine if the changes in nephrin phosphorylation contribute to the development of disease as a direct result of altered nephrin signaling or if they simply occur after the disease has developed as a consequence of changes in other signaling pathways.

Despite differing theories, our inability to directly block the phosphorylation of a specific nephrin tyrosine residue means that there has been no way to date to resolve this significant question of whether nephrin phosphorylation is essential for podocyte functions *in vivo*.

## 1.8 RATIONALE, HYPOTHESES, RESEARCH QUESTION AND OBJECTIVES

Evidence from podocyte-specific Nck knockout mice (Jones *et al.*, 2006; Jones *et al.*, 2009) has established a role for Nck in the podocyte; however, this work does not directly implicate a particular Nck binding partner in this process. The importance of Nck in the podocyte, combined with the evidence that the SH2 domain of Nck can interact with three YDxV based motifs in the cytoplasmic tail of nephrin led to the following hypothesis: *Nck signaling in the podocyte is mediated through phosphorylated nephrin*.

At the same time, evidence from other research groups suggested that levels of nephrin phosphorylation could be decreased in human patients with some forms of human kidney disease (Uchida *et al.*, 2008). This information, when combined with our initial hypothesis, led us to refine our hypothesis as follows: *Removal of the YDxV motifs from nephrin* in vivo *will result in the loss of Nck signaling within the podocyte and therefore to the collapse of the podocyte actin cytoskeleton as observed in podocyte-specific Nck knockout mice*.

Consideration of these hypotheses led me to formulate the following research question for my doctoral thesis: ***What is the significance of nephrin tyrosine phosphorylation and associated signaling within the podocyte?***

Given that little is known about the function of nephrin phosphorylation or how it is regulated, I have taken several approaches to explore this question. I chose to focus on three main objectives within this thesis:

1. Generation of phospho-nephrin antibodies and characterization of nephrin phosphorylation *in vivo*

2. Investigation of signaling pathways that regulate nephrin phosphorylation

3. Generation of a mouse model expressing mutant nephrin lacking key Nck binding tyrosine residues to investigate the function of nephrin phosphorylation *in vivo*

## 1.9 THESIS ORGANIZATION

In this thesis, I begin with a short chapter briefly describing the development of phospho-specific nephrin antibodies and their use to demonstrate nephrin phosphorylation in the adult kidney (Chapter 2). The reagents developed therein are used in subsequent chapters. I then continue with a description of the role I uncovered for the SH3 domains of Nck in the recruitment of the kinase Fyn, which phosphorylates nephrin, generating a positive feedback loop where binding of Nck to phosphorylated nephrin actively maintains nephrin phosphorylation (Chapter 3). Finally, I outline the characterization of the nephrin$^{Y3F/Y3F}$ mouse (Chapter 4), and find that, although lack of nephrin phosphorylation does not impede podocyte foot process development, nephrin phosphorylation does play an important role in the maintenance of foot process structures, demonstrating unequivocally that phosphorylation is required for proper nephrin function. I conclude with a discussion and suggestions for future research (Chapter 5).

## 1.10 ATTRIBUTIONS

Chapter 1

Some of the material in Chapter 1 was adapted from an unpublished 2011 review article entitled “Nephrin expression and tyrosine phosphorylation in human glomerular diseases and associated experimental models”, written by myself, Kelly Keithlin and Colin Stringer and edited by Nina Jones.

Chapter 2

Chapter 2 is adapted from the following article published in 2009:

Jones N, **New LA**, Fortino MA, Eremina V, Ruston J, Blasutig IM, Aoudjit L, Zou Y, Liu X, Yu GL, Takano T, Quaggin SE, Pawson T. (2009) Essential role of Nck proteins in the adult kidney filtration barrier. *Journal of the American Society of Nephrology*. 20:1533-43.

I designed and conducted some of the experiments and prepared Figure 2.1C and Figure 2.2A.

Megan Fortino assisted with antibody testing and preparation of Figure 2.1B. Antibody purification was performed by Epitomics Inc. The experiments shown in Figure 2.2B and Figure 2.2C were designed and performed in the laboratory of Dr. Tomoko Takano. Nina Jones oversaw all experiments and wrote the manuscript and prepared Figure 2.1A.

Chapter 3

Chapter 3 was published as an article in 2013:

**New, LA**, Keyvani-Chahi, A, Jones, N. (2013) Direct regulation of nephrin tyrosine phosphorylation by Nck adaptor proteins. *Journal of Biological Chemistry*. 288:1500-10

I designed and conducted experiments, prepared all figures and wrote and edited the manuscript.

Ava Keyvani-Chahi conducted experiments for Figure 3.5B, Figure 3.6A and Figure 3.6C and edited the manuscript. Mackenzie Smith performed the experiments shown in Figure 3.7B. Melanie Wills produced the illustration in Figure 3.8. Nina Jones designed experiments and revised and edited the manuscript.

Chapter 4

Chapter 4 has been submitted for publication as:

**New LA**, Scott RP, Stringer CDM, Samborska B, Platt MJ, Eremina V, Simpson JA, Quaggin SE, Jones N. (2013) Nephrin tyrosine phosphorylation is required for maintenance of podocyte foot process architecture and response to injury. (Submitted October 2013 to the *Journal of Clinical Investigation*)

I designed and conducted experiments, collected urine samples, performed the ACR assay, prepared the graphs, figures and tables, performed the statistical analyses, prepared and imaged SEM samples and wrote and edited the manuscript.

The staff at the University of Connecticut Health Center Gene Targeting and Transgenic Facility generated and inserted the construct to produce nephrin$^{Y3F/Y3F}$ mice. Megan Fortino produced Figure 4.1B. Martha Manning routinely collected urine samples from all mice, with occasional assistance from myself, Colin Stringer and Bozena Samborska. Martha Manning also performed the LPS injections and collected urine during the LPS experiments. Bozena Samborska performed the RNA isolation and ran the qPCR experiments, assisted with urine collection during the LPS experiments and ran the BCA assay and helped genotype animals. Colin Stringer performed all of the immunofluorescence, glomerular isolation and western blotting and helped genotype animals.

Rizaldy Scott took SEM, TEM and PAS images from the majority of samples. PAS samples were processed by the Pathology Core facility at the Toronto Centre for Phenogenomics. All TEM and most SEM samples were processed at the Advanced Bioimaging Centre in Toronto. Doug Holymard imaged some SEM and TEM samples. Vera Eremina and Sandy Smith also assisted with sample processing and imaging. Matt Platt and Jeremy Simpson collected all blood pressure data and weights of corresponding animals. Nina Jones designed experiments and edited the manuscript.

Chapter 5

Some of the material in Chapter 5 was adapted from my written contributions towards Nina Jones' 2013 Kidney Foundation of Canada grant application.

**Figure 1.1 The glomerulus.**

(A) Illustration of a cross-section through a simplified glomerulus (not to scale). Blood enters the glomerulus through the afferent arteriole and exits the glomerulus through the efferent arteriole. The glomerulus is surrounded by Bowman's capsule. Fenestrated endothelial cells (red) line each capillary. The foot processes of podocyte cells (blue) are found on the outside of the capillary, with the GBM (green) between them. The capillaries are held in place by the mesangium (yellow). Adapted from (Quaggin and Kreidberg, 2008). (B) PAS stained section of a glomerulus. Pink colour indicates extracellular matrix, purple colour indicates nuclei. All of the cell types shown in A can be observed in the higher magnification image (right). Scale bar = 50 µm. C. TEM image of a segment of a glomerular capillary labeled as in A and B. Red blood cells are visible inside of capillaries. Individual podocyte foot processes are almost visible. Scale bar = 5 µm.

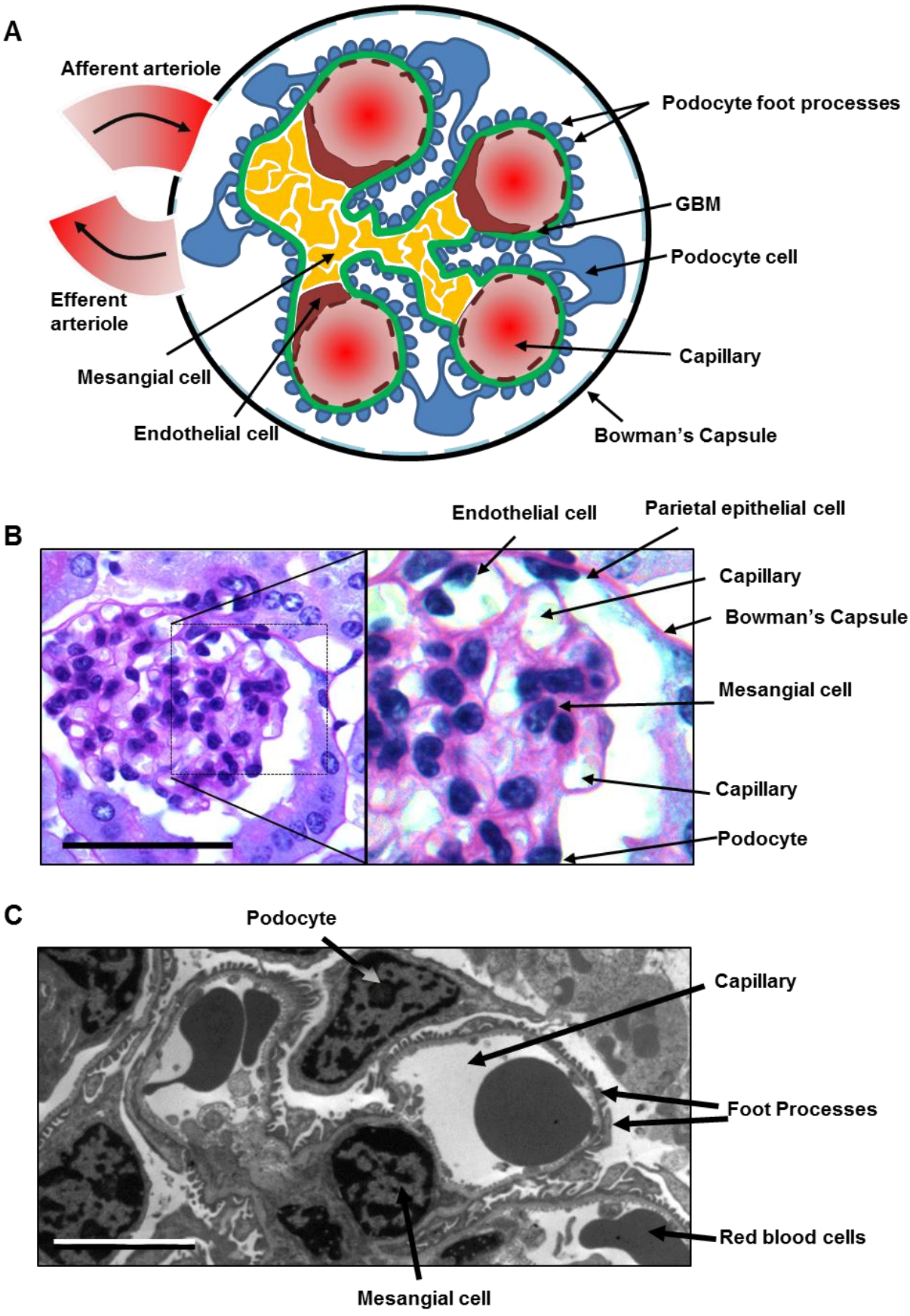
A
Afferent arteriole
Podocyte foot processes
GBM
Podocyte cell
Efferent arteriole
Capillary
Mesangial cell
Endothelial cell
Bowman's Capsule
B
Endothelial cell
Parietal epithelial cell
Capillary
Bowman's Capsule
Mesangial cell
Capillary
Podocyte
C
Podocyte
Capillary
Foot Processes
Red blood cells
Mesangial cell

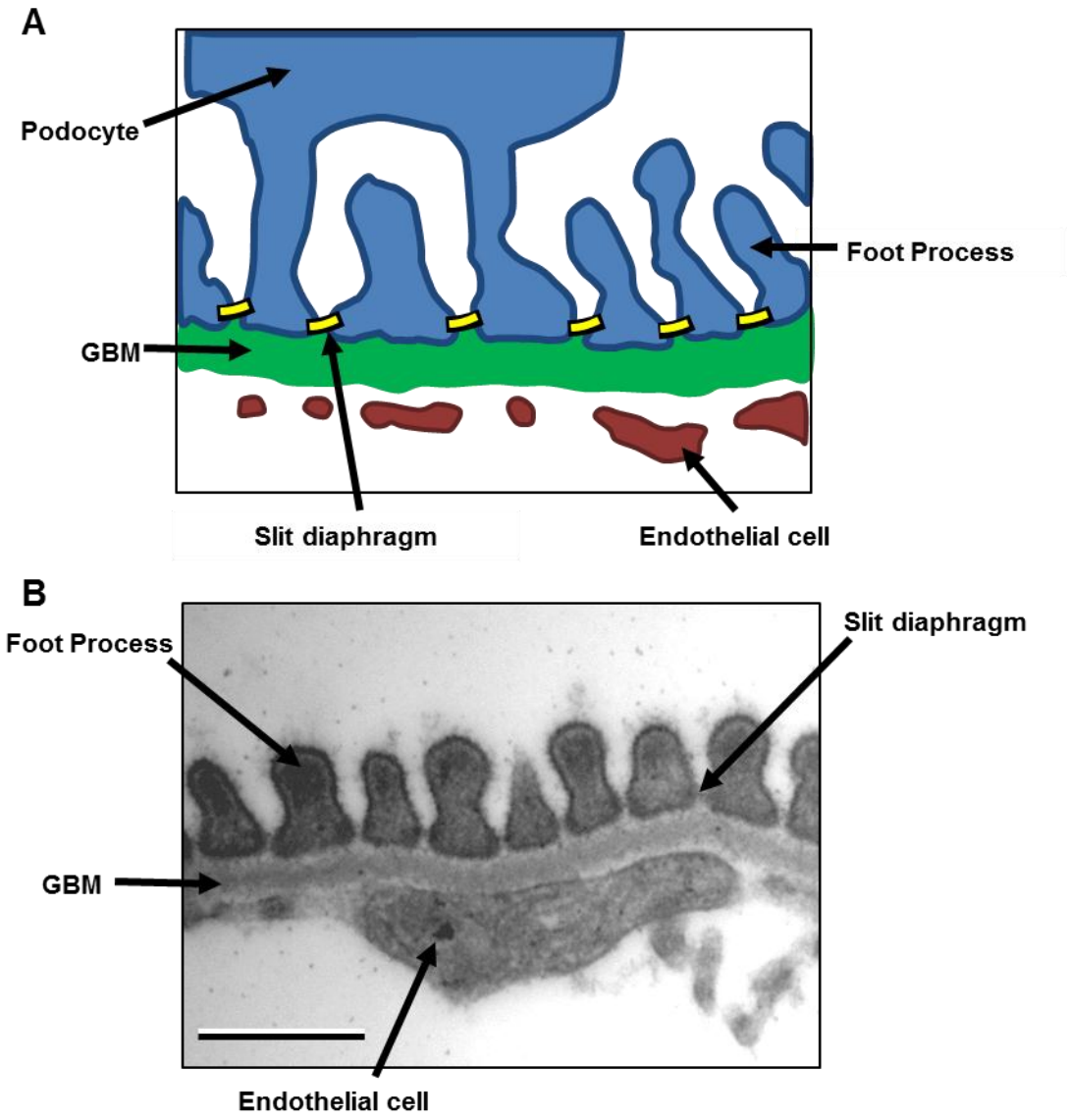


**Figure 1.2 The glomerular filtration barrier.**

(A) Illustration of segment of a glomerular capillary loop. Interdigitating foot processes line the outside of the capillary. The slit diaphragm junction is formed between neighbouring foot processes. Podocytes are attached to the glomerular basement membrane (GBM). On the inner surface, fenestrated endothelial cells are attached to the GBM. (B) TEM image of a segment of a glomerular capillary labeled as in A. The slit diaphragm is visible as an electron dense (dark) line connecting adjacent foot processes. Scale bar = 500 nm.

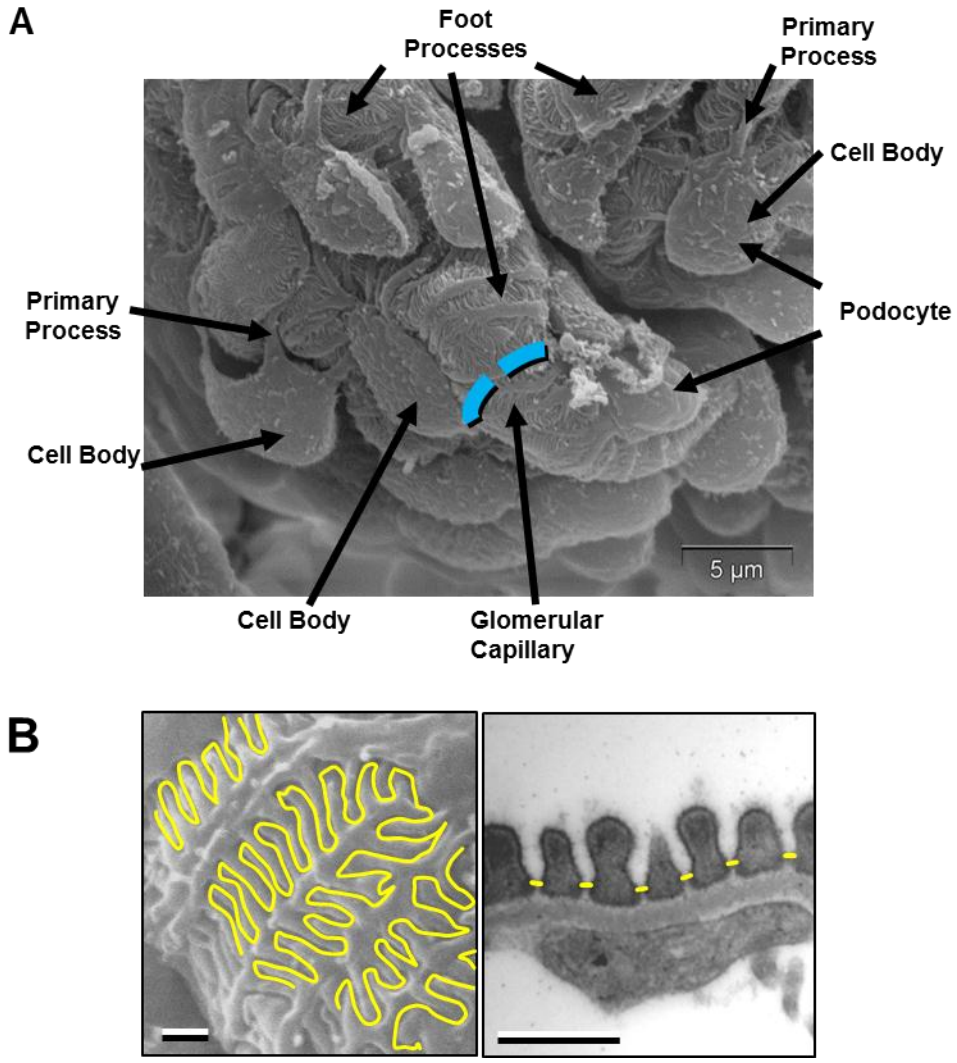


**Figure 1.3 The podocyte forms the outer layer of the glomerular filtration barrier.**

(A) SEM image of a section of a glomerulus. Each glomerular capillary is enveloped by a network of podocyte cells. The podocyte cell body floats above the capillary. It extends a number of primary processes, which branch into secondary processes and then extend many small foot processes. (B) The slit diaphragm (outlined in yellow) is formed between adjacent podocyte foot processes. Left panel, SEM image of a segment of a glomerular capillary. Right panel, TEM image of a segment of a glomerular capillary. Scale bars: A: 5 µm. B: 500 nm (both panels)

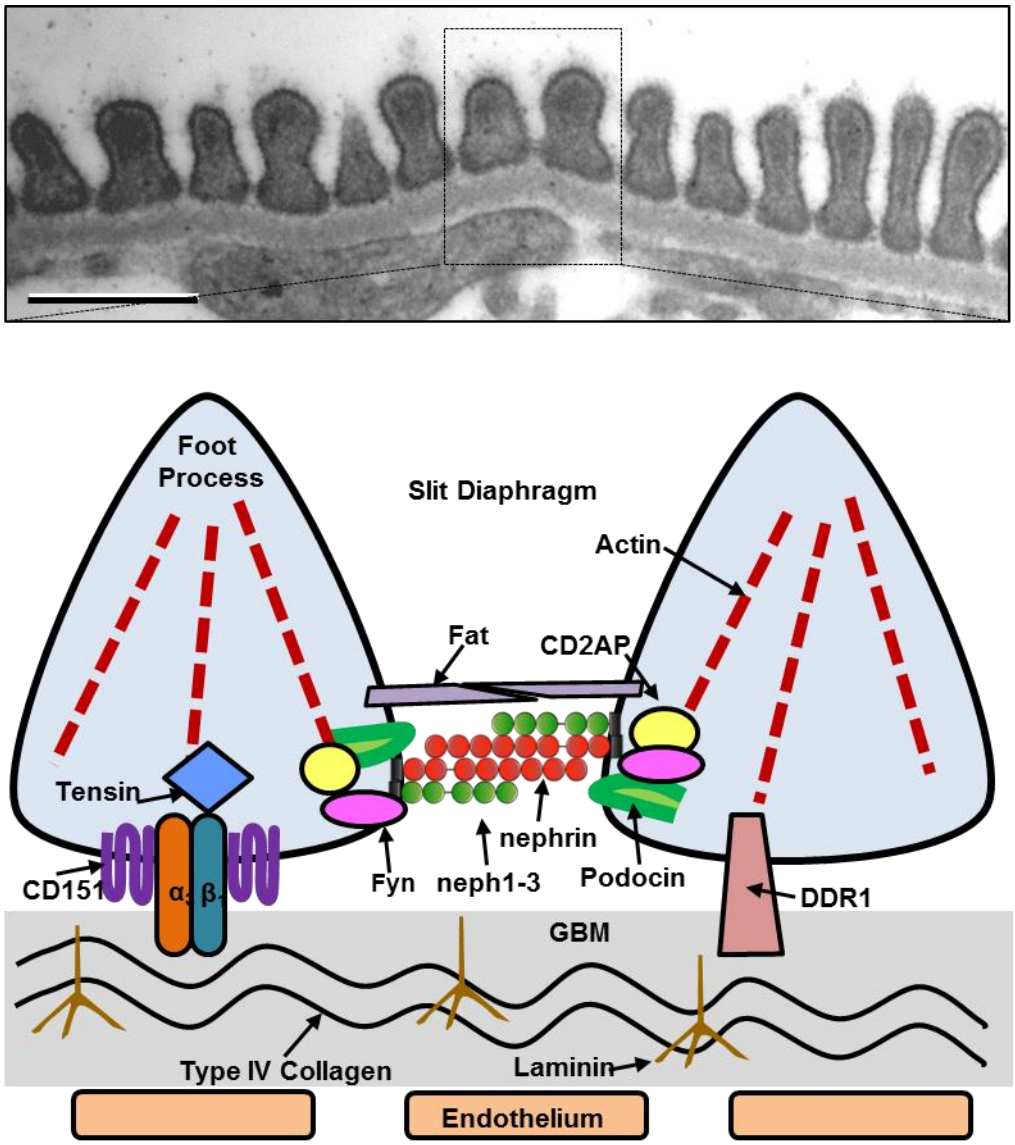


**Figure 1.4 Cartoon of the molecular architecture of the podocyte.**

Sizes are not to scale. The podocyte slit diaphragm is composed of nephrin, the neph family (neph1, neph2 and neph3), podocin and Fat. Inside the cytoplasm, nephrin and podocin interact with CD2AP which links the complex to the actin cytoskeleton. Foot processes are anchored to the glomerular basement membrane (GBM) via integrin $\alpha_3\beta_1$ in combination with tetraspanin CD151. Tensin links integrins to the actin cytoskeleton. Foot processes are also anchored to the GBM by DDR1. Scale bar: 500 nm. Adapted from (Zenker *et al*., 2009).

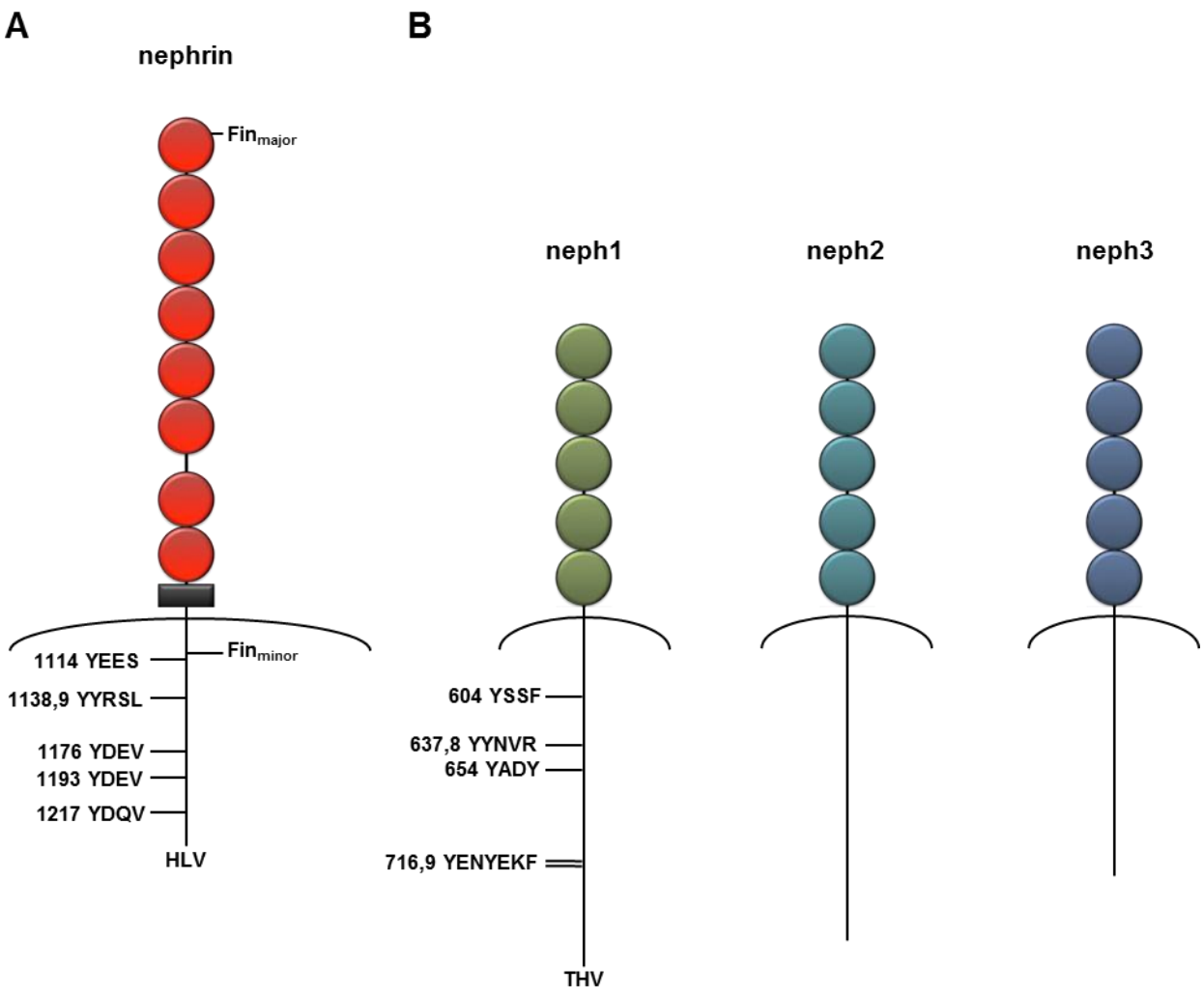


**Figure 1.5 Illustration of the neph-nephrin family of proteins.**

The proteins structures are not drawn to scale, but the lengths of the cytoplasmic tails are comparable relative to each other. (A) Structure of nephrin. On the right side, the locations of the $Fin_{major}$ and $Fin_{minor}$ mutations are indicated. The positions of the six most highly conserved tyrosine motifs are shown in the cytoplasmic tail. (B) Structure of the neph family of proteins. The neph family is composed of three closely related proteins, neph1, neph2 and neph3. Conserved tyrosine motifs are indicated in neph1.

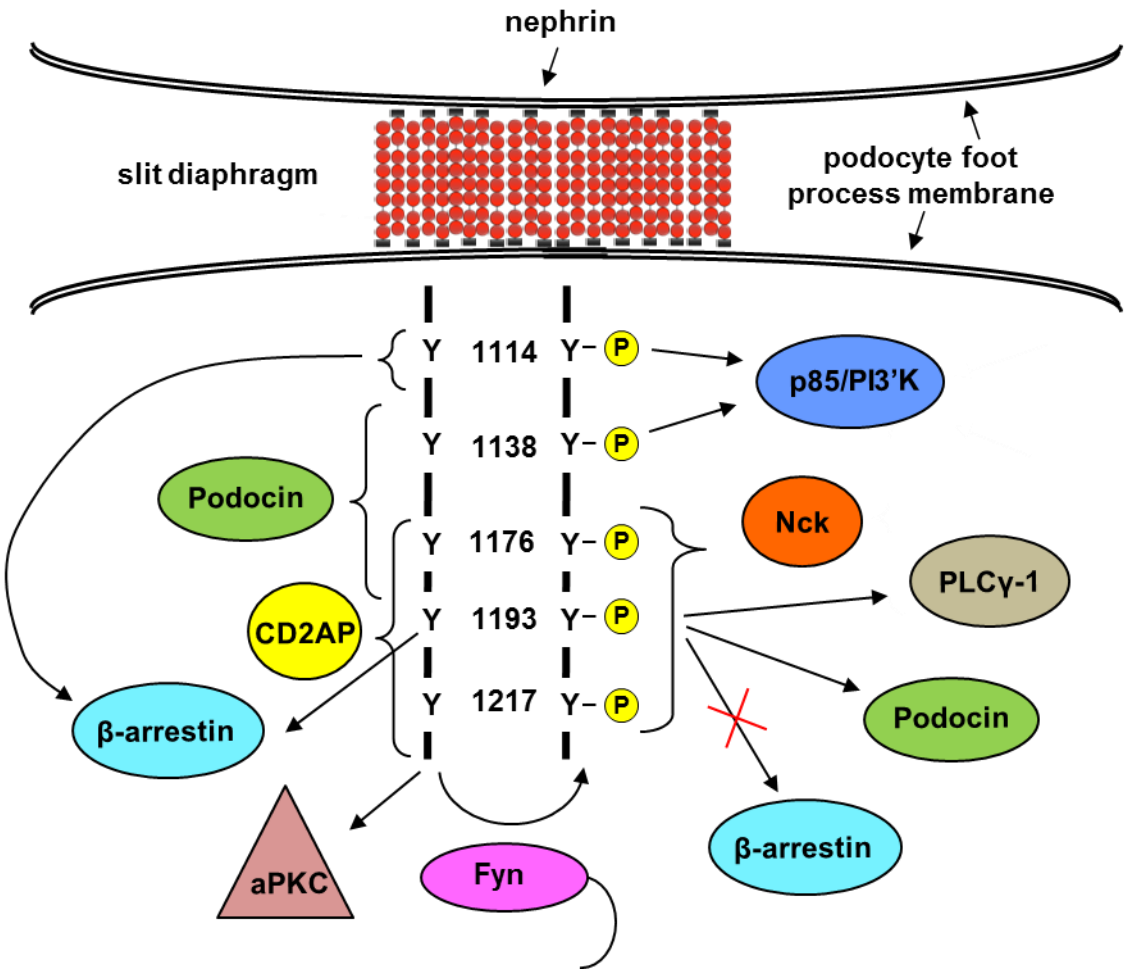


**Figure 1.6 Phospho-independent (left side) and phospho-dependent (right side) interactions of the cytoplasmic tail of nephrin.**

The cytoplasmic tail of nephrin contains 5 conserved tyrosine residues known to influence binding to other proteins. Tyrosine residues are numbered as in human nephrin. Binding of podocin, aPKC and CD2AP to nephrin is phospho-independent. β-arrestin binds to nephrin around 1120 but only when Y1193 is not phosphorylated. Fyn phosphorylates nephrin and can also bind to phosphorylated nephrin. Y1114 and Y1138 are binding sites for p85. PLCγ-1 interacts with Y1193. Phosphorylation of Y1193 increases affinity for podocin. Nck can bind to three sites, Y1176, Y1193 and Y1217.

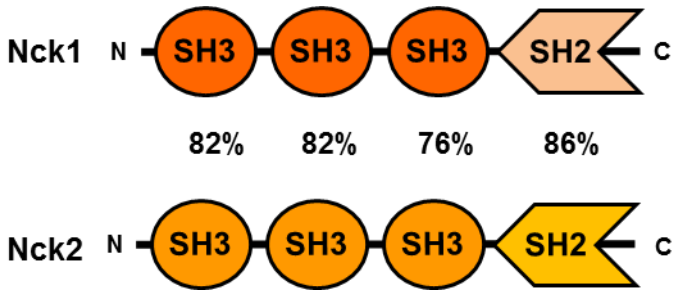


**Figure 1.7 The Nck family of adaptor proteins.**

The Nck family is composed of two members, Nck1 and Nck2. Both proteins contain three tandem SH3 domains followed by a single SH2 domain. The values in between the domains represent the percent amino acid identity of Nck2 with Nck1. Adapted from (Lettau *et al*., 2009).

# CHAPTER 2:

# GENERATION OF PHOSPHO-NEPHRIN ANTIBODIES AND CHARACTERIZATION OF NEPHRIN PHOSPHORYLATION *IN VIVO*

## 2.1 ABSTRACT

The trans-membrane protein nephrin is a key component of the glomerular slit diaphragm, and alterations in nephrin function lead to defective actin organization and changes in podocyte foot process morphology (effacement), ultimately resulting in loss of proper blood filtration and renal disease. Upon clustering of adjacent nephrin molecules, the cytoplasmic tail becomes phosphorylated on a series of conserved tyrosine residues within YDxV motifs, and we have recently demonstrated that each of these residues can recruit the Nck SH2/SH3 adaptor proteins and initiate actin reorganization. Moreover, we have also shown that selective deletion of Nck from either developing or established podocytes results in foot process effacement and renal disease. However, the regulation of nephrin tyrosine phosphorylation and Nck binding at the slit diaphragm and the role of this signaling pathway in the development and maintenance of podocyte foot processes is presently not well understood. To investigate the phosphorylation status of nephrin in the kidney and its potential ability to associate with Nck under different conditions, we have generated a series of antibodies that specifically recognize each of the three Nck binding sites found on mouse and human nephrin. We have characterized the specificity of these antibodies and used them to analyze nephrin tyrosine phosphorylation in cells and in adult rodent kidneys. Our data indicate that nephrin can be phosphorylated on all three tyrosine residues *in vitro* and that nephrin is also phosphorylated *in vivo* on multiple tyrosine residues. These results support the emerging hypothesis that Nck is connected to these phosphorylation sites in both developing and mature podocytes, and that loss of this signaling pathway results in actin rearrangement and subsequent foot process effacement.

## 2.2 MATERIALS AND METHODS

### 2.2.1 *GENERATION OF PHOSPHO-SPECIFIC NEPHRIN ANTIBODIES*

We generated rabbit monoclonal antibodies (RAbMAbs) in collaboration with Epitomics® (Burlingame, CA). Briefly, peptides specific to phosphorylated mouse nephrin were synthesized and used to immunize rabbits. Upon screening for sera reactive with phosphorylated nephrin

expressed from HEK293T cells, B cells were isolated from spleens and used to generate rabbit hybridoma cells. Pooled hybridoma cells were next screened for reactivity with phosphorylated nephrin, followed by screening of clonal lines from positive pools. A single production clone for each antibody was selected for final immunoanalysis of nephrin phosphorylation, with 0.5 μg of phosphoantibody used for immunoprecipitation and 0.07 μg/ml used for immunoblotting. We used the following peptides: AFPGHLpYDEVERC (mouse Y1191 = human Y1176); GVWGPLpYDEVQMC (mouse Y1208 = human Y1193); and DPRGIpYDQVAADC (mouse Y1232 = human Y1217). Antibodies are labeled with human numbering throughout the text for consistency.

### 2.2.2 *ANTIBODIES*

We obtained the following antibodies from commercial sources: polyclonal anti-GFP 290 (Abcam, Cambridge, MA) and monoclonal anti-phosphotyrosine clone 4G10 (Upstate-Millipore, Bedford, MA). Polyclonal antibodies to rat nephrin have been described previously (Li *et al.*, 2004). We quantified protein content in immunoblots using scanning densitometry (Image J software, NIH, Bethesda, MD) and used the t-test to determine significant differences between two groups.

### 2.2.3 *PLASMIDS*

Construction of CD16/7-nephrin(WT)IC and CD16/7-nephrin(Y3F)IC have been described previously (Jones *et al.*, 2006). Here, we amplified the intracellular domains of human nephrin containing tyrosine to phenylalanine substitutions at one or two YDxV sites by PCR to generate in-frame fusions with the extracellular domain of CD16 and the intracellular domain of CD7 (CD16/7) followed by a carboxy-terminal EGFP epitope tag. We confirmed all constructs by DNA sequencing.

### 2.2.4 *Cell Culture*

We grew HEK 293T cells in high glucose Dulbecco's modified Eagle's medium (DMEM) supplemented with 10% fetal bovine serum (Hyclone, Logan, UT). Transient transfections were performed using polyethyleneimine.

### 2.2.5 *Immunoprecipitations and Immunoblotting*

Immunoprecipitation and immunoblotting procedures have been described previously (Jones *et al.*, 2006). Briefly, for phosphorylation analyses and co-immunoprecipitation experiments, cells were starved overnight and stimulated for 10 min at 37°C using a 1 μg/ml dilution of anti-CD16 antibody. We prepared lysates from transfected cells, rodent kidney cortex biopsies, or rat glomeruli using PLC lysis buffer supplemented with fresh protease inhibitors [50 mM HEPES (pH 7.5), 150 mM NaCl, 10% glycerol, 1% Triton X-100, 1.5 mM $MgCl_2$, 1 mM EGTA, 10 mM NaPPi, 100 mM NaF, supplemented with 1 mM sodium orthovanadate, 1 mM PMSF, 10 μg/ml aprotinin, and 10 μg/ml leupeptin].

### 2.2.6 *Induction of PAN Nephrosis*

We obtained male Sprague Dawley rats (250 to 300 g) from Charles River (St. Constant, QU). We used a single injection of puromycin aminonucleoside (50 mg/kg body wt) to induce podocyte injury, as described previously (Zhu *et al.*, 2008).

## 2.3 **Results**

### 2.3.1 *Development of Nephrin Phospho-Specific Antibodies*

The results from our genetic experiments indicate that Nck expression is critical in adult podocytes to retain foot process morphology. We thus hypothesized that Nck may interact with

nephrin in both developing and established podocyte foot processes, and that this interaction is required to maintain connections with the underlying actin cytoskeleton. Increasing evidence suggests that nephrin is tyrosine phosphorylated in normal glomeruli of adult rodents (Verma *et al.*, 2003; Li *et al.*, 2004; Jones *et al.*, 2006; Li *et al.*, 2006). To investigate the tyrosine phosphorylation status of nephrin in the adult kidney and its potential ability to associate with Nck, we generated a series of antibodies that specifically recognize each of the three Nck binding sites found on mouse and human nephrin (Figure 2.1A). We used peptides encompassing each tyrosine phosphorylated YDxV site on nephrin to immunize rabbits and generate rabbit monoclonal antibodies (RAbMAbs). We assessed the specificity of each affinity-purified antibody using a series of human nephrin proteins harboring tyrosine (Y) to phenylalanine (F) substitutions at amino acid positions 1176, 1193, and 1217. In each of these proteins, the intracellular domain of nephrin (which includes a GFP tag) has been fused to the extracellular domain of the Ig receptor CD16 and the transmembrane domain of CD7 to facilitate activation of nephrin signaling upon addition of CD16 antibody. Chimeric proteins were expressed in HEK 293T cells, and lysates from CD16-stimulated cells were immunoprecipitated with anti-GFP antibody and subjected to immunoblotting with the phospho-nephrin antibodies. We have previously used this approach to demonstrate that nephrin is tyrosine phosphorylated on multiple YDxV sites following CD16 stimulation (Jones *et al.*, 2006). Figure 2.1B shows that all three Nck binding sites on nephrin are indeed tyrosine phosphorylated upon CD16-induced clustering, as each phospho-specific antibody can detect the wild-type (WT) protein. The nephrin pY1193 antibody appears to be specific to this Tyr residue, as it does not recognize the Y1193F mutant, nor does it detect the Y1176/1193F or Y1193/1217F double mutants (Figure 2.1B). Similarly, the pY1217 antibody also appears to be specific, as it does not recognize the Y1217F mutant, or the Y1176/1217F or Y1193/1217F double mutants (Figure 2.1B). In contrast, the pY1176 antibody appears to display weak cross-reactivity with the other YDEV motif at Tyr 1193, as it can detect low levels of the Y1176F mutant but not the Y1176/1193F double mutant (which still contains the YDQV motif at Tyr 1217) (Figure 2.1B). However, since there was no reduction in intensity with the Y1193F mutant when compared with the dramatic reduction with the Y1176F mutant, it suggests that this antibody has high affinity for Tyr 1176. None of the antibodies could detect the Y3F triple mutant, indicating their specificity for phosphorylated YDxV sites on nephrin. We also examined the ability of these antibodies to specifically immunoprecipitate

phosphorylated chimeric nephrin from lysates of transfected HEK 293T cells. Indeed, each of these antibodies showed an ability to immunoprecipitate chimeric nephrin, and in each case, this was markedly increased following anti-CD16 cross-linking, suggesting that nephrin stimulation increases phosphorylation at each YDxV site (Figure 2.1C). We observed similar patterns of phosphorylation with chimeric nephrin proteins bearing a Myc-epitope tag in place of GFP (data not shown). These results confirm that nephrin phosphorylation induced by CD16 clustering in HEK 293T cells occurs on all three Nck binding sites, and that these reagents are specific to the multiple YDxV sites on nephrin.

### 2.3.2 *Nephrin Phosphorylation is Maintained in the Adult Glomerulus*

We next wanted to utilize these reagents to pursue the possibility that endogenous nephrin might be phosphorylated in adult rodent kidneys under normal physiologic conditions. Rat nephrin contains a single YDEV site (corresponding to human Tyr 1193) as well as the YDQV site (corresponding to human Tyr 1217), while mouse nephrin contains all three YDxV sites. To bypass any potential artifacts that could arise in the sieving procedure wherein glomeruli are isolated from intact kidneys, we chose to first prepare lysates directly from kidney cortex. Cortical lysates from normal adult rat kidneys were immunoprecipitated with various phospho- or pan-nephrin antibodies followed by anti-nephrin immunoblotting. Endogenous nephrin appears as a doublet of 180 and 170 kD, and the upper band is tyrosine phosphorylated (Figure 2.2A) (Jones *et al.*, 2006). As shown in Figure 2.2A, each of the phospho-nephrin antibodies specifically immunoprecipitated the 180-kD phosphorylated species. Although a site corresponding to human Tyr 1176 is not present in rat nephrin, the ability of the pY1176 antibody to cross-react with the corresponding rat Tyr 1193 site likely allows this antibody to immunoprecipitate phosphorylated nephrin from rat kidney lysates. These data clearly demonstrate that a basal level of nephrin tyrosine phosphorylation exists in normal adult rat kidneys. Similar results were obtained with mouse kidney lysates, where each antibody again detected the 180-kD phosphorylated nephrin species (data not shown), and we found no reactivity with IgG alone. Taken together, these results indicate that the Nck binding sites on nephrin are phosphorylated in normal adult kidney.

Altered dynamics of nephrin tyrosine phosphorylation have been observed during foot process effacement *in vivo* (Li *et al.*, 2004; Verma *et al.*, 2006; Li *et al.*, 2006). To investigate whether these changes in phosphorylation occur on the YDxV sites, we examined nephrin phosphorylation in the puromycin aminonucleoside (PAN) nephrosis model of podocyte injury. We prepared glomerular extracts from PAN-treated rats at multiple time-points corresponding to the onset (day 4) and peak period (day 7 and 14) of proteinuria. Phosphorylation on the YDQV site (human Tyr 1217, corresponding to rat Tyr 1228) was clearly observed in untreated control rats, and it decreased significantly over the course of PAN nephrosis, whereas overall expression of nephrin did not change (Figure 2.2B). Upon normalizing for the amount of total nephrin in each lysate, the reduction in phosphorylation on this site was nearly 50% during the peak of proteinuria (Figure 2.2C). These findings, therefore, indicate a decrease in nephrin tyrosine phosphorylation on Nck binding sites upon podocyte injury.

## 2.4 DISCUSSION

To further investigate the nature of nephrin phosphorylation, we have developed and characterized a series of phospho-specific antibodies that recognize each of the conserved Nck SH2 domain binding motifs on nephrin. Using these three antibodies, we demonstrated that all of the YDxV motifs on nephrin appear to be phosphorylated in adult rat and mouse kidneys. As each of these sites has a similar affinity for the Nck SH2 domain (Jones *et al.*, 2006; Blasutig *et al.*, 2008), these observations correlate well with the notion that multiple Nck SH2 domain bindings motifs on nephrin act cooperatively to initiate and sustain robust levels of actin polymerization (Blasutig *et al.*, 2008).

Two other laboratories recently reported *in vivo* phosphorylation of the Nck binding sites on nephrin. Uchida *et al*. (Uchida *et al.*, 2008) developed two antibodies that recognize the conserved Nck binding sites on rat nephrin (corresponding to human Tyr 1193 and Tyr 1217), while Verma *et al*. (Verma *et al.*, 2006) developed a single antibody that recognizes both YDEV sites on mouse nephrin (corresponding to human Tyr 1176 and Tyr 1193). Interestingly, although Verma *et al*. (Verma *et al.*, 2006) could detect nephrin phosphorylation in developing glomeruli at the capillary loop stage, they were unable to detect nephrin phosphorylation on the Nck

binding sites in adult glomeruli. It was, therefore, speculated that since nephrin was not phosphorylated in mature mouse podocytes, it may connect to actin via phosphorylation-independent mechanisms in established podocytes. These findings contrast with those reported here and in Uchida *et al*. (Uchida *et al.*, 2008) and may reflect differences in the specificity and sensitivity of these various antibodies. Accordingly, it is important to note that this latter antibody does not appear to recognize the third Nck binding site on mouse and human nephrin (Verma *et al.*, 2006), which is contained within a YDQV motif and is conserved on rat nephrin. Taken together, our data support those of Uchida *et al*. (Uchida *et al.*, 2008) and are consistent with a model in which nephrin is phosphorylated on the Nck binding sites in both developing and mature podocytes, thereby providing a continuous and dynamic connection to the actin machinery that controls foot process morphology.

Phosphorylation of Tyr 1193 appears to be particularly sensitive to nephrin clustering, as very little phosphorylation of this site could be seen in unstimulated cells when compared with Tyr 1176 and Tyr 1217 (Figure 2.1C). While we must consider that this reduction could be due to lower antibody affinity, it is interesting to note that the phosphorylation status of Tyr 1193 may be an important regulator of nephrin signaling, through controlling the expression of nephrin on the cell surface. Phosphorylation of this site has been shown by Quack and colleagues (Quack *et al.*, 2006) to function as a switch to determine whether podocin or β-arrestin2 is recruited to nephrin. Phosphorylation of Tyr 1193 by Src kinases Fyn and Yes induces podocin binding and AP-1 transactivation (Li *et al.*, 2004; Quack *et al.*, 2006). In contrast, unphosphorylated nephrin or a Y1193F mutant can interact with β-arrestin2, and this interaction is disrupted in the presence of Yes kinase. Association of nephrin with β-arrestin2 promotes nephrin endocytosis and reduces nephrin signaling. This "switch" at Tyr 1193 is, therefore, hypothesized to function as a mechanism by which podocytes can sense the structural integrity of the slit diaphragm. Unpaired nephrin molecules, such as those that are mislocalized or have lost extracellular contacts, will not be phosphorylated on this residue, thus promoting interaction with β-arrestin2 and nephrin internalization. Indeed, in our experiments where nephrin is not clustered via CD16 antibodies, phosphorylation of Tyr 1193 was virtually undetectable, consistent with the potential for β-arrestin2 binding and nephrin endocytosis. Phosphorylation of Tyr 1193 is also reduced in rats with foot process effacement (Uchida *et al.*, 2008).

Alterations in nephrin phosphorylation may be an important indicator of slit diaphragm integrity during glomerular disease. Our results showing a reduction in phosphorylation on the YDQV site in PAN-induced nephrosis confirm those of Uchida *et al.*, where foot process effacement and proteinuria coincide with a decrease in phosphorylation on both Nck binding sites on rat nephrin (Uchida *et al.*, 2008). Moreover, the interaction between nephrin and Nck is reduced in glomeruli isolated from rats with PAN-induced nephrosis (Li *et al.*, 2006), and a decrease in the amount of F-actin is also observed (Uchida *et al.*, 2008). A reduction in phosphorylation of the YDQV site on nephrin is also associated with human minimal change nephrosis (Uchida *et al.*, 2008). These findings raise the intriguing possibility that loss of connection between nephrin and Nck may contribute to foot process effacement in such patients. In contrast, other models of podocyte damage, including protamine sulfate perfusion, passive Heymann nephritis and 27A antibody injection, result in an increase in nephrin phosphorylation (Simons *et al.*, 2001; Li *et al.*, 2004; Verma *et al.*, 2006), and it is plausible that such hyperphosphorylation of nephrin may also contribute to nephropathy under certain circumstances. Alternatively, hyperphosphorylation of certain tyrosine residues may be required at certain time points in the course of recovery as a compensatory mechanism. The phospho-specific nephrin antibodies described here will be a useful tool for deciphering how nephrin phosphorylation and Nck binding are regulated under both physiologic and pathologic conditions in the glomerulus.

**Figure 2.1. Conserved tyrosine residues on nephrin are recognized by phospho-specific antibodies.**

(A) The intracellular region of human nephrin contains a series of conserved tyrosine residues within YDxV motifs that can bind the Nck SH2 domain. (B) Peptides encompassing each tyrosine phosphorylated YDxV motif on nephrin were used to immunize rabbits and generate rabbit monoclonal antibodies (RAbMAbs). HEK 293T cells were transfected with a series of GFP-tagged chimeric human nephrin proteins with tyrosine (Y)-to-phenylalanine (F) substitutions at amino acid positions 1176, 1193, and 1217. Nephrin phosphorylation was induced by CD16 clustering, and lysates were immunoprecipitated (IP) with GFP antibodies to isolate nephrin. Separated proteins were immunoblotted (IB) with affinity-purified phospho-nephrin antibodies or GFP. Both the nephrin pY1193 and pY1217 antibodies appear to be specific to each respective Tyr residue, while the pY1176 antibody appears to recognize YDEV (1176 and also 1193 to a limited extent) but not YDQV (1217) sites. None of the antibodies could detect the Y3F triple mutant, indicating their specificity for phosphorylated YDxV sites on nephrin. Exposure time for the pY1176 and pY1193 blots is 30 min, and exposure time for the pY1217 blot is 10 min. (C) HEK 293T cells expressing wildtype (WT) chimeric nephrin were stimulated with anti-CD16 or left unstimulated, and lysates were immunoprecipitated (IP) with each phospho-nephrin antibody or GFP. Separated proteins were immunoblotted (IB) with GFP or phosphotyrosine (pY) antibodies. Nephrin clustering results in increased tyrosine phosphorylation on each YDxV site.

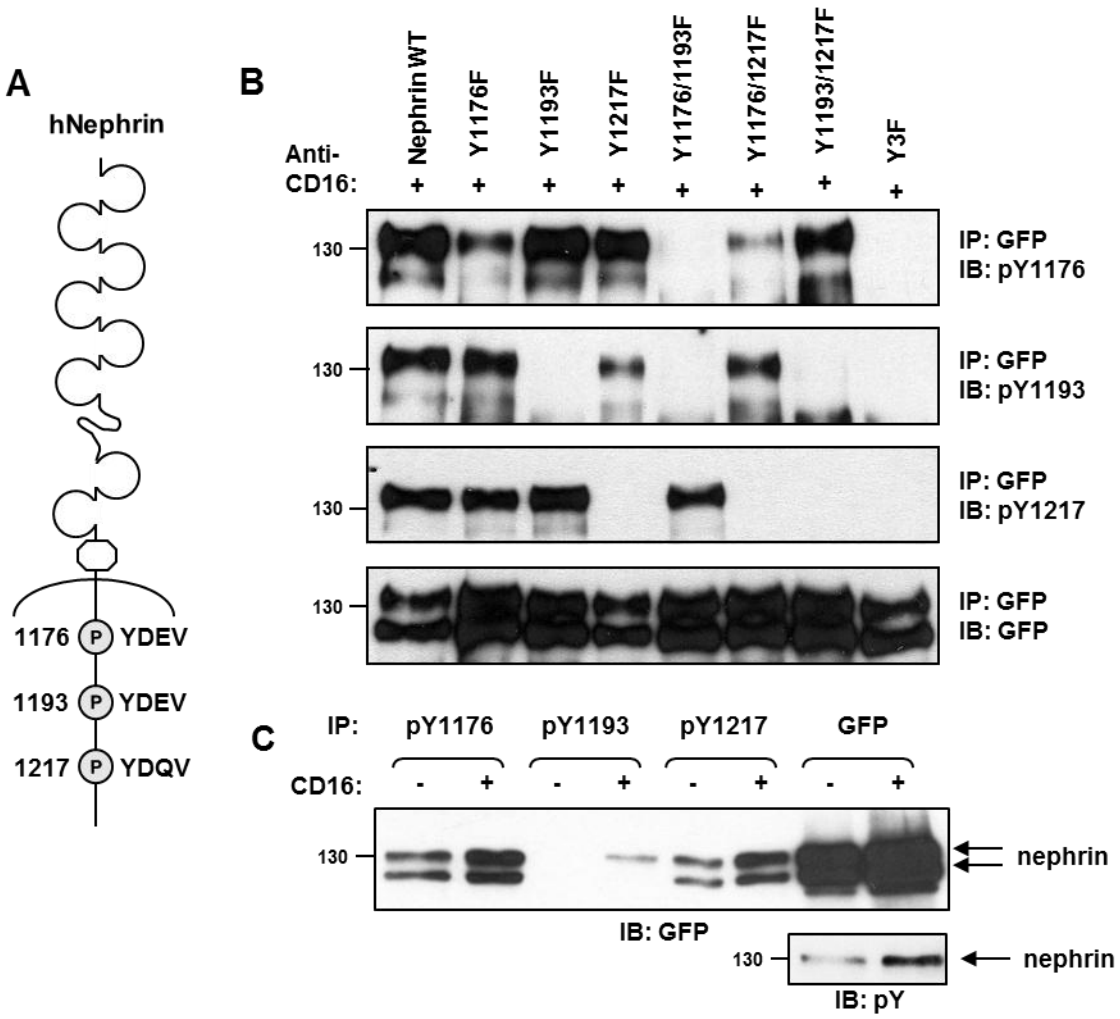
A
hNephrin
1176 P YDEV
1193 P YDEV
1217 P YDQV
B
Anti-CD16:
+ Nephrin WT
+ Y1176F
+ Y1193F
+ Y1217F
+ Y1176/1193F
+ Y1176/1217F
+ Y1193/1217F
+ Y3F
130
IP: GFP
IB: pY1176
IP: GFP
IB: pY1193
IP: GFP
IB: pY1217
IP: GFP
IB: GFP
C
IP: pY1176 pY1193 pY1217 GFP
CD16: - + - + - + - +
130
nephrin
IB: GFP
130
nephrin
IB: pY

**Figure 2.2. Nephrin is phosphorylated on YDxV sites in normal adult kidneys and a decrease is associated with podocyte injury.**

(A) Adult rat kidney cortex lysates were immunoprecipitated (IP) with each phospho-nephrin antibody or pan-nephrin, and separated proteins were immunoblotted (IB) with nephrin antibodies. Endogenous nephrin appears as a doublet of 180 and 170 kD, and each of the phospho-nephrin antibodies detected the 180-kD tyrosine-phosphorylated upper species. (B) Glomerular lysates from rats with PAN nephrosis at various time-points or untreated control rats were immunoblotted with phospho-nephrin or nephrin antibodies. We utilized the pY1217 antibody as it displays superior sensitivity. Equivalent amounts of lysate are indicated by tubulin. Data shown are representative of four independent experiments. (C) Densitometric quantitation of phosphorylated nephrin normalized to total nephrin (p-nephrin/nephrin) indicates a decrease in nephrin phosphorylation on the YDQV site upon podocyte injury. $*P < 0.05$ *versus* control, $n = 4$.

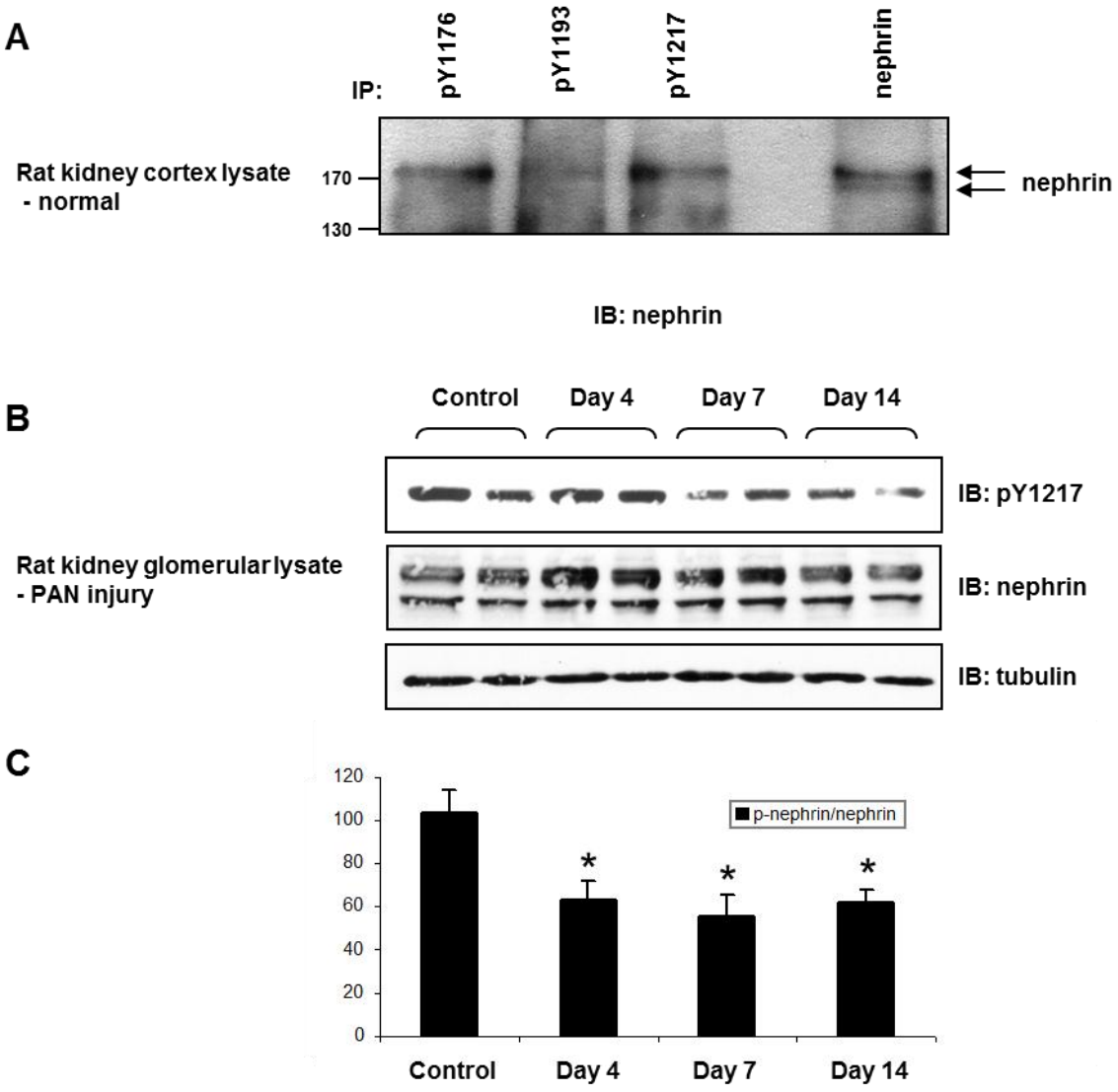
A
IP:
pY1176
pY1193
pY1217
nephrin
Rat kidney cortex lysate
- normal
170
130
nephrin
IB: nephrin
B
Control
Day 4
Day 7
Day 14
IB: pY1217
Rat kidney glomerular lysate
- PAN injury
IB: nephrin
IB: tubulin
C
120
100
80
60
40
20
0
p-nephrin/nephrin
*
*
*
Control
Day 4
Day 7
Day 14

# CHAPTER 3:

# DIRECT REGULATION OF NEPHRIN TYROSINE PHOSPHORYLATION BY NCK ADAPTOR PROTEINS

## 3.1 ABSTRACT

The transmembrane protein nephrin is a key component of the kidney slit diaphragm that contributes to the morphology of podocyte foot processes through signaling to the underlying actin cytoskeleton. We have recently reported that tyrosine phosphorylation of the cytoplasmic tail of nephrin facilitates recruitment of Nck SH2/SH3 adaptor proteins and subsequent actin remodeling, and that phosphorylation of the Nck binding sites on nephrin is decreased during podocyte injury. We now demonstrate that Nck directly modulates nephrin phosphorylation through formation of a signaling complex with the Src family kinase (SFK) Fyn. The ability of Nck to enhance nephrin phosphorylation is compromised in the presence of the SFK inhibitor PP2, and when the SH3 domains of Nck are mutated. Furthermore, induced loss of Nck expression in podocytes *in vivo* is associated with a rapid reduction in nephrin tyrosine phosphorylation. Our results suggest that Nck may facilitate dynamic signaling events at the slit diaphragm by promoting Fyn-dependent phosphorylation of nephrin, which may be important in the regulation of foot process morphology and response to podocyte injury.

## 3.2 INTRODUCTION

Podocytes are a specialized type of epithelial cell which comprise the outer layer of the blood filtration barrier of the kidney glomerulus (Pavenstadt *et al.*, 2003). These cells have a unique three dimensional structure formed by the extension of many small actin rich foot processes, which interdigitate with one another to form a lattice like structure. Adjacent foot processes are connected via a specialized intercellular junction known as the slit diaphragm.

One of the primary causes of many forms of podocyte damage is alteration in the integrity of the slit diaphragm concomitant with morphological changes to the actin cytoskeleton of the foot processes, resulting in a flattening, or effacement, of foot processes as well as a loss of slit diaphragms (Kriz *et al.*, 1996). Together, these perturbations can lead to the development of renal disease. A key component of the slit diaphragm is the transmembrane IgG family protein nephrin, which interacts with neighbouring nephrin molecules to form both an external structural

barrier through its IgG domains and an internal signaling hub using its cytoplasmic tail, which is connected to the podocyte actin cytoskeleton (Welsh and Saleem, 2010).

Several aspects of foot process architecture appear to be dependent on proper phosphorylation of podocyte proteins induced by Src family kinases (SFKs). Mice lacking both Fyn and Yes develop proteinuria and foot process effacement by 4 weeks of age (Verma *et al.*, 2003), while Fyn knockout mice present with altered foot process architecture (Yu *et al.*, 2001; Verma *et al.*, 2003) and have been reported to develop proteinuria (Yu *et al.*, 2001). Targets of phosphorylation by SFKs include a number of structural components of the slit diaphragm, such as nephrin (Verma *et al.*, 2003) and the Neph1/2/3 family (Garg *et al.*, 2007; Harita *et al.*, 2008) of IgG adhesion molecules, whose phosphorylated tyrosines serve to recruit downstream signaling proteins. Phosphorylated nephrin has been reported to interact with p85 (Huber *et al.*, 2003b; Zhu *et al.*, 2008; Garg *et al.*, 2010), podocin (Li *et al.*, 2004; Quack *et al.*, 2006), Nck1/2 (Li *et al.*, 2006; Verma *et al.*, 2006; Jones *et al.*, 2006), and PLC-γ (Harita *et al.*, 2009), while phosphorylated neph1 has been shown to interact with Grb2 (Garg *et al.*, 2007; Harita *et al.*, 2008) and Csk (Harita *et al.*, 2008).

Three of the six highly conserved tyrosine residues of the cytoplasmic tail of human nephrin—Y1176, Y1193 and Y1217—are contained within YDxV motifs. We (Jones *et al.*, 2006; Blasutig *et al.*, 2008) and others (Li *et al.*, 2006; Verma *et al.*, 2006) have demonstrated that, when phosphorylated, each of these residues can recruit the Nck family of SH2/SH3 adaptor proteins. The single Nck SH2 domain binds the phosphorylated YDxV motifs, while the three tandem SH3 domains mediate interactions with downstream effectors of the actin cytoskeleton, thereby providing a link between nephrin and podocyte actin dynamics. SH2 domain mediated recruitment of Nck to a phosphorylated substrate, followed by SH3 domain recruitment of modulators of the actin cytoskeleton has also been demonstrated for many other Nck interacting partners (Lettau *et al.*, 2009). Additionally, we have also demonstrated an essential role for Nck adaptors in both the development of podocyte structure (Jones *et al.*, 2006) as well as in the maintenance of foot process architecture in the adult mouse (Jones *et al.*, 2009).

Both the amount and significance of nephrin tyrosine phosphorylation at the slit diaphragm remain areas of ongoing investigation. There have been multiple reports demonstrating in vitro that nephrin can be phosphorylated by Fyn on more than one tyrosine residue (Li *et al.*, 2004; Verma *et al.*, 2006; Jones *et al.*, 2006; Harita *et al.*, 2009). Overall, it would appear that the conserved sites Y1193 and Y1217 are the strongest targets of Fyn kinase (Jones *et al.*, 2006; Harita *et al.*, 2009). Additionally, phosphorylation on Y1193 and Y1217 in the healthy kidney has been demonstrated in vivo through multiple reports using independently generated phospho-specific nephrin antibodies (Uchida *et al.*, 2008; Jones *et al.*, 2009; Zhang *et al.*, 2010a). A separate study using mass-spectroscopy reported phosphorylation on Y1193 in samples from normal rat kidneys (Zhang *et al.*, 2010b).

Phosphorylation of nephrin on specific sites has also been examined during the development of renal disease, with decreases in nephrin phosphorylation on Y1217 reported in human patients with minimal change disease (Uchida *et al.*, 2008) as well as in the corresponding rat PAN model (Uchida *et al.*, 2008; Jones *et al.*, 2009) and the mouse LPS model of transient foot process effacement (Zhang *et al.*, 2010a). However, despite changes in nephrin phosphorylation being associated with disease, the mechanisms regulating the dynamics of nephrin phosphorylation and their role in the development and maintenance of podocyte structure are currently not well understood.

In the present study, we have characterized a role for the Nck family of adaptor proteins in the regulation of nephrin phosphorylation. We demonstrate that both Nck1 and Nck2 increase nephrin phosphorylation in vitro and that this effect is dependent on functional SH3 domains of Nck. Further, we found that, when recruited to nephrin, Nck was able to interact with the kinase Fyn and that this interaction correlated with an increase in Fyn activity. Lastly, using a mouse model to perform a podocyte-specific deletion of both Nck1 and Nck2, we show that reduction of Nck in vivo is associated with rapid loss of nephrin phosphorylation. These data suggest an additional role for Nck adaptor proteins in cellular signaling which could contribute to the pathogenesis of kidney disease.

## 3.3 MATERIALS AND METHODS

### 3.3.1 *PLASMIDS*

Constructs encoding human Myc-tagged nephrin, CD16-nephrin-GFP, human Flag-tagged Nck1 and Nck2 and mutants thereof have been previously described (Jones *et al.*, 2006; Blasutig *et al.*, 2008). HA-Akt was provided by Jim Woodgett (SLRI, Toronto, Ontario), pcDNA3-HA-Nck2 was a gift from Bruce Mayer (University of Connecticut, Framington, CT) and pcDNA3-HA-Grb2 was provided by Tony Pawson (SLRI, Toronto, Ontario).

### 3.3.2 *ANTIBODIES*

The following antibodies were obtained commercially: rabbit anti-GFP (#ab290) (Abcam), mouse anti-GAPDH (#G041) (Applied Biological Materials Inc), mouse anti-Nck (BD Pharmingen), and guinea pig anti-nephrin (#20R-NP002) (Fitzgerald Inc.). Rabbit anti-$pS^{473}$ Akt (#4060), rabbit anti-$pS^{3}$-cofilin (#3311), mouse anti-Myc 9B11 (#2276) and rabbit anti-$Y^{527}$ (active) Src (#2107) were obtained from Cell Signaling. Mouse anti-CD16 (#sc-19620), rabbit anti-$pT^{308}$ Akt (#sc-16646) and rabbit anti-Fyn (#sc-16) were obtained from Santa Cruz Biotechnology. Rabbit anti-cofilin (#C8736), mouse anti-Flag clone M2 (#F3165) and anti-Flag M2-HRP (#A8592) were from Sigma-Aldrich. Mouse anti-HA clone 12CA5 and anti-pY clone 4G10 were provided by Sunnybrook Hybridoma Bank, Toronto, Ontario. Generation and testing of the following antibodies has previously been reported: rabbit anti-nephrin (Li *et al.*, 2004), phospho-specific nephrin $pY^{1193}$ and $pY^{1217}$ (Jones *et al.*, 2009).

### 3.3.3 *CELL CULTURE*

HEK293T cells were grown in Dulbecco's modified Eagle's medium-high glucose (Hyclone) supplemented with 10% fetal bovine serum and 1% penicillin/streptomycin. Cells were kept at 37°C with 5% $CO_2$. Transfections were performed using polyethyleneimine.

### 3.3.4 *CELL LYSIS, IMMUNOPRECIPITATION AND WESTERN BLOTTING*

For phosphorylation analyses and coimmunoprecipitation experiments, cells expressing CD16-nephrin were starved in serum free medium overnight, then stimulated for 10 min at 37°C by using a 1 µg/ml dilution of anti-CD16 antibody. For inhibition of SFK activity, cells were treated with 10µM PP2 (Sigma-Aldrich) for 3 hours prior to CD16 stimulation as described above in the continued presence of PP2. Lysates were prepared from transfected cells by using phospholipase C lysis buffer (50 mM HEPES, pH 7.5, 150 mM NaCl, 10% glycerol, 1% Triton X-100, 15 mM $MgCl_2$, 1 mM EGTA, 10 mM Na-$PP_i$, 100 mM NaF) supplemented with fresh protease inhibitors. Immunoprecipitation procedures have been described previously (Blasutig *et al.*, 2008).

For Western blotting, total lysates and immunoprecipitates were resolved on 8% SDS-PAGE gels, followed by semi-dry transfer to PVDF membrane, blocked for 30 minutes in TBST containing either 5% non-fat milk powder or BSA and incubated with the indicated primary antibody overnight at 4ºC. Detection was performed using ECL Western blotting substrate (Pierce). Blots were imaged using a ChemiDoc XRS+ (Biorad) or exposed to film (Pierce). Values used for densitometry were obtained using ImageLab v2.0 analysis software (Biorad).

### 3.3.5 *ANALYSIS OF NCK CONDITIONAL INDUCIBLE MUTANT MICE*

Inducible podocyte-specific Nck2 knockout mice on a Nck1 null background (referred to here as Nck1/2-cKO mice) containing the following transgenes (Podocin-rtTA; TetO-Cre; Nck2 $^{flx/flx;}$ Nck1 $^{-/-}$) have been described previously (Jones *et al.*, 2009).

We housed Nck1/2-cKO mice and their littermate controls (Nck2 $^{flx/flx;}$ Nck1 $^{-/-}$) together and collectively treated them with doxycycline in their food (2,000 mg/kg) (TD.09751 Harlan Tecklad; Madison, WI). Doxycycline was administered using this method for 1-2 weeks to generate animals with reduced Nck expression in podocytes. The duration of doxycycline treatment was determined to be the minimum length to allow sufficient reduction of Nck prior to development of proteinuria. Animal husbandry was approved by the University of Guelph

Animal Care Committee and carried out in accordance with Canadian Council on Animal Care protocols.

Mice were euthanized with $CO_2$ and immediately perfused with saline, followed directly by removal of the kidneys. Kidneys were either processed for immunofluorescence as described below or protein samples were prepared for Western blotting. For protein extraction, the renal cortex was separated and lysed (1mL/0.4 g tissue) in RIPA buffer (50 mM Tris pH 7.5, 150 mM NaCl, 10% glycerol, 1% NP-40, 0.25% Na-deoxycholate, 0.1% SDS, 1 mM EDTA), supplemented with fresh protease inhibitors via homogenization followed by sonication, then centrifuged at 13,000 rpm for 20 minutes to remove any debris. Total protein samples were prepared from the resulting supernatant.

### 3.3.6 *IMMUNOFLUORESCENCE*

Kidneys were flash frozen in cryomatrix (Thermo). 5µm sections were cut onto Superfrost Plus slides (Fisher) on a cryostat (Shandon). Sections were fixed and permeabilized in acetone for 10 minutes at -20°C, blocked in buffer containing 10% goat serum and phosSTOP tablet (Roche) and incubated with primary antibodies overnight at 4°C (guinea pig anti-nephrin (1:100) and rabbit anti-$pY^{1217}$ nephrin (1:50)). After washing, sections were incubated with secondary antibodies for 30 minutes at 25°C (goat anti-guinea pig Alexa Fluor 488 and goat anti-rabbit Alexa Fluor 594, both 1:400). Finally, slides were mounted using Prolong Gold antifade reagent with DAPI mounting media (Invitrogen). Cryosection slides were visualized using a Leica M2 125 epifluorescence microscope with a 40X objective lens. Images were captured using Volocity and processed with Adobe Photoshop. The Alexa fluorophore-conjugated secondary antibodies obtained from Invitrogen (Carlsbad, CA, USA) for immunofluorescence were: goat anti-guinea pig 488 (A-11076) and goat anti-rabbit 594 (A11037).

### 3.3.7 *STATISTICAL ANALYSIS*

Experiments were performed a minimum of three times. Differences between two groups were analyzed using the Student's *t* test, while differences between three or more groups were compared using ANOVA followed by Tukey's test with specific contrasts used for comparisons between multiple groups of means. Statistical significance was defined as $p<0.05$. Values are reported as mean ± standard error. Statistical analysis was performed using SAS version 9.2 (Cary, NC, USA) for ANOVA while GraphPad Prism version 5.04 (San Diego, CA, USA) was used for *t* tests. All graphs were prepared using GraphPad Prism.

## 3.4 **RESULTS**

### 3.4.1 *NCK AUGMENTS NEPHRIN TYROSINE PHOSPHORYLATION*

During our earlier analyses of interactions between nephrin and Nck (Blasutig *et al.*, 2008), we noticed increased levels of nephrin tyrosine phosphorylation upon co-expression of Nck, compared to expression of nephrin alone. This prompted us to investigate if Nck could be responsible for the difference in phosphorylation. We first confirmed that the presence of exogenous Nck1 or Nck2 could impact nephrin phosphorylation. When either Nck1 or Nck2 was co-expressed with full length nephrin in HEK293T cells, we observed increased amounts of nephrin tyrosine phosphorylation (Figure 3.1A). Similarly, using our chimeric CD16-nephrin construct containing the cytoplasmic tail of nephrin, which we have previously shown undergoes tyrosine phosphorylation following CD16-induced clustering (Blasutig *et al.*, 2008), we found that both Nck1 and Nck2 increased the basal amount of nephrin tyrosine phosphorylation observed in the absence of CD16-induced clustering, which increased further following CD16-induced clustering (Figure 3.1B).

We then used our phospho-specific antibodies against $Y^{1193}$ and $Y^{1217}$ (Jones *et al.*, 2009) to determine whether the increased phosphorylation on nephrin was occurring on these important downstream signaling sites. We found that, similar to total phosphotyrosine levels, there was

more nephrin phosphorylation with Nck1 and Nck2 at both $Y^{1193}$ and $Y^{1217}$ (Figure 3.1C). Interestingly, the observed increase in total nephrin phosphorylation as well as site specific phosphorylation was consistently larger with Nck2 as compared to Nck1. We also found that overall nephrin phosphorylation showed a dose-dependent increase with Nck expression (data not shown).

To verify that this change in phosphorylation was specific to Nck, we performed a similar experiment using the adaptor protein Grb2, which is also composed entirely of SH2 and SH3 domains. We observed no change in nephrin phosphorylation in the presence of Grb2 (Figure 3.1D), suggesting that the enhancement seen with Nck reflects a unique function of the Nck family.

### 3.4.2 *NEPHRIN PHOSPHORYLATION REQUIRES THE SH3 DOMAINS OF NCK*

Nck1 and Nck2 are both composed of three similar SH3 domains followed by a single SH2 domain (Figure 3.2A). To determine whether the SH3 domains contribute to increased nephrin phosphorylation, we employed mutant versions of Nck1 and Nck2, containing W-to-K substitutions in each of the SH3 domains (3xSH3*), rendering the domains unable to bind to their targets. We mutated all three SH3 domains as many Nck SH3 domain binding partners can bind to more than one Nck SH3 domain. As a control, we used Nck constructs with mutated SH2 domains (SH2*) containing an R-to-M substitution, which are unable to interact with nephrin (Verma *et al.*, 2006; Blasutig *et al.*, 2008).

Interestingly, we observed that expression of mutant versions of Nck1 or Nck2 lacking functional SH3 domains with CD16-nephrin significantly impaired Nck-mediated nephrin tyrosine phosphorylation (Figure 3.2B). We found that wildtype Nck1 produced around a 10 fold increase in CD16-nephrin phosphorylation relative to control cells expressing vector alone ($p<0.05$), whereas with the 3xSH3* mutant, only 43.1 ± 12.6% of the amount of phosphorylation seen with wildtype Nck1 was observed ($p<0.05$). More strikingly, wildtype Nck2 increased CD16-nephrin phosphorylation approximately 200 fold relative to CD16-nephrin alone ($p<0.05$). The amount of CD16-nephrin phosphorylation observed with 3xSH3* mutant Nck2 was 42.3 ±

5.3% of the amount of phosphorylation observed with wildtype Nck2 ($p<0.05$). Similar findings were obtained with full-length nephrin (Figure 3.3).

We observed that mutation of all three SH3 domains in Nck1 or Nck2 produced a similar relative decrease in nephrin phosphorylation (~40% of the amount seen with the corresponding wildtype Nck), suggesting that these domains perform equivalent functions in Nck1 and Nck2. To map the contributions of individual SH3 domains to nephrin phosphorylation, we expressed Nck1 mutants containing only a single functional SH3 domain (SH3-1, SH3-2, SH3-3) (as illustrated in Figure 3.2A) along with CD16-nephrin in HEK293T cells, with wildtype and 3xSH3* Nck1 serving as controls. We noted a significant reduction in nephrin phosphorylation with the SH3-2 construct (40.2 ± 9.3%) compared to wildtype Nck1 (100%) ($p<0.05$), which was equivalent to the reduction seen with the full 3xSH3* mutant (43.1 ± 12.6%) (Figure 3.2C). This effect was not seen with the SH3-1 (104.1 ± 19.8%) or SH3-3 (91.6 ± 7.2%) constructs, or when only the second SH3 domain was mutated (SH3-1,3; 85.3% ± 13.2% ) (Figure 3.2C). These results indicate that both the first and third SH3 domains of Nck can mediate binding to proteins that control nephrin tyrosine phosphorylation, while the second SH3 domain does not contribute appreciably to this process.

Similar to what we observed with Grb2 (Figure 3.1D), neither of the SH2* mutants altered nephrin phosphorylation relative to the amount observed with CD16-nephrin alone ($p>0.05$) (Figure 3.2B). As previous findings have clearly established that the interaction between nephrin and Nck requires binding of the Nck SH2 domain to phosphorylated tyrosine residues on nephrin (Jones *et al.*, 2006; Li *et al.*, 2006; Verma *et al.*, 2006; Blasutig *et al.*, 2008), our results suggest that the increase in nephrin phosphorylation seen with wildtype Nck is dependent on SH2-mediated recruitment of Nck to nephrin, and potentially via SH3-mediated association of a tyrosine kinase with Nck.

### 3.4.3 *HYPER-PHOSPHORYLATION OF NEPHRIN CORRELATES WITH FYN RECRUITMENT AND ACTIVATION*

The SFK Fyn plays a central role in podocyte foot process architecture, and given its ability to phosphorylate nephrin both *in vitro* (Harita *et al.*, 2009) and *in vivo* (Verma *et al.*, 2003), we examined whether this tyrosine kinase might be responsible for the increase in nephrin phosphorylation mediated by Nck adaptor proteins. To test if the increase in nephrin phosphorylation was a result of the action of SFKs, we blocked their activity using PP2, which is a SFK inhibitor. Treatment with PP2 suppressed the effect on Nck1-mediated CD16-nephrin phosphorylation, both in the presence and absence of CD16 clustering (Figure 3.4A). Similarly, PP2 decreased the amount of CD16-nephrin phosphorylation observed with Nck2 (Figure 3.4B). We also found that the interaction between nephrin and Nck induced by CD16 clustering was eliminated in cells treated with PP2 (Figure 3.4B).

Having observed that SFK activity was required to increase nephrin phosphorylation in the presence of Nck (Figure 3.4), we hypothesized that Nck and Fyn might form a signaling complex at the plasma membrane which affects nephrin phosphorylation. Using our CD16 clustering system, we expressed CD16-nephrin with wildtype as well as the SH2* and 3xSH3* mutants of Nck1 and Nck2, then examined binding between Fyn and Nck1 or Nck2 following clustering of CD16-nephrin (Figure 3.5A). We observed that the binding of wildtype and mutant Nck to Fyn by co-immunoprecipitation correlated closely with the results we previously obtained with the same Nck constructs regarding total nephrin phosphorylation. Analogous to the effect of Nck on nephrin phosphorylation, we observed the strongest interaction of Fyn with wildtype Nck, with Nck2 showing a more robust interaction than Nck1. We were able to detect a very weak interaction between Fyn and both 3xSH3* Ncks, which correlates with 3xSH3* mutant Nck having a lesser effect on nephrin phosphorylation. We did not observe any binding of SH2* Nck to Fyn as anticipated; Fyn is localized at the plasma membrane and as SH2* Nck cannot interact with nephrin (Verma *et al.*, 2006; Blasutig *et al.*, 2008), it is not recruited to the plasma membrane and so remains spatially segregated from Fyn in the cytoplasm.

We next investigated whether the presence of Nck might directly influence the activity of Fyn. To detect active Fyn, we used an antibody which recognizes the C-terminal SFK tyrosine $Y^{527}$ only when it is de-phosphorylated and therefore released from the inhibitory intra-molecular interaction with its SH2 domain. We utilized this antibody to detect active Fyn and compared it with total Fyn in order to determine the level of Fyn activity in lysates from cells expressing Nck2 and/or CD16-nephrin (Figure 3.5B). We observed a 2.3 ± 0.30 fold increase in active Fyn when CD16-nephrin was expressed with Nck2 as compared to CD16-nephrin alone ($p<0.05$) (Figure 3.5C). Notably, expression of Nck2 alone did not produce an increase in Fyn activity, ruling out a nephrin independent effect of Nck2 on Fyn activity. Collectively these data suggest that the mechanism by which Nck regulates nephrin phosphorylation occurs through an interaction with Fyn—likely involving the SH3 domains of Nck—which leads to increased Fyn activation.

### 3.4.4 *INCREASED NEPHRIN PHOSPHORYLATION CORRELATES WITH ACTIVATION OF NEPHRIN SIGNALING PATHWAYS*

Since we observed a global increase in nephrin tyrosine phosphorylation in the presence of Nck, we next asked whether this increase translated into the activation of downstream nephrin signaling pathways. In addition to Nck, phosphorylated nephrin recruits p85 and activates PI3K-dependent signaling (Zhu *et al.*, 2008), which includes phosphorylation of $T^{308}$ and $S^{473}$ on Akt. To examine changes in the activation state of Akt, we co-expressed HA-tagged Akt with CD16-nephrin and/or Nck2 in HEK293T cells and monitored Akt phosphorylation by Western blotting of cell lysates. We observed increased phosphorylation on both sites on Akt only when CD16-nephrin and Nck2 were co-expressed (Figure 3.6A). Specifically, Akt phosphorylation on $T^{308}$ was increased 2.2 ± 0.21 fold ($p<0.05$), while phosphorylation of $S^{473}$ was increased 5.9 ± 1.5 fold ($p<0.05$) with the addition of Nck2 as compared to CD16-nephrin alone (Figure 3.6B). Phosphorylation on both sites was not appreciably altered when Nck2 was expressed in the absence of CD16-nephrin (Figure 3.6A, right panel).

Another p85/PI3K signaling pathway which has recently been elucidated in the podocyte (Berger and Moeller, 2011) involves cofilin-1, which when activated by slingshot, can promote

actin rearrangement (Oser and Condeelis, 2009). We analyzed cofilin phosphorylation on $S^3$—which reflects its inactive state—when CD16-nephrin and Nck2 were expressed alone or in combination (Figure 3.6C). Quantitation of phosphorylated cofilin observed in each case revealed that the amount of phosphorylated cofilin observed when CD16-nephrin was clustered in the presence of Nck2 decreased by 40% (0.61 ± 0.056) compared to the amount observed with CD16-nephrin and vector alone (1.0) ($p<0.05$), while expression of Nck2 alone did not alter cofilin activity (Figure 3.6D). The decrease in phosphorylated cofilin indicates an increase in cofilin activation downstream of CD16-nephrin in the presence of Nck2. Together these data demonstrate that the Nck2 mediated increase in nephrin phosphorylation alters nephrin signaling more broadly as it leads to the activation of two separate pathways downstream of the nephrin p85/PI3K axis.

### 3.4.5 *NEPHRIN PHOSPHORYLATION IS REDUCED IN VIVO FOLLOWING PODOCYTE SPECIFIC DEPLETION OF NCK*

Our *in vitro* results clearly show that changes in Nck levels can alter nephrin phosphorylation. To validate these findings in an *in vivo* system, we took advantage of our existing mouse model system to conditionally modulate Nck levels. This system uses an inducible method (Podocin-rtTA/TetO-Cre) to genetically delete Nck2 specifically in podocytes of mice lacking Nck1 (Jones *et al.*, 2009), referred to here as Nck1/2-cKO mice. Using this system, we have previously demonstrated that loss of both Nck1 and Nck2 in podocytes of adult mice via administration of doxycycline (Dox) leads to progressive renal failure in about 4-6 weeks (Jones *et al.*, 2009). To avoid any complications related to the onset of renal disease, animals were induced for 1-2 weeks with lower levels of Dox, which allowed us to generate Nck1/2-cKO animals which had reduced, but not absent, levels of Nck2 in podocytes (Figure 3.7A) and which did not develop renal disease (data not shown). Analysis of nephrin phosphorylation on $Y^{1217}$ via immunoblotting of lysates prepared from the renal cortex of Nck1/2-cKO and control littermates revealed a striking decrease in phosphorylation upon removal of Nck expression in podocytes which was not seen in control animals also exposed to Dox (Figure 3.7A). Importantly, the levels of total nephrin expression remained unchanged (Figure 3.7A). We further confirmed these observations using immunofluorescence on kidney

cryosections obtained from Dox-treated animals. Nephrin phosphorylation on $Y^{1217}$ was clearly seen in the glomeruli of Nck1/2-cKO and control animals prior to Dox exposure (Figure 3.7B and data not shown). However, following treatment with Dox, glomeruli from Nck1/2-cKO animals showed reduced $Y^{1217}$ phosphorylation compared to control littermates, while levels of total nephrin remained comparable (Figure 3.7B). These results support the notion that the positive feedback loop that we have characterized *in vitro*, where Nck-based recruitment of Fyn contributes to nephrin phosphorylation, also occurs *in vivo*, as induced deletion of Nck expression in podocytes leads to rapid loss of nephrin phosphorylation.

## 3.5 DISCUSSION

We are interested in the mechanisms responsible for regulation of nephrin tyrosine phosphorylation by Fyn and related SFKs. In the present study, we observed that the Nck family of adaptors, which bind to phosphorylated nephrin, play a previously unappreciated role in modulating nephrin phosphorylation. We have shown that both Nck1 and Nck2 can increase nephrin phosphorylation *in vitro*, leading to engagement of downstream signaling pathways including activation of Akt and cofilin, and that reduced Nck expression in podocytes *in vivo* leads to rapid loss of nephrin phosphorylation. We have also provided evidence demonstrating that this enhanced phosphorylation of nephrin is likely due to Fyn activation, as the effects can be blocked by inhibition of SFK activity. Furthermore, we found increased activation of Fyn in the presence of Nck as well as SH3 domain-mediated association of Nck with Fyn, thereby providing a potential mechanism for Nck-mediated spatial control of nephrin phosphorylation and subsequent signaling.

### 3.5.1 *DIFFERENCES BETWEEN NCK1 AND NCK2*

Both Nck1 and Nck2 significantly increase nephrin phosphorylation, though the effect seems to be greater with Nck2. One explanation for increased phosphorylation with Nck2 could be that the SH2 domain of Nck2 has a higher affinity for the pY motifs of nephrin than Nck1, however studies have determined that the SH2 domains of Nck1 and Nck2 have similar binding

affinities to each of the three YDxV motifs of nephrin (Blasutig *et al.*, 2008) as well as to other known pY sequences (Frese *et al.*, 2006). Therefore, it seems more likely that the difference in the amount of nephrin phosphorylation between Nck1 and Nck2 should instead be attributed to variable recruitment of Fyn via the SH3 domains of Nck. Indeed, we found that there was a stronger interaction of Fyn with Nck2 than with Nck1, which is in agreement with Nck2 inducing a larger amount of nephrin phosphorylation. In both cases, mutation of the SH3 domains dramatically reduced Fyn binding, suggesting that Nck1 and Nck2 interact with Fyn through a similar mechanism. Despite the lesser amount of binding between Nck1 and Fyn, it is enough to augment nephrin phosphorylation, consistent with previous observations that Nck SH3 domains can participate in weak interactions which are functionally relevant (Vaynberg *et al.*, 2005; Hake *et al.*, 2008). Furthermore, examination of podocytes from Nck2 knockout mice did not reveal any abnormalities (Jones *et al.*, 2006), suggesting that Nck1 can compensate for Nck2 *in vivo*.

### 3.5.2 *Contributions of the SH3 domains of Nck to nephrin phosphorylation*

While we observed increased nephrin phosphorylation with wildtype Nck, this effect was compromised when either the SH2 domain or all of the SH3 domains of Nck were mutated. However, the reduction in nephrin phosphorylation is likely due to two different mechanisms. Firstly, as the SH2 domain of Nck is the sole mediator of the interaction between phosphorylated nephrin and Nck (Verma *et al.*, 2006; Li *et al.*, 2006), mutation of the SH2 domain effectively creates a version of Nck which cannot interact with nephrin and remains spatially segregated from nephrin signaling at the plasma membrane. SH2* Nck therefore does not have any effect on nephrin phosphorylation (Figure 3.2B), similar to what is seen with Grb2 (Figure 3.1D). Secondly, even when all three SH3 domains of Nck were mutated, this 3xSH3* Nck was still able to induce an increase in nephrin phosphorylation, though it was approximately 40% of the amount generated with wildtype Nck. When we examined the role of individual SH3 domains, we found that if only the first or third SH3 domain was functional, the level of nephrin phosphorylation was similar to that seen with wildtype Nck, and that the combination of the two SH3 domains together (SH3-1,3 Nck) did not further enhance phosphorylation levels. This

implies that there is no synergistic effect on nephrin phosphorylation with multiple Nck SH3 domains, consistent with our previous findings regarding actin polymerization (Blasutig *et al.*, 2008). By contrast, the second SH3 domain of Nck alone was not able to augment nephrin phosphorylation, suggesting that it may be unable to bind to Fyn. Given that the second SH3 domain binds strongly to N-WASp and is sufficient to induce full actin polymerization at sites of nephrin clustering (Blasutig *et al.*, 2008), it is reasonable to conclude that the multiple SH3 domains on Nck could simultaneously play divergent roles in nephrin signaling.

### 3.5.3 *Role of the SH3 domains of Nck in regulation of Fyn kinase activity*

Nck has previously been implicated in the alteration of kinase activity, though the mechanism by which this occurs is not well understood. The first and second SH3 domains of Nck1 were found to activate Abl kinase (Smith *et al.*, 1999) likely via binding of the second SH3 domain of Nck to a proline rich region of Abl (Miyoshi-Akiyama *et al.*, 2001). More recently, interaction of Nck2 with Fyn downstream of VEGFR-2 has been shown to lead to Fyn activation (Lamalice *et al.*, 2006), though no mechanism for the interaction was suggested. Consideration of potential interactions between Nck and Fyn in the context of our data suggests some possible mechanisms for how Nck could bind to Fyn and alter its activity. One possibility is that either the first or third SH3 domain of Nck could bind to the SH2-kinase linker region known to engage the SH3 domain of Fyn (Gonfloni *et al.*, 1997). Binding of Nck to the linker region could release the Fyn SH3 domain and allow it to bind to an external ligand which can promote Fyn activation (Solheim *et al.*, 2008).

Alternatively, one of the SH3 domains of Nck could be engaging in a non-canonical interaction with either the SH3 or SH2 domain of Fyn. This idea is not entirely without precedent, given that non-canonical interactions with other modular domains have been reported for a number of SH2 and SH3 domains, including the Fyn SH2 (Panchamoorthy *et al.*, 1994) and SH3 (Panchamoorthy *et al.*, 1994; Chan *et al.*, 2003) domains, as well as the second (Li *et al.*, 2009) and third (Tu *et al.*, 1998; Barda-Saad *et al.*, 2010) SH3 domains of Nck. Such an interaction would likely alter the conformation of the Fyn SH3 or SH2 domain, a process which has been found to result in Fyn activation through non-canonical binding of its SH3 domain to

the SH2 domain of SAP (Simarro *et al.*, 2004). Additionally, non-canonical interactions can engage different surfaces than those used for proline-based ligands, which may explain why W-to-K SH3 domain mutations which eliminate canonical binding do not significantly disrupt non-canonical binding (Panchamoorthy *et al.*, 1994; Tu *et al.*, 1998). Indeed, the W-to-K mutations in the Nck SH3 domains still allow some increase in nephrin phosphorylation and binding to Fyn. Further investigation into these possibilities may aid in determining the exact nature of the complex interaction between Nck and Fyn.

### 3.5.4 *IMPORTANCE OF NEPHRIN SIGNALING PATHWAYS TO PODOCYTE FUNCTION*

Signaling pathways downstream of phosphorylated nephrin are required for proper organization of the podocyte actin cytoskeleton which controls foot process architecture and ultimately podocyte function (Welsh and Saleem, 2010). In this work, we have uncovered a role for Nck in directly regulating Fyn-mediated phosphorylation of nephrin, which in turn potentiates activation of p85 signaling pathways known to influence podocyte cytoskeletal dynamics, namely Akt and cofilin. Disruption of these signaling pathways has been correlated with the development of renal disease. Decreased Akt phosphorylation on $S^{473}$ has been reported during the onset of proteinuria in the rat PAN model (Zhu *et al.*, 2008). Furthermore, mice with a podocyte-specific knockout of cofilin developed renal disease (Garg *et al.*, 2010), and phosphorylation of cofilin—corresponding with inactivation—was increased in some forms of human glomerular disease including minimal change disease (Ashworth *et al.*, 2010). Interestingly, decreased phosphorylation on the Nck binding sites $Y^{1193}$ and $Y^{1217}$ has been observed in the same animal models (Uchida *et al.*, 2008; Jones *et al.*, 2009) and human diseases (Uchida *et al.*, 2008) where decreased p85-based signaling has been reported (Zhu *et al.*, 2008; Ashworth *et al.*, 2010). Our findings thus suggest a model (see below) by which recruitment of Nck to nephrin contributes to the phosphorylation of additional tyrosine residues required for binding other key molecules. Such a global role for Nck in modulating nephrin phosphotyrosine-based signaling underscores the essential requirement for Nck expression in podocytes throughout life (Jones *et al.*, 2006; Jones *et al.*, 2009).

### 3.5.5 *MODEL FOR NCK-MEDIATED REGULATION OF NEPHRIN TYROSINE PHOSPHORYLATION*

We have outlined a possible model of how Nck could be contributing to regulation of nephrin phosphorylation in the podocyte (Figure 3.8). At the slit diaphragm, nephrin can be phosphorylated by Fyn, creating a binding site for the SH2 domain of Nck. Once Nck is recruited to phosphorylated nephrin, its SH3 domains appear to be able to promote activation of Fyn, through a still to be determined mechanism. This creates a positive feedback loop which allows for maximal phosphorylation of nephrin and recruitment of Nck as well as other binding partners, which together promote nephrin signaling.

This model is supported by observations that a fraction of nephrin is phosphorylated on $Y^{1193}$ in the normal rat glomerulus (Zhang *et al.*, 2010b), as well as evidence that nephrin, Fyn and Nck2 are all present in detergent resistant membranes isolated from mouse glomeruli (Verma *et al.*, 2006). Further, our *in vivo* results show that reduction of Nck2 protein levels specifically in podocytes is followed by a decrease in nephrin phosphorylation, which occurs prior to the onset of renal disease known to be mediated by podocyte-specific loss of Nck (Jones *et al.*, 2009). Together, this suggests that the pathway we have described may be actively occurring as part of normal podocyte dynamics.

In summary, our study demonstrates a role for Nck in the regulation of nephrin phosphorylation, which leads to the initiation of multiple downstream signals that coordinate efficient actin polymerization. This work supports the emerging hypothesis that—in the podocyte—the engagement of signaling pathways downstream of phosphorylated nephrin is an important contributor to the proper maintenance of podocyte foot process architecture.

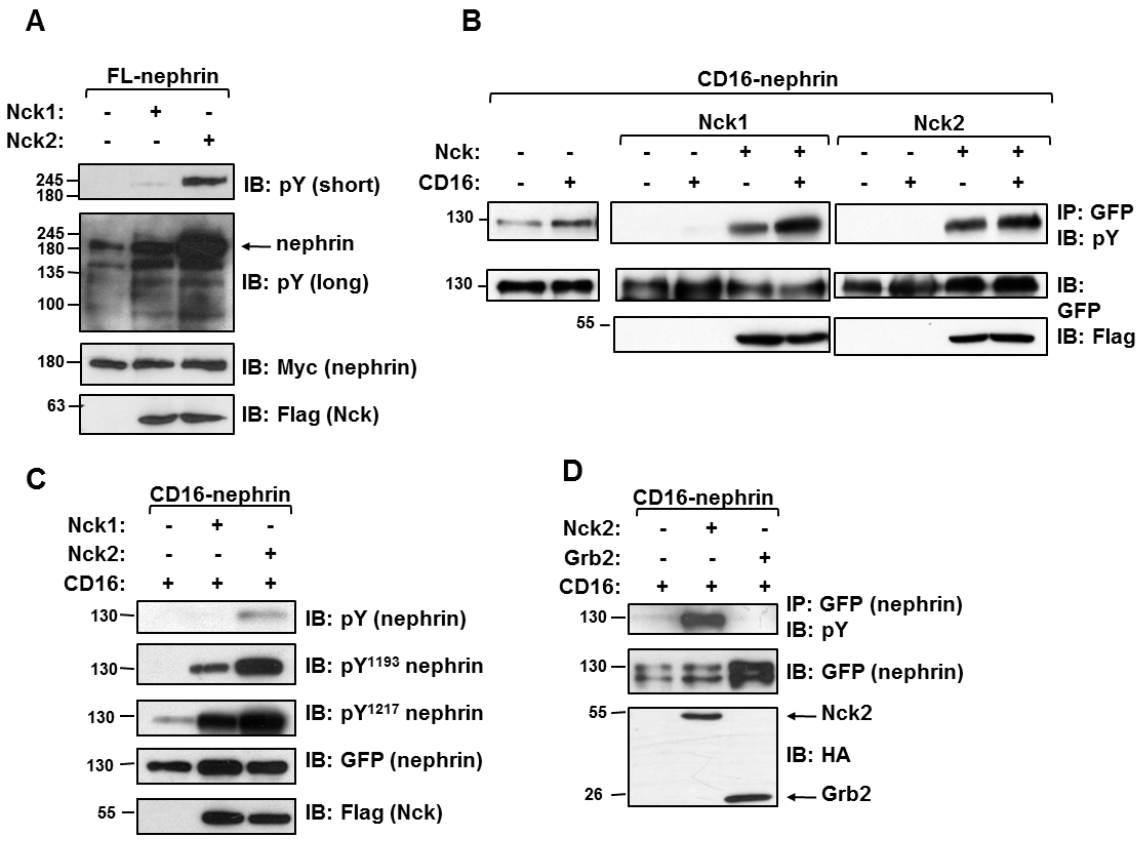


**Figure 3.1 Nck increases nephrin tyrosine phosphorylation.**

A) HEK293T cells were transfected with full length (FL) Myc-tagged nephrin and Flag-tagged Nck1 or Nck2 as indicated and lysates were immunoblotted (IB) for phosphotyrosine (pY), Myc or Flag. Coexpression of Nck1 or Nck2 increases overall nephrin phosphorylation compared to the baseline phosphorylation seen in the long exposure. B) HEK293T cells were transfected with GFP-tagged CD16-nephrin and Nck1 or Nck2, then stimulated with CD16 (+) or left untreated (–). CD16-clustering induces an increase in nephrin phosphorylation (left panel), which is enhanced in the presence of Nck1 or Nck2 and further increased after CD16 clustering (middle and right panels). Phosphorylation of CD16-nephrin alone can be seen after long pY exposure (left panel), while phosphorylation of CD16-nephrin co-expressed with Nck is visible in short pY exposures (middle and right panels). C) Lysates from CD16-stimulated HEK293T cells expressing CD16-nephrin with or without Nck1 or Nck2 were immunoblotted as indicated to reveal increased levels of nephrin phosphorylation on residues $Y^{1193}$ and $Y^{1217}$ in the presence of Nck1 and Nck2. D) HEK293T cells were transfected with CD16-nephrin and HA-tagged Nck2 or Grb2 as indicated. CD16-induced hyperphosphorylation of nephrin is seen with Nck2 but not Grb2.

**Figure 3.2 Increased nephrin phosphorylation is dependent on the SH3 domains of Nck.**

A) Schematic illustrating the structure of Nck and the amino acid residues mutated to generate the SH2* and various SH3* mutant constructs in Nck1. The corresponding residues were mutated in Nck2. B) HEK293T cells were transfected with CD16-nephrin and various mutants of Nck1 or Nck2 as indicated. CD16-stimulated (+) lysates were examined for nephrin phosphorylation and Nck binding by Western blotting followed by densitometry to determine the amount of nephrin phosphorylation relative to wildtype Nck. With wildtype (WT) Nck1 (white) or Nck2 (black) normalized to 100%, the SH2 domain mutants (SH2*) do not cause an increase in CD16-nephrin phosphorylation for either Nck1 (5.4± 1.4%) or Nck2 (1.1 ± 0.43%) relative to the amount of phosphorylation observed with CD16-nephrin alone (Nck1: 10.6 ± 2.0%; Nck2: 0.47 ± 0.044%). Mutation of all SH3 domains (3xSH3*) leads to a decrease in nephrin phosphorylation to 43.1 ± 12.6% for Nck1 and 42.3 ± 5.3% for Nck2 of that observed with the wildtype Nck. The amount of nephrin phosphorylation correlates with the amount of Nck immunoprecipitated (IP) with nephrin. * indicates $p<0.05$ compared to wildtype for Nck1(1) and Nck2(2). C) Transfection of HEK293T cells with additional SH3 domain mutants of Nck1 and CD16-nephrin followed by CD16 stimulation (+) revealed that the first and third SH3 domains either alone (SH3-1, 104.1 ± 19.8%; SH3-3, 91.6 ± 7.2%) or in combination (SH3-1,3, 85.3% ± 13.2%) increase nephrin phosphorylation similarly to wildtype Nck1 (100%), while the second SH3 domain alone (SH3-2, 40.2 ± 9.3%) is equivalent to the 3xSH3* mutant (43.1 ± 12.6%). * indicates $p<0.05$ compared to wildtype.

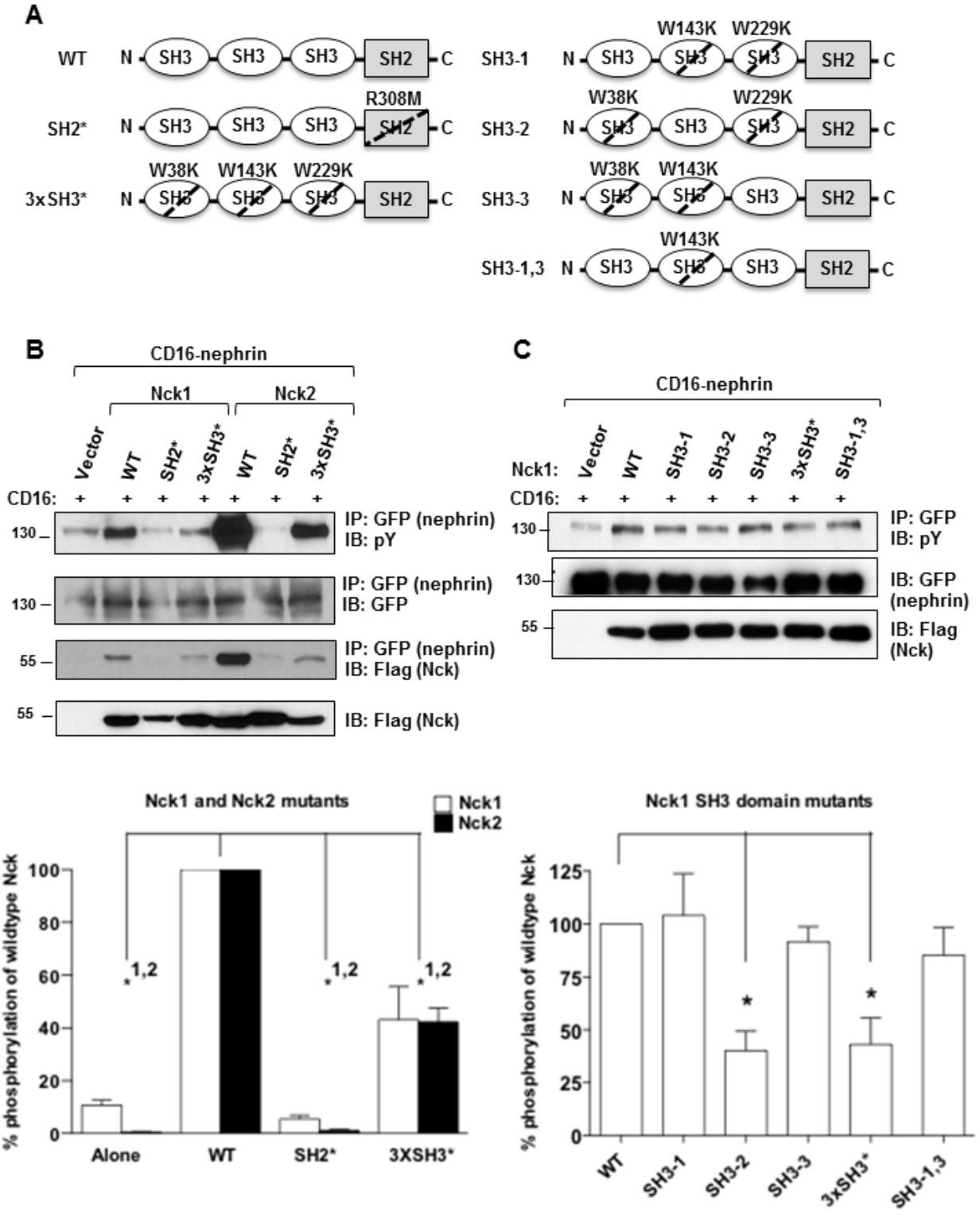
A
WT
SH2*
3xSH3*
SH3-1
SH3-2
SH3-3
SH3-1,3
N
C
SH3
SH2
R308M
W38K
W143K
W229K
B
CD16-nephrin
Nck1
Nck2
Vector
WT
SH2*
3xSH3*
CD16:
IP: GFP (nephrin)
IB: pY
IB: GFP
IB: Flag (Nck)
130
55
C
Nck1:
IP: GFP
IB: GFP (nephrin)
Nck1 and Nck2 mutants
Nck1
Nck2
% phosphorylation of wildtype Nck
Alone
Nck1 SH3 domain mutants

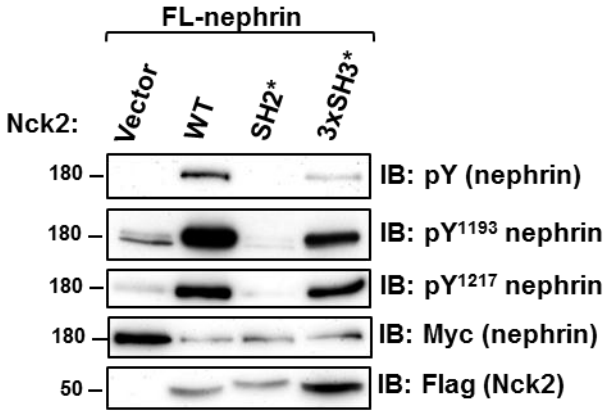


**Figure 3.3 Nck2 mutants have the same effect with full length nephrin as with the CD16 system.**

HEK 293T cells were transfected with full length (FL) Myc-tagged nephrin and Flag-tagged Nck2 as well as with the indicated Nck2 constructs. Lysates were immunoblotted for total nephrin and Nck as well as for nephrin phosphorylation using a general phosphotyrosine antibody as well as the phospho-specific pY1193 and pY1217 antibodies. As observed with the CD16 system, there is increased nephrin phosphorylation relative to the control with wild type Nck2, which does not occur with the SH2* mutant and there is reduced nephrin phosphorylation with the 3xSH3* mutant as compared to wild type Nck2.

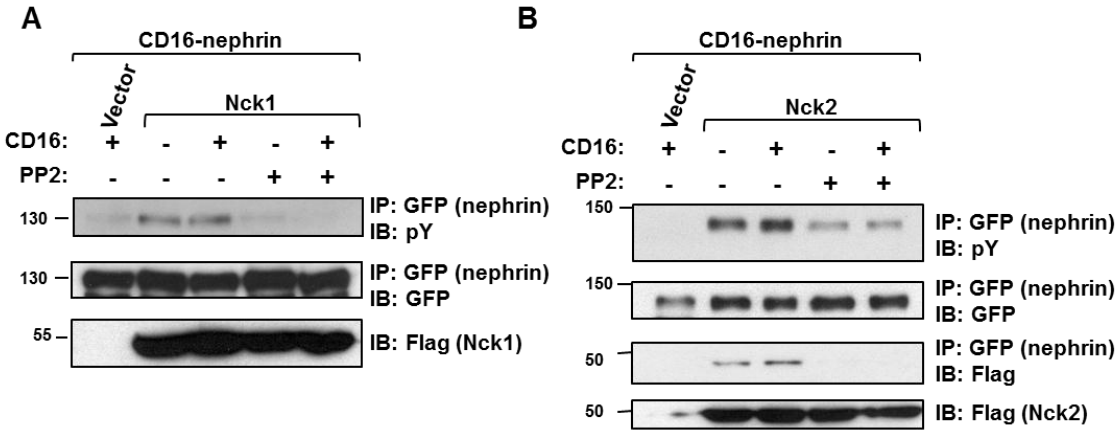


**Figure 3.4 Nck-induced hyperphosphorylation of nephrin requires SFK activity.**

A) HEK293T cells expressing CD16-nephrin and Nck1 were pre-treated with 10uM PP2 as indicated for 3 hours prior to stimulation with CD16 (+) to induce CD16-nephrin phosphorylation or left unstimulated (-). PP2 inhibition of SFKs blocks Nck1-mediated nephrin phosphorylation. B) Identical experiment as in A, except that Nck2 was used instead of Nck1. Treatment with PP2 reduces Nck2-induced hyperphosphorylation of nephrin and the interaction between Nck2 and nephrin as observed by co-immunoprecipitation (IP).

**Figure 3.5 Nck interacts with Fyn which increases nephrin phosphorylation and Fyn activation.**

A) HEK293T cells were transfected with CD16-nephrin and Nck1 or Nck2 constructs as indicated, then stimulated with CD16 (+) or left untreated (-). Both Nck1 and Nck2 co-immunoprecipitate (IP) with endogenous Fyn, however, we observed that the interaction with Fyn was much stronger for Nck2 compared to Nck1. The interaction between Fyn and Nck is very weak when all three SH3 domains are mutated and absent when the SH2 domain is mutated. The strength of these interactions correlates with the amount of nephrin phosphorylation seen in the lysates. B) HEK293T cells were transfected with Nck2 alone as a control, CD16-nephrin alone, or CD16-nephrin and Nck2 and those containing CD16-nephrin were stimulated with CD16 (+). Lysates were immunoblotted for un-phosphorylated $Y^{527}$ Src which recognizes activated SFKs and then reprobed for Fyn. C) Lysates were analyzed by densitometry to determine relative Fyn activity. Expression of Nck2 alone did not alter Fyn activity relative to CD16-nephrin alone. However, when Nck2 was co-expressed with CD16-nephrin, there was a $2.3 \pm 0.30$ fold increase in the amount of active Fyn relative to CD16-nephrin alone. * indicates $p<0.05$ compared to CD16-nephrin alone, n.s. indicates a non-significant difference.

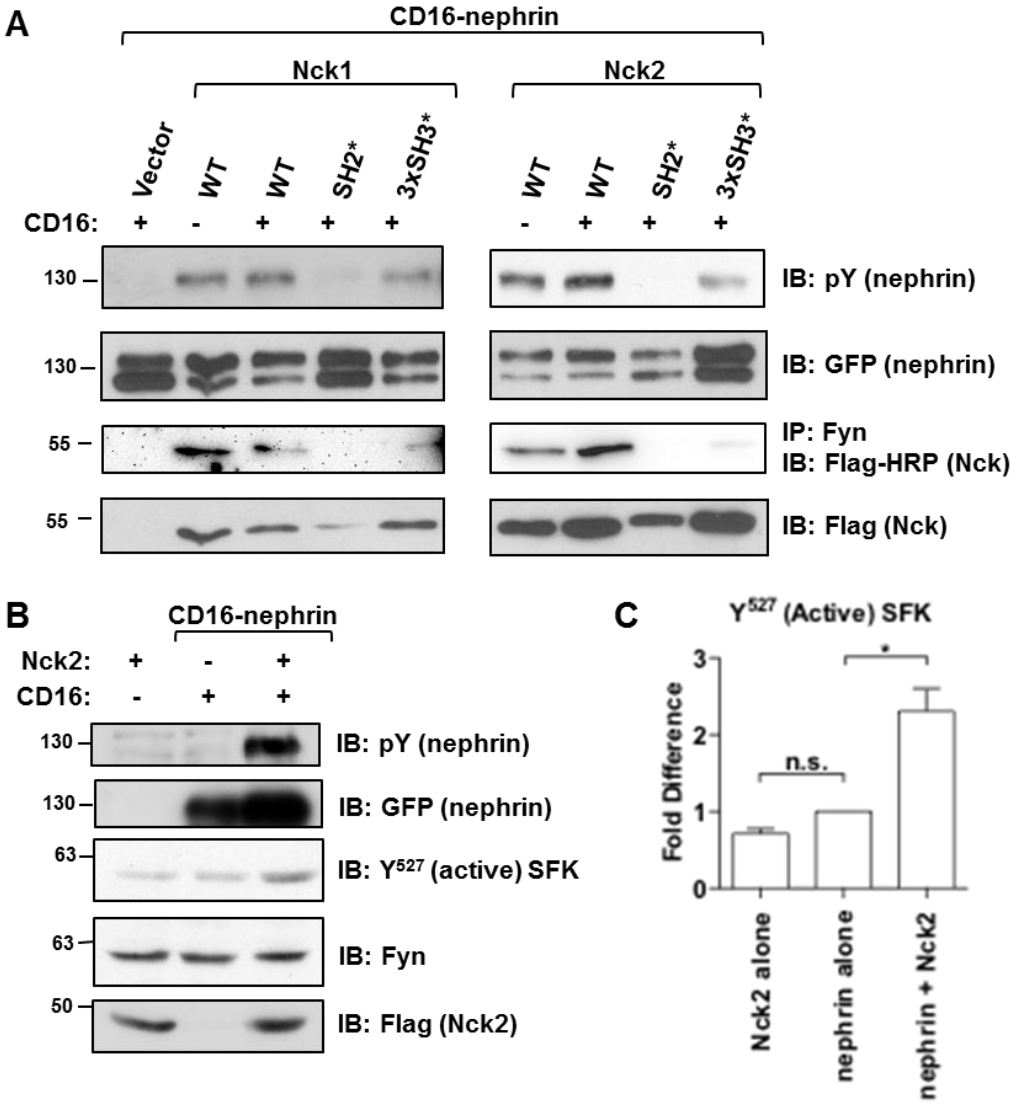
A
CD16-nephrin
Nck1
Nck2
Vector
WT
WT
SH2*
3xSH3*
WT
WT
SH2*
3xSH3*
CD16: + - + + + - + + +
130
130
55
55
IB: pY (nephrin)
IB: GFP (nephrin)
IP: Fyn
IB: Flag-HRP (Nck)
IB: Flag (Nck)
B
CD16-nephrin
Nck2: + - +
CD16: - + +
130
130
63
63
50
IB: pY (nephrin)
IB: GFP (nephrin)
IB: Y527 (active) SFK
IB: Fyn
IB: Flag (Nck2)
C
Y527 (Active) SFK
Fold Difference
3
2
1
0
n.s.
*
Nck2 alone
nephrin alone
nephrin + Nck2

**Figure 3.6 Hyperphosphorylation of nephrin correlates with increased downstream signaling activity.**

A) HEK293T cells were transfected with HA-tagged Akt, CD16-nephrin and Nck2, as indicated. All cells expressing CD16-nephrin were stimulated with CD16 (+) to induce nephrin phosphorylation. Western blotting was performed on lysates for phosphorylated and total Akt. Nck2 positively influenced Akt activation on both sites in the presence but not absence of CD16-nephrin. B) Densitometry showing that phosphorylation of Akt on $T^{308}$ increased 2.2 ± 0.21 fold, while phosphorylation of $S^{473}$ increased by 5.9 ± 1.5 fold with the addition of Nck2 to CD16-nephrin. Phosphorylation on these sites was not appreciably altered when Nck2 was expressed alone. C) HEK293T cells were transfected with Nck2 alone as a control, CD16-nephrin alone, or CD16-nephrin and Nck2 and those containing CD16-nephrin were stimulated with CD16 (+) to induce nephrin phosphorylation. Western blotting was performed on lysates for phosphorylated and total cofilin. D) Densitometry showing that the presence of Nck2 decreased cofilin phosphorylation by 40% (0.61 ± 0.056) compared to CD16-nephrin alone (1.0) and that expression of Nck2 alone did not alter cofilin activity. * indicates $p<0.05$ compared to CD16-nephrin alone in B and D, n.s. indicates a non-significant difference.

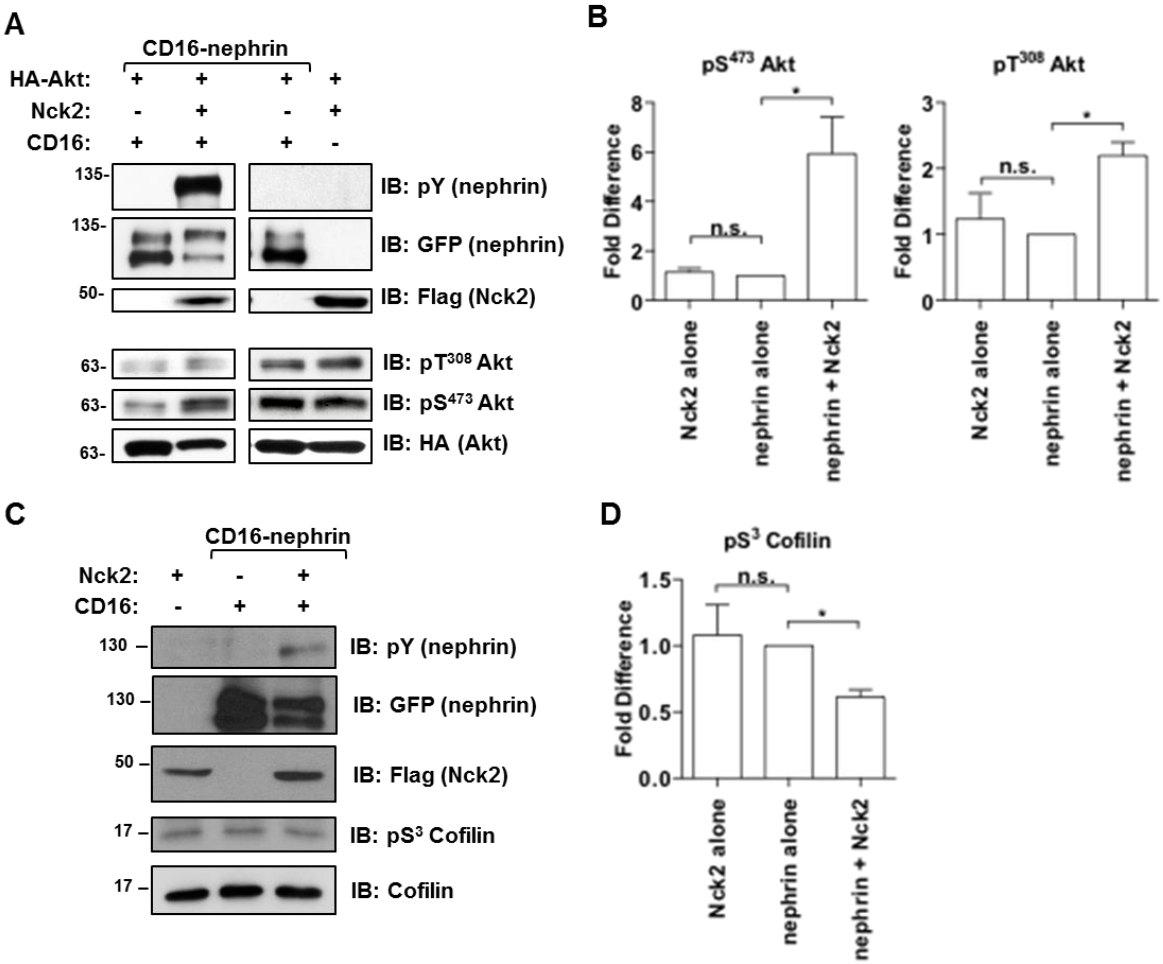
A
CD16-nephrin
HA-Akt: + + + +
Nck2: - + - +
CD16: + + + -
135-
IB: pY (nephrin)
135-
IB: GFP (nephrin)
50-
IB: Flag (Nck2)
63-
IB: pT308 Akt
63-
IB: pS473 Akt
63-
IB: HA (Akt)
B
pS473 Akt
pT308 Akt
Fold Difference
n.s.
*
Nck2 alone
nephrin alone
nephrin + Nck2
C
CD16-nephrin
Nck2: + - +
CD16: - + +
130
IB: pY (nephrin)
130
IB: GFP (nephrin)
50
IB: Flag (Nck2)
17
IB: pS3 Cofilin
17
IB: Cofilin
D
pS3 Cofilin
Fold Difference
n.s.
*
Nck2 alone
nephrin alone
nephrin + Nck2

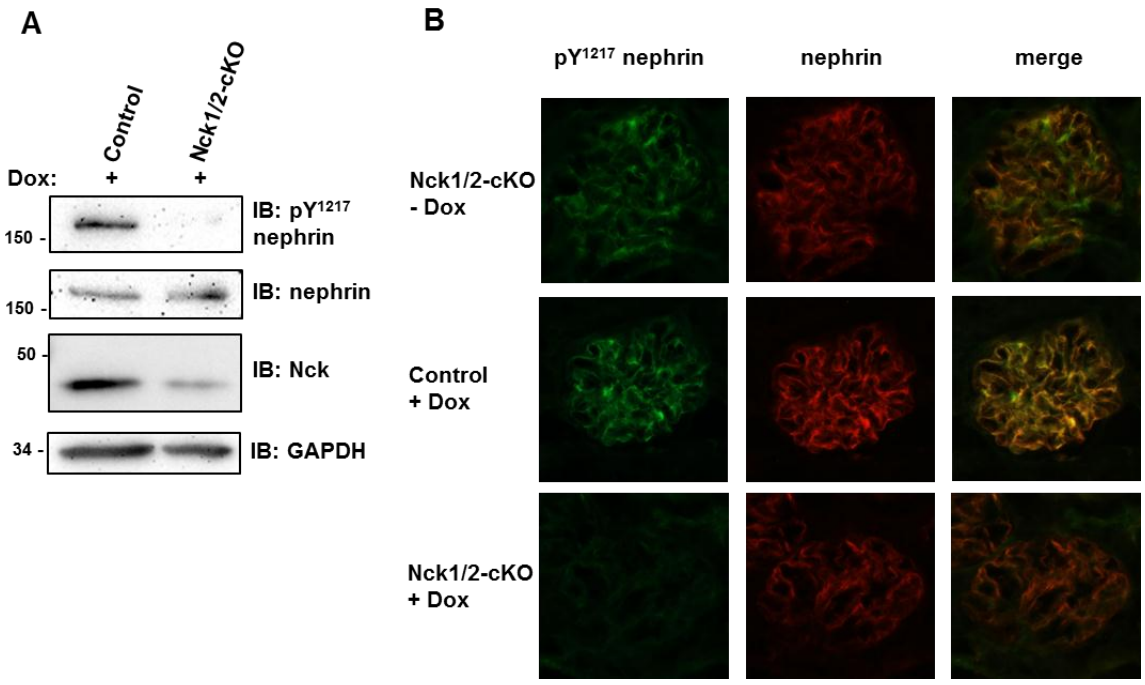


**Figure 3.7 Nephrin phosphorylation is reduced *in vivo* following podocyte-specific depletion of Nck2.**

A) Western blot analysis of kidney cortex lysates obtained from podocyte-specific Nck1/2 conditional knockout mice (Nck1/2-cKO) and control littermates exposed to doxycycline (Dox) for 1-2 weeks shows a decrease in phosphorylated (Y1217) nephrin but not total nephrin in Nck1/2-cKO animals. Reduced Nck expression is also only seen in Nck1/2-cKO animals, demonstrating the specificity of the Dox-induced gene excision. B) Dual immunofluorescence analysis of phosphorylated (pY1217) and total nephrin expression in glomeruli of Nck1/2-cKO mice and control littermates. Phosphorylated nephrin (green) and total nephrin (red) can be seen in Nck1/2-cKO animals prior to treatment with Dox (top panel). Upon Dox exposure, nephrin phosphorylation can still be readily observed in control animals (middle panel) but not Nck1/2-cKO animals (bottom panel). Despite the decreased nephrin phosphorylation, total nephrin expression remains unchanged in Dox treated Nck1/2-cKO animals.

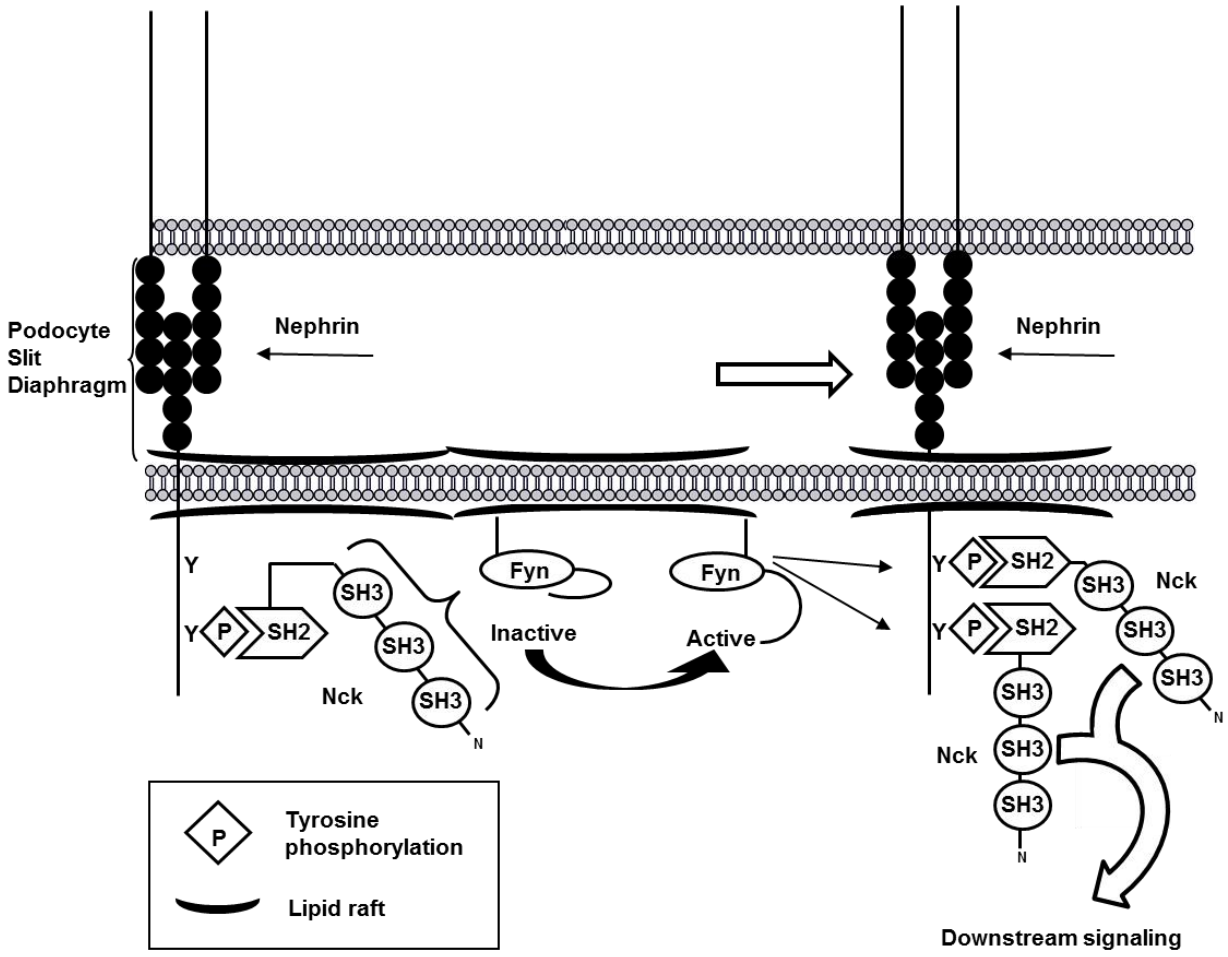


**Figure 3.8 Hypothetical model of Nck-mediated Fyn activation and its role in nephrin signaling at the slit diaphragm.**

At the podocyte slit diaphragm, nephrin is recruited into lipid rafts where it is initially phosphorylated by Fyn. Nephrin phosphorylation allows for the recruitment of Nck via its SH2 domain, thereby allowing the SH3 domains of Nck to interact with Fyn at the cell membrane, and in turn increase Fyn activation. This creates a positive feedback loop, wherein increased Fyn activity leads to the phosphorylation of adjacent nephrin molecules on multiple tyrosine residues. Additional Nck molecules as well as other binding partners can then be recruited to the newly phosphorylated nephrin complex, ultimately leading to the potentiation of downstream signaling pathways required for podocyte function.

# CHAPTER 4:

# ROLE OF NEPHRIN TYROSINE PHOSPHORYLATION IN MAINTENANCE OF PODOCYTE FOOT PROCESS ARCHITECTURE AND RESPONSE TO INJURY

## 4.1 ABSTRACT

Nephrin is a transmembrane component of the kidney slit diaphragm that plays a central role in organizing the unique morphology of actin-rich podocyte foot processes. The intracellular domain of nephrin contains several tyrosine residues that undergo phosphorylation, thereby initiating signaling events linking the slit diaphragm to the actin cytoskeleton. Human renal diseases characterized by podocyte foot process effacement and decreased filtration barrier function are associated with loss of this phosphorylation; however, it has not been clear whether phospho-nephrin signaling plays a causative or compensatory role in disease. To explore the function of nephrin tyrosine phosphorylation *in vivo*, we generated knock-in mice bearing tyrosine to phenylalanine mutations at three key adaptor protein binding sites, which seemingly compromise all nephrin phosphotyrosine-based signaling. Surprisingly, absence of nephrin tyrosine phosphorylation does not affect the initial formation of podocyte foot processes; however, as the mice age, they develop albuminuria accompanied by structural changes in the filtration barrier, including dilated capillary loops, irregular thickening of the glomerular basement membrane and podocyte foot process effacement, the extent of which are all influenced by genetic background. Furthermore, loss of nephrin tyrosine phosphorylation on these sites enhanced the susceptibility to transient podocyte injury. Our findings are consistent with a model in which dynamic changes in phosphotyrosine-based signaling confer plasticity to the podocyte actin cytoskeleton.

## 4.2 INTRODUCTION

Blood filtration in the kidney occurs in the glomerulus. Glomerular capillaries are composed of three layers: a fenestrated endothelium (Haraldsson and Nystrom, 2012), a glomerular basement membrane (GBM) (Abrahamson, 2012), and an outer layer of visceral epithelial cells known as podocytes. While damage to any of the three components can lead to kidney disease, research over the past two decades has established that podocyte injury is a significant contributor to many forms of renal failure (Leeuwis *et al.*, 2010).

Podocytes adopt a unique and complex three-dimensional architecture. Their cell bodies extend many microtubule-based primary and secondary processes, which branch into a regular pattern of smaller actin rich foot processes. Adjacent foot processes are connected to each other by a specialized cell-cell junction called the slit diaphragm, which plays an integral role in the mechanism of blood filtration.

The IgG family transmembrane protein nephrin is required for slit diaphragm formation, and mutations in nephrin lead to foot process effacement and proteinuria (Welsh and Saleem, 2010). The $Fin_{minor}$ mutation, which results in truncation of the cytoplasmic tail of nephrin, causes a similar disease phenotype as complete loss of nephrin, suggesting that this segment is essential for nephrin function. Within this segment, there are a number of conserved tyrosine residues (Table 4.1). Engagement of nephrin leads to their phosphorylation by Fyn kinase (Jones *et al.*, 2006; Verma *et al.*, 2006; Harita *et al.*, 2009) and recruitment of adapter proteins including p85/PI3K (Huber *et al.*, 2003b; Zhu *et al.*, 2008; Garg *et al.*, 2010), PLC-γ (Harita *et al.*, 2009) and Nck (Li *et al.*, 2006; Verma *et al.*, 2006; Jones *et al.*, 2006; Blasutig *et al.*, 2008), ultimately leading to the initiation of multiple signaling pathways including Akt activation (Huber *et al.*, 2003b; Zhu *et al.*, 2008; Garg *et al.*, 2010), actin polymerization (Jones *et al.*, 2006; Verma *et al.*, 2006; Blasutig *et al.*, 2008; Garg *et al.*, 2010; Venkatareddy *et al.*, 2011; George *et al.*, 2012), calcium signaling (Harita *et al.*, 2009) and lamellipodium formation (Zhu *et al.*, 2008; Venkatareddy *et al.*, 2011; George *et al.*, 2012). Interestingly, three of these tyrosine residues lie within YDxV-based binding motifs recognized by the Nck family of cytoskeletal adaptors, which we have previously shown are essential throughout life to initiate and maintain podocyte structure (Jones *et al.*, 2006; Jones *et al.*, 2009).

The dynamics of nephrin tyrosine phosphorylation in developing and mature podocytes, as well as in human kidney diseases and related animal models, have been examined using phospho-specific nephrin antibodies (Verma *et al.*, 2006; Uchida *et al.*, 2008; Jones *et al.*, 2009). While the significance of changes in nephrin tyrosine phosphorylation during podocyte health, injury and recovery remains somewhat unresolved (Patrakka and Tryggvason, 2007), as a whole, these studies have established that human kidney disease is generally associated with loss of both nephrin tyrosine phosphorylation and downstream signaling pathways. Nonetheless, it has not

been possible to determine whether perturbations in nephrin tyrosine phosphorylation directly contribute to the development of disease as a result of altered downstream signaling or rather if decreases in nephrin tyrosine phosphorylation occur during the progression of disease as a consequence of changes in other signaling pathways.

To resolve the significant question of whether nephrin tyrosine phosphorylation is required for podocyte function in both health and disease, we generated the nephrin$^{Y3F}$ knock-in mouse model which lacks all functional YDxV motifs. Surprisingly, absence of nephrin phosphorylation does not affect the initial formation of podocyte foot processes; however, as nephrin$^{Y3F/Y3F}$ mice age, they develop proteinuria accompanied by structural changes in the filtration barrier, including podocyte foot process effacement, irregular thickening of the GBM and dilated capillary loops, all of which are influenced by genetic background. Furthermore, nephrin$^{Y3F/Y3F}$ mice show enhanced susceptibility to transient podocyte injury. Our findings demonstrate that nephrin tyrosine phosphorylation plays an active role in the maintenance of podocyte foot processes and suggest there may be value in the investigation of potential therapeutic approaches which can increase nephrin phosphorylation.

## 4.3 MATERIALS AND METHODS

### 4.3.1 *GENERATION OF NEPHRIN$^{Y3F}$ MICE*

To generate nephrin$^{WT/Y3F}$ mice (official designation B6;129*Nphs1*$^{<Tm1.1>}$/Njns), three point mutations (p.Y1191F, p.Y1208F and p.Y1232F) were engineered into a construct containing the region from Exon 24 to Exon 29 of *Nphs1*. Homologous recombination of the targeting vector into C57Bl/6Jx129S6SvEv ES cells produced two independent clones. We examined nephrin$^{Y3F/Y3F}$ mice derived from both clones and saw similar phenotypes (data not shown). The animals used in this study were all derived from the same clone. After verification of germline transmission, mice were crossed to B6.129S1 Hprt-Cre mice in order to remove the floxed neomycin cassette. The resulting offspring were crossed once to C57Bl/6J and subsequently maintained on the C57Bl/6N background (#475; Charles River Canada).

Mice were genotyped by PCR using the primers *Nphs1*$^{Y3F}$-FW: (5'-GCATATGTGAACGCATGAGG-3') and *Nphs1*$^{Y3F}$-RV: (5'-GAAGGTGGTTGGTTGCAGTT-3'). PCR cycling conditions used were: 95ºC for 5 minutes, then 35 cycles of 94ºC (30 s), 59ºC (30 s), 72ºC (45 s), followed by a final extension at 72ºC for 5 minutes. DNA products were examined on 2% agarose gels.

B6;129 Nephrin$^{Y3F/Y3F}$ mice were bred onto the CD-1 (#472; Charles River Canada) background for 6 generations to generate CD-1.B6;129*Nphs1*$^{<Tm1.1>}$/Njns mice prior to intercrossing heterozygous animals. Data includes results from animals between generations 6 and 8. Independently, B6;129 nephrin$^{Y3F/Y3F}$ mice were crossed onto the FVB/N background (#207; Charles River Canada) for 5 generations to generate FVB.B6;129*Nphs1*$^{<Tm1.1>}$/Njns mice. The resulting mice were assessed by speed congenic analysis and animals with > 94 % FVB genome were intercrossed.

There were similar histological findings in male and female nephrin$^{Y3F/Y3F}$ mice, and data from both sexes is represented in this study. As the onset of proteinuria was generally earlier in males, male mice were used for all urine analysis, with the exception of the LPS study.

Animals were housed on a 12 hour / 12 hour artificial light cycle. They had free access to standard chow (#2014; Harlan Teklad) and drinking water.

### 4.3.2 *EVALUATION OF PROTEINURIA*

Mice were placed into a metabolic cage until they urinated freely. Urine samples (5µL) were diluted in 1x SDS Sample buffer, then run on 10% SDS-PAGE gels and stained with Coomassie brilliant blue R. The urinary albumin/creatinine ratio (ACR) was determined using the Albuwell M ELISA (Exocell) and creatinine companion (Exocell) kits according to the manufacturer's instructions.

### 4.3.3 *HISTOLOGICAL AND ULTRASTRUCTURAL ANALYSES*

For histology, kidneys were halved and fixed in 10% buffered formalin overnight before being embedded in paraffin. 4µm sections were cut and stained with PAS, or with PAAS (Feugas and Morikawa, 1989) to visualize the basement membrane. Slides were viewed on a Leica DM100. Images were prepared for presentation using Adobe Photoshop CS5.

For electron microscopy, sagittal slices (SEM) and small pieces (TEM) of kidney tissue were fixed in 0.1M sodium cacodylate buffer containing 4% paraformaldehyde and 2% gluteraldehyde (all from Electron Microscopy Sciences) and post fixed in 1% $OsO_4$, then dehydrated through graded ethanols. TEM samples were embedded in Quetol-Spurr resin. Ultrathin sections were cut and stained with uranyl acetate and lead citrate. TEM sections were viewed using a FEI CM100 TEM. For SEM, samples were critical point dried and sputter coated with gold. Samples were viewed using a FEI XL30 SEM or Hitachi S-540 SEM.

### 4.3.4 *LPS MODEL OF TRANSIENT PODOCYTE EFFACEMENT*

Non-proteinuric C57Bl/6 male and female control (n = 7) ($nephrin^{WT/WT}$ (n = 5) and $nephrin^{WT/Y3F}$ (n = 2)) and $nephrin^{Y3F/Y3F}$ mice (n = 9) between the ages of 3 and 6 months were used for this experiment. When required, mice were randomly assigned to LPS or PBS groups. We included $nephrin^{WT/Y3F}$ animals in the control group in order to have enough animals to perform a quantitative analysis as they do not develop foot process effacement with age (Figure S1). Mice were injected i.p with 200 ug LPS (1 mg/mL in PBS) (L2630, Sigma) or an equal volume of PBS. Spot urine samples were collected prior to injection and every 12 hours until 72 hours after injection. Urine samples (2µL) were run on SDS-PAGE gels and stained with Coomassie blue. Urinary protein concentrations were measured using a BCA kit (#23225, Pierce) according to the manufacturer's instructions.

### 4.3.5 *ANTIBODIES*

The commercial antibodies used were: mouse anti-GAPDH (#G041, Applied Biological Materials Inc), guinea pig anti-nephrin (#20R-NP002, Fitzgerald Inc.), rabbit anti-pS473 Akt (#4060), anti-Akt (#4691) and pY416 (active) Src (#2101)(Cell Signaling), rabbit anti-pY1217 human nephrin (also recognizes mouse pY1232) (#2423-1, Epitomics), mouse anti-β-actin (A5441, Sigma-Aldrich), rabbit anti-podocin (P0372, Sigma-Aldrich), rabbit anti-Src (Ab-529, Abcam). Rabbit anti-nephrin (Li *et al.*, 2004) was a kind gift from Dr. Tomoko Takano. Rabbit anti-Nck antibody has been described previously (Bladt *et al.*, 2003). Secondary antibodies for immunofluorescence from Invitrogen were: Goat anti-Rabbit Alexa Fluor 488 (A11008) and Goat anti-Guinea Pig Alexa Fluor 594 (A11076). Secondary antibodies for immunoblotting from Bio-Rad were: Goat anti-mouse HRP (170-6516) and Goat anti-rabbit HRP (170-6515).

### 4.3.6 *PREPARATION OF KIDNEY LYSATES AND IMMUNOPRECIPITATION*

Glomeruli were isolated from nephrin$^{WT/WT}$, nephrin$^{WT/Y3F}$ and nephrin$^{Y3F/Y3F}$ mice by differential sieving, pelleted, resuspended in 600 µL of RIPA+ lysis buffer (50 mM Tris pH 7.5, 150 mM NaCl, 10% glycerol, 1% NP-40, 0.25% Na-deoxycholate, 0.1% SDS, 1 mM EDTA) supplemented with fresh protease inhibitors, sonicated for 10 seconds on ice and centrifuged at 13,000 rpm for 10 minutes at 4°C. Supernatants were mixed with appropriate amounts of 5x SDS sample buffer and incubated at 100°C for 5 minutes. For immunoprecipitation, equal quantities of nephrin$^{WT/WT}$ and nephrin$^{Y3F/Y3F}$ kidney cortex were homogenized in RIPA+ lysis buffer, sonicated for 10 seconds on ice and centrifuged at 13,000 rpm for 10 minutes at 4°C. A portion of the supernatant was prepared as lysate in 5x SDS sample buffer and the remainder was diluted 1:4 in RIPA+ buffer and incubated overnight at 4°C with 0.5 µL rabbit anti-Nck or 2.5 µL rabbit anti-nephrin antibody and 80 µL of Protein A sepharose beads (GE Healthcare).

### 4.3.7 *IMMUNOBLOTTING*

Protein samples (glomeruli, cortex lysate, or immunoprecipitates) were resolved on 8% SDS-PAGE gels. Proteins were transferred to PVDF membrane (Millipore) and blocked in 5% skim milk or 5% bovine serum albumin in 1x TBST. Membranes were incubated with primary antibodies overnight at 4°C (rabbit: anti-nephrin (1:1000), anti-pY1232(1:2500), anti-pS473 Akt (1:2000), anti-Akt (1:1000), anti-pY416 Src (1:1000) and anti-Src (1:1000); mouse: GAPDH (1:1000), β-actin (1:2000)). After washing, membranes were incubated with HRP-conjugated secondary antibody diluted 1:10,000 in TBST for one hour at room temperature. Signals were detected using ECL (Pierce) or Luminata Crescendo (Millipore). Blots were imaged using a ChemiDoc XRS+ (Biorad) or exposed to film (Pierce).

### 4.3.8 *INDIRECT IMMUNOFLUORESCENCE OF TISSUE SECTIONS*

Kidneys were flash frozen in Cryomatrix (Fisher Sci). 6um sections were dried at room temperature for 10 minutes, then fixed and permeabilised in acetone at -20ºC for 10 minutes. When using the pY1232 antibody, a phosSTOP tablet (Roche) was added to all solutions. All subsequent steps were carried out at room temperature. Slides were blocked for 1 hour in 10% goat serum, then incubated with primary antibodies for 1 hour (guinea pig anti-nephrin (1:100), rabbit anti-pY1232-nephrin (1:50) or anti-podocin (1:100)). After 3 washes in PBS, slides were incubated with secondary antibodies for 1 hour (Goat anti-Rabbit Alexa-488 and Goat anti-Guinea Pig Alexa-594, both 1:400). Slides were washed, then mounted using Prolong Gold anti-fade mounting medium (Invitrogen). Epifluoresence images were obtained using Volocity software version 5.3.2 (Improvision) on a DMIRE2 microscope (Leica) using a 63x oil immersion objective. Stacks were captured at 0.2um z-intervals, then deconvolved using an iterative restoration function (95% confidence with 15 iterations) in Volocity.

### 4.3.9 *REAL-TIME PCR*

For mRNA isolation, kidney cortex was dissected from nephrin$^{WT/WT}$ (n=3) and nephrin$^{Y3F/Y3F}$ (n=3) mice, immediately flash frozen and stored at -80ºC. mRNA was isolated from the cortex using TriZol (Invitrogen) and mRNA concentrations were measured on a nanodrop (Thermo Sci.) after DNase I (Invitrogen) treatment. RNA integrity was verified on a Bioanalzyer (Agilent); all samples used for analysis had a RIN value of at least 7. cDNA synthesis was performed on 1 µg RNA with the Superscript II kit (Invitrogen) using random primers. qRT-PCR reactions were carried out using SsoFast EvaGreen Supermix (Bio-Rad) on a CFX96 Real-Time PCR Detection System (Bio-Rad). Primer sequences used in this study are listed in Table 4.3. Standard curves were generated for all primer pairs used and melt curves were examined to verify that there was a single amplicon. No reverse transcriptase and no template controls were included in all runs. Expression differences were calculated using the $\Delta^{Ct}$ method, corrected for primer efficiency. Differences were normalized to the reference genes *Gapdh* and *Hprt*. All calculations were performed in CFX Manager 3.0 (Bio-Rad).

### 4.3.10 *BLOOD PRESSURE MEASUREMENTS*

Mice were anesthetized with a 2%:98% mix of isoflurane and oxygen. Body temperature was maintained at 37°C using a battery operated rectal thermometer in combination with a 100W heating lamp. A small incision was made and a 1.2F catheter (FTS-1211B-0018, Scisense Inc.) was inserted into the right carotid artery, through the aortic valve, and into the left ventricle. Pressures were digitized at a sampling rate of 2000 Hz and recorded using iWorx® analytic software (Labscribe2).

### 4.3.11 *STATISTICS*

Values are presented as mean ± S.E.M. Differences between more than two groups were analyzed by ANOVA using SAS version 9.3 (SAS Inc). Statistical analysis of qRT-PCR data

was performed in CFX Manager software (Bio-Rad). Graphs were prepared using Graphpad Prism version 5.0 (Graphpad Software). $P < 0.05$ was considered statistically significant.

#### 4.3.12 *STUDY APPROVAL*

Animal studies were approved by the University of Guelph Animal Care Committee and carried out in accordance with Canadian Council on Animal Care protocols.

## 4.4 **RESULTS**

### 4.4.1 *GENERATION OF NEPHRIN$^{Y3F/Y3F}$ KNOCK-IN MICE AND CHARACTERIZATION OF NEPHRIN-Y3F EXPRESSION IN VIVO*

To generate mice with disrupted nephrin tyrosine phosphorylation, the three YDxV tyrosines 1191, 1208 and 1232 of nephrin were converted to phenylalanine, an amino acid which mimics the structure of tyrosine but cannot undergo phosphorylation (Figure 4.1A). A targeting vector containing appropriate nucleotide point mutations was constructed (Figure 4.1B), and the three mutations were incorporated into the endogenous *Nphs1* locus by homologous recombination. Successful targeting led to the generation of nephrin$^{WT/Y3F}$ mice on a mixed B6/129 background, which we subsequently bred onto the C57Bl/6 background. When we intercrossed heterozygous nephrin$^{WT/Y3F}$ mice, we observed the birth of nephrin$^{WT/WT}$ (WT), nephrin$^{WT/Y3F}$ (HET) and nephrin$^{Y3F/Y3F}$ (Y3F) animals (Figure 4.1C) in the expected Mendelian ratios ($0.23^{(WT/WT)}$: $0.46^{(WT/Y3F)}$: $0.31^{(Y3F/Y3F)}$; n=68). The presence of the three mutations was verified by DNA sequencing (data not shown).

To examine the expression and biochemical function of the mutant nephrin allele, we first isolated RNA from the kidney cortex of nephrin$^{WT/WT}$ and nephrin$^{Y3F/Y3F}$ animals and used quantitative PCR to compare the amount of mRNA expression of the two *Nphs1* alleles as well as the podocyte markers *Actn4*, *Nphs2* and *Wt1* (Figure 4.2A). We observed similar amounts of *Nphs1* mRNA in nephrin$^{WT/WT}$ and nephrin$^{Y3F/Y3F}$ animals, suggesting that insertion of our

knock-in mutation did not affect nephrin promoter activity or mRNA stability. There were no significant differences in expression of the other podocyte markers. We next isolated glomeruli from nephrin$^{WT/WT}$, nephrin$^{WT/Y3F}$, and nephrin$^{Y3F/Y3F}$ animals and performed western blots to analyze nephrin expression (Figure 4.2B). Comparable levels of nephrin relative to GAPDH were seen in all genotypes and as expected, using our phospho-specific Y1232 nephrin antibody (Jones *et al.*, 2009), we detected phosphorylation of Y1232 in nephrin$^{WT/WT}$ animals, which was decreased in nephrin$^{WT/Y3F}$ animals and absent from nephrin$^{Y3F/Y3F}$ animals (Figure 4.2B).

Investigation of nephrin localization within the glomerulus via immunofluorescence staining revealed that both nephrin-WT and nephrin-Y3F proteins were expressed in a pattern characteristic of podocyte proteins (Figure 4.2C). Most of the nephrin protein appeared to be phosphorylated on Y1232 in nephrin$^{WT/WT}$ animals, while we could not detect any signal in nephrin$^{Y3F/Y3F}$ animals (Figure 4.2C). We obtained similar results using a phospho-specific antibody against Y1208 (data not shown). Given that nephrin phosphorylation can affect nephrin-podocin interactions (Li *et al.*, 2004; Quack *et al.*, 2006), we performed dual immunofluorescence staining for nephrin and podocin (Figure 4.2D) and found that both proteins were similarly expressed in a continuous pattern in the glomeruli of nephrin$^{WT/WT}$ and nephrin$^{Y3F/Y3F}$ animals, with no readily apparent differences between the two.

Finally, we examined the effect of the mutant allele on nephrin signaling. Phosphorylation of these tyrosines is required for nephrin-Nck binding *in vitro* (Verma *et al.*, 2006; Jones *et al.*, 2006; Li *et al.*, 2006), thus we validated that the interaction was disrupted *in vivo* using immunoprecipitation on kidney lysates from nephrin$^{WT/WT}$ and nephrin$^{Y3F/Y3F}$ animals (Figure 4.2E). Nephrin phosphorylation on other tyrosine residues has been linked to p85-based signaling pathways (Zhu *et al.*, 2008; Garg *et al.*, 2010; Venkatareddy *et al.*, 2011; George *et al.*, 2012) and we have shown it to influence SFK activity (New *et al.*, 2013). We examined these two signaling pathways by western blot on glomeruli isolated from nephrin$^{WT/WT}$ and nephrin$^{Y3F/Y3F}$ animals. We observed decreased p-Akt and p-Src levels in nephrin$^{Y3F/Y3F}$ animals compared to nephrin$^{WT/WT}$ animals (Figure 4.2F). Together, these observations suggest that mutant nephrin-Y3F protein is expressed in similar amounts as the wildtype form, and that the

absence of these three phosphorylation sites compromises overall nephrin phosphotyrosine signaling *in vivo*.

### 4.4.2 *PODOCYTE FOOT PROCESSES OF C57BL/6 NEPHRIN$^{Y3F/Y3F}$ MICE FORM NORMALLY*

We looked at nephrin tyrosine phosphorylation during glomerular development and found that, in accord with the observations of others (Verma *et al.*, 2006), nephrin phosphorylation on Y1217 was detectable beginning in the late capillary loop stage (Figure 4.3). However, despite early expression, it would appear that tyrosine phosphorylated nephrin, like nephrin itself (Ruotsalainen *et al.*, 2000; Putaala *et al.*, 2001; Rantanen *et al.*, 2002; Hamano *et al.*, 2002; Kramer-Zucker *et al.*, 2005), is not required for podocyte foot process formation. Although nephrin-Y3F can form slit diaphragms, it cannot interact with Nck, suggesting the hypothesis that loss of this interaction in nephrin$^{Y3F/Y3F}$ mice would result in a similar phenotype to that of podocyte-specific Nck1/2 knockout mice (Jones *et al.*, 2006). Therefore, we examined nephrin$^{Y3F/Y3F}$ mice at 4 weeks of age for signs of proteinuria, glomerular damage and foot process effacement, all of which are observed by that age in podocyte-specific Nck1/2 knockout mice (Jones *et al.*, 2006). Surprisingly, we could not detect any overt proteinuria in nephrin$^{Y3F/Y3F}$ mice (Figure 4.4A), nor did we observe any signs of glomerular damage in PAS stained kidney sections (Figure 4.4B,C). We examined podocyte foot process architecture using scanning electron microscopy (SEM) and observed that nephrin$^{Y3F/Y3F}$ mice formed regularly spaced foot processes like those found in nephrin$^{WT/WT}$ animals (Figure 4.4D,E). We also examined glomerular architecture using transmission electron microscopy (TEM) and found that there were no differences between the podocytes, GBM and endothelium of nephrin$^{WT/WT}$ and nephrin$^{Y3F/Y3F}$ mice (Figure 4.4F,G). The observation that podocyte foot processes form normally in the absence of nephrin-Nck interactions suggests that there are likely additional regulators of Nck-mediated actin polymerization in the podocyte.

### 4.4.3 *C57BL/6 NEPHRIN$^{Y3F/Y3F}$ MICE DEVELOP MILD ALBUMINURIA AND FOOT PROCESS DISORGANIZATION WITH AGE*

Although the foot processes of nephrin$^{Y3F/Y3F}$ mice appeared normal at 1 month of age, we followed a cohort of nephrin$^{WT/WT}$ and nephrin$^{Y3F/Y3F}$ animals over time to determine whether they developed podocyte alterations with age. We collected urine monthly and monitored urinary albumin excretion in the same animals by Coomassie stained gels (Figure 4.5A) and by measurement of the albumin/creatinine ratio (ACR) (Figure 4.5B). We observed an increase in the ACR of nephrin$^{Y3F/Y3F}$ animals at 6 months of age (76.1 ± 12.0 [Y3F] vrs 38.2 ± 8.2 [WT]; $P = 0.059$) which attained statistical significance by 8 months of age (71.3 ± 12.1 [Y3F] vrs 22.8 ± 12.1 [WT]; $P = 0.047$) compared to nephrin$^{WT/WT}$ littermates.

We examined the kidneys of nephrin$^{WT/WT}$ and nephrin$^{Y3F/Y3F}$ animals at 6 and 11 months of age. Light microscopy did not reveal any obvious structural changes in the glomeruli of nephrin$^{Y3F/Y3F}$ mice at 6 months of age (Figure 4.5D); however, by SEM, we observed that podocytes of 6 month old nephrin$^{Y3F/Y3F}$ mice contained areas of broadened and mildly disorganized foot processes (Figure 4.5F) and using TEM, found that there were segmental regions of foot process effacement in nephrin$^{Y3F/Y3F}$ mice (Figure 4.5H, arrow) which tended to be associated with areas of increased GBM thickness.

When we looked at 11 months of age, we did not detect severe glomerulosclerosis in nephrin$^{Y3F/Y3F}$ mice by PAS staining (Figure 4.5J). However, many glomeruli had dilated capillary loops (Figure 4.5J, arrows) and we found proteinaceous casts in the tubules of some nephrin$^{Y3F/Y3F}$ animals (data not shown). Examination of podocyte ultrastructure using SEM revealed that in nephrin$^{WT/WT}$ animals, foot process branching patterns were normal (Figure 4.5K), whereas in nephrin$^{Y3F/Y3F}$ animals, there were a number of foot process alterations (Figure 4.5L), with more extensive regions of effacement (Figure 4.5L, arrowhead). Furthermore, the remaining foot processes appeared shorter, contained curves or bends and extended from secondary processes at multiple different angles (Figure 4.5L, arrows). When we looked at glomerular morphology using TEM, nephrin$^{WT/WT}$ animals had normal capillary loops with many podocyte foot processes visible (Figure 4.5M). In nephrin$^{Y3F/Y3F}$ animals, while there were

regions of normal foot processes in some capillary loops (Figure 4.5N, arrowheads), foot process effacement was evident in adjacent regions and in neighboring capillary loops (Figure 4.5N, arrows). Additionally, in some areas there were regions of GBM thickening with 'spikes' of matrix deposition (Figure 4.5N, ^). In contrast, heterozygous nephrin$^{WT/Y3F}$ littermates did not develop significant foot process effacement even by 14 months of age (Figure 4.6).

### 4.4.4 *GENETIC BACKGROUND CONTRIBUTES TO THE NEPHRIN$^{Y3F/Y3F}$ PHENOTYPE*

The phenotype we observed in nephrin$^{Y3F/Y3F}$ mice is very different from the one observed in podocyte-specific Nck knockout mice which present with congenital foot process effacement and proteinuria (Jones *et al.*, 2006). While some of the difference between the phenotypes is likely due to nephrin independent functions of Nck in the podocyte, we also wondered if it could be attributed to the C57Bl/6 genetic background of the nephrin$^{Y3F/Y3F}$ mice. This genetic background can significantly decrease the severity of renal phenotypes observed in genetically altered mice (Gao *et al.*, 2004; Kang *et al.*, 2006; Baleato *et al.*, 2008; Nishino *et al.*, 2010; Sachs *et al.*, 2012; Johnstone *et al.*, 2013). In addition, C57Bl/6 mice show resistance to several types of renal injury—including multiple models of membranous nephropathy and diabetic nephropathy—compared with other strains (Chen *et al.*, 2004; Zheng *et al.*, 2005; Qi *et al.*, 2005; Gurley *et al.*, 2010; Xu *et al.*, 2010; Chua *et al.*, 2010; Zhang *et al.*, 2012a).

Therefore, we bred our nephrin$^{Y3F/Y3F}$ mice off the C57Bl/6 background onto other genetic backgrounds—the inbred FVB background and the outbred CD-1 background—to see whether this would alter their phenotype. We crossed onto the FVB background for 5 generations, using speed congenics to verify that the resulting genome was > 95% FVB origin, before intercrossing heterozygous mice together. We followed FVB nephrin$^{Y3F/Y3F}$ animals from birth until 6 months of age but did not detect an increase in proteinuria (data not shown). Simultaneously, we crossed for 6 generations onto the CD-1 background, then bred heterozygous mice together to generate CD-1 nephrin$^{Y3F/Y3F}$ animals and examined them to see if the change of genetic background affected the phenotype. In contrast to C57Bl/6 nephrin$^{Y3F/Y3F}$ and FVB nephrin$^{Y3F/Y3F}$ mice, CD-1 nephrin$^{Y3F/Y3F}$ mice developed an early onset phenotype.

### 4.4.5 *CD-1 NEPHRIN$^{Y3F/Y3F}$ MICE DEVELOP PROTEINURIA AND SEVERE FOOT PROCESS DISORGANIZATION BY 15 WEEKS OF AGE*

We monitored for the development of proteinuria in CD-1 nephrin$^{Y3F/Y3F}$ mice, and found that we could detect mild proteinuria at 4 weeks, which progressed to severe proteinuria by 12-15 weeks and continued to increase (Figure 4.7A). We examined glomeruli at four time points: at the earliest sign of proteinuria (4 weeks), at the onset of moderate proteinuria (9 weeks), after the progression to severe proteinuria (15 weeks) and finally after a period of chronic proteinuria (26 weeks) (Figure 4.7B-I). At 4 weeks of age, we did not observe any significant alterations by light microscopy in the glomeruli of nephrin$^{Y3F/Y3F}$ mice (Figure 4.7C), but at 9 weeks, we observed that some glomeruli of nephrin$^{Y3F/Y3F}$ mice had enlarged capillary loops (Figure 4.7E, arrows). At 15 weeks, there also appeared to be a slight thickening of the GBM, and we observed irregular GBM bulges or 'spikes' in nephrin$^{Y3F/Y3F}$ animals (Figure 4.7G, inset, higher magnification). By 26 weeks, we noticed a larger number of nephrin$^{Y3F/Y3F}$ glomeruli with morphological alterations, including some with numerous dilated capillary loops (Figure 4.7I, arrows). We also examined the glomeruli of 26 week old nephrin$^{WT/WT}$ and nephrin$^{Y3F/Y3F}$ mice using silver staining to better visualize the GBM (Figure 4.7J-L). In nephrin$^{Y3F/Y3F}$ mice, this highlighted the extent of changes to the architecture of the GBM (Figure 4.7K,L arrows) and the presence of 'spikes' as shown in two representative glomeruli (Figure 4.7K,L higher magnification insets).

We also examined nephrin$^{WT/WT}$ and nephrin$^{Y3F/Y3F}$ podocyte architecture using SEM at the same timepoints of 4, 9, 15 and 26 weeks. The majority of foot processes appeared normal at 4 weeks of age in both genotypes (Figure 4.7M,N). At 9 weeks, we found that nephrin$^{Y3F/Y3F}$ podocyte foot processes extended from secondary processes in a variety of random orientations (Figure 4.7P). They contained more curves than usual (Figure 4.7P), and there also appeared to be a mild increase in the number of branched foot processes (Figure 4.7P, arrowhead). At 15 weeks of age, foot process organization in nephrin$^{Y3F/Y3F}$ mice had become visibly altered (Figure 4.7R) and by 26 weeks, those foot processes which could be found in nephrin$^{Y3F/Y3F}$ mice were short and curvy and were not arranged in a discernible pattern (Figure 4.7T). We observed

varying degrees of damage to the glomeruli of individual animals, ranging from glomeruli that appeared almost normal to those where no foot processes could be seen at all (data not shown).

### 4.4.6 *Proteinuric nephrin$^{Y3F/Y3F}$ mice do not have altered blood pressure, regardless of genetic background*

To be certain that the dilated capillary loops we observed in nephrin$^{Y3F/Y3F}$ mice were not a response to increased blood pressure, we measured blood pressure in proteinuric male nephrin$^{WT/WT}$ and nephrin$^{Y3F/Y3F}$ mice (Table 4.2). We saw no difference in mean arterial pressure (MAP) between 10 month old C57Bl/6 nephrin$^{WT/WT}$ and nephrin$^{Y3F/Y3F}$ mice (MAP 86 ± 8 [WT] vrs 80 ± 3 [Y3F] mmHg; $P = 0.548$). There was also no difference between 4 month old nephrin$^{WT/WT}$, nephrin$^{WT/Y3F}$ and nephrin$^{Y3F/Y3F}$ mice on the CD-1 background (MAP 88 ± 3 [WT] vrs 87 ± 8 [Y3F] mmHg; $P = 0.877$).

### 4.4.7 *C57Bl/6 nephrin$^{Y3F/Y3F}$ mice are more susceptible to LPS-induced podocyte injury*

Altered nephrin tyrosine phosphorylation has been reported in several models of podocyte injury (Li *et al.*, 2004; Verma *et al.*, 2006; Jones *et al.*, 2009; Zhang *et al.*, 2010a), though it is not entirely clear whether phospho-nephrin signaling has a positive or negative role during podocyte foot process effacement, and whether it is required for foot process repair. Given that our nephrin$^{Y3F/Y3F}$ develop normally on the C57Bl/6 background while lacking key tyrosine phosphorylation sites, we reasoned that they would provide a suitable model to examine the role of phospho-nephrin signaling in a setting of acute podocyte injury causing rapid reversible foot process remodeling. To do this, we chose to use the LPS model of transient injury whereby injection of LPS leads to an increase in proteinuria at 24 hours, which subsequently returns to normal by 72 hours (Pippin *et al.*, 2009). We injected non-proteinuric nephrin$^{WT/WT}$ and nephrin$^{Y3F/Y3F}$ mice with PBS or LPS and collected spot urine prior to injection and at 24 hours after injection (Figure 4.8A). PBS injection did not alter urinary protein levels, while injection with LPS led to an increase in urinary protein levels in both nephrin$^{WT/WT}$ and nephrin$^{Y3F/Y3F}$ mice after 24 hours (Figure 4.8A). To measure the amplitude of this response, and monitor the

kinetics of recovery, we performed a larger experiment collecting spot urine samples every 6-12 hours until 72 hours after LPS injection. We ran urine samples from the timepoints on a gel and stained with Coomassie (Figure 4.8B). LPS injection produced a peak of proteinuria at 24 hours which was more pronounced in nephrin$^{Y3F/Y3F}$ mice compared to nephrin$^{WT/WT}$ mice, with both genotypes returning to baseline at 72 hours (Figure 4.8B). Quantitation of the total urinary protein levels in mice injected with LPS every 12 hours between 0 and 72 hours (Figure 4.8C) showed that average protein levels were higher in nephrin$^{Y3F/Y3F}$ mice at both 24 hours (1.752 ± 0.382 [Y3F] vrs 0.927 ± 0.098 mg/mL in controls) and 36 hours (1.441 ± 0.157 [Y3F] vrs 0.968 ± 0.075 mg/mL in controls) after injection with LPS compared to the control group.

## 4.5 DISCUSSION

It has been hypothesized that signaling pathways downstream of tyrosine phosphorylated nephrin, such as those involving Nck cytoskeletal adaptor proteins (Jones *et al.*, 2006; Verma *et al.*, 2006), might be required during glomerular development for the establishment of actin-rich podocyte foot processes (Patrakka and Tryggvason, 2007). Nephrin$^{Y3F/Y3F}$ mice provide a unique opportunity to evaluate this hypothesis as they demonstrate *in vivo* decoupling of nephrin-Nck signaling. To our surprise, we found that foot process development proceeds normally in nephrin$^{Y3F/Y3F}$ mice as compared to the distinct lack of foot processes seen in podocyte-specific Nck-knockout mice (Jones *et al.*, 2006). This strongly suggests that Nck utilizes alternate pathways to facilitate actin remodeling during podocyte foot process formation. Indeed, the podocyte-specific knockouts of Nck binding partners N-Wasp (Schell *et al.*, 2013), dynamin (Soda *et al.*, 2012), synaptojanin (Soda *et al.*, 2012) and Pinch1/2 (Hodgin *et al.*, 2011) all develop early onset proteinuria similar to Nck-knockouts. Although these results suggest that nephrin-Nck signaling is not essential during foot process formation, we cannot rule out the possibility that disruption of phospho-nephrin-Nck signaling contributes to the renal disease that develops in adult nephrin$^{Y3F/Y3F}$ mice, as we have previously demonstrated that active Nck signaling is also required for the maintenance of established podocyte foot processes (Jones *et al.*, 2009).

Despite the difference in foot process formation observed between podocyte-specific Nck-knockout mice and nephrin$^{Y3F/Y3F}$ mice, it is important to note that the development of foot processes in nephrin$^{Y3F/Y3F}$ mice is in keeping with the literature regarding the importance of nephrin to the initial stages of foot process formation, namely that nephrin is not required for podocyte survival (Done *et al.*, 2007) or foot process formation (Ruotsalainen *et al.*, 2000; Putaala *et al.*, 2001; Rantanen *et al.*, 2002; Hamano *et al.*, 2002; Kramer-Zucker *et al.*, 2005). Further, it is likely that targeting of nephrin to the nascent slit diaphragm occurs via a phospho-independent mechanism, namely the c-terminal PDZ recognition motif (HLV) which mediates binding to Par3 in the aPKC-Par3-CDC42 polarity complex (Hartleben *et al.*, 2008), and it has been suggested that the Par complex may recruit nephrin to the developing slit diaphragm (Huber *et al.*, 2009). The PDZ binding motif of nephrin is evolutionarily conserved, in support of this concept, whereas the three YDxV tyrosine motifs are distinctly absent in lower vertebrates and invertebrates (data not shown).

Podocyte nephrin expression is first detected baso-laterally in the early capillary loop stage, where it colocalizes with other components of the future slit diaphragm (Ruotsalainen *et al.*, 2000; Huber *et al.*, 2009; Babayeva *et al.*, 2013). In contrast, we and others (Verma *et al.*, 2006) detect nephrin tyrosine phosphorylation beginning only in the late capillary loop stage in the basal domain of those areas where podocyte foot processes have begun to invade the glomerular capillaries and maturing slit diaphragms have started to form. Once established, nephrin tyrosine phosphorylation is maintained in the glomerulus throughout life. Based on these observations, we propose that nephrin tyrosine phosphorylation be considered a marker of the mature slit diaphragm. This is supported by evidence that nephrin mutations in patients which result in slit diaphragm instability have decreased levels of nephrin tyrosine phosphorylation (Shono *et al.*, 2009, Jones, unpublished observations), suggesting a link between nephrin phosphorylation and slit diaphragm stability. More importantly, the phenotype observed in our nephrin$^{Y3F/Y3F}$ mice strongly supports an active role for nephrin tyrosine phosphorylation in the proper functioning of the mature podocyte.

One of the most prominent features of the nephrin$^{Y3F/Y3F}$ phenotype is the irregular thickening of the GBM, characterized by spike-like protrusions or bulges which form on the

epithelial face of the GBM beneath podocytes. It has been hypothesized that the development of membrane spikes may represent increased matrix deposition in an attempt to compensate for decreased podocyte adhesion to the underlying GBM (Gross *et al.*, 2004; Sachs and Sonnenberg, 2013). As such, these structures have been reported in a number of other mouse models including DDR1 knockout mice (Gross *et al.*, 2004), tetraspanin CD151 knockout mice (Sachs *et al.*, 2006; Baleato *et al.*, 2008), α2 integrin (Girgert *et al.*, 2010) and α3 integrin (Sachs *et al.*, 2006) knockout mice and ICGN mice (Ogura *et al.*, 1989). Interestingly, most of these proteins are directly involved in podocyte adhesion to the major GBM components type IV collagen (DDR1 and α2β1 integrin) and laminin-521 (α3β1 integrin and CD151), while the ICGN mouse has a premature stop codon in tensin2 (Cho *et al.*, 2006), which links integrins to the actin cytoskeleton (Calderwood *et al.*, 2003). It is tempting to speculate that phospho-nephrin signaling may help to induce proper adhesion of podocyte foot processes to the GBM via recruitment of an Nck2-Pinch-integrin-linked kinase complex (Yang *et al.*, 2005), which could link the slit diaphragm to β1 integrin in the basal domain of the podocyte which contacts the GBM. Defective cell adhesion could also explain the other striking observation in nephrin$^{Y3F/Y3F}$ mice—the appearance of enlarged capillary loops. Inability of the slit diaphragm to directly signal to the GBM via nephrin/Nck could result in insufficient force generation by the podocyte actin cytoskeleton against the intercapillary pressure of the glomerulus (Endlich and Endlich, 2012).

After birth, there is a significant increase in systemic blood pressure (Huang *et al.*, 2006) and in the rate of glomerular blood flow (Baum *et al.*, 2013). These changes result in increased force on the podocyte and their ability to respond appropriately may depend on actin signaling from the slit diaphragm. Adult blood pressure levels in mice are only achieved around five weeks of age (Huang *et al.*, 2006), making it likely that any instability inherent in nephrin$^{Y3F}$ containing slit diaphragms would begin to manifest starting in the subsequent weeks. This is in keeping with the onset of the phenotype in CD-1 nephrin$^{Y3F/Y3F}$ mice at nine weeks, whereas in C57Bl/6 nephrin$^{Y3F/Y3F}$ mice, proteinuria is only observed beginning at six months of age. In agreement with the differences in phenotype that we observe, blood pressure in CD-1 mice is higher than in age matched C57Bl/6 mice (Leelahavanichkul *et al.*, 2010). Further, increased blood pressure can overcome C57Bl/6 resistance to renal disease in CD151 knockout mice (Sachs *et al.*, 2012),

which have a similar GBM phenotype to the one observed in nephrin$^{Y3F/Y3F}$ mice. While we have not yet attempted to artificially adjust blood pressure in our mice, we plan to do so in the near future.

In addition to kidney podocytes, nephrin expression has also been reported in the brain (Putaala *et al.*, 2001; Beltcheva *et al.*, 2003; Morikawa *et al.*, 2007; Nishida *et al.*, 2010; Li *et al.*, 2011), skeletal muscle (Komori *et al.*, 2008; Sohn *et al.*, 2009), heart (Wagner *et al.*, 2011), pancreas (Putaala *et al.*, 2001; Palmen *et al.*, 2001; Beltcheva *et al.*, 2003; Zanone *et al.*, 2005) and testis (Liu *et al.*, 2001; Juhila *et al.*, 2010). Nephrin$^{Y3F/Y3F}$ mice did not display any obvious behavioural or locomotive difficulties, their blood pressure was comparable to that of wildtype mice and male nephrin$^{Y3F/Y3F}$ mice were fertile. In contrast, nephrin-rescue mice, which express rat nephrin specifically in podocytes of nephrin knockout mice, had altered brain architecture and male mice were infertile due to abnormal gonad development (Juhila *et al.*, 2010). The disparity between nephrin$^{Y3F/Y3F}$ and nephrin-rescue mice may simply be due to strain effects, as the phenotype of nephrin$^{Y3F/Y3F}$ mice is strongly affected by genetic background, with a significant difference in the onset and severity of proteinuria between C57Bl/6, CD-1 and FVB strains. Alternatively, it may be that phospho-independent nephrin functions predominate in extra-renal tissues, whereas phospho-nephrin signaling plays a significant role only within the podocyte. Perhaps the mode of nephrin signaling within the podocyte, or some aspect of podocyte structure and function, necessitates a greater dependence on phospho-nephrin signaling than is observed in other murine tissues. In this regard, it is interesting to note that despite having reduced tyrosine phosphorylation, nephrin$^{WT/Y3F}$ mice did not show any obvious podocyte derangements. Indeed, despite all we have learned about nephrin, unanswered questions about its function remain (Li *et al.*, 2013).

Tyrosine phosphorylation is a tightly regulated process and its reduction in nephrin$^{Y3F/Y3F}$ mice leads to foot process effacement, supporting a direct role for phospho-nephrin signaling via YDxV motifs in the maintenance of podocyte architecture. This concept is of clinical relevance as recent evidence has shown that nephrin phosphorylation patterns are altered in disease. Loss of phosphorylation on these same tyrosine residues is seen in patients with minimal change disease (Uchida *et al.*, 2008) and membranous nephropathy (Ohashi *et al.*, 2010), and moreover,

is accompanied by changes in the expression of proteins known to control nephrin phosphorylation. Decreased gal-1 expression is observed in minimal change disease (Shimizu *et al.*, 2009) and increased c-mip expression is seen in both minimal change disease (Zhang *et al.*, 2010a) and membranous nephropathy (Sendeyo *et al.*, 2013). Nephrin phosphorylation is also reduced in the PAN model of minimal change disease (Li *et al.*, 2006; Zhu *et al.*, 2008; Uchida *et al.*, 2008; Jones *et al.*, 2009; Zhu *et al.*, 2010), and this could be due to increased expression of PTP-PEST (Aoudjit *et al.*, 2011) or TMSF10 (Azhibekov *et al.*, 2011), both of which have been shown to negatively regulate nephrin phosphorylation through their effects on Fyn kinase activity, or by increased expression of the phosphatase PTP1β, which we have previously shown can de-phosphorylate nephrin YDxV sites (Aoudjit *et al.*, 2011). Interestingly, genetic deletion or chemical inactivation of this phosphatase protects against LPS-induced proteinuria (Kumagai *et al.*, 2012). Given our findings that nephrin$^{Y3F/Y3F}$ mice are more susceptible to transient LPS-induced injury, it follows that precise control of nephrin phosphorylation is important for the podocyte's ability to sense and respond to stress.

Importantly, decreased nephrin phosphorylation in both human and animal renal disease is not merely a disease biomarker, but is also associated with the disruption of multiple key signaling pathways. Distinct tyrosine residues on nephrin link Nck and p85 to the podocyte actin cytoskeleton, and in animal models of disease, reduced nephrin phosphorylation correlates with a decrease in both nephrin-Nck (Verma *et al.*, 2006; Li *et al.*, 2006; Zhang *et al.*, 2010a) and nephrin-p85 (Zhu *et al.*, 2008) interactions, thereby suppressing further downstream signaling, as evidenced by reduced activation of Pak (Zhu *et al.*, 2010) and Akt (Zhu *et al.*, 2008; Zhang *et al.*, 2010a). In concordance with the changes seen in animal models, both Akt activation (Zhang *et al.*, 2010a) and cofilin activity (Ashworth *et al.*, 2010) are decreased in human minimal change disease. Interestingly, mutation of the YDxV sites in nephrin$^{Y3F/Y3F}$ mice appears to compromise overall nephrin tyrosine phosphorylation, and as a result we found a similar decrease in Akt signaling. This observation is in agreement with other reports in the literature which suggest that phosphorylation of these sites is required for effective nephrin signaling through both Nck and p85 based pathways (Venkatareddy *et al.*, 2011; George *et al.*, 2012; New *et al.*, 2013). Taken together, our observations and those of others suggest a paradigm whereby dynamic signaling pathways controlled by nephrin tyrosine phosphorylation promote podocyte foot process and slit

diaphragm integrity—and that a reduction in nephrin phosphorylation with concomitant downregulation of associated signaling pathways is a crucial step in the initiation of podocyte damage.

In closing, the potential for the cytoplasmic tail of nephrin to be regulated by tyrosine phosphorylation has been recognized since the initial characterization of nephrin (Kestila *et al.*, 1998; Lahdenpera *et al.*, 2003). Since then, numerous efforts have been made to determine the existence and purpose of this modification. Our nephrin$^{Y3F}$ knock-in mouse model now demonstrates unequivocally that signaling pathways regulated by nephrin phosphorylation play a significant role in the maintenance of podocyte function, and suggest there may be value in the investigation of potential therapeutic approaches which can increase nephrin phosphorylation. Additionally, our observation that the severity of the phenotype is affected by genetic background could potentially lead to insights into factors affecting kidney disease susceptibility in humans.

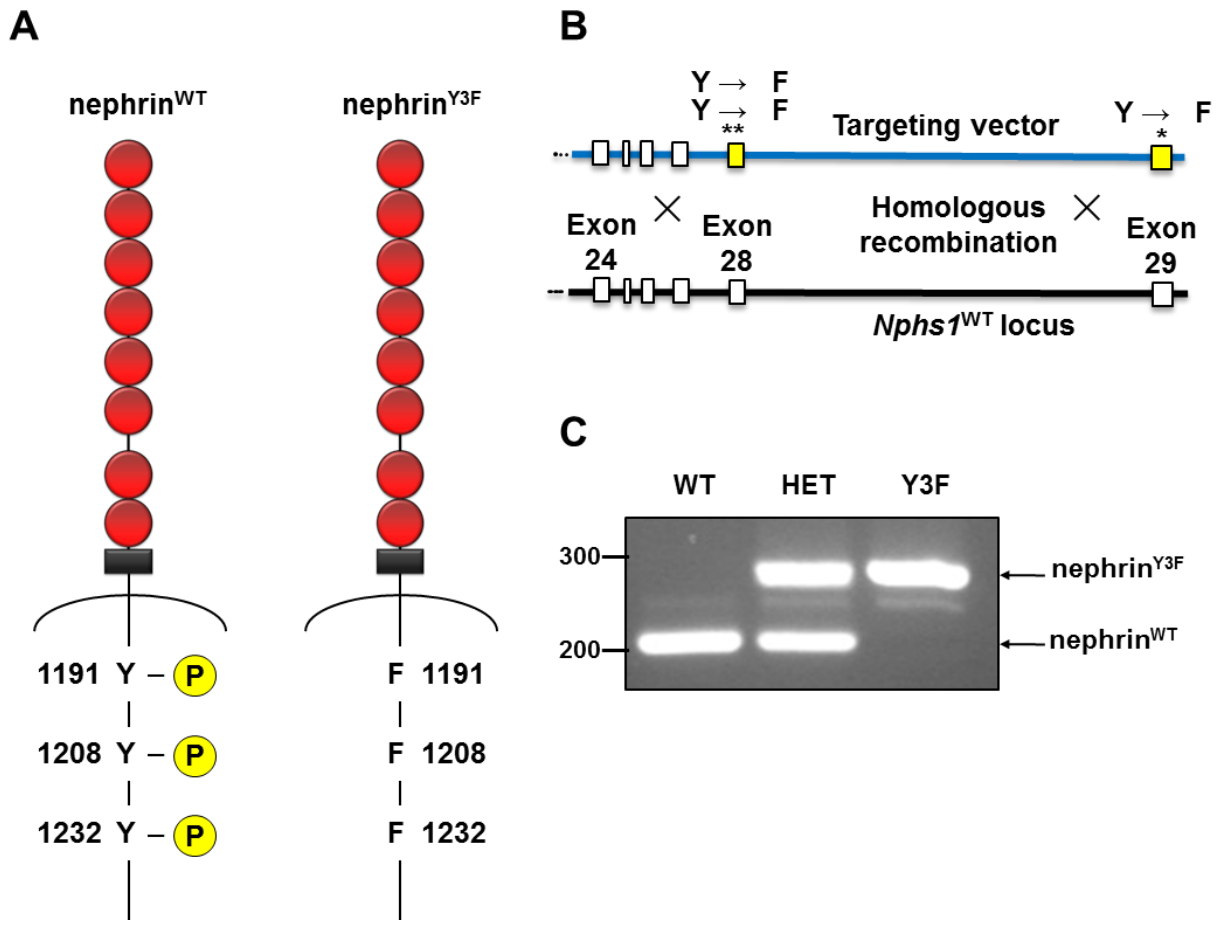


**Figure 4.1 Generation of nephrin$^{Y3F/Y3F}$ mice.**

A) Cartoon of mouse nephrin protein indicating the positions of the three phosphorylated (P) tyrosine (Y) residues within the cytoplasmic tail mutated to phenylalanine (F) to create nephrin$^{Y3F}$. B) Schematic of the targeting vector used to generate the murine *Nphs1*$^{Y3F}$ allele. Site directed mutagenesis was used to introduce 3 single nucleotide substitutions (A→T) to convert the tyrosines shown in A) to phenylalanine. The modified exons (28 and 29) are indicated in yellow. The targeting vector was inserted into the wildtype *Nphs1* locus by homologous recombination. C) PCR analysis illustrates the ability to distinguish between the *Nphs1*$^{WT}$ and *Nphs1*$^{Y3F}$ alleles using genomic DNA samples from representative nephrin$^{WT/WT}$, nephrin$^{WT/Y3F}$ and nephrin$^{Y3F/Y3F}$ animals.

**Figure 4.2 Validation of expression and function of *Nphs1*$^{Y3F}$ mutant allele.**

A) Real-time PCR analysis of mRNA levels in glomeruli isolated from 1 month old nephrin$^{WT/WT}$ (WT; n=3) and nephrin$^{Y3F/Y3F}$ (Y3F; n=3) animals for *Nphs1* and podocyte markers *Actn4*, *Nphs2* and *Wt1*. For each gene, expression in nephrin$^{WT/WT}$ animals was adjusted to 1.0. No significant differences were observed between the two genotypes in the levels of expression of any of the genes (*Actn4*: $P = 0.91$, *Nphs1*: $P = 0.15$, *Nphs2*: $P = 0.39$, *Wt1*: $P = 0.29$). B) Nephrin protein expression and phosphorylation was evaluated using immunoblotting (IB) for the indicated antibodies on glomeruli isolated from nephrin$^{WT/WT}$ (WT), nephrin$^{WT/Y3F}$ (HET) and nephrin$^{Y3F/Y3F}$ (Y3F) mice. Similar total levels of nephrin protein were observed in all genotypes. Using a phospho-specific antibody (p-nephrin) against Y1232, phosphorylation of that site is highest in nephrin$^{WT/WT}$ (WT) mice, reduced in nephrin$^{WT/Y3F}$ (HET) mice and absent in nephrin$^{Y3F/Y3F}$ (Y3F) mice. C) Dual immunofluorescence staining was performed for total nephrin (red) and p-nephrin (Y1232) (green) on kidney sections of nephrin$^{WT/WT}$ and nephrin$^{Y3F/Y3F}$ animals. The pattern of nephrin staining is comparable between genotypes, while p-nephrin (Y1232) staining is present in nephrin$^{WT/WT}$ (WT) mice and absent in nephrin$^{Y3F/Y3F}$ (Y3F) animals. D) As in C), dual immunofluorescence staining was performed for nephrin (red) and podocin (green). The overlap between nephrin and podocin (merge, yellow) in similar in both nephrin$^{WT/WT}$ (WT) and nephrin$^{Y3F/Y3F}$ (Y3F) animals. E) The nephrin-Nck interaction is disrupted in nephrin$^{Y3F/Y3F}$ mice. Kidney cortex lysates from nephrin$^{WT/WT}$ (WT) and nephrin$^{Y3F/Y3F}$ (Y3F) mice were immunoprecipitated (IP) for nephrin (top panel) or Nck (middle panel) and immunoblotted for nephrin. Expression of actin is shown as a loading control. Co-immunoprecipitation between Nck and nephrin is observed in nephrin$^{WT/WT}$ (WT) mice, but not in nephrin$^{Y3F/Y3F}$ (Y3F) mice. F) Impaired nephrin signaling in nephrin$^{Y3F/Y3F}$ mice. Glomerular lysates from nephrin$^{WT/WT}$ (WT) and nephrin$^{Y3F/Y3F}$ (Y3F) mice were immunoblotted with the indicated antibodies. Total phospho-nephrin (pY), phospho-tyrosine-1232-nephrin (Y1232), p-Akt (S473) and p-Src (Y416) levels are decreased in nephrin$^{Y3F/Y3F}$ (Y3F) mice compared to nephrin$^{WT/WT}$ (WT) mice. Expression of GAPDH is shown as a loading control.

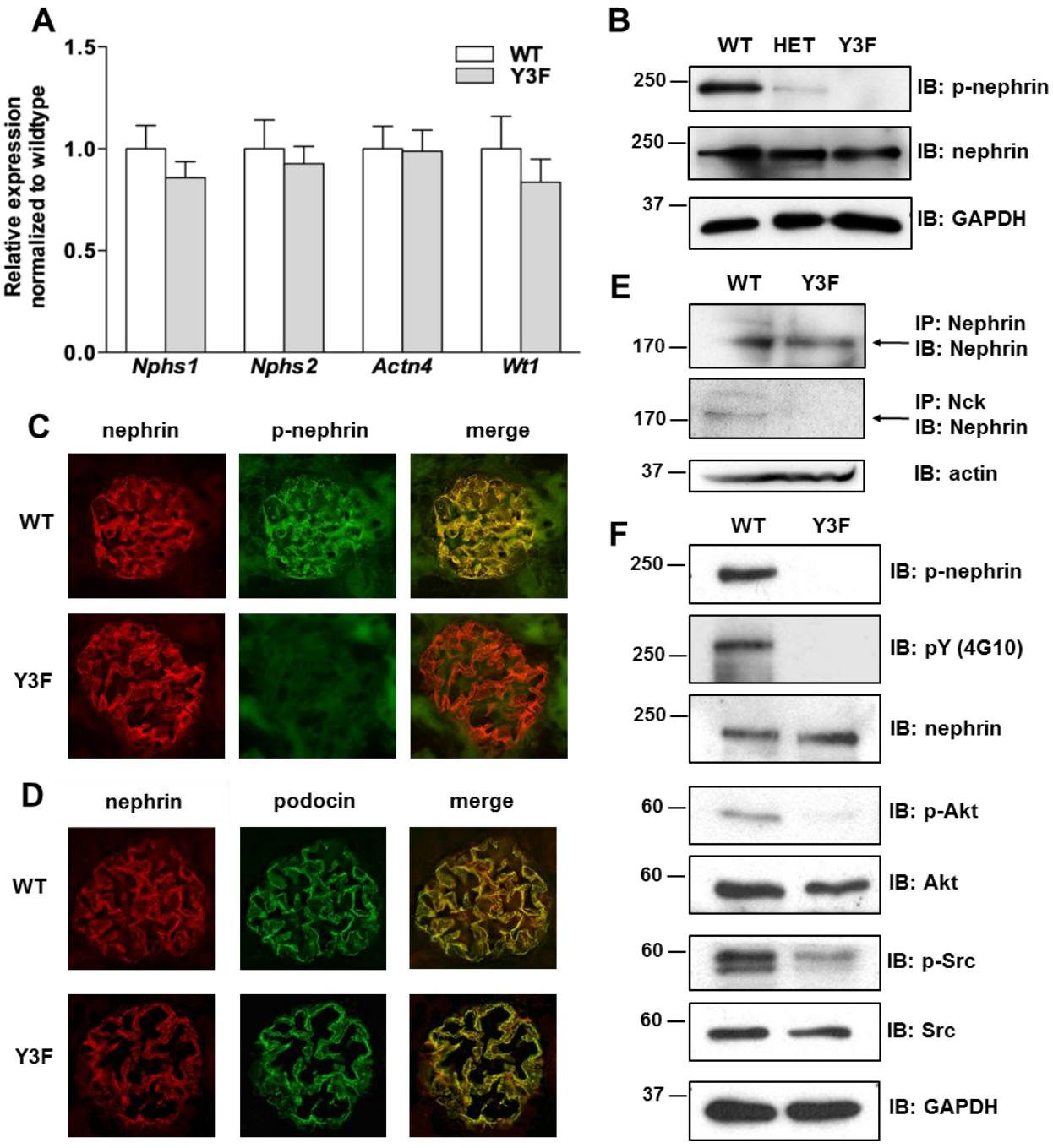
A
Relative expression normalized to wildtype
1.5
1.0
0.5
0.0
WT
Y3F
Nphs1
Nphs2
Actn4
Wt1
B
WT HET Y3F
250
IB: p-nephrin
250
IB: nephrin
37
IB: GAPDH
C
nephrin
p-nephrin
merge
WT
Y3F
D
nephrin
podocin
merge
WT
Y3F
E
WT Y3F
170
IP: Nephrin
IB: Nephrin
170
IP: Nck
IB: Nephrin
37
IB: actin
F
WT Y3F
250
IB: p-nephrin
250
IB: pY (4G10)
250
IB: nephrin
60
IB: p-Akt
60
IB: Akt
60
IB: p-Src
60
IB: Src
37
IB: GAPDH

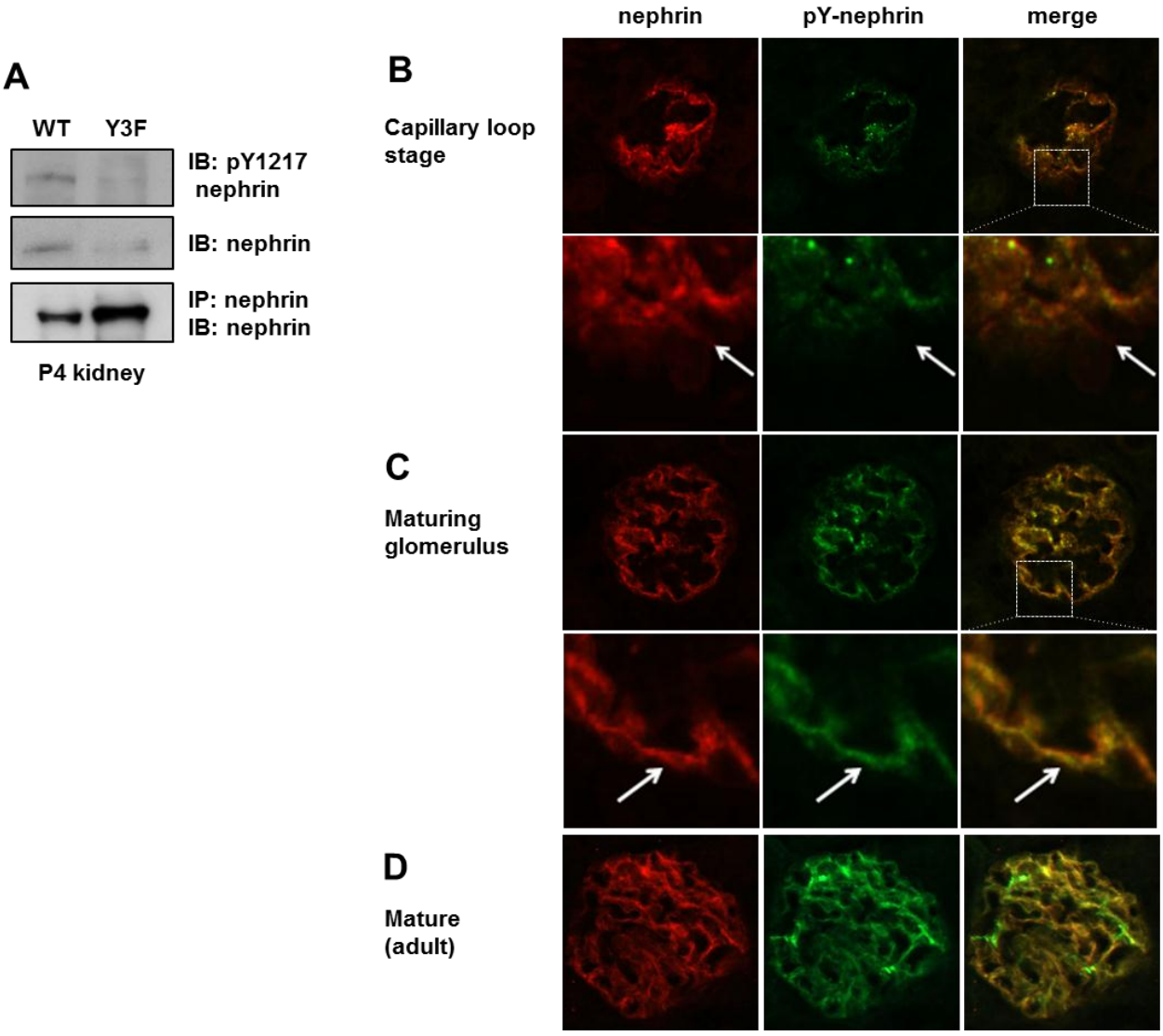


**Figure 4.3 Nephrin phosphorylation during glomerular development.**

(A) Nephrin is phosphorylated on Y1232 at P4. Kidney lysates from nephrin$^{WT/WT}$ (WT) and nephrin$^{Y3F/Y3F}$ (Y3F) mice were immunoblotted for pY-1232 nephrin (top panel) and total nephrin (middle panel). Lysates were also immunoprecipitated (IP) for nephrin (bottom panel) and immunoblotted for nephrin. Nephrin phosphorylation on Y1232 is observed in nephrin$^{WT/WT}$ (WT) mice, but not in nephrin$^{Y3F/Y3F}$ (Y3F) mice. (B,C) Nephrin expression preceeds nephrin tyrosine phosphorylation during development. In early capillary loop stage podocytes, nephrin is not phosphorylated (B, inset, arrow). In the maturing glomerulus, nephrin is now located at presumptive slit diaphragms and appears to be tyrosine phosphorylated (C, inset, arrow). (D) Nephrin tyrosine phosphorylation is maintained in the mature glomerulus.

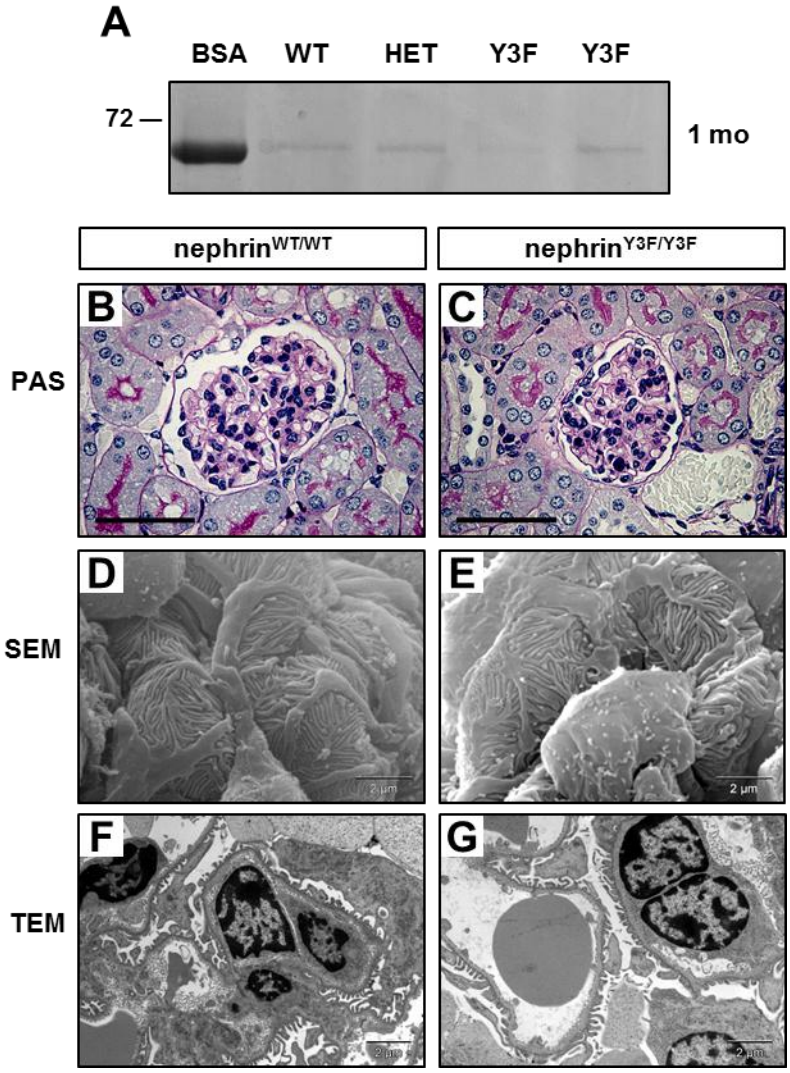


**Figure 4.4 One month old C57Bl/6 nephrin$^{Y3F/Y3F}$ mice have a normal glomerular filtration barrier.**

A) Coomassie stained gel of urine samples from 1 month old mice of the indicated genotypes. (B and C) PAS stained sections from 1 month old nephrin$^{WT/WT}$ B) and nephrin$^{Y3F/Y3F}$ C) animals. (D and E) Scanning electron microscopy (SEM) images of podocyte foot processes in 1 month old nephrin$^{WT/WT}$ D) and nephrin$^{Y3F/Y3F}$ E) mice. The characteristic interdigitation pattern of podocyte foot processes is visible in both nephrin$^{WT/WT}$ and nephrin$^{Y3F/Y3F}$ mice. (F and G) Transmission electron microscopy (TEM) images of podocyte foot processes in 1 month old nephrin$^{WT/WT}$ F) and nephrin$^{Y3F/Y3F}$ G) mice. The architecture of podocyte foot processes, GBM and endothelium of nephrin$^{Y3F/Y3F}$ mice appears similar to that observed in nephrin$^{WT/WT}$ mice. Scale bars: 50 µm (B and C); 2 µm (D-G).

**Figure 4.5 C57Bl/6 nephrin$^{Y3F/Y3F}$ mice develop progressive proteinuria and segmental foot process effacement with age.**

A) Coomassie stained gels of urine samples from littermate nephrin$^{WT/WT}$ and nephrin$^{Y3F/Y3F}$ animals between 2 and 9 months of age. B) Quantification using the albumin/creatinine ratio (ACR) of the urine samples shown in (A). The ACR of nephrin$^{Y3F/Y3F}$ animals is significantly increased relative to nephrin$^{WT/WT}$ littermates starting at 8 months of age (n=3 / genotype); *, $P < 0.05$ by ANOVA. (C-H) Morphological analysis of 6 month old nephrin$^{WT/WT}$ and nephrin$^{Y3F/Y3F}$ mice. No differences are visible in PAS stained sections by light microscopy (C and D). Scanning electron microscopy (SEM) images (E and F) show segments of broadened foot processes in nephrin$^{Y3F/Y3F}$ mice (F, arrow). Transmission electron microscopy (TEM) (G and H) shows that nephrin$^{Y3F/Y3F}$ mice have regions of preserved foot processes (H, arrowhead) adjacent to regions of effacement (H, arrow). (I-N) Morphological analysis of 11 month old nephrin$^{WT/WT}$ and nephrin$^{Y3F/Y3F}$ mice. PAS stained sections of nephrin$^{WT/WT}$ mice show normal glomerular histology (I), while nephrin$^{Y3F/Y3F}$ animals develop dilated capillary loops (J, arrows). Scanning electron microscopy (SEM) shows normal foot processes are observed in nephrin$^{WT/WT}$ animals (K). In nephrin$^{Y3F/Y3F}$ animals (L), foot processes appear curved (L, arrow) with regions of significant effacement visible (L, arrowhead). (M and N) Transmission electron microscopy (TEM) images from nephrin$^{WT/WT}$ (M) and nephrin$^{Y3F/Y3F}$ animals (N). Nephrin$^{Y3F/Y3F}$ mice show segmental changes - some normal foot processes are visible (N, arrowheads), while in regions of effacement (N, arrows), increased matrix deposition resulting in spike-like protrusions on the epithelial face of the GBM can be observed (N,^). Scale bars: 50 µm (C and D); 2 µm (E-H); 50 µm (I and J); 2 µm (K-N).

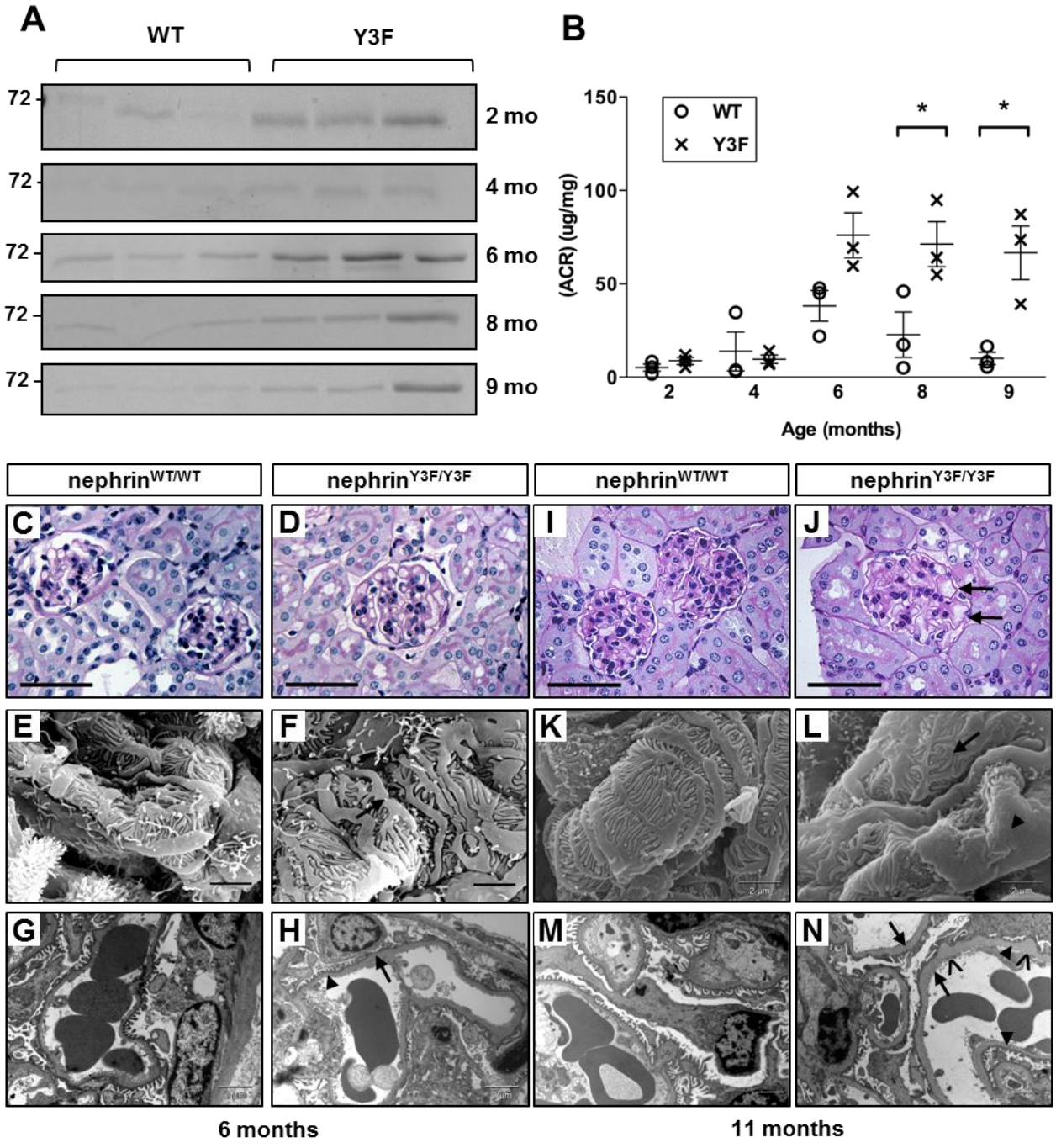
A
WT
Y3F
72
2 mo
72
4 mo
72
6 mo
72
8 mo
72
9 mo
B
150
100
50
0
WT
Y3F
(ACR) (ug/mg)
2
4
6
8
9
Age (months)
*
*
nephrin WT/WT
nephrin Y3F/Y3F
nephrin WT/WT
nephrin Y3F/Y3F
C
D
I
J
E
F
K
L
G
H
M
N
6 months
11 months

**Figure 4.6 No significant foot process abnormalities develop in C57Bl/6 nephrin$^{WT/Y3F}$ mice with age.**

(A-C) Scanning electron microscopy analysis of podocyte morphology in nephrin$^{WT/WT}$ (A), nephrin$^{WT/Y3F}$ (B) and nephrin$^{Y3F/Y3F}$ (C) animals at 1 month of age. Podocyte foot process architecture is similar across all genotypes. (D-L) Transmission electron microscopy analysis of podocyte morphology in nephrin$^{WT/WT}$, nephrin$^{WT/Y3F}$ and nephrin$^{Y3F/Y3F}$ animals at the ages of 4 months (D-F), 6 months (G-I) and 14 months (J-L). Foot process architecture in nephrin$^{WT/Y3F}$ mice remains comparable to nephrin$^{WT/WT}$ mice at all timepoints, whereas foot process effacement is visible in nephrin$^{Y3F/Y3F}$ mice (I and L). Scale bar: 2 μm (A-L).

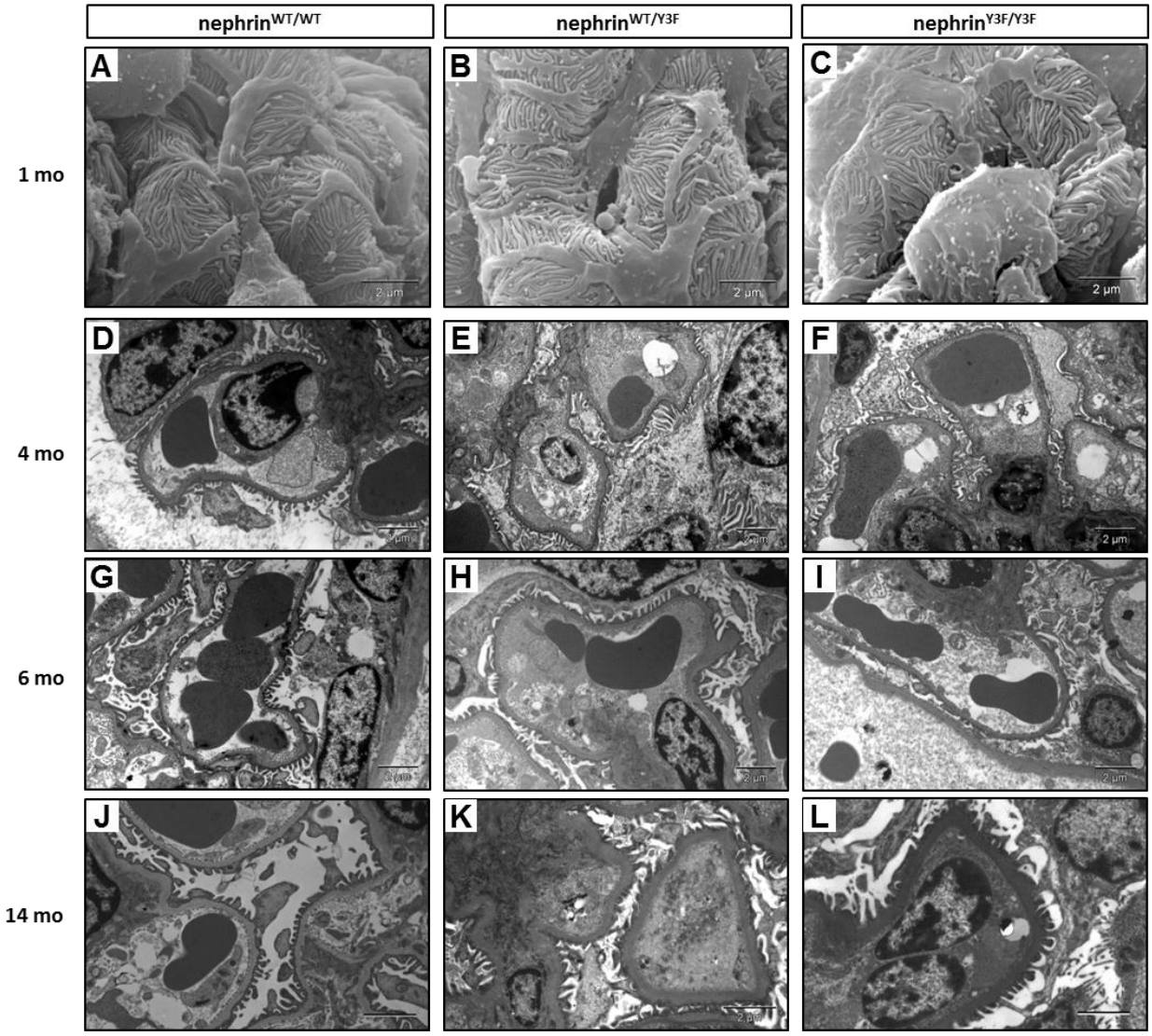
nephrin^WT/WT
nephrin^WT/Y3F
nephrin^Y3F/Y3F
1 mo
4 mo
6 mo
14 mo
A
B
C
D
E
F
G
H
I
J
K
L
2 µm

**Figure 4.7 Nephrin$^{Y3F/Y3F}$ mice develop an accelerated phenotype on the CD-1 background.** (A) Coomassie stained gels of urine samples from CD-1 nephrin$^{WT/WT}$ (WT), nephrin$^{WT/Y3F}$ (HET) and nephrin$^{Y3F/Y3F}$ (Y3F) animals at the indicated time points. CD-1 nephrin$^{Y3F/Y3F}$ animals develop progressively severe proteinuria beginning at 4 weeks of age, whereas no proteinuria is evident in nephrin$^{WT/WT}$ or nephrin$^{WT/Y3F}$ animals even at 26 weeks of age. (B-I) Light microscopy analysis of PAS stained sections of CD-1 nephrin$^{WT/WT}$ and nephrin$^{Y3F/Y3F}$ animals at 4 weeks (B and C), 9 weeks (D and E), 15 weeks (F and G) and 26 weeks (H and I). Increased capillary loop diameters can be observed in nephrin$^{Y3F/Y3F}$ animals (C,E,G and I, arrows). GBM spikes can also be seen in nephrin$^{Y3F/Y3F}$ mice (G, inset). (J-L) Light microscopy analysis of basement membrane morphology in PAAS silver stained sections of 26 week old nephrin$^{WT/WT}$ (J) and nephrin$^{Y3F/Y3F}$ (K,L) mice. Increased GBM deposition is clearly visible in nephrin$^{Y3F/Y3F}$ mice (K,L arrows) and in the increased magnification insets in the bottom panel. (M-T) Scanning electron microscopy analysis of podocyte morphology in CD-1 nephrin$^{WT/WT}$ and nephrin$^{Y3F/Y3F}$ animals at 4 weeks (M and N), 9 weeks (O and P), 15 weeks (Q and R) and 26 weeks (S and T). At 9 weeks of age, nephrin$^{Y3F/Y3F}$ animals have branched and disorganized foot processes (P, arrows). This progresses to severe foot process disorganization at 15-26 weeks (R and T). Scale bars: 50 μm (B-L); 2 μm (M-T).

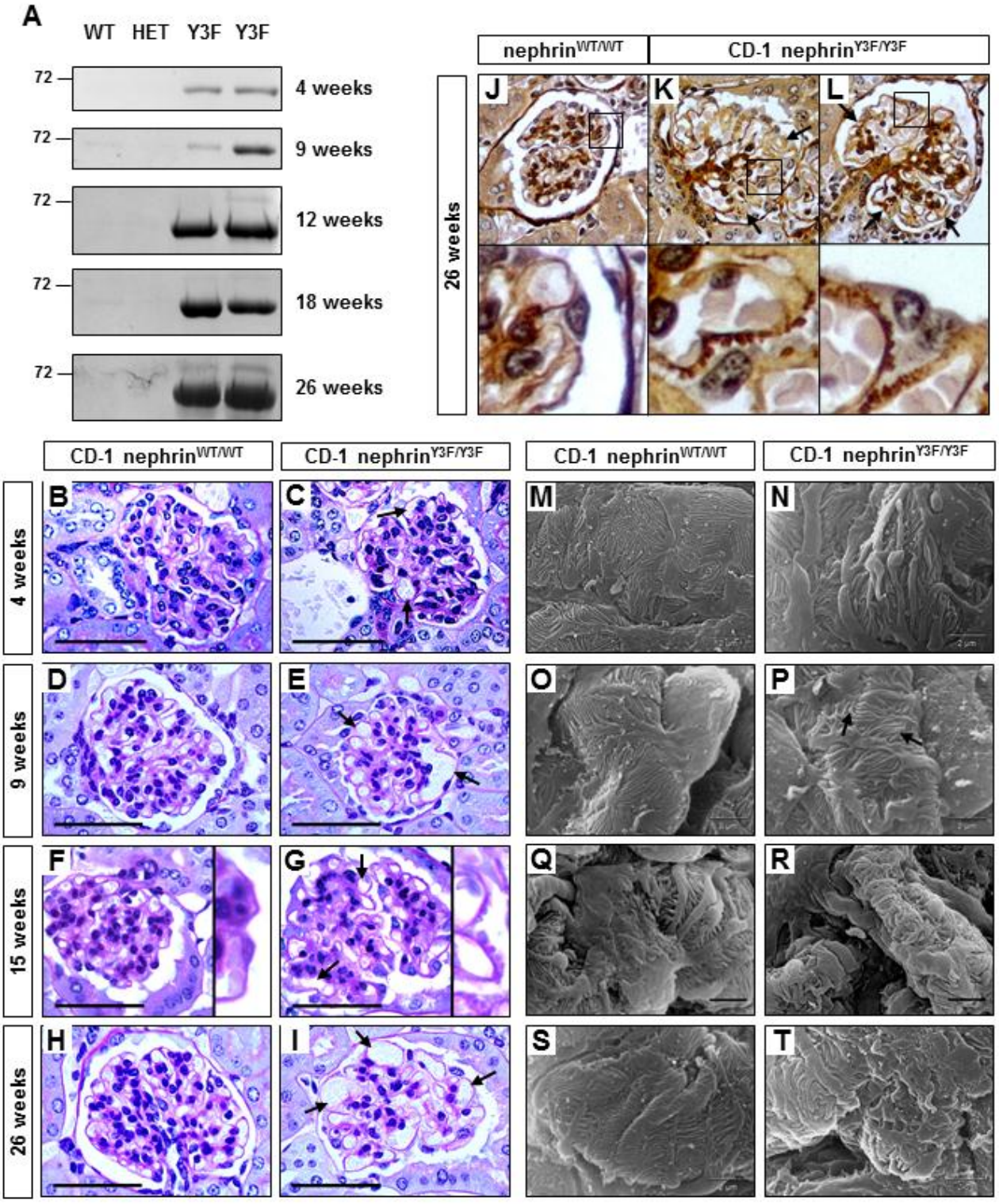
A
WT HET Y3F Y3F
72
4 weeks
9 weeks
12 weeks
18 weeks
26 weeks
nephrin WT/WT
CD-1 nephrin Y3F/Y3F
26 weeks
J
K
L
CD-1 nephrin WT/WT
CD-1 nephrin Y3F/Y3F
CD-1 nephrin WT/WT
CD-1 nephrin Y3F/Y3F
4 weeks
9 weeks
15 weeks
26 weeks
B
C
D
E
F
G
H
I
M
N
O
P
Q
R
S
T

**Figure 4.8 C57Bl/6 nephrin$^{Y3F/Y3F}$ mice have an enhanced response to LPS-induced podocyte injury.**

(A) Nephrin$^{WT/WT}$ (WT; n=2) and nephrin$^{Y3F/Y3F}$ (Y3F; n=2) mice were injected with LPS or an equal volume of PBS as a control. Urine samples were collected at T = 0 and T = 24 hours. Urine samples were analyzed qualitatively via Coomassie staining. Urinary albumin levels are similar in nephrin$^{WT/WT}$ (WT) and nephrin$^{Y3F/Y3F}$ (Y3F) animals prior to injection and there is no change following injection of PBS. LPS injection causes an increase in albumin excretion at T = 24 hours which appears greater in nephrin$^{Y3F/Y3F}$ animals. (B) Coomassie stained gels of albumin excretion over the course (0 to 72 hours) of LPS induced proteinuria in representative nephrin$^{WT/WT}$ (WT) and nephrin$^{Y3F/Y3F}$ (Y3F) animals. (C) Quantification of urinary protein levels (mg/mL) during the time course of LPS induced proteinuria (as in B) in control (nephrin$^{WT/WT}$ and nephrin$^{WT/Y3F}$; n = 7) and nephrin$^{Y3F/Y3F}$ (Y3F; n = 9) animals. The average amount of urinary protein is higher in nephrin$^{Y3F/Y3F}$ (Y3F) animals relative to the control group at 24 and 36 hours after injection.

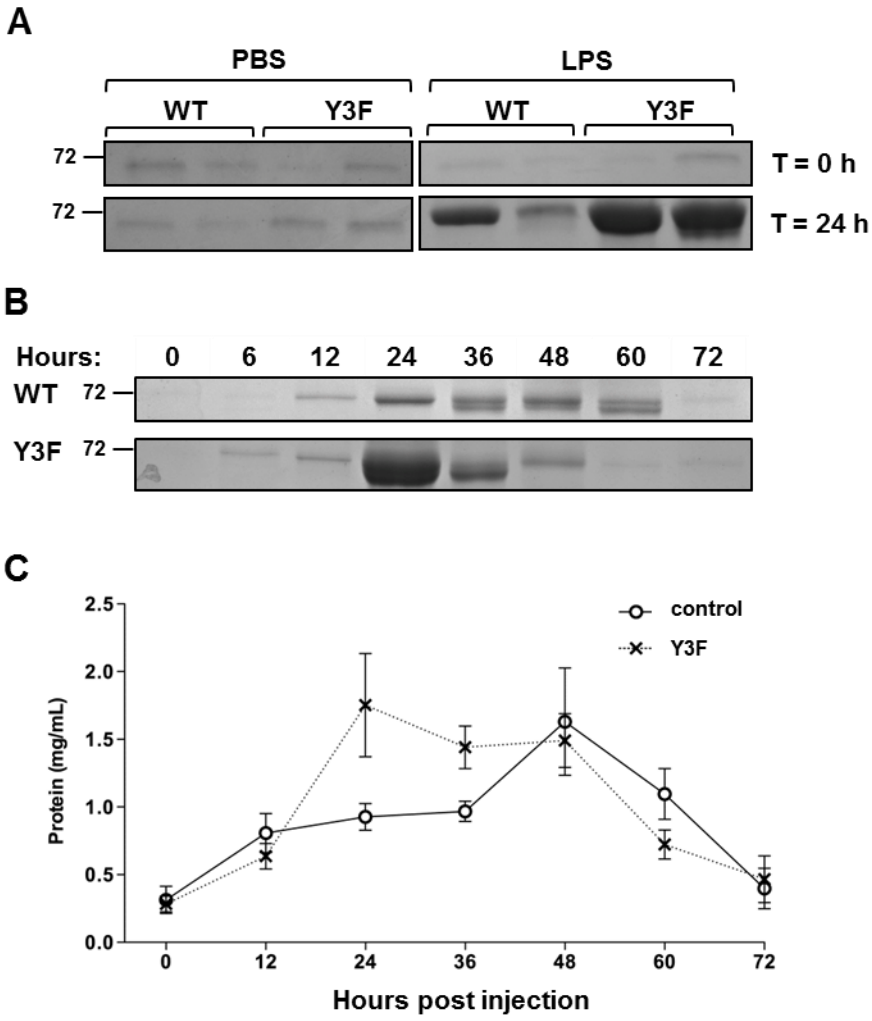
A
PBS
LPS
WT
Y3F
WT
Y3F
72
72
T = 0 h
T = 24 h
B
Hours:
0
6
12
24
36
48
60
72
WT
72
Y3F
72
C
control
Y3F
Protein (mg/mL)
2.5
2.0
1.5
1.0
0.5
0.0
0
12
24
36
48
60
72
Hours post injection

**Table 4.1 Conserved tyrosine residues shared between human, mouse and rat nephrin**

| | Human | Mouse | Rat |
|---|---|---|---|
| * | **1114 - YEES** | **1128 - YEES** | **1127 - YEES** |
| | **1138 - YYRS** | **1153 - YYSM** | **1152 - YYSM** |
| | **1158 - YSRG** | **1172 - YRQA** | **1171 - YHQG** |
| | **1176 - YDEV** | **1191 - YDEV** | |
| | **1183 - YPPS** | **1198 - YGPP** | **1194 - YGPP** |
| * | **1193 - YDEV** | **1208 - YDEV** | **1204 - YDEV** |
| | | **1216 - YDLR** | **1212 - YDLR** |
| | **1210 - YQDP** | **1225 - YEDP** | |
| * | **1217 - YDQV** | **1232 - YDQV** | **1228 - YDQV** |

Sites marked with * are conserved between all three species. Boxes indicate YDxV motifs.

**Table 4.2 Blood pressures of proteinuric male nephrin$^{Y3F/Y3F}$ mice on different genetic backgrounds**

| **Background:** | **C57Bl/6** | | **CD-1** | |
|---|---|---|---|---|
| **Age:** | **10 months** | | **4 months** | |
| **Genotype** | **WT** | **Y3F** | **WT / HET** | **Y3F** |
| | **n=3** | **n=3** | **n=4** | **n=4** |
| **Weight (g)** | 48.9 ± 0.8 | 46.6 ± 2.4 | 49.2 ± 3.2 | 47.1 ± 4.7 |
| **Systolic (mm Hg)** | 109 ± 8 | 101 ± 5 | 106 ± 4 | 105 ± 9 |
| **Diastolic (mm Hg)** | 74 ± 7 | 70 ± 2 | 80 ± 3 | 78 ± 7 |
| **MAP (mm Hg)** | 86 ± 8 | 80 ± 3 | 88 ± 3 | 87 ± 8 |
| **Heart Rate (beats/min)** | 498 ± 24 | 510 ± 20 | 571 ± 43 | 543 ± 56 |

**Table 4.3 Primer sequences used for real-time PCR analysis**

| Gene | Forward Primer (5'-3') | Reverse Primer (5'-3') | Size |
|---|---|---|---|
| *Actn4* | ATGGTCTCCGACATCAACAA | TCATTCAGCAGCCATTCTTC | 77 |
| *Nphs1* | GGAAGAGGTGTCATATCGCC | CTCAAAGGGCAGAGAACCAG | 250 |
| *Nphs2* | TCCATGAGGTGGTAACCAAA | CTTTGGACACATGGGCTAGA | 111 |
| *Wt1* | ACGTCCTTTCATGTGTGCAT | TTTCTCACCAGTGTGCTTCC | 94 |
| *Gapdh* | AGGTCGGTGTGAACGGATTTG | GGGGTCGTTGATGGCAACA | 95 |
| *Hprt* | CATGGACTGATTATGGACAGGACTG | ATCCAGCAGGTCAGCAAAGAACT | 126 |

# CHAPTER 5:

# DISCUSSION AND FUTURE DIRECTIONS

## 5.1 SUMMARY

The work outlined in this thesis has increased our understanding of the role of nephrin tyrosine phosphorylation through the exploration of three complementary avenues—generation of reagents to observe site-specific phosphorylation of nephrin, definition of an additional role for Nck in mediating nephrin activation, and characterization of the role of nephrin phosphorylation *in vivo* using a mouse model of nephrin that lacks three key nephrin tyrosine residues. Four key aspects are examined. First, new reagents composed of a set of phospho-tyrosine-specific nephrin antibodies are characterized. Development of these antibodies allows us to demonstrate that nephrin can become tyrosine phosphorylated on these sites *in vitro* and that phosphorylation of these sites can also be detected in healthy mouse and rat kidneys *in vivo*. An outline of the biochemical and signaling mechanisms regulating nephrin phosphorylation reveals that Nck, after binding phosphorylated nephrin via its SH2 domain can use its SH3 domains to recruit and activate Fyn, thus increasing nephrin tyrosine phosphorylation and further promoting the engagement of nephrin signaling pathways. In addition, the importance of nephrin tyrosine phosphorylation in the podocyte *in vivo* is examined through characterization of the nephrin$^{Y3F}$ mouse model. The inability to phosphorylate the three YDxV motif tyrosine residues in these mice does not prevent slit diaphragm formation, but results in podocyte foot process effacement and proteinuria with age. The model also shows that nephrin phosphorylation likely plays a protective role in the LPS model of injury. Finally, the phenotype is affected by genetic background, suggesting that the role of nephrin phosphorylation may be more complex than had been thought previously. Taken together, these results provide clear evidence in support of a functional role for nephrin tyrosine phosphorylation *in vivo*.

## 5.2 USE OF PHOSPHO-SPECIFIC NEPHRIN ANTIBODIES TO EXAMINE NEPHRIN PHOSPHORYLATION IN DISEASE

The phospho-specific antibodies described in this thesis were produced in collaboration with Epitomics Inc., which has since been acquired by Abcam. Although we initially attempted to generate three phospho-specific antibodies against each of the individual tyrosines pY1176, pY1193 and pY1217, it became clear during testing that the pY1176 antibody continued to

cross-react with pY1193 and it was therefore re-named pY1176/1193 to indicate that it recognizes both pY1176 and Y1193. Following the publication of our article describing their characterization in 2009 (Jones *et al.*, 2009), Epitomics began selling the pY1217 antibody (Cat # 2423-1), and later, they began to also offer the pY1176/1193 antibody (Cat # 2452-1).

In the five years since the commercial release of these antibodies, we have continued to use them in subsequent studies (Aoudjit *et al.*, 2011; Heikkila *et al.*, 2011; Jin *et al.*, 2012, Chapter 4; New *et al.*, 2013). It is also worth noting that similar phospho-specific nephrin antibodies have also been developed by other groups (Table 5.1). The availability of phospho-specific nephrin antibodies has allowed researchers to examine if there are changes in nephrin phosphorylation on specific tyrosines during the development and progression of a variety of models of glomerular injury. Contexts where changes in nephrin phosphorylation have been studied include the protamine sulfate model, the PAN model, the LPS model, and diabetic nephropathy. The current understanding of the role of nephrin phosphorylation in each of these cases is described below.

### 5.2.1 *PROTAMINE SULFATE MODEL*

The model where altered nephrin phosphorylation was first investigated was the protamine sulfate model, which is a model of rapid foot process effacement and recovery (Pippin *et al.*, 2009). Those investigations found that phosphorylation of both Y1176 and Y1193 was increased *in vitro* and *in vivo* after protamine sulfate treatment (Verma *et al.*, 2006; Harita *et al.*, 2009). Protamine sulfate-induced phosphorylation of Y1217 has been detected *in vitro* (Jeon *et al.*, 2012), but to my knowledge no one has directly examined phosphorylation of Y1217 following protamine sulfate infusion *in vivo*. The use of our Y1193 and Y1217 antibodies in immunofluorescence imaging of sections from protamine sulfate treated wildtype mice could allow us to confirm phosphorylation of Y1193 and could also provide evidence that protamine sulfate treatment induces Y1217 phosphorylation *in vivo*.

### 5.2.2 *PUROMYCIN AMINONUCLOSIDE (PAN) MODEL*

Another experimental model where nephrin phosphorylation has been examined is the PAN model. Decreased nephrin phosphorylation has been reported in the PAN model (Li *et al.*, 2006; Zhu *et al.*, 2008; Uchida *et al.*, 2008; Jones *et al.*, 2009; Zhu *et al.*, 2010), including both total phospho-tyrosine (Zhu *et al.*, 2008) and site-specific phosphorylation of Y1193 (Uchida *et al.*, 2008) and Y1217 (Uchida *et al.*, 2008; Jones *et al.*, 2009). The most likely explanation for the decrease in nephrin phosphorylation is altered regulation of nephrin phosphorylation. PAN treated animals show increased expression of a number of negative regulators of nephrin phosphorylation including PTP1β (Aoudjit *et al.*, 2011), PTP-PEST (Aoudjit *et al.*, 2011), and TMSF10 (Azhibekov *et al.*, 2011). As discussed, we have demonstrated that the phosphatase PTP1β can directly dephosphorylate nephrin and that its expression is upregulated on day 7 of PAN (Aoudjit *et al.*, 2011). This time point marks the onset of proteinuria and it is also when decreased nephrin phosphorylation is detected (Uchida *et al.*, 2008, Chapter 2). In addition, as described in the next section, LPS-induced proteinuria has been shown to be improved by treatments which can increase nephrin phosphorylation (Zhang *et al.*, 2010a; Kumagai *et al.*, 2012). Therefore, this suggests that similar treatment during the PAN model could also increase nephrin phosphorylation and possibly affect proteinuria. To test this hypothesis, we could examine the effects of PTP1β inhibition *in vivo* by treatment of animals with a PTP1β inhibitor (Calbiochem #539741, CAS # 765317-72-4) during the course of the PAN model. We could examine nephrin phosphorylation using the phospho-nephrin antibodies by western blot as well as by immunofluorescence staining of glomeruli at several timepoints and compare the results seen in animals with and without PTP1β inhibitor treatment. In addition, we could monitor the level of proteinuria in the animals by determination of the albumin/creatinine ratio during the course of PAN, and look at differences seen on day 7 as an experimental outcome, for example.

### 5.2.3 *LIPOPOLYSACCHRIDE (LPS) MODEL*

More recently, altered nephrin phosphorylation has also been examined in the LPS model. Decreased nephrin phosphorylation on Y1176/Y1193 has been reported in LPS treated mice (Zhang *et al.*, 2010a), and the *in vivo* blockade of c-mip—a negative regulator of Fyn kinase—

prior to LPS treatment resulted in increased nephrin phosphorylation and decreased proteinuria (Zhang *et al.*, 2010a). In addition, mice lacking the phosphatase PTP1β—which we have previously shown can de-phosphorylate nephrin on YDxV tyrosines (Aoudjit *et al.*, 2011) —are protected from LPS proteinuria (Kumagai *et al.*, 2012). Furthermore, the treatment of wildtype mice with a PTP1β inhibitor reduced LPS-induced proteinuria (Kumagai *et al.*, 2012). It would be useful to confirm LPS-induced nephrin dephosphorylation using our phospho-nephrin antibodies on wildtype mice treated with LPS for different amounts of time. In addition, as PTP1β may dephosphorylate Y1193 more effectively than Y1217 (Aoudjit *et al.*, 2011), it would also be interesting to use the Y1193 and Y1217 antibodies on samples from LPS treated mice to determine if the amount of LPS induced nephrin dephosphorylation differs between Y1193 and Y1217.

### 5.2.4 *DIABETIC NEPHROPATHY*

A final case where nephrin phosphorylation may be altered is diabetic nephropathy. There are currently a small number of studies which have examined nephrin phosphorylation in diabetic nephropathy (Mima *et al.*, 2012; Denhez *et al.*, 2013; Dessapt-Baradez *et al.*, 2013). One such study detected increased nephrin phosphorylation in STZ treated diabetic mice (Dessapt-Baradez *et al.*, 2013), which is consistent with a report that high glucose increases nephrin phosphorylation *in vitro* (Jeon *et al.*, 2012). However, a different study found nephrin phosphorylation was decreased in diabetic Akita mice (Denhez *et al.*, 2013). This study attributed the decrease in nephrin phosphorylation to increased nephrin dephosphorylation by the phosphatase SHP-1 (Denhez *et al.*, 2013). SHP-1 expression has recently been recognized to be upregulated in diabetes and to contribute to the effects of diabetes on the podocyte (Mima *et al.*, 2012; Drapeau *et al.*, 2013). As these two studies saw opposite results, we could aid in clarification of the status of nephrin phosphorylation in diabetes through use of our Y1193 and Y1217 antibodies on samples from non-diabetic and diabetic mice and see if we observe a difference in the amount of nephrin phosphorylation. Further research may show stronger associations than have been discovered to date.

## 5.3 INSIGHTS INTO THE REGULATION OF NEPHRIN TYROSINE PHOSPHORYLATION

The cytoplasmic tail of human nephrin contains three YDxV motifs; this is the only tyrosine motif found in the cytoplasmic tail of nephrin which is consistently duplicated across other mammalian species. We have previously shown that Nck is recruited to phosphorylated nephrin and that this initiates actin polymerization *in vitro* (Blasutig *et al.*, 2008). We have also demonstrated that co-expression of nephrin and Nck leads to increased nephrin phosphorylation relative to when nephrin is expressed alone. This effect is dependent on the SH3 domains of Nck and on Src family kinase activity and we provided evidence that it was caused by recruitment of Fyn to nephrin by Nck. Further, we were able to show that loss of podocyte Nck *in vivo* results in decreased nephrin phosphorylation, confirming that our *in vitro* hypothesis is also relevant in an *in vivo* context. Our data suggests an unanticipated role for Nck in promoting increased nephrin phosphorylation. What reasons might there be for the development of such a phenomenon? The most likely explanation for the augmentation of nephrin phosphorylation by Nck is that this increases nephrin phosphorylation, leading to the generation of additional Nck binding sites; further recruitment of Nck to those sites therefore ultimately results in a significant increase in the local Nck concentration.

The importance of the local Nck concentration has recently become clear—it appears to represent a finely tuned mechanism for tightly controlled spatial regulation of Arp2/3 based actin dynamics. We have previously determined the minimum number of binding sites required for robust initiation of actin polymerization downstream of the nephrin-Nck interface using an *in vitro* chimeric CD16-nephrin clustering system (Blasutig *et al.*, 2008). It appears that the combination of a single nephrin pY site and a single Nck SH3 domain cannot initiate actin remodeling, whereas a single nephrin pY site is sufficient provided that all Nck SH3 domains are available (Blasutig *et al.*, 2008). In addition, others have clearly established that stoichiometry requirements dictate the minimum local concentration of Nck required for actin polymerization to occur (Ditlev *et al.*, 2012). Recently, Li *et al.* postulated another potential mechanism explaining why activation of actin polymerization only occurs above a certain Nck concentration (Li *et al.*, 2012). They found that binding of high avidity complexes with multiple tandem binding sites such as can be found in a nephrin-Nck-N-WASp complex can induce a phase

transition from a liquid phase into a gel-like polymer structure, and that this transition correlates strongly with biological activity (Li *et al.*, 2012). Notably, the threshold concentration of Nck required to trigger the phase transition decreased two-fold with the addition of a peptide from the cytoplasmic tail of nephrin containing two pYDxV sites and there was an even larger decrease larger when nephrin contained three pYDxV sites (Li *et al.*, 2012).

These ideas lend support to the concept that there could be multiple pools of nephrin within the podocyte, which has been suggested by observations that only a fraction of total rat nephrin was phosphorylated on Y1193 (Zhang *et al.*, 2010b), and also that only a fraction of total nephrin was present in lipid rafts (Yuan *et al.*, 2002). In fact, given these findings, it seems likely to be the case that only a small fraction of the total amount of nephrin in the podocyte is phosphorylated on all three YDxV motifs at any given moment. Further, it is clear that this high degree of phosphorylation appears necessary to actively drive actin polymerization (Li *et al.*, 2012) and it may also act as a threshold to ensure the pathway is only activated in response to an appropriate level of stimulus (Ditlev *et al.*, 2012). Despite representing a small percentage of total nephrin, this could represent an important mechanism used within the podocyte to maintain the connection between the podocyte slit diaphragm and the internal actin cytoskeleton when linked with our data demonstrating that Nck promotes increased nephrin phosphorylation and therefore raises the local Nck concentration, which is essential for initiation of downstream Nck signaling.

## 5.4 FURTHER ANALYSIS OF NEPHRIN$^{Y3F/Y3F}$ MICE

We have described an initial characterization of the nephrin$^{Y3F/Y3F}$ mouse model with reduced nephrin tyrosine phosphorylation due to three Y-to-F mutations in the three YDxV motifs of the cytoplasmic tail of nephrin. Although these phosphorylation sites are absent, it does not seem to affect the formation of normal podocyte foot process architecture. On the C57Bl/6 genetic background, however, nephrin$^{Y3F/Y3F}$ mice develop proteinuria beginning at 8 months of age. Their glomeruli have dilated capillary loops and their podocyte foot processes are disorganized. On the CD-1 genetic background, the onset of the phenotype is accelerated. In CD-1 nephrin$^{Y3F/Y3F}$ mice, mild changes in foot process patterning are detectable by 9 weeks of age,

and mice progress to significant proteinuria and loss of normal podocyte architecture by 15 weeks of age. Both C57Bl/6 nephrin$^{Y3F/Y3F}$ and CD-1 nephrin$^{Y3F/Y3F}$ develop dilated capillary loops and show irregular thickening of the GBM into 'spikes' following the onset of proteinuria. There does not appear to be a difference in systolic blood pressure between nephrin$^{WT/WT}$ and nephrin$^{Y3F/Y3F}$ mice of either strain, suggesting that increased capillary loop size is not a direct response to increased blood pressure. These efforts have described the effects of the nephrin$^{Y3F}$ mutation on podocyte foot process architecture, and they generate a number of follow-up questions about the specific molecular mechanisms behind these observations.

### 5.4.1 *Determine the composition of the altered GBM seen in nephrin$^{Y3F/Y3F}$ mice*

A significant aspect of the phenotype of nephrin$^{Y3F/Y3F}$ mice is the prominent GBM alterations, which present primarily as spike-like protrusions which form on the epithelial face of the GBM beneath podocytes. However, the normal appearance of the GBM in C57Bl/6 nephrin$^{Y3F/Y3F}$ mice at four weeks of age suggests that the initial production of the GBM is not affected. The more pronounced GBM phenotype observed in CD-1 nephrin$^{Y3F/Y3F}$ than in C57Bl/6 nephrin$^{Y3F/Y3F}$ mice is consistent with the level of proteinuria in each strain. Therefore, it is recommended that CD-1 background mice be used in any future experiments that would examine GBM composition as outlined below.

To be able to determine how the GBM of CD-1 nephrin$^{Y3F/Y3F}$ mice changes during the development of disease, we would likely need to examine TEM images from mice at multiple ages. A logical place to begin would be with the examination of 4 week old CD-1 nephrin$^{Y3F/Y3F}$ mice which would allow us to confirm that the GBM appears normal by TEM, which would be in agreement with light microscopy results. After this, I would recommend the examination of TEM images from CD-1 nephrin$^{Y3F/Y3F}$ mice at other ages. For example, one possible age is 9 weeks, which is the earliest age where we can observe minor changes in podocyte foot process architecture by SEM, and we can also begin to see a few spikes in some glomeruli by light microscopy. Another possible age is shortly after the onset of severe proteinuria, which generally occurs between 13-15 weeks of age. At this age, light microscopy data indicates that spikes become more wide spread and they are clearly visible in a large number of glomeruli.

The alterations to the GBM seen in nephrin$^{Y3F/Y3F}$ mice develop with age, suggesting that changes to the GBM are likely due to altered GBM deposition or remodeling in response to the high capillary pressure of the glomerulus. One possible source for these changes is the altered expression of proteins involved in the formation or maintenance of the GBM. The changes to the GBM in nephrin$^{Y3F/Y3F}$ mice could be the result of enhanced synthesis of GBM components such as the various laminin and type IV collagen isoforms which are expressed in the glomerulus. One suggested method to analyze the GBM in CD-1 nephrin$^{Y3F/Y3F}$ mice would be to evaluate the expression levels of the major GBM components found in both the developing and mature glomerulus (Abrahamson, 2012; Miner, 2012), which could include laminins α1, α2, α4, and α5; laminins-β1 and β2; type IV collagens α1 - α6; and fibronectin. Expression and localization of these proteins within the glomerulus could be monitored using immunohistochemistry and immunofluorescence techniques. The comparison of an early time point (such as 4 weeks), when the GBM appears normal, with a later time point (such as 15 weeks), when abnormal GBM spikes are visible, would allow us to categorize which GBM components are being incorporated into the altered GBM structures which form in nephrin$^{Y3F/Y3F}$ mice.

Another possible cause of increased GBM proteins is decreased turnover of the GBM which is mediated by matrix metalloproteinases (MMPs). Both increased and decreased levels of several different MMPs have been reported in glomerular disease (Veron *et al.*, 2010; Kato *et al.*, 2011; Reidy *et al.*, 2013). In order to look at changes in MMPs, we could evaluate MMP protein levels by western blot and MMP activity by gelatin zymography in glomerular lysates from 15 week old nephrin$^{WT/WT}$ and nephrin$^{Y3F/Y3F}$ mice. Two likely candidate MMPs which are highly expressed in the glomerulus are MMP-2 and MMP-9, which mediate degradation of laminins and type IV collagen respectively (Rawlings *et al.*, 2013). While we could also analyze levels of MMPs and GBM components by qPCR, that approach would not provide any information about the spatial arrangements of the proteins; in addition, changes in mRNA levels do not always correlate with altered protein levels.

As discussed previously, GBM alterations similar to those seen in nephrin$^{Y3F/Y3F}$ mice are also observed in Alport mice (Meehan *et al.*, 2009) and tetraspanin CD151 knockout mice

(Baleato *et al.*, 2008). Alport syndrome is caused by the absence of type IV collagen (α3, α4, α5) from the GBM (Kruegel *et al.*, 2013). Therefore, the resulting GBM that is produced in Alport syndrome contains only type IV collagen (α1, α2, α1), which generates an abnormal GBM that is more elastic than the usual mature GBM (Gunwar *et al.*, 1998; Wyss *et al.*, 2011). One commonality between Alport syndrome and CD151-knockout mice is increased glomerular strain (Sachs *et al.*, 2012; Zallocchi *et al.*, 2013), which in CD151-knockout mice is due to reduced adhesion of α3β1 integrin to laminin-521 in the GBM because the integrins are no longer distributed throughout a tetraspanin web (Sachs *et al.*, 2012). Zallocchi *et al*. recently reported on a potential cause of the GBM thickening seen in both Alport mice and CD151 knockout mice (Zallocchi *et al.*, 2013). They determined that due to the underlying GBM adhesion defects described above, increased biomechanical strain on the glomerulus activates mesangial cell process invasion of the capillary loop GBM and the ectopic deposition of mesangial laminin-211 (Zallocchi *et al.*, 2013). Given the similarities between the GBM alterations seen in these models and in nephrin$^{Y3F/Y3F}$ mice, it would be very interesting to test the hypothesis that the GBM alterations in nephrin$^{Y3F/Y3F}$ mice occur through a similar mechanism.

Overall, it is clear that there are a number of possible explanations for the GBM changes seen in nephrin$^{Y3F/Y3F}$ mice, and I am hopeful that future efforts will be able to provide a plausible answer to this puzzle. As for why such GBM changes might occur in nephrin$^{Y3F/Y3F}$ mice, I will leave that question for future scientists, but can offer the suggestion that it would appear that pY1217 nephrin can be detected in small amounts on the basal surface of healthy podocyte foot processes *in vivo*, and that it is also present on the basal surface of foot processes which have regenerated during the course of disease (Ohashi *et al.*, 2010). It will be up to others to determine if these observations might be connected to altered podocyte adhesion.

### 5.4.2 *Analyze the phenotype of FVB nephrin$^{Y3F/Y3F}$ mice*

As described in this thesis, we initially generated nephrin$^{Y3F/Y3F}$ mice on the C57Bl/6 background. We saw mild proteinuria by six months and some degree of foot process alteration and GBM thickening by 11 months of age. To test if the C57Bl/6 genetic background was

responsible for the mild phenotype, we migrated the mutation to the CD-1 (outbred) and the FVB (inbred) backgrounds. After migrating the mutation to the CD-1 background, we observed a more severe phenotype than the one which we originally characterized on the C57Bl/6 background, with proteinuria occurring by one month of age. In contrast to the CD-1 background, we did not observe any proteinuria in nephrin$^{Y3F/Y3F}$ mice on the FVB background, even by six months of age. The glomerular phenotype of nephrin$^{Y3F/Y3F}$ mice on the FVB background has not yet been fully characterized; therefore, any future work should begin with a thorough analysis of podocyte foot process architecture in FVB nephrin$^{Y3F/Y3F}$ mice. The use of SEM and TEM for this analysis is recommended, as this would permit the detection of foot process effacement and subtle changes to glomerular architecture. For this reason, a complete SEM and TEM analysis of the structure of the GBM in one month old FVB nephrin$^{Y3F/Y3F}$ mice is strongly suggested, as this would provide an important baseline for comparisons with later time points.

If these efforts do not detect any significant morphological changes in FVB nephrin$^{Y3F/Y3F}$ mice, it is possible that some element of the FVB genetic background could be responsible for the mild phenotype. For example, a recent study investigated possible reasons for the well-established strain-dependent difference in levels of microalbuminuria between C57Bl/6 and FVB mice, with FVB mice having higher levels than C57Bl/6 mice (Long *et al.*, 2013). They found that FVB mice have reduced expression of podocin and synaptopodin mRNA compared to C57Bl/6 mice and they also had decreased levels of type IV Collagen α1 (*Col4a1*) mRNA (Long *et al.*, 2013). These findings are of interest as differences in podocin expression have been recently shown to affect the severity of human kidney disease (Agrawal *et al.*, 2013). In addition, differences in the expression of collagen isoforms have been reported to affect the severity of renal disease in mice. For example, type IV Collagen α3 (*Col4a3*) knockout mice, which model Alport syndrome (Kruegel *et al.*, 2013), show an increased survival rate on the C57Bl/6 background compared to the 129 background due to inherent differences in the expression level of type IV Collagen α6 (*Col4a6*) between the two strains (Kang *et al.*, 2006).

Another possibility is that some C57Bl/6 chromosomal segments could still be present in FVB nephrin$^{Y3F/Y3F}$ mice. When we performed a speed congenic analysis of potential FVB

nephrin$^{WT/Y3F}$ breeders in 2011 using the services of IDEXX-RADIL, there were four markers in our selected animals which were still heterozygous for the C57Bl/6 genome. Backcrossing to FVB has continued since that time, and whether any markers are still heterozygous for the C57Bl/6 genome in the current population can be readily determined via another round of speed congenic genetic analysis. It is tempting to hypothesize that one of the genes found in those regions which retained C57Bl/6 genetic material could still exist in the population and that it could be responsible for the lack of phenotype in FVB mice; this type of phenomenon has been recently reported in the literature (Prakash *et al.*, 2011). During the mapping of quantitative trait loci (QTLs) controlling susceptibility to HIV-associated nephropathy using Balb/c (resistant) and FVB (susceptible) strains, the authors noted that a genetic bottleneck resulted in the loss of susceptibility in one of their FVB breeding colonies (Prakash *et al.*, 2011). They analyzed the genetic makeup of their resistant FVB mice using a single nucleotide polymorphism (SNP) panel and found that 13 out of 1305 SNPs were not consistent with being from the FVB strain; these SNPs corresponded to two different chromosomal segments which covered the Balb/c resistant locus they previously identified, strongly suggesting that their resistant FVB mice acquired a high frequency of the Balb/c resistant locus during their genetic bottleneck (Prakash *et al.*, 2011).

Further investigation will be required to determine whether either of the possibilities described above hold in FVB nephrin$^{Y3F/Y3F}$ mice. Alternatively, several examples appear in the literature where migration to the FVB background did not produce a phenotype. Recent reports investigating the phenotype of podocyte-specific *Myh9* knockout mice on multiple genetic backgrounds found that podocyte-specific *Myh9* knockout mice did not develop a phenotype either on the FVB background (Johnstone *et al.*, 2013) or on the C57Bl/6 background (Johnstone *et al.*, 2011). However, these outcomes contrast with an independent effort which reported a phenotype in podocyte-specific *Myh9* knockout mice on a mixed background of C57BL/6, BALB/c, and 129/SJ (Zhang *et al.*, 2012b). This suggests the possibility that the heterozygosity seen in the mixed background could be a contributor to the *Myh9* phenotype as compared to the two inbred backgrounds. Similarly, we observed the strongest phenotype of nephrin$^{Y3F/Y3F}$ mice on the CD-1 outbred background, as compared to the exact same two inbred backgrounds.

We faced an additional difficulty during the analysis of FVB nephrin$^{Y3F/Y3F}$ mice, as a smaller number of nephrin$^{Y3F/Y3F}$ animals were born than we anticipated. We attempted to generate FVB nephrin$^{Y3F/Y3F}$ mice through the crossing of heterozygous nephrin$^{WT/Y3F}$ parents. In eight litters of mice (n=69), there were a total of nine nephrin$^{Y3F/Y3F}$ mice born, with one dying shortly after birth. Of the 68 FVB mice genotyped at weaning, the resulting Mendelian ratios were $0.35^{(WT/WT)}$: $0.53^{(WT/Y3F)}$: $0.12^{(Y3F/Y3F)}$ (Figure 5.1), meaning that the percentage of FVB nephrin$^{Y3F/Y3F}$ mice born was approximately half the value predicted (0.25). In comparison, both C57Bl/6 and CD-1 nephrin$^{Y3F/Y3F}$ mice were born in the expected Mendelian ratio (Figure 5.1), indicating that some FVB nephrin$^{Y3F/Y3F}$ mice might be dying *in utero*.

Why might this be occurring? It is important to remember that the nephrin$^{Y3F}$ mutation is expressed throughout the whole animal. Indeed, while nephrin is highly expressed in the kidney, its expression can also be found in other organs in the mouse including the brain (Putaala *et al.*, 2001; Beltcheva *et al.*, 2003; Morikawa *et al.*, 2007; Nishida *et al.*, 2010; Li *et al.*, 2011), testes (Liu *et al.*, 2001; Juhila *et al.*, 2010) and heart (Wagner *et al.*, 2011). The study of nephrin expression in the heart, which was performed on the FVB background, found that approximately 25% of nephrin-knockout mice died before birth between E12.5 and E15.5 due to severe cardiac dysfunction based on alterations to the epicardium (Wagner *et al.*, 2011). This contrasts with the results of a different group that generated nephrin-rescue mice which expressed rat nephrin specifically in the podocytes of nephrin-knockout mice. These mice were on the CD-1 background and there were no heart defects detected in six week old nephrin-rescue mice (Juhila *et al.*, 2010). It was also reported in their study that the birth rate of mice homozygous for the nephrin-knockout allele from crosses of heterozygous parents was 20% (Juhila *et al.*, 2010), which is similar to the ratio we observed for nephrin$^{Y3F/Y3F}$ mice on both the CD-1 and C57Bl/6 backgrounds (Figure 5.1).

One possible explanation for the difference between the results obtained on the FVB background and the results seen on other backgrounds is that there are significant differences in baseline cardiac function between FVB and other strains (Barnabei *et al.*, 2010). This difference is known to translate into significantly different phenotypes, such as in the case of a mutation in α-tropomyosin (Glu180Gly), which is associated with the development of familial hypertrophic

cardiomyopathy in humans. When the α-tropomyosin mutation was expressed on the FVB background, it resulted in severe cardiac alterations leading to death by 4-5 months of age (Prabhakar *et al.*, 2001). In contrast, when it was expressed on the C57Bl/6 background, no significant histological changes were seen in mutant mice at 12 months of age (Michele *et al.*, 2002).

Based on these ideas, it would be interesting to determine if FVB nephrin$^{Y3F/Y3F}$ mice are dying during development due to a heart defect similar to the one detected in FVB nephrin-knockout mice (Wagner *et al.*, 2011). In order to do so, we would need to perform timed matings and determine the number of embryos of each genotype at E12.5, as this is prior to the age when FVB nephrin-knockout embryos begin to die from heart malformation defects (Wagner *et al.*, 2011). This would allow us to calculate the frequency of FVB nephrin$^{Y3F/Y3F}$ mice at that age, and to determine if it is closer to 25%. At the same time, we could also compare the epicardium morphology in FVB nephrin$^{Y3F/Y3F}$ mice at E12.5 with that reported by Wagner *et al*. in E12.5 FVB nephrin-knockout mice (Wagner *et al.*, 2011). In addition, an analysis of the hearts of C57Bl/6 nephrin$^{Y3F/Y3F}$ mice at E12.5 would provide a good control to be able to fully attribute any changes seen in the developing heart in FVB nephrin$^{Y3F/Y3F}$ mice to an effect of the FVB genetic background on the nephrin$^{Y3F}$ mutation. It would also be interesting to directly compare nephrin$^{Y3F/Y3F}$ mice and nephrin-knockout mice. We happen to have nephrin-knockout mice in our mouse colony (Jax strain 005692), however they are on a mixed C57Bl/6 and 129 genetic background (Jackson Labs,; Hamano *et al.*, 2002). This would likely make it difficult to use them to compare and contrast with FVB nephrin$^{Y3F/Y3F}$ mice, as the nephrin-knockout mice could have normal hearts due to the strain-dependent differences described (Michele *et al.*, 2002). Therefore, another possibility would be to ask the researchers that generated the FVB nephrin-knockout mice (Wagner *et al.*, 2011) if they would be willing to share their animals with us.

The results from the experiments outlined above would allow us to be able to compare and contrast the effects of the total absence of nephrin in nephrin-knockout mice with the effects of the loss of nephrin phospho-tyrosine signaling through the three tyrosine residues mutated in nephrin$^{Y3F/Y3F}$ mice. If the findings in FVB nephrin$^{Y3F/Y3F}$ mice are similar to those seen in FVB

nephrin-knockout mice, this would provide us with some important new insights into the roles of nephrin and nephrin phosphorylation in the developing heart.

### 5.4.3 *INVESTIGATE THE RESPONSE OF NEPHRIN$^{Y3F/Y3F}$ MICE TO PROTAMINE SULFATE TREATMENT*

Nephrin tyrosine phosphorylation has been shown to increase in the protamine sulfate model of experimental podocyte injury and decrease following recovery (Verma *et al.*, 2006), leading to the hypothesis that phospho-nephrin signaling is actually driving the effacement process (Patrakka and Tryggvason, 2007). Examination of the response of nephrin$^{Y3F/Y3F}$ mice to protamine sulfate-induced injury provides an elegant method to test this hypothesis.

In the protamine sulfate model, kidneys are perfused with protamine sulfate, which is thought to neutralize the negative surface charge of the podocyte, resulting in foot process effacement within 15 minutes (Pippin *et al.*, 2009). After treatment with protamine sulfate, kidneys can also be perfused with heparin sulfate for an additional 15 minutes, which neutralizes the charge of the protamine sulfate and results in the recovery of normal foot process structures. The potential outcomes from performing this model in genetically altered mice are protection from effacement following protamine sulfate perfusion, as seen in animals lacking Crk1/2 adaptor proteins (George *et al.*, 2012), or the inability to restore normal foot process architecture following heparin sulfate perfusion, as seen in mutant mice lacking the actin-associated protein synaptopodin (Asanuma *et al.*, 2005). Alternatively, there could be no difference seen in genetically altered mice.

I recommend that such experiments are performed using four week old C57Bl/6 nephrin$^{Y3F/Y3F}$ mice. This will make it easier to compare the effects of protamine sulfate treatment on C57Bl/6 nephrin$^{WT/WT}$ and nephrin$^{Y3F/Y3F}$ mice because podocyte foot process architecture, the GBM and the endothelium all appear normal in nephrin$^{Y3F/Y3F}$ mice at this age. One method which could be used to quantitatively assess the effects of protamine sulfate on podocyte foot process architecture is the use of morphometric analysis to evaluate the differences in foot process effacement between the different genotypes. This method calculates the frequency of foot processes/unit length of GBM, and the measure is proportional to the average

foot process width (van den Berg *et al.*, 2004). We could begin by confirming that the experiment has been performed successfully by examining the effects of protamine sulfate and heparin sulfate treatments in wildtype mice using both visual inspection and morphometric analysis of TEM images. Once validated, these methods could then be used to test how both treatments affect nephrin$^{Y3F/Y3F}$ mice.

Preliminary evidence from a pilot study that we performed (New *et al*, unpublished observations) suggests that nephrin$^{Y3F/Y3F}$ mice undergo foot process effacement following protamine sulfate infusion. These results must be confirmed using a larger cohort of mice. As well, it is not known if protamine sulfate treated nephrin$^{Y3F/Y3F}$ mice will recover from effacement after treatment with heparin sulfate. The increased proteinuria in nephrin$^{Y3F/Y3F}$ mice seen in the LPS model suggests that phospho-nephrin signaling could be associated with the preservation of podocyte function. If this holds more generally, then it is likely that the inability to activate tyrosine phosphorylation-dependent signaling pathways in nephrin$^{Y3F/Y3F}$ mice will prevent restoration of normal foot process morphology after heparin sulfate treatment. This hypothesis requires validation with experimental evidence, however. Regardless of the results obtained from these experiments, they will provide new data on whether nephrin phosphorylation is required for rearrangement of the podocyte actin cytoskeleton as part of the mechanisms driving effacement. In addition, they will also provide a suggestion on whether nephrin phosphorylation plays an important role in the mechanisms responsible for the restoration of podocyte architecture.

### 5.4.4 *INVESTIGATE THE RESPONSE OF NEPHRIN$^{Y3F/Y3F}$ MICE TO THE DIABETIC MILIEU*

Not only is nephrin found in the glomerulus, but it is also found in pancreatic beta cells (Palmen *et al.*, 2001; Beltcheva *et al.*, 2003; Zanone *et al.*, 2005), where it associates with insulin containing vesicles (Fornoni *et al.*, 2010) and is required for their transport to the plasma membrane in response to glucose (Fornoni *et al.*, 2010; Jeon *et al.*, 2012). Further, elevated glucose concentrations increase nephrin phosphorylation in beta cells on Y1176/Y1193 (Jeon *et al.*, 2012), and the equivalent mutations in human nephrin to those found in our nephrin$^{Y3F/Y3F}$ mice prevent nephrin-mediated insulin release from beta cells (Jeon *et al.*, 2012). While we have

not examined the glucose levels of nephrin$^{Y3F/Y3F}$ mice, they do not exhibit classical symptoms of diabetes such as increased water consumption and urination, suggesting that the beta cells of nephrin$^{Y3F/Y3F}$ mice are able to regulate insulin release appropriately.

In addition, in recent years, it has also become clear that podocytes are insulin sensitive cells and that nephrin is involved in the podocyte insulin response (Coward *et al.*, 2007; Welsh *et al.*, 2010). In podocytes, nephrin is required for proper trafficking of the constitutive glucose transporter GLUT1 and the insulin-sensitive glucose transporter GLUT4 to the plasma membrane in response to insulin (Coward *et al.*, 2007; Wasik *et al.*, 2012). Moreover, recent evidence suggests that the effects of glucose on nephrin phosphorylation may not be limited to the pancreas, and that the development of diabetic nephropathy may be influenced by the effects of glucose on nephrin phosphorylation in the glomerulus. However, the relationship between glucose, nephrin phosphorylation, and diabetic nephropathy is not well understood. One study reported that diabetic mice have decreased levels of Angiopoietin-1 (Ang-1) and increased levels of nephrin phosphorylation on Y1176/Y1193 (Dessapt-Baradez *et al.*, 2013). They found that induction of podocyte-specific Ang-1 expression in diabetic mice increased Ang-1 levels and decreased proteinuria; this also resulted in a reduction in nephrin phosphorylation on Y1176/Y1193 (Dessapt-Baradez *et al.*, 2013). In contrast, other studies have shown that nephrin phosphorylation on Y1176/Y1193 is decreased in diabetic mice (Denhez *et al.*, 2013) and in diabetic rats (Mima *et al.*, 2012).The decreased nephrin phosphorylation in diabetic mice was linked to increased nephrin dephosphorylation by the tyrosine phosphatase SHP-1 (Denhez *et al.*, 2013), which is upregulated in the podocytes of diabetic animals (Mima *et al.*, 2012), where it impairs both insulin signaling (Drapeau *et al.*, 2013) and VEGF-A signaling (Mima *et al.*, 2012). Additionally, the prevention of increased SHP-1 expression in diabetes reduces symptoms of diabetic nephropathy (Mima *et al.*, 2012). PKC-delta activation is required for SHP-1 expression (Geraldes *et al.*, 2009), and diabetic PKC-delta knockout mice, which do not have elevated SHP-1 expression, show reduced levels of proteinuria (Mima *et al.*, 2012).

There are several different approaches that we could take to help resolve the current differences in the literature regarding nephrin phosphorylation during diabetes, specifically, whether nephrin phosphorylation is increased or decreased during diabetes, and also whether

nephrin phosphorylation plays a positive or negative role in the pathogenesis of diabetic nephropathy. The first question can be answered using our phospho-specific antibodies. For example, diabetic PKC-delta knockout mice, which do not have elevated SHP-1 levels because PKC-delta activation is required for SHP-1 expression (Geraldes *et al.*, 2009), show reduced levels of proteinuria (Mima *et al.*, 2012). The phospho-specific nephrin antibodies could be used on diabetic PKC-delta knockout mice to determine if they show increased nephrin phosphorylation relative to diabetic wildtype mice. If this were to be observed, it would support the hypothesis that SHP-1 mediated nephrin dephosphorylation could be a contributor to the development of diabetic nephropathy (Denhez *et al.*, 2013).

The role of nephrin phosphorylation in diabetic nephropathy can be answered by modeling diabetes in our nephrin$^{Y3F/Y3F}$ mice. One of the standard methods to model diabetes in mice is to use the STZ model in male C57Bl/6 mice (Brosius *et al.*, 2009). Although wildtype C57Bl/6 mice are generally resistant to the development of diabetic nephropathy relative to other strains (Qi *et al.*, 2005), some genetically altered mice on the C57Bl/6 background develop diabetic nephropathy (Kanetsuna *et al.*, 2007). If we performed the STZ model with male nephrin$^{WT/WT}$ and nephrin$^{Y3F/Y3F}$ mice on the C57Bl/6 background, this would allow us to determine if the nephrin$^{Y3F}$ mutations increase susceptibility to diabetic nephropathy. To test the converse hypothesis, we could perform the STZ model using male FVB nephrin$^{WT/WT}$ and nephrin$^{Y3F/Y3F}$ mice. As FVB mice are likely more prone to diabetic nephropathy than C57Bl/6 mice (Qi *et al.*, 2005), this experiment could provide insight into the question of whether the nephrin$^{Y3F}$ mutations were protective against the development of diabetic nephropathy; if this hypothesis were true, we would expect to see decreased levels of proteinuria in diabetic FVB nephrin$^{Y3F/Y3F}$ mice compared to diabetic FVB nephrin$^{WT/WT}$ mice. However, given our difficulties generating FVB nephrin$^{Y3F/Y3F}$ mice (see section 5.4.2), this may not be a practical experiment to attempt. Alternatively, if we were to use male mice on the CD-1 background, this could allow us to determine if diabetes exacerbates the renal disease phenotype which develops in those animals.

While the experiments described above may provide some insights, it is clear that a significant amount of additional research will be required in order to fully clarify the relationship between nephrin phosphorylation and diabetes.

### 5.4.5 *ANALYZE THE EFFECTS OF THE NEPHRIN$^{Y3F}$ MUTATION IN VITRO USING A NEPHRIN$^{Y3F}$ PODOCYTE CELL LINE*

Further analysis of nephrin$^{Y3F/Y3F}$ mice as described in the preceding sections will allow us to learn more about how nephrin$^{Y3F}$ functions *in vivo*, however, those types of studies do not generally result in significant mechanistic insights unless accompanied by complementary *in vitro* data using a relevant cell line. Podocytes are terminally differentiated cells and they do not normally proliferate in culture. Luckily, the Immorto™ mouse has provided a method to generate *in vitro* cell lines from transgenic mouse models (Noble *et al.*, 1995). Briefly, the SV40 large T antigen transgene present in Immorto™ mice allows researchers to develop conditionally immortalized podocyte cell lines which proliferate at 33°C when treated with interferon-gamma (Shankland *et al.*, 2007). This allows for continued growth and passage of 'undifferentiated' podocytes at 33°C. To induce 'differentiation', podocytes are plated at a low density and transferred to 37°C where they are grown without interferon supplement. The lack of interferon, coupled with the temperature change, results in the degradation of SV40 and halts proliferation. Over a period of 14 days, the podocytes undergo a remarkable increase in cell size and shape, and begin to express markers of podocyte differentiation such as synaptopodin. After the 14 day differentiation period, the cells are ready to be used for experiments.

The methods required to passage podocyte cell lines are relatively straight forward, though more labour intensive than other cell lines as podocytes require increased care, including having their medium changed every third day. In contrast, the *de novo* generation of a podocyte cell line from a mouse model can be much more difficult. During the course of my doctoral studies, I was privileged to be awarded with a Michael Smith Foreign Study Supplement from NSERC. This award allowed me to travel to Boston, Massachusetts for the summer of 2012, where I worked in the lab of Dr. Peter Mundel with the aim to successfully generate podocyte cell lines from nephrin$^{WT/WT}$ and nephrin$^{Y3F/Y3F}$ littermates. During my stay in Boston, I successfully isolated podocytes from both genotypes of mice. These initial podocytes were a mixed population, and I began the process of generating individual clones of both lines. At the end of my stay, the

podocytes were shipped back to Guelph, where I have been collaborating with a fellow graduate student, Claire Martin, to continue their characterization.

The next phase of the project plans to focus on validation of the lines by differentiating them and verifying that they express podocyte proteins such as nephrin, podocin, synaptopodin and WT-1. Some groups have reported that cultured podocytes have low levels of nephrin expression (Takano *et al.*, 2007). If we are unable to detect nephrin expression by Western blot, we could consider the use of supplements in the medium such as retinoic acid or vitamin D which can increase nephrin expression (Takano *et al.*, 2007; Okamura *et al.*, 2009). Alternatively, we could consider stably expressing our myc-tagged human nephrin$^{WT}$ and nephrin$^{Y3F}$ constructs in the corresponding cell lines; this would allow us to more reliably increase nephrin expression, which could potentially affect cell-cell adhesion (Heikkila *et al.*, 2011; Jeon *et al.*, 2012).

Once we have established nephrin$^{WT}$ and nephrin$^{Y3F}$ podocyte lines with adequate nephrin expression, there are a number of avenues which we could pursue with them. A likely first step would be to stain them with actin and tubulin to determine if nephrin$^{Y3F}$ podocytes have any obvious differences in the arrangement of their cytoskeleton. We could also measure the average shape and size of differentiated nephrin$^{WT}$ and nephrin$^{Y3F}$ podocytes to see if they have changes in overall cell architecture. In addition, we could perform a number of assays which measure the functional properties of podocytes *in vitro* and use them to compare the properties of nephrin$^{WT}$ and nephrin$^{Y3F}$ podocytes. Examples of possible assays include albumin permeability (Li *et al.*, 2008), response to calcium flux (Hunt *et al.*, 2005; Foster *et al.*, 2010), the effects of stretch (Martineau *et al.*, 2004; Schordan *et al.*, 2011; Eekhoff *et al.*, 2011) and migration rates (Chittiprol *et al.*, 2011).

Lastly, it would be exciting to attempt to model podocytes *in vitro* in a more representational manner. Podocytes create a unique three dimensional (3D) shape *in vivo*, which is not replicated in a two dimensional (2D) environment. The effects of 3D culture compared to 2D culture have been well documented in cultured mammary epithelial cells, which, when grown in 3D, form alveolar-like structures and can even be induced to produce milk proteins (Barcellos-Hoff *et al.*, 1989). There have been a number of recent innovations for the production of different 3D

scaffolds which could possibly be used to grow podocytes (Knight *et al.*, 2011; Sharma *et al.*, 2013; Puschmann *et al.*, 2013). There are also scaffolds which have been designed to have some of the properties found in basement membranes that have been used to test the co-culture of podocytes with either endothelial cells or mesangial cells (Wang and Takezawa, 2005; Slater *et al.*, 2011).

## 5.5 THE EMERGING RELATIONSHIP BETWEEN NEPHRIN TYROSINE PHOSPHORYLATION AND NEPHRIN ENDOCYTOSIS

Phosphorylation and endocytosis are tightly regulated processes; the precise relationship between nephrin tyrosine phosphorylation and nephrin endocytosis is not well understood. Endocytosis is essential for the maintenance of cellular junctions and is also involved in the regulation of signaling pathways. Both clathrin-dependent and clathrin-independent (raft-mediated) routes of endocytosis can mediate junction turnover. One example of a dynamic junction which is a likely site of active remodelling *in vivo* is the podocyte slit diaphragm; however, the role of endocytosis in the maintenance of the slit diaphragm remains an open area of investigation within the podocyte field (Soda and Ishibe, 2013; Swiatecka-Urban, 2013; Grahammer *et al.*, 2013). The main component of the slit diaphragm, nephrin, can be internalized via both clathrin-mediated (Quack *et al.*, 2006; Qin *et al.*, 2009) and raft-mediated (Qin *et al.*, 2009) endocytic pathways, and recent evidence suggests that both forms of nephrin endocytosis may be regulated by patterns of nephrin phosphorylation on specific tyrosine residues (Figure 5.2). Both we and others have observed that nephrin hyper-phosphorylation increases basal rates of nephrin endocytosis (Qin *et al.*, 2009; Jeon *et al.*, 2012 New et al., unpublished observations) and it appears that nephrin phosphorylation on Y1176/Y1193 may regulate raft-mediated but not clathrin-mediated nephrin endocytosis (Qin *et al.*, 2009). However, the mechanisms linking specific patterns of nephrin tyrosine phosphorylation with particular forms of endocytosis are not well characterized. Clarification of these connections requires the systematic examination of those treatments known to affect either nephrin tyrosine phosphorylation or nephrin endocytosis to determine if they cause changes to both.

### 5.5.1 *MODULATION OF NEPHRIN TURNOVER BY PHOSPHORYLATION OF SPECIFIC TYROSINE RESIDUES*

The best way to dissect the role of the phosphorylation status of each of the YDxV motifs in directing nephrin endocytosis towards raft or clathrin pathways is to examine them both alone and in combination. One method would be to use our pY1193 and pY1217 nephrin antibodies (Jones *et al.*, 2009) to monitor changes in site-specific nephrin phosphorylation in combination with various nephrin mutants, while using other methods to monitor nephrin surface expression and total protein (Tossidou *et al.*, 2010). There are a number of possible treatments which have been suggested to affect nephrin phosphorylation or nephrin endocytosis. These include vanadate (Verma *et al.*, 2006; Jeon *et al.*, 2012), PMA (Tossidou *et al.*, 2010), protamine sulfate (Harita *et al.*, 2009; Jeon *et al.*, 2012), high glucose (Tossidou *et al.*, 2010; Quack *et al.*, 2011; Jeon *et al.*, 2012), Wnt5a (Babayeva *et al.*, 2013) and sFlt1 (Jin *et al.*, 2012).

Human, mouse and rat nephrin all contain one conserved YDQV tyrosine motif (human Y1217) and one YDEV tyrosine motif (human Y1193), with human and mouse nephrin containing a second YDEV motif (human Y1176). These motifs all match the phospho-tyrosine-based endocytosis signal pattern of YxxØ (Bonifacino and Traub, 2003; Swiatecka-Urban, 2013). Qin *et al*. found that phosphorylation of the YDEV motif (Y1176/Y1193) is required to trigger raft-mediated nephrin endocytosis but that it does not affect clathrin-mediated endocytosis (Qin *et al.*, 2009). The phosphorylation status of the YDQV motif was not examined. Similarly, the results of Jeon *et al*. suggest that phosphorylation of YDEV motifs (Y1176/Y1193) promotes nephrin endocytosis resulting in nephrin signaling (Jeon *et al.*, 2012). However, they observed that phosphorylation of the YDQV motif (Y1217) promotes nephrin endocytosis leading to the attenuation of nephrin signaling and nephrin degradation (Jeon *et al.*, 2012). When both YDEV and YDQV motifs were phosphorylated, this led to attenuation of nephrin signaling (Jeon *et al.*, 2012), suggesting the hypothesis that phosphorylation of the YDQV (Y1217) motif represents a switch which triggers nephrin attenuation/degradation rather than nephrin signaling (Jeon *et al.*, 2012). These studies were carried out in pancreatic beta cells, not podocytes, so it is not clear if their results can translate into similar findings regarding nephrin endocytosis in the podocyte.

A big concern is that the patterns of nephrin phosphorylation on specific tyrosines may differ between species (Jones *et al.*, 2006; Verma *et al.*, 2006; Harita *et al.*, 2009; Shimizu *et al.*, 2009); but more importantly, the patterns of phosphorylation of individual nephrin molecules are likely to be an important regulator in this process (Lothrop *et al.*, 2013) and they cannot be determined from the global average seen by Western blot. Using sequences from human, mouse and rat nephrin in the same set of experiments could assist with determining if there are any more subtle differences between the three species. In addition, precise phosphorylation patterns can be detected in a semi-quantitative manner (Steen *et al.*, 2005; Singh *et al.*, 2012) with newer techniques such as multiple-reaction-monitoring (Picotti and Aebersold, 2012; Surinova *et al.*, 2013). The analysis of these results will allow a much needed evaluation of whether there is any correlation between the phosphorylation states of Y1176, Y1193 and Y1217 and the observed rates of nephrin endocytosis and nephrin degradation between species.

### 5.5.2 *THE RELATIONSHIP BETWEEN NEPHRIN TYROSINE PHOSPHORYLATION, SLIT DIAPHRAGM TURNOVER AND PODOCYTE FOOT PROCESS ARCHITECTURE*

The distinction between clathrin-mediated and raft-mediated nephrin endocytosis may be relevant to the function of the slit diaphragm, as protamine sulfate treatment, which causes foot process effacement and increases nephrin phosphorylation on Y1176/Y1193 tyrosines *in vivo* (Verma *et al.*, 2006), has been associated with a significant increase in the number of endocytic pits visible in electron micrographs of podocyte foot processes (Qin *et al.*, 2009). The opposite scenario, decreased nephrin phosphorylation, is observed in human kidney disease (Uchida *et al.*, 2008; Ohashi *et al.*, 2010). It also appears in our nephrin$^{Y3F/Y3F}$ mouse model, which lacks nephrin phosphorylation on Y1176/Y1193/Y1217, but it is not known if these decreases in nephrin phosphorylation affect nephrin endocytosis. Generating appropriate data requires performing an analysis on nephrin in a circumstance where it is hyper-phosphorylated as well as where it is hypo-phosphorylated, as represented by the protamine sulfate mouse model (Verma *et al.*, 2006) and the nephrin$^{Y3F/Y3F}$ mouse model, respectively.

The nephrin$^{Y3F/Y3F}$ mouse model represents a valuable tool to evaluate the effects of decreased nephrin phosphorylation *in vivo* in a controlled manner. In each case, a suggested

method to evaluate the amount of nephrin endocytosis compared to controls would be to use high magnification TEM images to count the total number of budding vesicles in at least 200 podocyte foot process cross sections and then determine an average value. An increase in the number of vesicles after protamine sulfate treatment would indicate agreement with the results of Qin *et al*. from protamine-sulfate-treated rats (Qin *et al.*, 2009). In the case of the nephrin$^{Y3F/Y3F}$ mouse model, the nephrin$^{Y3F}$ protein may not be efficiently internalized by raft-mediated endocytosis, although it should still be able to undergo clathrin-mediated endocytosis (Qin *et al.*, 2009), suggesting a possibility of altered trafficking of the nephrin$^{Y3F}$ protein. This would predict an observation of decreased nephrin endocytosis in nephrin$^{Y3F/Y3F}$ mice. The opposite could also be true, however. Turnover of the slit diaphragm might be affected by altered nephrin phosphorylation (Soda and Ishibe, 2013); for instance, nephrin$^{Y3F}$ can likely be internalized by clathrin-mediated endocytosis (Qin *et al.*, 2009), and dephosphoryation of nephrin at Y1193 promotes association of nephrin with beta-arrestin, a known mediator of clathrin-based endocytosis (Quack *et al.*, 2006). If this were to be the case in nephrin$^{Y3F/Y3F}$ mice, then there could be increased clathrin-based nephrin endocytosis due to altered slit diaphragm turnover.

There are several methods which could be used to resolve the differences between these possibilities. First, the use of immuno-gold labeling of nephrin during TEM sample preparation would provide a mechanism to investigate if any altered endocytic activity is a reflection of increased nephrin endocytosis. Secondly, collection of sufficiently high magnification images would allow a more accurate examination of the type of endocytic structures being observed. In this way, the proportions of clathrin and non-clathrin (raft) structures could be more accurately determined. Ultimately, collection of important *in vivo* data about the relationship between nephrin endocytosis and nephrin phosphorylation, when correlated with *in vitro* observations will allow us to generate a more accurate model.

## 5.6 THE RELATIONSHIP BETWEEN NEPHRIN PHOSPHORYLATION, NCK AND THE PODOCYTE ACTIN CYTOSKELETON

We examined whether or not there were any changes to downstream nephrin signaling pathways as a result of introducing the nephrin$^{Y3F}$ mutations. As we and others have previously shown *in vitro* (Verma *et al.*, 2006; Jones *et al.*, 2006; Li *et al.*, 2006; Blasutig *et al.*, 2008), the interaction between nephrin and Nck is dependent on phosphorylation of those tyrosine residues, and this interaction was disrupted in nephrin$^{Y3F/Y3F}$ mice. However, the phenotype we observed in nephrin$^{Y3F/Y3F}$ mice is distinct from the one we reported for podocyte specific Nck knockout mice (Jones *et al.*, 2006; Jones *et al.*, 2009). While decreased nephrin phosphorylation is observed following initial loss of Nck (New *et al.*, 2013), the rapid progression of the inducible adult Nck knockout phenotype (Jones *et al.*, 2009) suggests that interactions between Nck and other podocyte proteins make a more significant contribution to the adult Nck knockout phenotype than decreased nephrin-Nck signaling does. Supporting this argument, podocyte-specific deletion of several other Nck binding partners leads to early onset proteinuria and foot process effacement in both developmental (Hodgin *et al.*, 2011; Soda *et al.*, 2012; Schell *et al.*, 2013) and adult contexts (Schell *et al.*, 2013).

While we have focused on nephrin-Nck-N-WASp-mediated actin polymerization, there are other pathways which involve Nck and result in modulation of the actin cytoskeleton (Lettau *et al.*, 2009). For example, in neurons, an interaction between a proline rich region on the Roundabout receptor Robo and the SH3 domains of Nck was required for both dendrite elongation and branching, presumably in an actin polymerization dependent fashion (Round and Sun, 2011). Nephrin (Sugie *et al.*, 2010; Juhila *et al.*, 2010), Nck (Fawcett *et al.*, 2007) and Robo (Hocking *et al.*, 2010) are involved in neuronal guidance, and there are a number of similarities between podocytes and neurons (Kobayashi *et al.*, 2004; Rastaldi *et al.*, 2006; Li *et al.*, 2011; Brunskill *et al.*, 2011; Sistani *et al.*, 2013). Therefore, it is possible to conceive of neuronal proteins such as Robo potentially being found in the podocyte. Mice lacking Robo2 globally show severe podocyte disorganization at three weeks of age, although this occurs at a much later timepoint (seven months) when Robo2 is deleted specifically from podocytes. The difference in onset between the global and podocyte-specific knockouts implies an important role for Robo2

in endothelial and mesangial cells as well as being also expressed in the podocyte (Fan *et al.*, 2012).

Activation of Robo2 by its ligand Slit antagonises nephrin-Nck-mediated actin polymerization *in vitro*, suggesting that the Robo2 podocyte phenotype was due to increased nephrin-Nck-mediated actin polymerization in the absence of Robo2 (Fan *et al.*, 2012). However, the foot process alterations in Robo2 knockout mice are reminiscent of those observed in nephrin$^{Y3F/Y3F}$ mice, despite the elimination of nephrin-Nck interactions in nephrin$^{Y3F/Y3F}$ mice. This apparent discrepancy would be explained if Robo2-Nck signaling plays a second role in the podocyte in addition to its antagonistic function towards nephrin-Nck signaling. If this were the case, then the similarities between nephrin$^{Y3F/Y3F}$ and Robo2 knockout mice could be explained by a loss of Robo2-Nck signaling in nephrin$^{Y3F/Y3F}$ mice, which would be the case if recruitment of Nck to phosphorylated nephrin via its SH2 domain occurs prior to binding of Nck to Robo2 via its SH3 domains. Indeed, it is possible that Robo-Nck, nephrin-Nck and nephrin-Nck-Robo signaling all play distinct but complementary roles in foot process branching. More generally, it appears that regulation of nephrin-Nck signaling is more complex than was originally anticipated, and that additional studies are required to clarify the process.

## 5.7 THE ROLE OF NEPHRIN TYROSINE PHOSPHORYLATION IN THE PODOCYTE SLIT DIAPHRAGM DURING DEVELOPMENT, HOMEOSTASIS AND DISEASE

During glomerular development, podocytes undergo a remarkable transformation from a layer of columnar epithelial cells into the complex architecture of the mature podocyte (Quaggin and Kreidberg, 2008, Figure 5.3). The formation of occluding junctions in the apical region of presumptive podocytes begins in the S-shaped body stage of glomerular development (Figure 5.3A,B). In the capillary loop stage, the apical membrane area of the podocytes expands as these junctions begin migrating baso-laterally (Figure 5.3C,D). In the late capillary loop stage, podocytes begin to extend processes and the occluding junctions reach the location of the future slit diaphragm (Figure 5.3E). As the glomerulus matures, these junctions are replaced by mature slit diaphragms as the podocytes begin to wrap around the newly forming capillary loops (Figure 5.3F).

Nephrin expression is first detected in the podocytes of late S-stage / early capillary loop stage glomeruli, where it co-localizes with other components of the future slit diaphragm in the baso-lateral domain (Ruotsalainen *et al.*, 2000; Huber *et al.*, 2009; Babayeva *et al.*, 2013). As the capillary loop stage proceeds, the apical domain increases in size, and both nephrin and the slit diaphragm components migrate towards the basal domain. This coincides with the expression of laminin-511 in the GBM (Abrahamson, 2012) and the start of podocyte process formation. These initial processes are connected with nephrin-containing occluding junctions. In the late capillary loop stage, podocytes begin to extend additional processes as they wrap around the newly forming capillary loops, the GBM transitions to the 'adult' laminin, laminin-521 (Abrahamson, 2012), and slit diaphragms begin to appear as the glomerulus matures. This also marks when tetraspanin CD151/α3β1 integrin complexes begin to form (Sachs *et al.*, 2012). Although nephrin expression is necessary for slit diaphragm maturation (Done *et al.*, 2007), it is not required for podocyte foot process formation (Ruotsalainen *et al.*, 2000; Putaala *et al.*, 2001; Rantanen *et al.*, 2002; Hamano *et al.*, 2002; Kramer-Zucker *et al.*, 2005).

Whereas nephrin expression is found laterally between podocytes in the early capillary loop stage (Figure 5.3D), we and others (Verma *et al.*, 2006) detect nephrin tyrosine phosphorylation beginning later in the capillary loop stage in the basal domain of those regions where podocytes have begun to invade the glomerular capillaries and maturing slit diaphragms have started to develop (Figure 5.3E,F). Once established, nephrin tyrosine phosphorylation is maintained throughout life. For this reason, we propose a model in which nephrin tyrosine phosphorylation is considered a marker of the mature slit diaphragm. In this model, nephrin is recruited to developing slit diaphragm complexes in the early capillary loop stage via its C-terminal PDZ recognition motif which mediates binding to Par3 in the aPKC-Par3-CDC42 polarity complex (Hartleben *et al.*, 2008) via a phosphorylation-independent mechanism. In support of this concept, the PDZ binding motif of nephrin is evolutionarily conserved. In the late capillary loop stage / beginning of glomerular maturation, foot processes begin to mature, and nephrin begins to be detected in the characteristic pattern of the adult glomerulus next to the GBM. Nephrin tyrosine phosphorylation also begins to be detected in a similar pattern, it increases as the glomerulus continues to mature and it is maintained in the adult glomerulus.

We have shown that there is a continued requirement for phospho-nephrin signaling in the maintenance of mature podocyte foot processes as nephrin$^{Y3F/Y3F}$ mice, which lack all three YDxV tyrosine residues, develop significant proteinuria accompanied by structural changes characterized by dilated capillary loops, thickening of the GBM and podocyte foot process effacement. We also detected phosphorylated nephrin in heterozygous nephrin$^{WT/Y3F}$ mice, albeit at lower levels—suggesting that the wildtype nephrin being expressed is properly phosphorylated and ruling out a dominant negative effect of nephrin$^{Y3F}$. Indeed, heterozygous nephrin$^{WT/Y3F}$ mice do not develop proteinuria. There is not likely a dose-dependent requirement for effective phospho-nephrin signaling as the amount of phosphorylated nephrin present in nephrin$^{WT/Y3F}$ mice generates sufficient phospho-nephrin signaling to maintain podocyte architecture. Other nephrin mutations which result in slit diaphragm instability have decreased levels of nephrin tyrosine phosphorylation (Shono *et al.*, 2009, Jones, unpublished observations), however, suggesting there could potentially be a link between levels of nephrin phosphorylation and slit diaphragm stability.

This relationship is also supported by the results of our LPS challenge experiment, which showed that healthy C57Bl/6 nephrin$^{Y3F/Y3F}$ mice developed more severe proteinuria than their nephrin$^{WT/WT}$ counterparts after LPS challenge. One possible explanation for this difference is that, in nephrin$^{WT/WT}$ mice, the early effects of LPS-mediated signaling pathways which induce podocyte damage are counteracted by phospho-nephrin-signaling pathways involved in the maintenance of podocyte foot process architecture. In nephrin$^{Y3F/Y3F}$ mice, earlier initiation of podocyte damage and increased proteinuria after 24 hours occurs because phospho-nephrin signaling pathways cannot be engaged following LPS injection. A further beneficial role for phospho-nephrin signaling in the prevention of podocyte damage is demonstrated in that mice lacking the phosphatase PTP1β—which we have previously shown can de-phosphorylate nephrin YDxV sites (Aoudjit *et al.*, 2011) —are protected from both LPS and Adriamycin-induced proteinuria (Kumagai *et al.*, 2012). As well, treatment of wildtype mice with a PTP1β inhibitor reduces LPS-induced proteinuria (Kumagai *et al.*, 2012). Taken together, our observations and those of others suggest a paradigm in which phospho-nephrin-based signaling pathways promote podocyte foot process and slit diaphragm integrity, especially in response to certain types of

stress. A crucial step in the initiation of podocyte damage is therefore a reduction in nephrin phosphorylation with concomitant downregulation of associated signaling pathways.

## 5.8 NEPHRIN TYROSINE PHOSPHORYLATION AS A THERAPEUTIC TARGET

Taken together, the work outlined in this thesis suggests that nephrin tyrosine phosphorylation has the potential to be a therapeutic target in human kidney disease. A small number of studies have examined the effects of treatments on proteinuria and nephrin phosphorylation and suggest that they could be linked. Increased nephrin phosphorylation on Y1217 was observed in dexamethasone-treated cultured podocytes (Ohashi *et al.*, 2011). In another study, reduced proteinuria and increased nephrin tyrosine phosphorylation in adriamycin-treated rats was detected following both prednisone (glucocorticoid) and lisinopril (ACE inhibitor) therapies (Fan *et al.*, 2009). Additionally, increased Y1176/Y1193 nephrin phosphorylation was associated with reduced LPS-induced proteinuria in mice following c-mip siRNA treatment. These studies represent proof of the principle that modulation of nephrin phosphorylation can affect the progression of disease. However, it is important to note that the reported increases in nephrin phosphorylation could be a secondary effect of the primary treatments. It is possible that the primary treatments decreased proteinuria through a nephrin-independent mechanism, and that the increase in nephrin phosphorylation occurred as part of a general response to decreased proteinuria. Regardless of the relationship, it appears that increased nephrin phosphorylation is correlated with decreased proteinuria, and that the analysis of nephrin phosphorylation could potentially be used as an additional marker when testing new treatments in animal models and in humans.

Any therapy targeted towards altering levels of nephrin phosphorylation is likely to use indirect means aimed at directly targeting activators and inhibitors of nephrin phosphorylation, given that nephrin does not intrinsically possess kinase activity. One possible therapeutic target is the protein c-mip, an inhibitor of nephrin phosphorylation. Increased c-mip expression is found in minimal change disease and membranous nephropathy, both of which are associated with decreased nephrin tyrosine phosphorylation. In addition, c-mip expression may also be involved in the development of negative renal side effects associated with anti-VEGF therapy in

cancer treatment that uses receptor tyrosine kinase inhibitors such as sorafenib (Izzedine *et al.*, 2013). A possible explanation for this phenomenon was recently postulated based on evidence that sorafenib can directly increase c-mip expression (Izzedine *et al.*, 2013), suggesting that decreased nephrin phosphorylation could also be present in these cases.

Another possible therapeutic target is the tyrosine phosphatase PTP1β. It has been demonstrated that treatment of mice with a PTP1β inhibitor (CAS #765317-72-4) reduces LPS-induced proteinuria (Kumagai *et al.*, 2012) and it may be possible to evaluate the effectiveness of the inhibitor in the PAN model as well. PTP1β expression is upregulated in PAN rats at the onset of proteinuria (Aoudjit *et al.*, 2011); in addition, proteinuria is associated with decreased nephrin phosphorylation on Y1193 and Y1217 (Uchida *et al.*, 2008; Jones *et al.*, 2009). As we have shown that PTP1β can directly dephosphorylate nephrin (Aoudjit *et al.*, 2011), this suggests that PTP1β inhibition during PAN could result in increased nephrin phosphorylation and decreased proteinuria analogous to the results seen in other models (Fan *et al.*, 2009; Kumagai *et al.*, 2012). If successful, this concept could be easily tested in humans as PTP1β inhibitors are actively being investigated for use in type II diabetes (Thareja *et al.*, 2012). One inhibitor has already been tested in clinical trials (Swarbrick *et al.*, 2009), and if nephrin phosphorylation is found to be decreased in either type I or type II diabetes, these inhibitors could possibly have an additional benefit for those at risk of developing diabetic nephropathy.

Overall, nephrin phosphorylation may be more suited to being a biomarker of slit diaphragm integrity. Knowledge of how the modulation of other possible therapeutic targets could affect nephrin phosphorylation is, however, necessary to consider when evaluating the potential and actual effects of treatments for kidney dysfunction. It could well provide a mechanism for evaluating the potential worth of treatments based on how successful they are at increasing nephrin phosphorylation.

## 5.9 CONCLUSION

The goal of this thesis was to investigate the role of nephrin phosphorylation and associated signaling pathways in the podocyte. Originally, the potential for the cytoplasmic tail of nephrin

to be regulated by tyrosine phosphorylation was recognized when nephrin was initially characterized (Kestila *et al.*, 1998; Lahdenpera *et al.*, 2003), and this has led to efforts to determine the purpose of this post-translational modification. Initial efforts suggested that phosphorylated nephrin is present during podocyte differentiation and in diseased podocytes, but not in the healthy glomerulus. This implied that nephrin phosphorylation was involved in changing foot process architecture, but that it was not needed for the ongoing maintenance of foot processes. Further research aided by the development of phospho-nephrin antibodies has demonstrated that, in fact, phosphorylated nephrin is present in the healthy glomerulus, and it appears that decreased nephrin phosphorylation is observed in both human and animal forms of kidney disease. These observations suggest a view of the role of nephrin phosphorylation as important for homeostasis, and that its loss could be a detrimental event associated with disruption of normal foot process architecture. Complementing this work is the identification of a mechanism whereby nephrin phosphorylation is positively regulated by Nck through increased activation of Fyn, which supports the idea that mature foot processes continue to need ongoing nephrin phosphorylation. Finally, characterization of the nephrin$^{Y3F/Y3F}$ mouse model demonstrates unequivocally that signaling pathways regulated by nephrin phosphorylation play a significant role in the maintenance of podocyte function *in vivo*. This work provides a strong foundation for future efforts, which can now focus productively on defining the precise relationship between phospho-nephrin signaling and foot process alterations during disease, and also on the further expansion of our understanding of the roles of nephrin *in vivo* through detailed characterization of the precise nephrin signaling mechanisms whose alteration produces the changes seen in nephrin$^{Y3F/Y3F}$ mice.

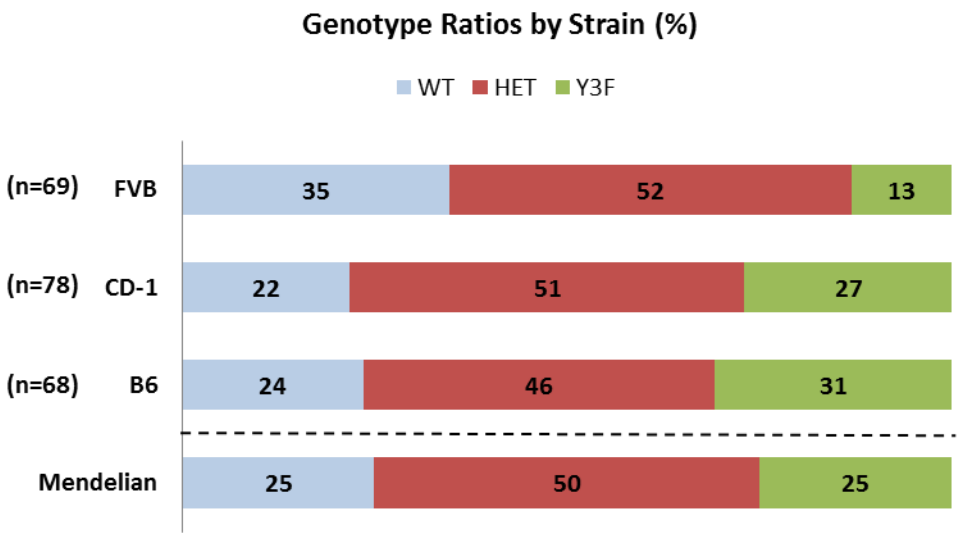


**Figure 5.1 A comparison of the expected Mendelian ratios with the observed percentage of each genotype from the mating of heterozygous nephrin$^{WT/Y3F}$ mice on the FVB, CD-1 and C57Bl/6 (B6) genetic backgrounds.**

The percentages of all genotypes seen on the B6 and CD-1 backgrounds are in accordance with the expected Mendelian ratios, whereas on the FVB background, the observed percentage of nephrin$^{Y3F/Y3F}$ mice is half of the expected value.

**Figure 5.2 Hypothetical model of the relationship between nephrin tyrosine phosphorylation and slit diaphragm turnover.**

(Left) Nephrin at the slit diaphragm is tyrosine phosphorylated by Fyn and preferentially interacts with podocin. The slit diaphragm complex is slowly turned over by raft-mediated endocytosis. Damage to the integrity of podocyte foot process architecture results in increased mobility of nephrin out of the slit diaphragm into the plasma membrane. (Right) There, nephrin becomes dephosphorylated, enabling binding of β-arrestin and triggering clathrin-mediated endocytosis of nephrin, which could result in nephrin degradation and proteinuria.

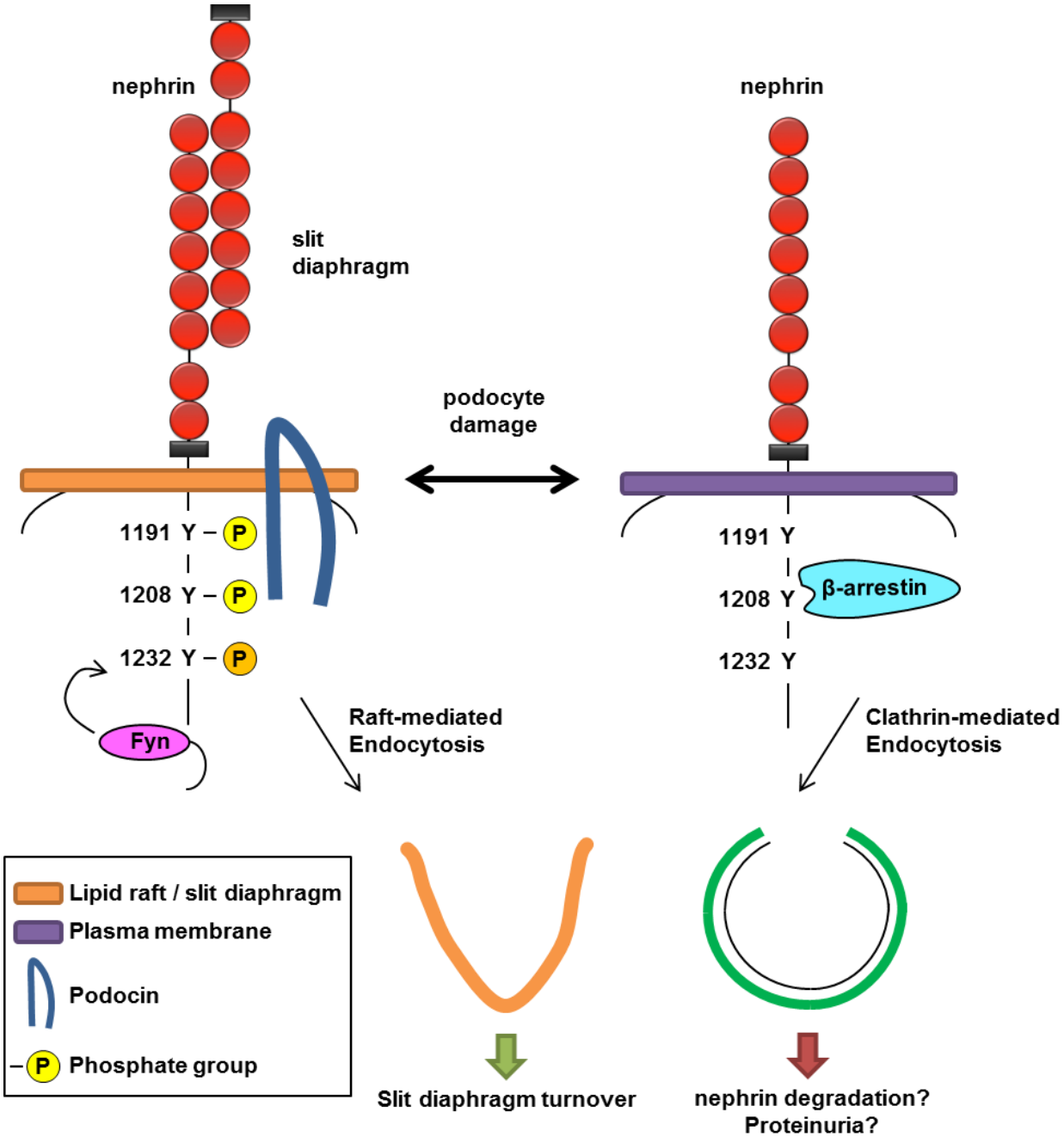
nephrin
slit
diaphragm
podocyte
damage
nephrin
1191 Y – P
1208 Y – P
1232 Y – P
Fyn
1191 Y
1208 Y
β-arrestin
1232 Y
Raft-mediated
Endocytosis
Clathrin-mediated
Endocytosis
Lipid raft / slit diaphragm
Plasma membrane
Podocin
– P Phosphate group
Slit diaphragm turnover
nephrin degradation?
Proteinuria?

**Figure 5.3 Model of glomerular development and slit diaphragm formation with an emphasis on nephrin expression and phosphorylation.**

Each stage is illustrated (drawings are not to scale) and the components of the GBM present during that stage are noted on the right (LM, laminin; Col, collagen). (A) Podocytes originate in the S-shaped body as columnar epithelial cells. (B) During the S-shaped body stage of glomerular development, podocytes form apically-located occluding junctions. (C) In the late S-stage and early capillary loop stages, the apical membrane area of the podocyte expands and their occluding junctions begin migrating baso-laterally. Nephrin begins to be expressed during the capillary loop stage. (D) As the capillary loop stage proceeds, the apical domain continues to increase in size, and both nephrin and the other future slit diaphragm components migrate towards the basal domain. This coincides with the expression of laminin-511 in the GBM and the start of podocyte process formation. These initial podocyte processes are now connected with nephrin-containing occluding junctions. (E) In the late capillary loop stage, the nephrin-containing occluding junctions reach the location of the future slit diaphragm. As the glomerulus matures, podocytes begin to extend additional processes as they wrap around the newly forming capillary loops, the GBM transitions to laminin-521, and preliminary slit diaphragm structures containing tyrosine phosphorylated nephrin appear. (F) In the mature glomerulus, podocyte foot processes are connected by fully assembled slit diaphragm junctions which contain tyrosine phosphorylated nephrin. After Hartleben *et al.* (Hartleben *et al.*, 2012) and Abrahamson (Abrahamson, 2012).

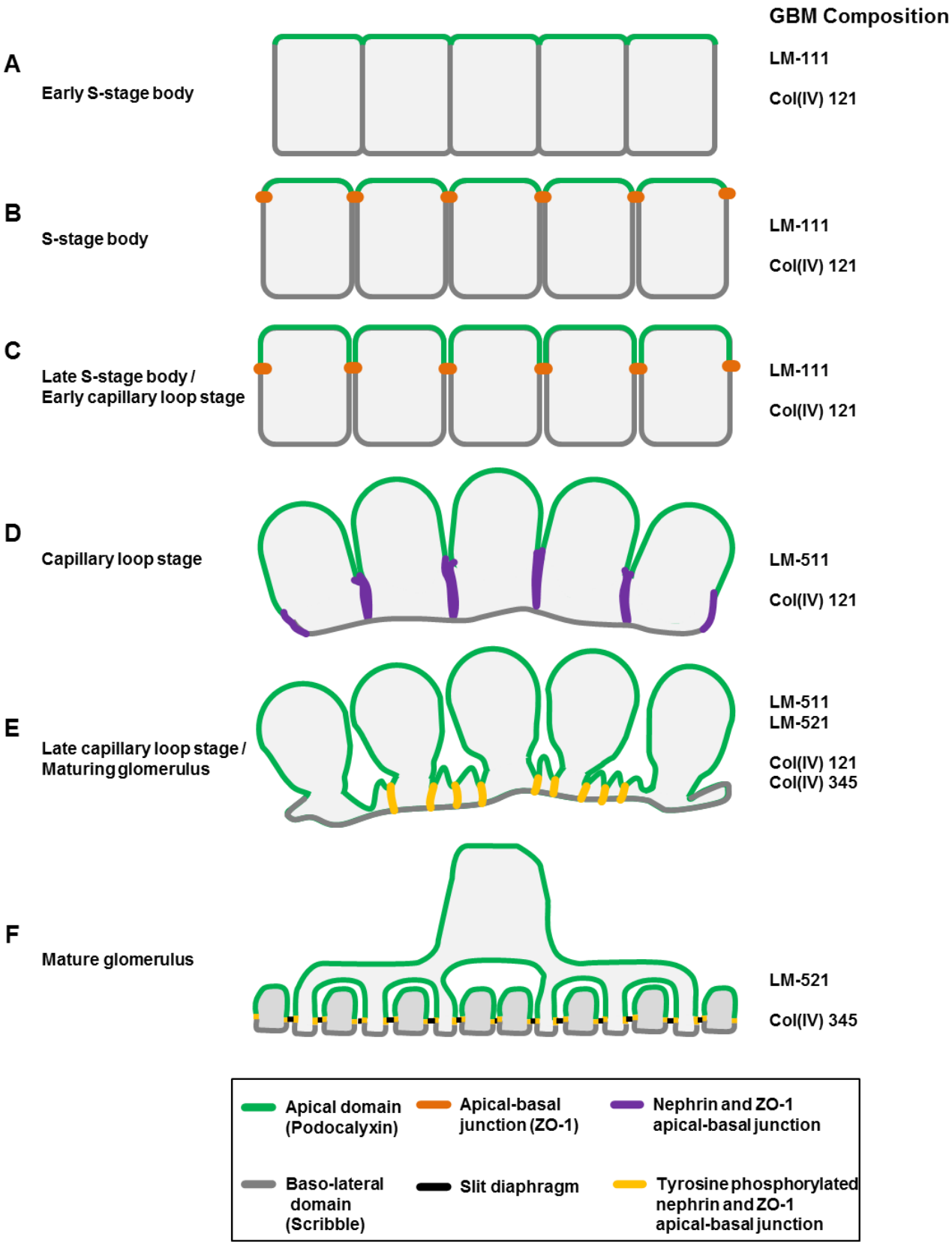
GBM Composition
A
Early S-stage body
LM-111
Col(IV) 121
B
S-stage body
LM-111
Col(IV) 121
C
Late S-stage body /
Early capillary loop stage
LM-111
Col(IV) 121
D
Capillary loop stage
LM-511
Col(IV) 121
E
Late capillary loop stage /
Maturing glomerulus
LM-511
LM-521
Col(IV) 121
Col(IV) 345
F
Mature glomerulus
LM-521
Col(IV) 345
Apical domain (Podocalyxin)
Apical-basal junction (ZO-1)
Nephrin and ZO-1 apical-basal junction
Baso-lateral domain (Scribble)
Slit diaphragm
Tyrosine phosphorylated nephrin and ZO-1 apical-basal junction

**Table 5.1 Summary of published phospho-nephrin antibodies raised against YDxV motifs**

| Antibody Characterization | Antibody name | Antibody type | Peptide Sequence | Peptide Species |
|---|---|---|---|---|
| Jones *et al*. (Jones *et al.*, 2009) | pY1176/1193 | Rabbit monoclonal | AFPGHL(pY)DEVER**C** | Mouse |
| Jones *et al*. (Jones *et al.*, 2009) | pY1193 | Rabbit monoclonal | GVWGPL(pY)DEVQM**C** | Mouse |
| Jones *et al*. (Jones *et al.*, 2009) | pY1217 | Rabbit monoclonal | DPRGI(pY)DQVAAD**C** | Mouse |
| Uchida *et al*. (Uchida *et al.*,2008) | pY1228 | Rabbit polyclonal | DPRGI(pY)DQVA**C** | Rat |
| Uchida *et al*. (Uchida *et al.*, 2008) | pY1204 | Rabbit polyclonal | **C**WGPL(pY)DEVQM | Mouse |
| Verma *et al*. (Verma *et al.*, 2006) | pY1176/1193 | Rabbit polyclonal | WGPL(pY)DEVQM | Mouse |
| Harita *et al*. (Harita *et al.*, 2009) | pY1204 | Rabbit polyclonal | **C**AWGPL(pY)DEVRMD | Rat |

# REFERENCES


Abmayr SM, Pavlath GK. Myoblast fusion: Lessons from flies and mice. *Development*. 2012;139(4):641-656.

Abrahamson DR. Role of the podocyte (and glomerular endothelium) in building the GBM. *Semin Nephrol*. 2012;32(4):342-349.

Agrawal V, Prasad N, Jain M, Pandey R. Reduced podocin expression in minimal change disease and focal segmental glomerulosclerosis is related to the level of proteinuria. *Clin Exp Nephrol*. 2013.

Aoudjit L, Jiang R, Lee TH, New LA, Jones N, Takano T. Podocyte protein, nephrin, is a substrate of protein tyrosine phosphatase 1B. *J Signal Transduct*. 2011;2011:376543.

Arora P, Vasa P, Brenner D, Iglar K, McFarlane P, Morrison H, Badawi A. Prevalence estimates of chronic kidney disease in canada: Results of a nationally representative survey. *CMAJ*. 2013;185(9):E417-23.

Asanuma K, Kim K, Oh J, Giardino L, Chabanis S, Faul C, Reiser J, Mundel P. Synaptopodin regulates the actin-bundling activity of {alpha}-actinin in an isoform-specific manner. *J Clin Invest*. 2005;115(5):1188-1198.

Ashworth S, Teng B, Kaufeld J, Miller E, Tossidou I, Englert C, Bollig F, Staggs L, Roberts IS, Park JK, Haller H, Schiffer M. Cofilin-1 inactivation leads to proteinuria--studies in zebrafish, mice and humans. *PLoS One*. 2010;5(9):e12626. doi: 10.1371/journal.pone.0012626.

Astrom E, Rinta-Valkama J, Gylling M, Ahola H, Miettinen A, Timonen T, Holthofer H. Nephrin in human lymphoid tissues. *Cell Mol Life Sci*. 2006;63(4):498-504.

Audard V, Zhang SY, Copie-Bergman C, Rucker-Martin C, Ory V, Candelier M, Baia M, Lang P, Pawlak A, Sahali D. Occurrence of minimal change nephrotic syndrome in classical hodgkin lymphoma is closely related to the induction of c-mip in hodgkin-reed sternberg cells and podocytes. *Blood*. 2010;115(18):3756-3762.

Azhibekov TA, Wu Z, Padiyar A, Bruggeman LA, Simske JS. TM4SF10 and ADAP interaction in podocytes: Role in fyn activity and nephrin phosphorylation. *Am J Physiol Cell Physiol*. 2011;301(6):C1351-9.

Babayeva S, Rocque B, Aoudjit L, Zilber Y, Li J, Baldwin C, Kawachi H, Takano T, Torban E. Planar cell polarity pathway regulates nephrin endocytosis in developing podocytes. *J Biol Chem*. 2013;288(33):24035-24048.

Baleato RM, Guthrie PL, Gubler MC, Ashman LK, Roselli S. Deletion of CD151 results in a strain-dependent glomerular disease due to severe alterations of the glomerular basement membrane. *Am J Pathol*. 2008;173(4):927-937.

Bao S, Cagan R. Preferential adhesion mediated by hibris and roughest regulates morphogenesis and patterning in the drosophila eye. *Dev Cell*. 2005;8(6):925-935.

Bao S, Fischbach KF, Corbin V, Cagan RL. Preferential adhesion maintains separation of ommatidia in the drosophila eye. *Dev Biol*. 2010;344(2):948-956.

Barcellos-Hoff MH, Aggeler J, Ram TG, Bissell MJ. Functional differentiation and alveolar morphogenesis of primary mammary cultures on reconstituted basement membrane. *Development*. 1989;105(2):223-235.

Barda-Saad M, Shirasu N, Pauker MH, Hassan N, Perl O, Balbo A, Yamaguchi H, Houtman JC, Appella E, Schuck P, Samelson LE. Cooperative interactions at the SLP-76 complex are critical for actin polymerization. *EMBO J*. 2010;29(14):2315-2328.

Barletta GM, Kovari IA, Verma RK, Kerjaschki D, Holzman LB. Nephrin and Neph1 co-localize at the podocyte foot process intercellular junction and form cis hetero-oligomers. *J Biol Chem*. 2003;278(21):19266-19271.

Barnabei MS, Palpant NJ, Metzger JM. Influence of genetic background on ex vivo and in vivo cardiac function in several commonly used inbred mouse strains. *Physiol Genomics*. 2010;42A(2):103-113.

Baum M, Gattineni J, Satlin LM. Chapter 27 - postnatal renal development. In: Alpern RJ, Moe OW, Caplan M, eds. *Seldin and giebisch's the kidney (fifth edition).* Academic Press; 2013:911-931.

Beall MH, Amidi F, Gayle DA, Wang S, Beloosesky R, Ross MG. Placental and fetal membrane nephrin and Neph1 gene expression: Response to inflammation. *J Soc Gynecol Investig*. 2005;12(5):298-302.

Beck LH,Jr, Bonegio RG, Lambeau G, Beck DM, Powell DW, Cummins TD, Klein JB, Salant DJ. M-type phospholipase A2 receptor as target antigen in idiopathic membranous nephropathy. *N Engl J Med*. 2009;361(1):11-21.

Beltcheva O, Hjorleifsdottir EE, Kontusaari S, Tryggvason K. Sp1 specifically binds to an evolutionarily conserved DNA segment within a region necessary for podocyte-specific expression of nephrin. *Nephron Exp Nephrol*. 2010;114(1):e15-22.

Beltcheva O, Kontusaari S, Fetissov S, Putaala H, Kilpelainen P, Hokfelt T, Tryggvason K. Alternatively used promoters and distinct elements direct tissue-specific expression of nephrin. *J Am Soc Nephrol*. 2003;14(2):352-358.

Benesch S, Lommel S, Steffen A, Stradal TEB, Scaplehorn N, Way M, Wehland J, Rottner K. Phosphatidylinositol 4,5-biphosphate (PIP2)-induced vesicle movement depends on N-WASP and involves nck, WIP, and Grb2. *J Biol Chem*. 2002;277(40):37771-37776.

Benzing T. The promise of well-being: Stay in shape with N(i)ck. *J Am Soc Nephrol*. 2009;20(7):1425-1427.

Berger K, Moeller MJ. Cofilin-1 in the podocyte: A molecular switch for actin dynamics. *Int Urol Nephrol*. 2011;43(1):273-275.

Bertani T, Poggi A, Pozzoni R, Delaini F, Sacchi G, Thoua Y, Mecca G, Remuzzi G, Donati MB. Adriamycin-induced nephrotic syndrome in rats: Sequence of pathologic events. *Lab Invest*. 1982;46(1):16-23.

Bertuccio C, Veron D, Aggarwal PK, Holzman L, Tufro A. Vascular endothelial growth factor receptor 2 direct interaction with nephrin links VEGF-A signals to actin in kidney podocytes. *J Biol Chem*. 2011;286(46):39933-39944.

Bladt F, Aippersbach E, Gelkop S, Strasser GA, Nash P, Tafuri A, Gertler FB, Pawson T. The murine nck SH2/SH3 adaptors are important for the development of mesoderm-derived embryonic structures and for regulating the cellular actin network. *Mol Cell Biol*. 2003;23(13):4586-4597.

Blasutig IM, New LA, Thanabalasuriar A, Dayarathna TK, Goudreault M, Quaggin SE, Li SSC, Gruenheid S, Jones N, Pawson T. Phosphorylated YDXV motifs and nck SH2/SH3 adaptors act cooperatively to induce actin reorganization. *Mol Cell Biol*. 2008;28(6):2035-2046.

Bohle A, Aeikens B, Eenboom A, Fronholt L, Plate WR, Xiao JC, Greschniok A, Wehrmann M. Human glomerular structure under normal conditions and in isolated glomerular disease. *Kidney Int Suppl*. 1998;67:S186-8.

Bonifacino JS, Traub LM. Signals for sorting of transmembrane proteins to endosomes and lysosomes. *Annu Rev Biochem*. 2003;72:395-447.

Braverman LE, Quilliam LA. Identification of Grb4/nckbeta, a src homology 2and 3Domain-containing adapter protein having similar binding and biological properties to nck. *J Biol Chem*. 1999;274(9):5542-5549.

Brosius FC,3rd, Alpers CE, Bottinger EP, Breyer MD, Coffman TM, Gurley SB, Harris RC, Kakoki M, Kretzler M, Leiter EH, Levi M, McIndoe RA, Sharma K, Smithies O, Susztak K, Takahashi N, Takahashi T, Animal Models of Diabetic Complications Consortium. Mouse models of diabetic nephropathy. *J Am Soc Nephrol*. 2009;20(12):2503-2512.

Bruggeman LA, Martinka S, Simske JS. Expression of TM4SF10, a claudin/EMP/PMP22 family cell junction protein, during mouse kidney development and podocyte differentiation. *Dev Dyn*. 2007;236(2):596-605.

Brunskill EW, Georgas K, Rumballe B, Little MH, Potter SS. Defining the molecular character of the developing and adult kidney podocyte. *PLoS One*. 2011;6(9):e24640.

Buday L, Wunderlich L, Tamas P. The nck family of adapter proteins: Regulators of actin cytoskeleton. *Cell Signal*. 2002;14(9):723-731.

Calderwood DA, Fujioka Y, de Pereda JM, Garcia-Alvarez B, Nakamoto T, Margolis B, McGlade CJ, Liddington RC, Ginsberg MH. Integrin beta cytoplasmic domain interactions with phosphotyrosine-binding domains: A structural prototype for diversity in integrin signaling. *Proc Natl Acad Sci U S A*. 2003;100(5):2272-2277.

Chaki SP, Rivera GM. Integration of signaling and cytoskeletal remodeling by nck in directional cell migration. *Bioarchitecture*. 2013;3(3):57-63.

Chan B, Lanyi A, Song HK, Griesbach J, Simarro-Grande M, Poy F, Howie D, Sumegi J, Terhorst C, Eck MJ. SAP couples fyn to SLAM immune receptors. *Nat Cell Biol*. 2003;5(2):155-160.

Chao DL, Shen K. Functional dissection of SYG-1 and SYG-2, cell adhesion molecules required for selective synaptogenesis in C. elegans. *Mol Cell Neurosci*. 2008;39(2):248-257.

Chen JS, Chen A, Chang LC, Chang WS, Lee HS, Lin SH, Lin YF. Mouse model of membranous nephropathy induced by cationic bovine serum albumin: Antigen dose-response relations and strain differences. *Nephrol Dial Transplant*. 2004;19(11):2721-2728.

Chen M, She H, Kim A, Woodley DT, Li W. Nckbeta adapter regulates actin polymerization in NIH 3T3 fibroblasts in response to platelet-derived growth factor bb. *Mol Cell Biol*. 2000;20(21):7867-7880.

Chittiprol S, Chen P, Petrovic-Djergovic D, Eichler T, Ransom RF. Marker expression, behaviors, and responses vary in different lines of conditionally immortalized cultured podocytes. *Am J Physiol Renal Physiol*. 2011;301(3):F660-71.

Cho ME, Kopp JB. Focal segmental glomerulosclerosis amd collapsing glomerulopathy. In: Wilcox CS, ed. *Therapy in nephrology & hypertension: A companion to brenner & rector's the kidney.* 3rd ed. Philadelphia, PA: Saunders/Elsevier; 2008:220-238.

Cho AR, Uchio-Yamada K, Torigai T, Miyamoto T, Miyoshi I, Matsuda J, Kurosawa T, Kon Y, Asano A, Sasaki N, Agui T. Deficiency of the tensin2 gene in the ICGN mouse: An animal model for congenital nephrotic syndrome. *Mamm Genome*. 2006;17(5):407-416.

Chua S,Jr, Li Y, Liu SM, Liu R, Chan KT, Martino J, Zheng Z, Susztak K, D'Agati VD, Gharavi AG. A susceptibility gene for kidney disease in an obese mouse model of type II diabetes maps to chromosome 8. *Kidney Int*. 2010;78(5):453-462.

Chugh SS, Clement LC, Mace C. New insights into human minimal change disease: Lessons from animal models. *Am J Kidney Dis*. 2012;59(2):284-292.

Coenen MJ, Hofstra JM, Debiec H, Stanescu HC, Medlar AJ, Stengel B, Boland-Auge A, Groothuismink JM, Bockenhauer D, Powis SH, Mathieson PW, Brenchley PE, Kleta R, Wetzels JF, Ronco P. Phospholipase A2 receptor (PLA2R1) sequence variants in idiopathic membranous nephropathy. *J Am Soc Nephrol*. 2013;24(4):677-683.

Couser WG, Schulze M, Pruchno CJ. Role of C5b-9 in experimental membranous nephropathy. *Nephrol Dial Transplant*. 1992;7 Suppl 1:25-31.

Couser WG, Steinmuller DR, Stilmant MM, Salant DJ, Lowenstein LM. Experimental glomerulonephritis in the isolated perfused rat kidney. *J Clin Invest*. 1978;62(6):1275-1287.

Coward RJ, Welsh GI, Koziell A, Hussain S, Lennon R, Ni L, Tavare JM, Mathieson PW, Saleem MA. Nephrin is critical for the action of insulin on human glomerular podocytes. *Diabetes*. 2007;56(4):1127-1135.

D'Agati VD. Pathobiology of focal segmental glomerulosclerosis: New developments. *Curr Opin Nephrol Hypertens*. 2012;21(3):243-250.

D'Agati VD, Fogo AB, Bruijn JA, Jennette JC. Pathologic classification of focal segmental glomerulosclerosis: A working proposal. *Am J Kidney Dis*. 2004;43(2):368-382.

Deb DK, Wang Y, Zhang Z, Nie H, Huang X, Yuan Z, Chen Y, Zhao Q, Li YC. Molecular mechanism underlying 1,25-dihydroxyvitamin D regulation of nephrin gene expression. *J Biol Chem*. 2011;286(37):32011-32017.

Dember LM, Salant DJ. Minimal change disease. In: Wilcox CS, ed. *Therapy in nephrology & hypertension: A companion to brenner & rector's the kidney*. 3rd ed. Philadelphia, PA: Saunders/Elsevier; 2008:205-219.

Denhez B, Lizotte F, Guimond M, Geraldes P: New mechanism for podocyte dysfunction: Regulation of nephrin by SHP-1 [Abstract]. *Canadian Journal of Diabetes*. 2013;37:S8.

Dessapt-Baradez C, Woolf AS, White KE, Pan J, Huang JL, Hayward AA, Price KL, Kolatsi-Joannou M, Locatelli M, Diennet M, Webster Z, Smillie SJ, Nair V, Kretzler M, Cohen CD, Long DA, Gnudi L. Targeted glomerular angiopoietin-1 therapy for early diabetic kidney disease. *J Am Soc Nephrol*. 2013.

Dirks J. A world perspective on renal care: The challenges of prevention and treatment. *EDTNA ERCA J*. 2005;31(2):72-74.

Ditlev JA, Michalski PJ, Huber G, Rivera GM, Mohler WA, Loew LM, Mayer BJ. Stoichiometry of nck-dependent actin polymerization in living cells. *J Cell Biol*. 2012;197(5):643-658.

Done SC, Takemoto M, He L, Sun Y, Hultenby K, Betsholtz C, Tryggvason K. Nephrin is involved in podocyte maturation but not survival during glomerular development. *Kidney Int*. 2007.

Donoviel DB, Freed DD, Vogel H, Potter DG, Hawkins E, Barrish JP, Mathur BN, Turner CA, Geske R, Montgomery CA, Starbuck M, Brandt M, Gupta A, Ramirez-Solis R, Zambrowicz BP, Powell DR. Proteinuria and perinatal lethality in mice lacking NEPH1, a novel protein with homology to NEPHRIN. *Mol Cell Biol*. 2001;21(14):4829-4836.

Downward J. The GRB2/sem-5 adaptor protein. *FEBS Lett*. 1994;338(2):113-117.

Drapeau N, Lizotte F, Denhez B, Guay A, Kennedy CR, Geraldes P. Expression of SHP-1 induced by hyperglycemia prevents insulin actions in podocytes. *Am J Physiol Endocrinol Metab*. 2013;304(11):E1188-98.

Eekhoff A, Bonakdar N, Alonso JL, Hoffmann B, Goldmann WH. Glomerular podocytes: A study of mechanical properties and mechano-chemical signaling. *Biochem Biophys Res Commun*. 2011;406(2):229-233.

Endlich N, Endlich K. The challenge and response of podocytes to glomerular hypertension. *Semin Nephrol*. 2012;32(4):327-341.

Fan Q, Xing Y, Ding J, Guan N. Reduction in VEGF protein and phosphorylated nephrin associated with proteinuria in adriamycin nephropathy rats. *Nephron Exp Nephrol*. 2009;111(4):e92-e102.

Fan X, Li Q, Pisarek-Horowitz A, Rasouly HM, Wang X, Bonegio RG, Wang H, McLaughlin M, Mangos S, Kalluri R, Holzman LB, Drummond IA, Brown D, Salant DJ, Lu W. Inhibitory effects of Robo2 on nephrin: A crosstalk between positive and negative signals regulating podocyte structure. *Cell Rep*. 2012;2(1):52-61.

Farquhar MG, Saito A, Kerjaschki D, Orlando RA. The heymann nephritis antigenic complex: Megalin (gp330) and RAP. *J Am Soc Nephrol*. 1995;6(1):35-47.

Fawcett JP, Georgiou J, Ruston J, Bladt F, Sherman A, Warner N, Saab BJ, Scott R, Roder JC, Pawson T. Nck adaptor proteins control the organization of neuronal circuits important for walking. *Proc Natl Acad Sci U S A*. 2007;104(52):20973-20978.

Feugas P, Morikawa L. Periodic acid-ammoniacal silver (PAAS) method for the demonstration of glomerular basement membranes using the microwave oven. *The J Histotechnol*. 1989;2:105-107.

Fischbach KF, Linneweber GA, Andlauer TF, Hertenstein A, Bonengel B, Chaudhary K. The irre cell recognition module (IRM) proteins. *J Neurogenet*. 2009;23(1-2):48-67.

Fornoni A, Jeon J, Varona Santos J, Cobianchi L, Jauregui A, Inverardi L, Mandic SA, Bark C, Johnson K, McNamara G, Pileggi A, Molano RD, Reiser J, Tryggvason K, Kerjaschki D, Berggren PO, Mundel P, Ricordi C. Nephrin is expressed on the surface of insulin vesicles and facilitates glucose-stimulated insulin release. *Diabetes*. 2010;59(1):190-199.

Foster RR, Welsh GI, Satchell SC, Marlow RD, Wherlock MD, Pons D, Mathieson PW, Bates DO, Saleem MA. Functional distinctions in cytosolic calcium regulation between cells of the glomerular filtration barrier. *Cell Calcium*. 2010;48(1):44-53.

Frese S, Schubert W, Findeis AC, Marquardt T, Roske YS, Stradal TEB, Heinz DW. The phosphotyrosine peptide binding specificity of Nck1 and Nck2 src homology 2 domains. *J Biol Chem*. 2006;281(26):18236-18245.

Fukasawa H, Bornheimer S, Kudlicka K, Farquhar MG. Slit diaphragms contain tight junction proteins. *J Am Soc Nephrol*. 2009;20(7):1491-1503.

Gao F, Maiti S, Sun G, Ordonez NG, Udtha M, Deng JM, Behringer RR, Huff V. The Wt1+/R394W mouse displays glomerulosclerosis and early-onset renal failure characteristic of human denys-drash syndrome. *Mol Cell Biol*. 2004;24(22):9899-9910.

Garg P, Verma R, Nihalani D, Johnstone DB, Holzman LB. Neph1 cooperates with nephrin to transduce a signal that induces actin polymerization. *Mol Cell Biol*. 2007;27(24):8698-8712.

Garg P, Verma R, Cook L, Soofi A, Venkatareddy M, George B, Mizuno K, Gurniak C, Witke W, Holzman LB. Actin-depolymerizing factor cofilin-1 is necessary in maintaining mature podocyte architecture. *J Biol Chem*. 2010;285(29):22676-22688.

George B, Holzman LB. Signaling from the podocyte intercellular junction to the actin cytoskeleton. *Semin Nephrol*. 2012;32(4):307-318.

George B, Verma R, Soofi AA, Garg P, Zhang J, Park TJ, Giardino L, Ryzhova L, Johnstone DB, Wong H, Nihalani D, Salant DJ, Hanks SK, Curran T, Rastaldi MP, Holzman LB. Crk1/2-dependent signaling is necessary for podocyte foot process spreading in mouse models of glomerular disease. *J Clin Invest*. 2012;122(2):674-692.

Geraldes P, Hiraoka-Yamamoto J, Matsumoto M, Clermont A, Leitges M, Marette A, Aiello LP, Kern TS, King GL. Activation of PKC-delta and SHP-1 by hyperglycemia causes vascular cell apoptosis and diabetic retinopathy. *Nat Med*. 2009;15(11):1298-1306.

Gerke P, Huber TB, Sellin L, Benzing T, Walz G. Homodimerization and heterodimerization of the glomerular podocyte proteins nephrin and NEPH1. *J Am Soc Nephrol*. 2003;14(4):918-926.

Gerke P, Sellin L, Kretz O, Petraschka D, Zentgraf H, Benzing T, Walz G. NEPH2 is located at the glomerular slit diaphragm, interacts with nephrin and is cleaved from podocytes by metalloproteinases. *J Am Soc Nephrol*. 2005;16(6):1693-1702.

Girgert R, Martin M, Kruegel J, Miosge N, Temme J, Eckes B, Muller GA, Gross O. Integrin alpha2-deficient mice provide insights into specific functions of collagen receptors in the kidney. *Fibrogenesis Tissue Repair*. 2010;3:19-1536-3-19.

Glassock RJ. The pathogenesis of membranous nephropathy: Evolution and revolution. *Curr Opin Nephrol Hypertens*. 2012;21(3):235-242.

Gonfloni S, Williams JC, Hattula K, Weijland A, Wierenga RK, Superti-Furga G. The role of the linker between the SH2 domain and catalytic domain in the regulation and function of src. *EMBO J*. 1997;16(24):7261-7271.

Grahammer F, Schell C, Huber TB. The podocyte slit diaphragm-from a thin grey line to a complex signalling hub. *Nat Rev Nephrol*. 2013;9(10):587-598.

Grimbert P, Valanciute A, Audard V, Pawlak A, Le gouvelo S, Lang P, Niaudet P, Bensman A, Guellaen G, Sahali D. Truncation of C-mip (tc-mip), a new proximal signaling protein, induces c-maf Th2 transcription factor and cytoskeleton reorganization. *J Exp Med*. 2003;198(5):797-807.

Gross O, Beirowski B, Harvey SJ, McFadden C, Chen D, Tam S, Thorner PS, Smyth N, Addicks K, Bloch W, Ninomiya Y, Sado Y, Weber M, Vogel WF. DDR1-deficient mice show localized subepithelial GBM thickening with focal loss of slit diaphragms and proteinuria. *Kidney Int*. 2004;66(1):102-111.

Gruenheid S, DeVinney R, Bladt F, Goosney D, Gelkop S, Gish GD, Pawson T, Finlay BB. Enteropathogenic E. coli tir binds nck to initiate actin pedestal formation in host cells. *Nat Cell Biol*. 2001;3(9):856-859.

Guan S, Chen M, Woodley D, Li W. Nck{beta} adapter controls neuritogenesis by maintaining cellular paxillin level. *Mol Cell Biol*. 2007;17:6001-6011.

Gunwar S, Ballester F, Noelken ME, Sado Y, Ninomiya Y, Hudson BG. Glomerular basement membrane. identification of a novel disulfide-cross-linked network of alpha3, alpha4, and alpha5 chains of type IV collagen and its implications for the pathogenesis of alport syndrome. *J Biol Chem*. 1998;273(15):8767-8775.

Guo G, Morrison DJ, Licht JD, Quaggin SE. WT1 activates a glomerular-specific enhancer identified from the human nephrin gene. *J Am Soc Nephrol*. 2004;15(11):2851-2856.

Gurley SB, Mach CL, Stegbauer J, Yang J, Snow KP, Hu A, Meyer TW, Coffman TM. Influence of genetic background on albuminuria and kidney injury in Ins2(+/C96Y) (akita) mice. *Am J Physiol Renal Physiol*. 2010;298(3):F788-95.

Hake MJ, Choowongkomon K, Kostenko O, Carlin CR, Sönnichsen FD. Specificity determinants of a novel nck interaction with the juxtamembrane domain of the epidermal growth factor receptor, *Biochemistry*. 2008;47(10):3096-3108.

Hamano Y, Grunkemeyer JA, Sudhakar A, Zeisberg M, Cosgrove D, Morello R, Lee B, Sugimoto H, Kalluri R. Determinants of vascular permeability in the kidney glomerulus. *J Biol Chem*. 2002;277(34):31154-31162.

Haraldsson B, Nystrom J. The glomerular endothelium: New insights on function and structure. *Curr Opin Nephrol Hypertens*. 2012;21(3):258-263.

Haraldsson B, Nystrom J, Deen WM. Properties of the glomerular barrier and mechanisms of proteinuria. *Physiol Rev*. 2008;88(2):451-487.

Harita Y, Kurihara H, Kosako H, Tezuka T, Sekine T, Igarashi T, Hattori S. Neph1, a component of the kidney slit diaphragm, is tyrosine phosphorylated by src-family tyrosine kinase and modulates intracellular signaling by binding to Grb2. *J Biol Chem*. 2008;283(14):9177-9186.

Harita Y, Kurihara H, Kosako H, Tezuka T, Sekine T, Igarashi T, Ohsawa I, Ohta S, Hattori S. Phosphorylation of nephrin triggers Ca2+ signaling by recruitment and activation of phospholipase C-{gamma}1. *J Biol Chem*. 2009;284(13):8951-8962.

Hartleben B, Widmeier E, Wanner N, Schmidts M, Kim ST, Schneider L, Mayer B, Kerjaschki D, Miner JH, Walz G, Huber TB. Role of the polarity protein scribble for podocyte differentiation and maintenance. *PLoS One*. 2012;7(5):e36705.

Hartleben B, Schweizer H, Lubben P, Bartram MP, Moller CC, Herr R, Wei C, Neumann-Haefelin E, Schermer B, Zentgraf H, Kerjaschki D, Reiser J, Walz G, Benzing T, Huber TB. Neph-nephrin proteins bind the Par3-Par6-atypical protein kinase C (aPKC) complex to regulate podocyte cell polarity. *J Biol Chem*. 2008;283(34):23033-23038.

Heikkila E, Ristola M, Havana M, Jones N, Holthofer H, Lehtonen S. Trans-interaction of nephrin and Neph1/Neph3 induces cell adhesion that associates with decreased tyrosine phosphorylation of nephrin. *Biochem J*. 2011;435(3):619-628.

Helmstadter M, Luthy K, Godel M, Simons M, Ashish, Nihalani D, Rensing SA, Fischbach KF, Huber TB. Functional study of mammalian neph proteins in drosophila melanogaster. *PLoS One*. 2012;7(7):e40300.

Heymann W, Hackel DB, Harwood S, Wilson SG, Hunter JL. Production of nephrotic syndrome in rats by freund's adjuvants and rat kidney suspensions. *Proc Soc Exp Biol Med*. 1959;100(4):660-664.

Hirabayashi S, Mori H, Kansaku A, Kurihara H, Sakai T, Shimizu F, Kawachi H, Hata Y. MAGI-1 is a component of the glomerular slit diaphragm that is tightly associated with nephrin. *Lab Invest*. 2005;85(12):1528-1543.

Hirose T, Satoh D, Kurihara H, Kusaka C, Hirose H, Akimoto K, Matsusaka T, Ichikawa I, Noda T, Ohno S. An essential role of the universal polarity protein, aPKClambda, on the maintenance of podocyte slit diaphragms. *PLoS One*. 2009;4(1):e4194.

Hocking JC, Hehr CL, Bertolesi GE, Wu JY, McFarlane S. Distinct roles for Robo2 in the regulation of axon and dendrite growth by retinal ganglion cells. *Mech Dev*. 2010;127(1-2):36-48.

Hodgin JB, Qu H, Liang X, Blattner SM, Chen K, Vining CM, Wylie S, Nishio M, Chen J, Wu C, Kretzler M: PINCH-1 and -2 Are essential for podocyte adhesion, shape modulation and maintenance of glomerular filtration barrier function [Abstract]. *J Am Soc Nephrol*. 2011;22:7A.

Holthofer H, Ahola H, Solin M, Wang S, Palmen T, Luimula P, Miettinen A, Kerjaschki D. Nephrin localizes at the podocyte filtration slit area and is characteristically spliced in the human kidney. *Am J Pathol*. 1999;155(5):1681-1687.

Holzman LB, St John PL, Kovari IA, Verma R, Holthofer H, Abrahamson DR. Nephrin localizes to the slit pore of the glomerular epithelial cell. *Kidney Int*. 1999;56(4):1481-1491.

Hu G, Jiao B. Mechanism of podocyte detachment: Targeting transmembrane molecules between podocytes and glomerular basement membrane. *Biomedicine & Aging Pathology*. 2013;3(1):36-42.

Huang Y, Guo X, Kassab GS. Axial nonuniformity of geometric and mechanical properties of mouse aorta is increased during postnatal growth. *Am J Physiol Heart Circ Physiol*. 2006;290(2):H657-64.

Huber TB, Schermer B, Benzing T. Podocin organizes ion channel-lipid supercomplexes: Implications for mechanosensation at the slit diaphragm. *Nephron Exp Nephrol*. 2007;106(2):e27-31.

Huber TB, Hartleben B, Winkelmann K, Schneider L, Becker JU, Leitges M, Walz G, Haller H, Schiffer M. Loss of podocyte aPKClambda/iota causes polarity defects and nephrotic syndrome. *J Am Soc Nephrol*. 2009;20(4):798-806.

Huber TB, Simons M, Hartleben B, Sernetz L, Schmidts M, Gundlach E, Saleem MA, Walz G, Benzing T. Molecular basis of the functional podocin-nephrin complex: Mutations in the NPHS2 gene disrupt nephrin targeting to lipid raft microdomains. *Hum Mol Genet*. 2003a;12(24):3397-3405.

Huber TB, Hartleben B, Kim J, Schmidts M, Schermer B, Keil A, Egger L, Lecha RL, Borner C, Pavenstadt H, Shaw AS, Walz G, Benzing T. Nephrin and CD2AP associate with phosphoinositide 3-OH kinase and stimulate AKT-dependent signaling. *Mol Cell Biol*. 2003b;23(14):4917-4928.

Hunt JL, Pollak MR, Denker BM. Cultured podocytes establish a size-selective barrier regulated by specific signaling pathways and demonstrate synchronized barrier assembly in a calcium switch model of junction formation. *J Am Soc Nephrol*. 2005;16(6):1593-1602.

Hussain S, Romio L, Saleem M, Mathieson P, Serrano M, Moscat J, Diaz-Meco M, Scambler P, Koziell A. Nephrin deficiency activates NF-kappaB and promotes glomerular injury. *J Am Soc Nephrol*. 2009;20(8):1733-1743.

Izzedine H, Mangier M, Ory V, Zhang SY, Sendeyo K, Bouachi K, Audard V, Pechoux C, Soria JC, Massard C, Bahleda R, Bourry E, Khayat D, Baumelou A, Lang P, Ollero M, Pawlak A, Sahali D. Expression patterns of RelA and c-mip are associated with different glomerular diseases following anti-VEGF therapy. *Kidney Int*. 2013.

Jackson Labs. JAX mice database - 005692. http://jaxmice.jax.org/strain/005692.html. Accessed 10/09, 2013.

Jeon J, Leibiger I, Moede T, Walter B, Faul C, Maiguel D, Villarreal R, Guzman J, Berggren PO, Mundel P, Ricordi C, Merscher-Gomez S, Fornoni A. Dynamin-mediated nephrin phosphorylation regulates glucose-stimulated insulin release in pancreatic beta cells. *J Biol Chem*. 2012;287(34):28932-28942.

Jia CYH, Nie J, Wu C, Li C, Li SS-. Novel src homology 3 domain-binding motifs identified from proteomic screen of a pro-rich region. *Mol Cell Proteomics*. 2005;4(8):1155-1166.

Jin J, Sison K, Li C, Tian R, Wnuk M, Sung HK, Jeansson M, Zhang C, Tucholska M, Jones N, Kerjaschki D, Shibuya M, Fantus IG, Nagy A, Gerber HP, Ferrara N, Pawson T, Quaggin SE. Soluble FLT1 binds lipid microdomains in podocytes to control cell morphology and glomerular barrier function. *Cell*. 2012;151(2):384-399.

Johnstone DB, Holzman LB. Clinical impact of research on the podocyte slit diaphragm. *Nat Clin Pract Nephrol*. 2006;2(5):271-282.

Johnstone DB, Ikizler O, Zhang J, Holzman LB. Background strain and the differential susceptibility of podocyte-specific deletion of Myh9 on murine models of experimental glomerulosclerosis and HIV nephropathy. *PLoS One*. 2013;8(7):e67839.

Johnstone DB, Zhang J, George B, Leon C, Gachet C, Wong H, Parekh R, Holzman LB. Podocyte-specific deletion of Myh9 encoding nonmuscle myosin heavy chain 2A predisposes mice to glomerulopathy. *Mol Cell Biol*. 2011;31(10):2162-2170.

Jones N, Blasutig IM, Eremina V, Ruston JM, Bladt F, Li HP, Huang HM, Larose L, Li SSC, Takano T, Quaggin SE, Pawson T. Nck adaptor proteins link nephrin to the actin cytoskeleton of kidney podocytes. *Nature*. 2006;440(7085):818-823.

Jones N, New LA, Fortino MA, Eremina V, Ruston J, Blasutig IM, Aoudjit L, Zou Y, Liu X, Yu GL, Takano T, Quaggin SE, Pawson T. Nck proteins maintain the adult glomerular filtration barrier. *J Am Soc Nephrol*. 2009;20(7):1533-1543.

Juhila J, Lassila M, Roozendaal R, Lehtonen E, Messing M, Langer B, Kerjaschki D, Verbeek JS, Holthofer H. Inducible nephrin transgene expression in podocytes rescues nephrin-deficient mice from perinatal death. *Am J Pathol*. 2010;176(1):51-63.

Kaipa BR, Shao H, Schafer G, Trinkewitz T, Groth V, Liu J, Beck L, Bogdan S, Abmayr SM, Onel SF. Dock mediates scar- and WASp-dependent actin polymerization through interaction with cell adhesion molecules in founder cells and fusion-competent myoblasts. *J Cell Sci*. 2013;126(Pt 1):360-372.

Kajiho Y, Harita Y, Kurihara H, Horita S, Matsunaga A, Tsurumi H, Kanda S, Sugawara N, Miura K, Sekine T, Hattori S, Hattori M, Igarashi T. SIRPalpha interacts with nephrin at the podocyte slit diaphragm. *FEBS J*. 2012;279(17):3010-3021.

Kanda S, Harita Y, Shibagaki Y, Sekine T, Igarashi T, Inoue T, Hattori S. Tyrosine phosphorylation-dependent activation of TRPC6 regulated by PLC-gamma1 and nephrin: Effect of mutations associated with focal segmental glomerulosclerosis. *Mol Biol Cell*. 2011;22(11):1824-1835.

Kanetsuna Y, Takahashi K, Nagata M, Gannon MA, Breyer MD, Harris RC, Takahashi T. Deficiency of endothelial nitric-oxide synthase confers susceptibility to diabetic nephropathy in nephropathy-resistant inbred mice. *Am J Pathol*. 2007;170(5):1473-1484.

Kang JS, Wang XP, Miner JH, Morello R, Sado Y, Abrahamson DR, Borza DB. Loss of alpha3/alpha4(IV) collagen from the glomerular basement membrane induces a strain-dependent isoform switch to alpha5alpha6(IV) collagen associated with longer renal survival in Col4a3-/- alport mice. *J Am Soc Nephrol*. 2006;17(7):1962-1969.

Kato H, Gruenwald A, Suh JH, Miner JH, Barisoni-Thomas L, Taketo MM, Faul C, Millar SE, Holzman LB, Susztak K. Wnt/beta-catenin pathway in podocytes integrates cell adhesion, differentiation, and survival. *J Biol Chem*. 2011;286(29):26003-26015.

Kebache S, Zuo D, Chevet E, Larose L. Modulation of protein translation by nck-1. *PNAS*. 2002;99(8):5406-5411.

Kerjaschki D, Schulze M, Binder S, Kain R, Ojha PP, Susani M, Horvat R, Baker PJ, Couser WG. Transcellular transport and membrane insertion of the C5b-9 membrane attack complex of complement by glomerular epithelial cells in experimental membranous nephropathy. *J Immunol*. 1989;143(2):546-552.

Kestila M, Lenkkeri U, Mannikko M, Lamerdin J, McCready P, Putaala H, Ruotsalainen V, Morita T, Nissinen M, Herva R, Kashtan CE, Peltonen L, Holmberg C, Olsen A, Tryggvason K. Positionally cloned gene for a novel glomerular protein--nephrin--is mutated in congenital nephrotic syndrome. *Mol Cell*. 1998;1(4):575-582.

Khoshnoodi J, Sigmundsson K, Ofverstedt LG, Skoglund U, Obrink B, Wartiovaara J, Tryggvason K. Nephrin promotes cell-cell adhesion through homophilic interactions. *Am J Pathol*. 2003;163(6):2337-2346.

Kim EY, Choi K, Dryer SE. Nephrin binds to the C-terminal of a large-conductance calcium-activated potassium channel isoform and regulates its expression on the cell surface. *Am J Physiol Renal Physiol*. 2008.

Knight E, Murray B, Carnachan R, Przyborski S. Alvetex(R): Polystyrene scaffold technology for routine three dimensional cell culture. *Methods Mol Biol*. 2011;695:323-340.

Kobayashi N, Gao SY, Chen J, Saito K, Miyawaki K, Li CY, Pan L, Saito S, Terashita T, Matsuda S. Process formation of the renal glomerular podocyte: Is there common molecular machinery for processes of podocytes and neurons? *Anat Sci Int*. 2004;79(1):1-10.

Kocherlakota KS, Wu JM, McDermott J, Abmayr SM. Analysis of the cell adhesion molecule sticks-and-stones reveals multiple redundant functional domains, protein-interaction motifs and phosphorylated tyrosines that direct myoblast fusion in drosophila melanogaster. *Genetics*. 2008;178(3):1371-1383.

Komori T, Gyobu H, Ueno H, Kitamura T, Senba E, Morikawa Y. Expression of kin of irregular chiasm-like 3/mKirre in proprioceptive neurons of the dorsal root ganglia and its interaction with nephrin in muscle spindles. *J Comp Neurol*. 2008;511(1):92-108.

Kramer-Zucker AG, Wiessner S, Jensen AM, Drummond IA. Organization of the pronephric filtration apparatus in zebrafish requires nephrin, podocin and the FERM domain protein mosaic eyes. *Dev Biol*. 2005;285(2):316-329.

Kremer BE, Adang LA, Macara IG. Septins regulate actin organization and cell-cycle arrest through nuclear accumulation of NCK mediated by SOCS7. *Cell*. 2007;130(5):837-850.

Kriz W, Kretzler M, Provoost AP, Shirato I. Stability and leakiness: Opposing challenges to the glomerulus. *Kidney Int*. 1996;49(6):1570-1574.

Kruegel J, Rubel D, Gross O. Alport syndrome--insights from basic and clinical research. *Nat Rev Nephrol*. 2013;9(3):170-178.

Kumagai T, Baldwin C, Aoudjit L, Zhu L, Takano T: PTP1B inhibition protects against podocyte injury and proteinuria [Abstract]. *J Am Soc Nephrol*. 2012;23:818A.

Kuusniemi AM, Kestila M, Patrakka J, Lahdenkari AT, Ruotsalainen V, Holmberg C, Karikoski R, Salonen R, Tryggvason K, Jalanko H. Tissue expression of nephrin in human and pig. *Pediatr Res*. 2004;55(5):774-781.

Lahdenpera J, Kilpelainen P, Liu XL, Pikkarainen T, Reponen P, Ruotsalainen V, Tryggvason K. Clustering-induced tyrosine phosphorylation of nephrin by src family kinases. *Kidney Int*. 2003;64(2):404-413.

Lamalice L, Houle F, Huot J. Phosphorylation of Tyr1214 within VEGFR-2 triggers the recruitment of nck and activation of fyn leading to SAPK2/p38 activation and endothelial cell migration in response to VEGF. *J Biol Chem*. 2006;281(45):34009-34020.

Le Roy C, Wrana JL. Clathrin- and non-clathrin-mediated endocytic regulation of cell signalling. *Nat Rev Mol Cell Biol*. 2005;6(2):112-126.

Leelahavanichkul A, Yan Q, Hu X, Eisner C, Huang Y, Chen R, Mizel D, Zhou H, Wright EC, Kopp JB, Schnermann J, Yuen PS, Star RA. Angiotensin II overcomes strain-dependent resistance of rapid CKD progression in a new remnant kidney mouse model. *Kidney Int*. 2010;78(11):1136-1153.

Leeuwis JW, Nguyen TQ, Dendooven A, Kok RJ, Goldschmeding R. Targeting podocyte-associated diseases. *Adv Drug Deliv Rev*. 2010;62(14):1325-1336.

Lehtonen S, Ryan JJ, Kudlicka K, Iino N, Zhou H, Farquhar MG. Cell junction-associated proteins IQGAP1, MAGI-2, CASK, spectrins, and alpha-actinin are components of the nephrin multiprotein complex. *Proc Natl Acad Sci U S A*. 2005;102(28):9814-9819.

Lemley KV, Elger M, Koeppen-Hagemann I, Kretzler M, Nagata M, Sakai T, Uiker S, Kriz W. The glomerular mesangium: Capillary support function and its failure under experimental conditions. *Clin Investig*. 1992;70(9):843-856.

Lettau M, Pieper J, Janssen O. Nck adapter proteins: Functional versatility in T cells. *Cell Commun Signal*. 2009;7:1. doi: 10.1186/1478-811X-7-1.

Li C, Schibli D, Li SS. The XLP syndrome protein SAP interacts with SH3 proteins to regulate T cell signaling and proliferation. *Cell Signal*. 2009;21(1):111-119.

Li H, Lemay S, Aoudjit L, Kawachi H, Takano T. Src-family kinase fyn phosphorylates the cytoplasmic domain of nephrin and modulates its interaction with podocin. *J Am Soc Nephrol*. 2004;15(12):3006-3015.

Li H, Zhu J, Aoudjit L, Latreille M, Kawachi H, Larose L, Takano T. Rat nephrin modulates cell morphology via the adaptor protein nck. *Biochem Biophys Res Commun*. 2006;349(1):310-316.

Li M, Armelloni S, Edefonti A, Messa P, Rastaldi MP. Fifteen years of research on nephrin: What we still need to know. *Nephrol Dial Transplant*. 2013;28(4):767-770.

Li M, Armelloni S, Ikehata M, Corbelli A, Pesaresi M, Calvaresi N, Giardino L, Mattinzoli D, Nistico F, Andreoni S, Puliti A, Ravazzolo R, Forloni G, Messa P, Rastaldi MP. Nephrin expression in adult rodent central nervous system and its interaction with glutamate receptors. *J Pathol*. 2011;225(1):118-128.

Li P, Banjade S, Cheng HC, Kim S, Chen B, Guo L, Llaguno M, Hollingsworth JV, King DS, Banani SF, Russo PS, Jiang QX, Nixon BT, Rosen MK. Phase transitions in the assembly of multivalent signalling proteins. *Nature*. 2012;483(7389):336-340.

Li W, Fan J, Woodley D. Nck/dock: An adapter between cell surface receptors and the actin cytoskeleton. *Oncogene*. 2001;20:6403-6417.

Li W, Hu P, Skolnik EY, Ullrich A, Schlessinger J. The SH2 and SH3 domain-containing nck protein is oncogenic and a common target for phosphorylation by different surface receptors. *Mol Cell Biol*. 1992;12(12):5824-5833.

Li Y, Kang YS, Dai C, Kiss LP, Wen X, Liu Y. Epithelial-to-mesenchymal transition is a potential pathway leading to podocyte dysfunction and proteinuria. *Am J Pathol*. 2008;172(2):299-308.

Liu G, Kaw B, Kurfis J, Rahmanuddin S, Kanwar YS, Chugh SS. Neph1 and nephrin interaction in the slit diaphragm is an important determinant of glomerular permeability. *J Clin Invest*. 2003;112(2):209-221.

Liu J, Li M, Ran X, Fan J, Song J. Structural insight into the binding diversity between the human Nck2 SH3 domains and proline-rich proteins. *Biochemistry*. 2006;45(23):7171-7184.

Liu L, Aya K, Tanaka H, Shimizu J, Ito S, Seino Y. Nephrin is an important component of the barrier system in the testis. *Acta Med Okayama*. 2001;55(3):161-165.

Liu XL, Kilpelainen P, Hellman U, Sun Y, Wartiovaara J, Morgunova E, Pikkarainen T, Yan K, Jonsson AP, Tryggvason K. Characterization of the interactions of the nephrin intracellular domain. *FEBS J*. 2005;272(1):228-243.

Long DA, Kolatsi-Joannou M, Price KL, Dessapt-Baradez C, Huang JL, Papakrivopoulou E, Hubank M, Korstanje R, Gnudi L, Woolf AS. Albuminuria is associated with too few glomeruli and too much testosterone. *Kidney Int*. 2013;83(6):1118-1129.

Lothrop AP, Torres MP, Fuchs SM. Deciphering post-translational modification codes. *FEBS Lett*. 2013;587(8):1247-1257.

Martineau LC, McVeigh LI, Jasmin BJ, Kennedy CR. p38 MAP kinase mediates mechanically induced COX-2 and PG EP4 receptor expression in podocytes: Implications for the actin cytoskeleton. *Am J Physiol Renal Physiol*. 2004;286(4):F693-701.

Matsui I, Ito T, Kurihara H, Imai E, Ogihara T, Hori M. Snail, a transcriptional regulator, represses nephrin expression in glomerular epithelial cells of nephrotic rats. *Lab Invest*. 2007;87(3):273-283.

Mayer BJ, Jackson PK, Van Etten RA, Baltimore D. Point mutations in the abl SH2 domain coordinately impair phosphotyrosine binding in vitro and transforming activity in vivo. *Mol Cell Biol*. 1992;12(2):609-618.

McGrogan A, Franssen CF, de Vries CS. The incidence of primary glomerulonephritis worldwide: A systematic review of the literature. *Nephrol Dial Transplant*. 2011;26(2):414-430.

Meehan DT, Delimont D, Cheung L, Zallocchi M, Sansom SC, Holzclaw JD, Rao V, Cosgrove D. Biomechanical strain causes maladaptive gene regulation, contributing to alport glomerular disease. *Kidney Int*. 2009;76(9):968-976.

Meisenhelder J, Hunter T. The SH2/SH3 domain-containing protein nck is recognized by certain anti-phospholipase C-gamma 1 monoclonal antibodies, and its phosphorylation on tyrosine is stimulated by platelet-derived growth factor and epidermal growth factor treatment. *Mol Cell Biol*. 1992;12(12):5843-5856.

Michele DE, Gomez CA, Hong KE, Westfall MV, Metzger JM. Cardiac dysfunction in hypertrophic cardiomyopathy mutant tropomyosin mice is transgene-dependent, hypertrophy-independent, and improved by beta-blockade. *Circ Res*. 2002;91(3):255-262.

Mima A, Kitada M, Geraldes P, Li Q, Matsumoto M, Mizutani K, Qi W, Li C, Leitges M, Rask-Madsen C, King GL. Glomerular VEGF resistance induced by PKCdelta/SHP-1 activation and contribution to diabetic nephropathy. *FASEB J*. 2012;26(7):2963-2974.

Miner JH. The glomerular basement membrane. *Exp Cell Res*. 2012;318(9):973-978.

Miyoshi-Akiyama T, Aleman LM, Smith JM, Adler CE, Mayer BJ. Regulation of cbl phosphorylation by the abl tyrosine kinase and the nck SH2/SH3 adaptor. *Oncogene*. 2001;20(30):4058-4069.

Moeller MJ, Kovari IA, Holzman LB. Evaluation of a new tool for exploring podocyte biology: Mouse Nphs1 5' flanking region drives LacZ expression in podocytes. *J Am Soc Nephrol*. 2000;11(12):2306-2314.

Moeller MJ, Sanden SK, Soofi A, Wiggins RC, Holzman LB. Two gene fragments that direct podocyte-specific expression in transgenic mice. *J Am Soc Nephrol*. 2002;13(6):1561-1567.

Mohamed AM, Chin-Sang ID. The C. elegans nck-1 gene encodes two isoforms and is required for neuronal guidance. *Dev Biol*. 2011;354(1):55-66.

Morikawa Y, Komori T, Hisaoka T, Ueno H, Kitamura T, Senba E. Expression of mKirre in the developing sensory pathways: Its close apposition to nephrin-expressing cells. *Neuroscience*. 2007;150(4):880-886.

Neumann-Haefelin E, Kramer-Zucker A, Slanchev K, Hartleben B, Noutsou F, Martin K, Wanner N, Ritter A, Godel M, Pagel P, Fu X, Muller A, Baumeister R, Walz G, Huber TB. A model organism approach: Defining the role of neph proteins as regulators of neuron and kidney morphogenesis. *Hum Mol Genet*. 2010;19(12):2347-2359.

New LA, Keyvani Chahi A, Jones N. Direct regulation of nephrin tyrosine phosphorylation by nck adaptor proteins. *J Biol Chem*. 2013;288(3):1500-1510.

Nishida K, Hoshino M, Kawaguchi Y, Murakami F. Ptf1a directly controls expression of immunoglobulin superfamily molecules nephrin and Neph3 in the developing central nervous system. *J Biol Chem*. 2010;285(1):373-380.

Nishino T, Sasaki N, Nagasaki K, Ahmad Z, Agui T. Genetic background strongly influences the severity of glomerulosclerosis in mice. *J Vet Med Sci*. 2010;72(10):1313-1318.

Noble M, Groves AK, Ataliotis P, Ikram Z, Jat PS. The H-2KbtsA58 transgenic mouse: A new tool for the rapid generation of novel cell lines. *Transgenic Res*. 1995;4(4):215-225.

Obeidat M, Obeidat M, Ballermann BJ. Glomerular endothelium: A porous sieve and formidable barrier. *Exp Cell Res*. 2012;318(9):964-972.

Ogura A, Asano T, Matsuda J, Takano K, Nakagawa M, Fukui M. Characteristics of mutant mice (ICGN) with spontaneous renal lesions: A new model for human nephrotic syndrome. *Lab Anim*. 1989;23(2):169-174.

Ohashi T, Uchida K, Uchida S, Sasaki S, Nitta K. Dexamethasone increases the phosphorylation of nephrin in cultured podocytes. *Clin Exp Nephrol*. 2011;15(5):688-693.

Ohashi T, Uchida K, Asamiya Y, Tsuruta Y, Ohno M, Horita S, Nitta K. Phosphorylation status of nephrin in human membranous nephropathy. *Clin Exp Nephrol*. 2010;14(1):51-55.

Okamura M, Takano Y, Saito Y, Yao J, Kitamura M. Induction of nephrin gene expression by selective cooperation of the retinoic acid receptor and the vitamin D receptor. *Nephrol Dial Transplant*. 2009;24(10):3006-3012.

Oser M, Condeelis J. The cofilin activity cycle in lamellipodia and invadopodia. *J Cell Biochem*. 2009;108(6):1252-1262.

Palmen T, Ahola H, Palgi J, Aaltonen P, Luimula P, Wang S, Jaakkola I, Knip M, Otonkoski T, Holthofer H. Nephrin is expressed in the pancreatic beta cells. *Diabetologia*. 2001;44(10):1274-1280.

Panchamoorthy G, Fukazawa T, Stolz L, Payne G, Reedquist K, Shoelson S, Songyang Z, Cantley L, Walsh C, Band H. Physical and functional interactions between SH2 and SH3 domains of the src family protein tyrosine kinase p59fyn. *Mol Cell Biol*. 1994;14(9):6372-6385.

Papeta N, Zheng Z, Schon EA, Brosel S, Altintas MM, Nasr SH, Reiser J, D'Agati VD, Gharavi AG. Prkdc participates in mitochondrial genome maintenance and prevents adriamycin-induced nephropathy in mice. *J Clin Invest*. 2010;120(11):4055-4064.

Patrakka J, Tryggvason K. Molecular make-up of the glomerular filtration barrier. *Biochem Biophys Res Commun*. 2010;396(1):164-169.

Patrakka J, Tryggvason K. Nephrin--a unique structural and signaling protein of the kidney filter. *Trends Mol Med*. 2007;13(9):396-403.

Pavenstadt H, Kriz W, Kretzler M. Cell biology of the glomerular podocyte. *Physiol Rev*. 2003;83(1):253-307.

Picotti P, Aebersold R. Selected reaction monitoring-based proteomics: Workflows, potential, pitfalls and future directions. *Nat Methods*. 2012;9(6):555-566.

Pippin JW, Brinkkoetter PT, Cormack-Aboud FC, Durvasula RV, Hauser PV, Kowalewska J, Krofft RD, Logar CM, Marshall CB, Ohse T, Shankland SJ. Inducible rodent models of acquired podocyte diseases. *Am J Physiol Renal Physiol*. 2009;296(2):F213-29.

Pitulescu ME, Adams RH. Eph/ephrin molecules--a hub for signaling and endocytosis. *Genes Dev*. 2010;24(22):2480-2492.

Pollard TD, Borisy GG. Cellular motility driven by assembly and disassembly of actin filaments. *Cell*. 2003;112(4):453-465.

Prabhakar R, Boivin GP, Grupp IL, Hoit B, Arteaga G, Solaro RJ, Wieczorek DF. A familial hypertrophic cardiomyopathy alpha-tropomyosin mutation causes severe cardiac hypertrophy and death in mice. *J Mol Cell Cardiol*. 2001;33(10):1815-1828.

Prakash S, Papeta N, Sterken R, Zheng Z, Thomas RL, Wu Z, Sedor JR, D'Agati VD, Bruggeman LA, Gharavi AG. Identification of the nephropathy-susceptibility locus HIVAN4. *J Am Soc Nephrol*. 2011;22(8):1497-1504.

Prince JE, Brignall AC, Cutforth T, Shen K, Cloutier JF. Kirrel3 is required for the coalescence of vomeronasal sensory neuron axons into glomeruli and for male-male aggression. *Development*. 2013;140(11):2398-2408.

Puschmann TB, de Pablo Y, Zanden C, Liu J, Pekny M. A novel method for 3D culture of central nervous system neurons. *Tissue Eng Part C Methods*. 2013.

Putaala H, Soininen R, Kilpelainen P, Wartiovaara J, Tryggvason K. The murine nephrin gene is specifically expressed in kidney, brain and pancreas: Inactivation of the gene leads to massive proteinuria and neonatal death. *Hum Mol Genet*. 2001;10(1):1-8.

Qi Z, Fujita H, Jin J, Davis LS, Wang Y, Fogo AB, Breyer MD. Characterization of susceptibility of inbred mouse strains to diabetic nephropathy. *Diabetes*. 2005;54(9):2628-2637.

Qin XS, Tsukaguchi H, Shono A, Yamamoto A, Kurihara H, Doi T. Phosphorylation of nephrin triggers its internalization by raft-mediated endocytosis. *J Am Soc Nephrol*. 2009;20(12):2534-2545.

Quack I, Woznowski M, Potthoff SA, Palmer R, Konigshausen E, Sivritas S, Schiffer M, Stegbauer J, Vonend O, Rump LC, Sellin L. PKC alpha mediates beta-arrestin2-dependent nephrin endocytosis in hyperglycemia. *J Biol Chem*. 2011;286(15):12959-12970.

Quack I, Rump LC, Gerke P, Walther I, Vinke T, Vonend O, Grunwald T, Sellin L. Beta-Arrestin2 mediates nephrin endocytosis and impairs slit diaphragm integrity. *PNAS*. 2006;103(38):14110-14115.

Quaggin SE, Kreidberg JA. Development of the renal glomerulus: Good neighbors and good fences. *Development*. 2008;135(4):609-620.

Rantanen M, Palmen T, Patari A, Ahola H, Lehtonen S, Astrom E, Floss T, Vauti F, Wurst W, Ruiz P, Kerjaschki D, Holthofer H. Nephrin TRAP mice lack slit diaphragms and show fibrotic glomeruli and cystic tubular lesions. *J Am Soc Nephrol*. 2002;13(6):1586-1594.

Rastaldi MP, Armelloni S, Berra S, Calvaresi N, Corbelli A, Giardino LA, Li M, Wang GQ, Fornasieri A, Villa A, Heikkila E, Soliymani R, Boucherot A, Cohen CD, Kretzler M, Nitsche A, Ripamonti M, Malgaroli A, Pesaresi M, Forloni GL, *et al*. Glomerular podocytes contain neuron-like functional synaptic vesicles. *FASEB J*. 2006;20(7):976-978.

Rawlings ND, Waller M, Barrett AJ, Bateman A. MEROPS: The database of proteolytic enzymes, their substrates and inhibitors. *Nucleic Acids Res*. 2013.

Reidy KJ, Aggarwal PK, Jimenez JJ, Thomas DB, Veron D, Tufro A. Excess podocyte semaphorin-3A leads to glomerular disease involving PlexinA1-nephrin interaction. *Am J Pathol*. 2013;183(4):1156-1168.

Reiser J, Polu KR, Moller CC, Kenlan P, Altintas MM, Wei C, Faul C, Herbert S, Villegas I, Avila-Casado C, McGee M, Sugimoto H, Brown D, Kalluri R, Mundel P, Smith PL, Clapham DE, Pollak MR. TRPC6 is a glomerular slit diaphragm-associated channel required for normal renal function. *Nat Genet*. 2005;37(7):739-744.

Reiser J, Kriz W, Kretzler M, Mundel P. The glomerular slit diaphragm is a modified adherens junction. *J Am Soc Nephrol*. 2000a;11(1):1-8.

Reiser J, Pixley FJ, Hug A, Kriz W, Smoyer WE, Stanley ER, Mundel P. Regulation of mouse podocyte process dynamics by protein tyrosine phosphatases. *Kidney Int*. 2000b;57(5):2035-2042.

Rigothier C, Auguste P, Welsh GI, Lepreux S, Deminiere C, Mathieson PW, Saleem MA, Ripoche J, Combe C. IQGAP1 interacts with components of the slit diaphragm complex in podocytes and is involved in podocyte migration and permeability in vitro. *PLoS One*. 2012;7(5):e37695.

Ristola M, Arpiainen S, Saleem MA, Holthofer H, Lehtonen S. Transcription of nephrin-Neph3 gene pair is synergistically activated by WT1 and NF-kappaB and silenced by DNA methylation. *Nephrol Dial Transplant*. 2012;27(5):1737-1745.

Ristola M, Arpiainen S, Saleem MA, Mathieson PW, Welsh GI, Lehtonen S, Holthofer H. Regulation of Neph3 gene in podocytes--key roles of transcription factors NF-kappaB and Sp1. *BMC Mol Biol*. 2009;10:83-2199-10-83.

Ristola M, Arpiainen S, Shimokawa T, Ra C, Tienari J, Saleem MA, Holthofer H, Lehtonen S. Regulation of nephrin gene by the ets transcription factor, GA-binding protein. *Nephrol Dial Transplant*. 2013;28(4):846-855.

Rivera GM, Antoku S, Gelkop S, Shin NY, Hanks SK, Pawson T, Mayer BJ. Requirement of nck adaptors for actin dynamics and cell migration stimulated by platelet-derived growth factor B. *PNAS*. 2006;103(25):9536-9541.

Rodewald R, Karnovsky MJ. Porous substructure of the glomerular slit diaphragm in the rat and mouse. *J Cell Biol*. 1974;60(2):423-433.

Round JE, Sun H. The adaptor protein Nck2 mediates Slit1-induced changes in cortical neuron morphology. *Mol Cell Neurosci*. 2011;47(4):265-273.

Ruotsalainen V, Ljungberg P, Wartiovaara J, Lenkkeri U, Kestila M, Jalanko H, Holmberg C, Tryggvason K. Nephrin is specifically located at the slit diaphragm of glomerular podocytes. *Proc Natl Acad Sci U S A*. 1999;96(14):7962-7967.

Ruotsalainen V, Patrakka J, Tissari P, Reponen P, Hess M, Kestila M, Holmberg C, Salonen R, Heikinheimo M, Wartiovaara J, Tryggvason K, Jalanko H. Role of nephrin in cell junction formation in human nephrogenesis. *Am J Pathol*. 2000;157(6):1905-1916.

Sachs N, Sonnenberg A. Cell-matrix adhesion of podocytes in physiology and disease. *Nat Rev Nephrol*. 2013;9(4):200-210.

Sachs N, Kreft M, van den Bergh Weerman MA, Beynon AJ, Peters TA, Weening JJ, Sonnenberg A. Kidney failure in mice lacking the tetraspanin CD151. *J Cell Biol*. 2006;175(1):33-39.

Sachs N, Claessen N, Aten J, Kreft M, Teske GJ, Koeman A, Zuurbier CJ, Janssen H, Sonnenberg A. Blood pressure influences end-stage renal disease of Cd151 knockout mice. *J Clin Invest*. 2012;122(1):348-358.

Saito Y, Okamura M, Nakajima S, Hayakawa K, Huang T, Yao J, Kitamura M. Suppression of nephrin expression by TNF-alpha via interfering with the cAMP-retinoic acid receptor pathway. *Am J Physiol Renal Physiol*. 2010;298(6):F1436-44.

Schell C, Baumhakl L, Salou S, Conzelmann AC, Meyer C, Helmstadter M, Wrede C, Grahammer F, Eimer S, Kerjaschki D, Walz G, Snapper S, Huber TB. N-wasp is required for stabilization of podocyte foot processes. *J Am Soc Nephrol*. 2013;24(5):713-721.

Schermer B, Benzing T. Lipid-protein interactions along the slit diaphragm of podocytes. *J Am Soc Nephrol*. 2009;20(3):473-478.

Schlondorff D, Banas B. The mesangial cell revisited: No cell is an island. *J Am Soc Nephrol*. 2009;20(6):1179-1187.

Schordan S, Schordan E, Endlich K, Endlich N. AlphaV-integrins mediate the mechanoprotective action of osteopontin in podocytes. *Am J Physiol Renal Physiol*. 2011;300(1):F119-32.

Schwarz K, Simons M, Reiser J, Saleem MA, Faul C, Kriz W, Shaw AS, Holzman LB, Mundel P. Podocin, a raft-associated component of the glomerular slit diaphragm, interacts with CD2AP and nephrin. *J Clin Invest*. 2001;108(11):1621-1629.

Seiler MW, Venkatachalam MA, Cotran RS. Glomerular epithelium: Structural alterations induced by polycations. *Science*. 1975;189(4200):390-393.

Sendeyo K, Audard V, Zhang SY, Fan Q, Bouachi K, Ollero M, Rucker-Martin C, Gouadon E, Desvaux D, Bridoux F, Guellaen G, Ronco P, Lang P, Pawlak A, Sahali D. Upregulation of c-mip is closely related to podocyte dysfunction in membranous nephropathy. *Kidney Int*. 2013;83(3):414-425.

Shankland SJ, Pippin JW, Reiser J, Mundel P. Podocytes in culture: Past, present, and future. *Kidney Int*. 2007;72(1):26-36.

Sharma R, Barakzai SZ, Taylor SE, Donadeu FX. Epidermal-like architecture obtained from equine keratinocytes in three-dimensional cultures. *J Tissue Eng Regen Med*. 2013.

Shelton C, Kocherlakota KS, Zhuang S, Abmayr SM. The immunoglobulin superfamily member hbs functions redundantly with sns in interactions between founder and fusion-competent myoblasts. *Development*. 2009;136(7):1159-1168.

Shen K, Fetter RD, Bargmann CI. Synaptic specificity is generated by the synaptic guidepost protein SYG-2 and its receptor, SYG-1. *Cell*. 2004;116(6):869-881.

Shih N, Li J, Cotran R, Mundel P, Miner JH, Shaw AS. CD2AP localizes to the slit diaphragm and binds to nephrin via a novel C-terminal domain. *Am J Pathol*. 2001;159(6):2303-2308.

Shimizu M, Khoshnoodi J, Akimoto Y, Kawakami H, Hirano H, Higashihara E, Hosoyamada M, Sekine Y, Kurayama R, Kurayama H, Joh K, Hirabayashi J, Kasai K, Tryggvason K, Ito N, Yan K. Expression of galectin-1, a new component of slit diaphragm, is altered in minimal change nephrotic syndrome. *Lab Invest*. 2009;89(2):178-195.

Shono A, Tsukaguchi H, Kitamura A, Hiramoto R, Qin XS, Doi T, Iijima K. Predisposition to relapsing nephrotic syndrome by a nephrin mutation that interferes with assembly of functioning microdomains. *Hum Mol Genet*. 2009;18(16):2943-2956.

Simarro M, Lanyi A, Howie D, Poy F, Bruggeman J, Choi M, Sumegi J, Eck MJ, Terhorst C. SAP increases FynT kinase activity and is required for phosphorylation of SLAM and Ly9. *Int Immunol*. 2004;16(5):727-736.

Simons M, Schwarz K, Kriz W, Miettinen A, Reiser J, Mundel P, Holthofer H. Involvement of lipid rafts in nephrin phosphorylation and organization of the glomerular slit diaphragm. *Am J Pathol*. 2001;159(3):1069-1077.

Singh S, Kirchner M, Steen JA, Steen H. A practical guide to the FLEXIQuant method. *Methods Mol Biol*. 2012;893:295-319.

Sistani L, Rodriguez PQ, Hultenby K, Uhlen M, Betsholtz C, Jalanko H, Tryggvason K, Wernerson A, Patrakka J. Neuronal proteins are novel components of podocyte major processes and their expression in glomerular crescents supports their role in crescent formation. *Kidney Int*. 2013;83(1):63-71.

Slater SC, Beachley V, Hayes T, Zhang D, Welsh GI, Saleem MA, Mathieson PW, Wen X, Su B, Satchell SC. An in vitro model of the glomerular capillary wall using electrospun collagen nanofibres in a bioartificial composite basement membrane. *PLoS One*. 2011;6(6):e20802.

Smith JM, Katz S, Mayer BJ. Activation of the abl tyrosine kinase in vivo by src homology 3 domains from the src homology 2/src homology 3 adaptor nck. *J Biol Chem*. 1999;274(39):27956-27962.

Soda K, Ishibe S. The function of endocytosis in podocytes. *Curr Opin Nephrol Hypertens*. 2013;22(4):432-438.

Soda K, Balkin DM, Ferguson SM, Paradise S, Milosevic I, Giovedi S, Volpicelli-Daley L, Tian X, Wu Y, Ma H, Son SH, Zheng R, Moeckel G, Cremona O, Holzman LB, De Camilli P, Ishibe S. Role of dynamin, synaptojanin, and endophilin in podocyte foot processes. *J Clin Invest*. 2012;122(12):4401-4411.

Sohn RL, Huang P, Kawahara G, Mitchell M, Guyon J, Kalluri R, Kunkel LM, Gussoni E. A role for nephrin, a renal protein, in vertebrate skeletal muscle cell fusion. *Proc Natl Acad Sci U S A*. 2009;106(23):9274-9279.

Solheim SA, Torgersen KM, Tasken K, Berge T. Regulation of FynT function by dual domain docking on PAG/cbp. *J Biol Chem*. 2008;283(5):2773-2783.

Sprinzak D, Lakhanpal A, Lebon L, Santat LA, Fontes ME, Anderson GA, Garcia-Ojalvo J, Elowitz MB. Cis-interactions between notch and delta generate mutually exclusive signalling states. *Nature*. 2010;465(7294):86-90.

Stanescu HC, Arcos-Burgos M, Medlar A, Bockenhauer D, Kottgen A, Dragomirescu L, Voinescu C, Patel N, Pearce K, Hubank M, Stephens HA, Laundy V, Padmanabhan S, Zawadzka A, Hofstra JM, Coenen MJ, den Heijer M, Kiemeney LA, Bacq-Daian D, Stengel B, *et al*. Risk HLA-DQA1 and PLA(2)R1 alleles in idiopathic membranous nephropathy. *N Engl J Med*. 2011;364(7):616-626.

Steen H, Jebanathirajah JA, Springer M, Kirschner MW. Stable isotope-free relative and absolute quantitation of protein phosphorylation stoichiometry by MS. *Proc Natl Acad Sci U S A*. 2005;102(11):3948-3953.

Sugie A, Umetsu D, Yasugi T, Fischbach KF, Tabata T. Recognition of pre- and postsynaptic neurons via nephrin/NEPH1 homologs is a basis for the formation of the drosophila retinotopic map. *Development*. 2010;137(19):3303-3313.

Suh JH, Miner JH. The glomerular basement membrane as a barrier to albumin. *Nat Rev Nephrol*. 2013;9(8):470-477.

Surinova S, Huttenhain R, Chang CY, Espona L, Vitek O, Aebersold R. Automated selected reaction monitoring data analysis workflow for large-scale targeted proteomic studies. *Nat Protoc*. 2013;8(8):1602-1619.

Swarbrick MM, Havel PJ, Levin AA, Bremer AA, Stanhope KL, Butler M, Booten SL, Graham JL, McKay RA, Murray SF, Watts LM, Monia BP, Bhanot S. Inhibition of protein tyrosine phosphatase-1B with antisense oligonucleotides improves insulin sensitivity and increases adiponectin concentrations in monkeys. *Endocrinology*. 2009;150(4):1670-1679.

Swiatecka-Urban A. Membrane trafficking in podocyte health and disease. *Pediatr Nephrol*. 2013;28(9):1723-1737.

Takano Y, Yamauchi K, Hiramatsu N, Kasai A, Hayakawa K, Yokouchi M, Yao J, Kitamura M. Recovery and maintenance of nephrin expression in cultured podocytes and identification of HGF as a repressor of nephrin. *Am J Physiol Renal Physiol*. 2007;292(5):F1573-1582.

Takemura M, Adachi-Yamada T. Cell death and selective adhesion reorganize the dorsoventral boundary for zigzag patterning of drosophila wing margin hairs. *Dev Biol*. 2011;357(2):336-346.

Thareja S, Aggarwal S, Bhardwaj TR, Kumar M. Protein tyrosine phosphatase 1B inhibitors: A molecular level legitimate approach for the management of diabetes mellitus. *Med Res Rev*. 2012;32(3):459-517.

Tossidou I, Teng B, Menne J, Shushakova N, Park JK, Becker JU, Modde F, Leitges M, Haller H, Schiffer M. Podocytic PKC-alpha is regulated in murine and human diabetes and mediates nephrin endocytosis. *PLoS One*. 2010;5(4):e10185.

Tu Y, Li F, Wu C. Nck-2, a novel src Homology2/3-containing adaptor protein that interacts with the LIM-only protein PINCH and components of growth factor receptor kinase-signaling pathways. *Mol Biol Cell*. 1998;9(12):3367-3382.

Uchida K, Suzuki K, Iwamoto M, Kawachi H, Ohno M, Horita S, Nitta K. Decreased tyrosine phosphorylation of nephrin in rat and human nephrosis. *Kidney Int*. 2008;73(8):926-932.

van den Berg JG, van den Bergh Weerman MA, Assmann KJ, Weening JJ, Florquin S. Podocyte foot process effacement is not correlated with the level of proteinuria in human glomerulopathies. *Kidney Int*. 2004;66(5):1901-1906.

Vaynberg J, Fukuda T, Chen K, Vinogradova O, Velyvis A, Tu Y, Ng L, Wu C, Qin J. Structure of an ultraweak protein-protein complex and its crucial role in regulation of cell morphology and motility. *Molecular Cell*. 2005;17(4):513-523.

Venkatareddy M, Cook L, Abuarquob K, Verma R, Garg P. Nephrin regulates lamellipodia formation by assembling a protein complex that includes Ship2, filamin and lamellipodin. *PLoS One*. 2011;6(12):e28710.

Verma R, Kovari I, Soofi A, Nihalani D, Patrie K, Holzman LB. Nephrin ectodomain engagement results in src kinase activation, nephrin phosphorylation, nck recruitment, and actin polymerization. *J Clin Invest*. 2006;116(5):1346-1359.

Verma R, Wharram B, Kovari I, Kunkel R, Nihalani D, Wary KK, Wiggins RC, Killen P, Holzman LB. Fyn binds to and phosphorylates the kidney slit diaphragm component nephrin. *J Biol Chem*. 2003;278(23):20716-20723.

Veron D, Reidy KJ, Bertuccio C, Teichman J, Villegas G, Jimenez J, Shen W, Kopp JB, Thomas DB, Tufro A. Overexpression of VEGF-A in podocytes of adult mice causes glomerular disease. *Kidney Int*. 2010;77(11):989-999.

Volker LA, Petry M, Abdelsabour-Khalaf M, Schweizer H, Yusuf F, Busch T, Schermer B, Benzing T, Brand-Saberi B, Kretz O, Hohne M, Kispert A. Comparative analysis of neph gene expression in mouse and chicken development. *Histochem Cell Biol*. 2012;137(3):355-366.

Wagner N, Morrison H, Pagnotta S, Michiels JF, Schwab Y, Tryggvason K, Schedl A, Wagner KD. The podocyte protein nephrin is required for cardiac vessel formation. *Hum Mol Genet*. 2011;20(11):2182-2194.

Wagner N, Wagner K, Xing Y, Scholz H, Schedl A. The major podocyte protein nephrin is transcriptionally activated by the wilms' tumor suppressor WT1. *J Am Soc Nephrol*. 2004;15(12):3044-3051.

Wang PC, Takezawa T. Reconstruction of renal glomerular tissue using collagen vitrigel scaffold. *J Biosci Bioeng*. 2005;99(6):529-540.

Wang R, St John PL, Kretzler M, Wiggins RC, Abrahamson DR. Molecular cloning, expression, and distribution of glomerular epithelial protein 1 in developing mouse kidney. *Kidney Int*. 2000a;57(5):1847-1859.

Wang Y, Wang YP, Tay YC, Harris DC. Progressive adriamycin nephropathy in mice: Sequence of histologic and immunohistochemical events. *Kidney Int*. 2000b;58(4):1797-1804.

Wanner N, Noutsou F, Baumeister R, Walz G, Huber TB, Neumann-Haefelin E. Functional and spatial analysis of C. elegans SYG-1 and SYG-2, orthologs of the neph/nephrin cell adhesion module directing selective synaptogenesis. *PLoS One*. 2011;6(8):e23598.

Wasik AA, Polianskyte-Prause Z, Dong MQ, Shaw AS, Yates JR,3rd, Farquhar MG, Lehtonen S. Septin 7 forms a complex with CD2AP and nephrin and regulates glucose transporter trafficking. *Mol Biol Cell*. 2012;23(17):3370-3379.

Wavreille A, Garaud M, Zhang Y, Pei D. Defining SH2 domain and PTP specificity by screening combinatorial peptide libraries. *Methods*. 2007;42(3):207-219.

Weavers H, Prieto-Sanchez S, Grawe F, Garcia-Lopez A, Artero R, Wilsch-Brauninger M, Ruiz-Gomez M, Skaer H, Denholm B. The insect nephrocyte is a podocyte-like cell with a filtration slit diaphragm. *Nature*. 2009;457(7227):322-326.

Weins A, Pollak MR. Inherited nephroses. In: Mount DB, Pollak MR, eds. *Molecular and genetic basis of renal disease: A companion to brenner & rector's the kidney*. Philadelphia: Saunders/Elsevier; 2008:141-150.

Welsh GI, Saleem MA. Nephrin-signature molecule of the glomerular podocyte? *J Pathol*. 2010;220(3):328-337.

Welsh GI, Hale LJ, Eremina V, Jeansson M, Maezawa Y, Lennon R, Pons DA, Owen RJ, Satchell SC, Miles MJ, Caunt CJ, McArdle CA, Pavenstadt H, Tavare JM, Herzenberg AM, Kahn CR, Mathieson PW, Quaggin SE, Saleem MA, Coward RJ. Insulin signaling to the glomerular podocyte is critical for normal kidney function. *Cell Metab*. 2010;12(4):329-340.

Wharram BL, Goyal M, Gillespie PJ, Wiggins JE, Kershaw DB, Holzman LB, Dysko RC, Saunders TL, Samuelson LC, Wiggins RC. Altered podocyte structure in GLEPP1 (ptpro)-deficient mice associated with hypertension and low glomerular filtration rate. *J Clin Invest*. 2000;106(10):1281-1290.

Wu F, Saleem MA, Kampik NB, Satchwell TJ, Williamson RC, Blattner SM, Ni L, Toth T, White G, Young MT, Parker MD, Alper SL, Wagner CA, Toye AM. Anion exchanger 1 interacts with nephrin in podocytes. *J Am Soc Nephrol*. 2010;21(9):1456-1467.

Wyss HM, Henderson JM, Byfield FJ, Bruggeman LA, Ding Y, Huang C, Suh JH, Franke T, Mele E, Pollak MR, Miner JH, Janmey PA, Weitz DA, Miller RT. Biophysical properties of normal and diseased renal glomeruli. *Am J Physiol Cell Physiol*. 2011;300(3):C397-405.

Xu J, Huang Y, Li F, Zheng S, Epstein PN. FVB mouse genotype confers susceptibility to OVE26 diabetic albuminuria. *Am J Physiol Renal Physiol*. 2010;299(3):F487-94.

Yang Y, Guo L, Blattner SM, Mundel P, Kretzler M, Wu C. Formation and phosphorylation of the PINCH-1-integrin linked kinase-alpha-parvin complex are important for regulation of renal glomerular podocyte adhesion, architecture, and survival. *J Am Soc Nephrol*. 2005;16(7):1966-1976.

Yu CC, Yen TS, Lowell CA, DeFranco AL. Lupus-like kidney disease in mice deficient in the src family tyrosine kinases lyn and fyn. *Curr Biol*. 2001;11(1):34-38.

Yu H, Rosen M, Shin T, Seidel-Dugan C, Brugge J, Schreiber S. Solution structure of the SH3 domain of src and identification of its ligand-binding site. *Science*. 1992;258(5088):1665-1668.

Yuan H, Takeuchi E, Salant DJ. Podocyte slit-diaphragm protein nephrin is linked to the actin cytoskeleton. *Am J Physiol Renal Physiol*. 2002;282(4):F585-91.

Zallocchi M, Johnson BM, Meehan DT, Delimont D, Cosgrove D. alpha1beta1 integrin/Rac1-dependent mesangial invasion of glomerular capillaries in alport syndrome. *Am J Pathol*. 2013;183(4):1269-1280.

Zanone MM, Favaro E, Doublier S, Lozanoska-Ochser B, Deregibus MC, Greening J, Huang GC, Klein N, Cavallo Perin P, Peakman M, Camussi G. Expression of nephrin by human pancreatic islet endothelial cells. *Diabetologia*. 2005;48(9):1789-1797.

Zeng R, Cannon JL, Abraham RT, Way M, Billadeau DD, Bubeck-Wardenberg J, Burkhardt JK. SLP-76 coordinates nck-dependent wiskott-aldrich syndrome protein recruitment with vav-1/Cdc42-dependent wiskott-aldrich syndrome protein activation at the T cell-APC contact site. *J Immunol*. 2003;171(3):1360-1368.

Zhang F, Zhao Y, Han Z. An in vivo functional analysis system for renal gene discovery in drosophila pericardial nephrocytes. *J Am Soc Nephrol*. 2013;24(2):191-197.

Zhang JJ, Malekpour M, Luo W, Ge L, Olaru F, Wang XP, Bah M, Sado Y, Heidet L, Kleinau S, Fogo AB, Borza DB. Murine membranous nephropathy: Immunization with alpha3(IV) collagen fragment induces subepithelial immune complexes and FcgammaR-independent nephrotic syndrome. *J Immunol*. 2012a;188(7):3268-3277.

Zhang SY, Kamal M, Dahan K, Pawlak A, Ory V, Desvaux D, Audard V, Candelier M, BenMohamed F, Matignon M, Christov C, Decrouy X, Bernard V, Mangiapan G, Lang P, Guellaen G, Ronco P, Sahali D. C-mip impairs podocyte proximal signaling and induces heavy proteinuria. *Sci Signal*. 2010a;3(122):ra39. doi: 10.1126/scisignal.2000678.

Zhang Y, Yoshida Y, Nameta M, Xu B, Taguchi I, Ikeda T, Fujinaka H, Mohamed SM, Tsukaguchi H, Harita Y, Yaoita E, Yamamoto T. Glomerular proteins related to slit diaphragm and matrix adhesion in the foot processes are highly tyrosine phosphorylated in the normal rat kidney. *Nephrol Dial Transplant*. 2010b;25(6):1785-1795.

Zhang Y, Conti MA, Malide D, Dong F, Wang A, Shmist YA, Liu C, Zerfas P, Daniels MP, Chan CC, Kozin E, Kachar B, Kelley MJ, Kopp JB, Adelstein RS. Mouse models of MYH9-related disease: Mutations in nonmuscle myosin II-A. *Blood*. 2012b;119(1):238-250.

Zheng Z, Pavlidis P, Chua S, D'Agati VD, Gharavi AG. An ancestral haplotype defines susceptibility to doxorubicin nephropathy in the laboratory mouse. *J Am Soc Nephrol*. 2006;17(7):1796-1800.

Zheng Z, Schmidt-Ott KM, Chua S, Foster KA, Frankel RZ, Pavlidis P, Barasch J, D'Agati VD, Gharavi AG. A mendelian locus on chromosome 16 determines susceptibility to doxorubicin nephropathy in the mouse. *Proc Natl Acad Sci U S A*. 2005;102(7):2502-2507.

Zhu J, Attias O, Aoudjit L, Jiang R, Kawachi H, Takano T. P21-activated kinases regulate actin remodeling in glomerular podocytes. *Am J Physiol Renal Physiol*. 2010;298(4):F951-61.

Zhu J, Sun N, Aoudjit L, Li H, Kawachi H, Lemay S, Takano T. Nephrin mediates actin reorganization via phosphoinositide 3-kinase in podocytes. *Kidney Int*. 2008;73(5):556-566.

Zhuang S, Shao H, Guo F, Trimble R, Pearce E, Abmayr SM. Sns and kirre, the drosophila orthologs of nephrin and Neph1, direct adhesion, fusion and formation of a slit diaphragm-like structure in insect nephrocytes. *Development*. 2009;136(14):2335-2344.